# Advances in Multidimensional Chromatography

by

Ahmed Mostafa

A thesis
presented to the University of Waterloo
in fulfillment of the
thesis requirement for the degree of
Doctor of Philosophy
in
Chemistry

Waterloo, Ontario, Canada, 2012

## AUTHOR'S DECLARATION

I hereby declare that I am the sole author of this thesis. This is a true copy of the thesis, including any required final revisions, as accepted by my examiners.

I understand that my thesis may be made electronically available to the public.

## Abstract

Comprehensive two-dimensional gas chromatography (GC×GC) is among the most powerful methods used to separate complex samples. Two columns of different selectivities are coupled in series through a special interface (modulator). The main role of the modulator is to trap and/or sample the primary column effluent and inject it into the secondary column. This results in an enhanced sensitivity, increased peak capacity and structured chromatograms. Practically all thermal modulators in use today are equipped with two trapping stages to prevent problems related to analyte breakthrough, which makes their design more complicated.

In this work, The sensitivity of GC×GC coupled to two different detectors, time-of-flight mass spectrometer (GC×GC-TOFMS) and flame ionization detector (GC×GC-FID) was compared to the sensitivity of conventional one-dimensional gas chromatography (GC-TOFMS and GC-FID) by determining the limits of detection (LOD) for a series of different compounds such as *n*-alkanes and alcohols using both approaches. Different modulation periods were used for GC×GC ranging from 2 to 8 seconds. In addition, different types of inlet ferrules were used to study their effect on both systems. In general, the LODs in GC×GC were lower by at least an order of magnitude.

A new liquid nitrogen-based single-stage cryogenic modulator was developed and characterized. In addition, a new liquid nitrogen delivery system was developed. Band breakthrough was prevented using changes in the carrier gas viscosity with temperature to reduce the carrier gas flow during desorption. Injection band widths for *n*-alkanes of 30-40 ms at half height were obtained. Most importantly, even the solvent peak could be perfectly modulated, which is impossible with any commercially available thermal modulator. Moreover, the newly developed liquid nitrogen supply system reduced liquid nitrogen consumption to ~30 L per day versus 50-100 L per day for commercially available modulators. Evaluation of the newly developed system for the GC×GC separation of some real samples such as regular gasoline and diesel fuel showed that the analytical performance of this single-stage modulator rivals that of the more complicated dual-stage designs.

The technique was tested in various applications. Headspace solid phase microextraction in combination with GC×GC coupled to time-of-flight mass spectrometry (HS-SPME-GC×GC-TOFMS) were used for the detailed investigation of the impact of malolactic fermentation (MLF) using three commercial *Oenococcus oeni* strains on the volatile composition of Pinotage wines. The technique was also

applied for the characterization of Pinotage wine volatiles and blue honeysuckle berries volatiles.

## Acknowledgements

Firstly, I would like to thank my supervisor Dr. Tadeusz Górecki for giving me the opportunity to work on this interesting project. His time spent in constructive discussions and comments is highly appreciated. I am deeply indebted to him for encouraging, supporting, guiding and giving me the chance to present my work at different prestigious conferences in North America and Europe. This helped me a lot to grasp and understand the most recent research areas and improve my presentation skills.

I wish to thank Dr. Susan Mikkelsen, Dr. Wojciech Gabryelski and Dr. Jacek Lipkowski, members of my advisory committee, for their advice and help along the way and for their critical review of my graduate work. I would like also to thank Dr. Frank Dorman for accepting to review my thesis and be part of my PhD defence committee.

Many thanks to all the people at Chemistry Department. I am grateful to all the people at the Science Technical Services (STS) and Information Systems and Technology (IST) at the University of Waterloo for their help in providing me with anything required to build my experimental setup.

Thanks to all the people at LECO, especially Olivier Niquette; Joe Macomber from Polymicro Technologies who supplied me with the optical fused silica fibers; and Richard Denis from Thermo Scientific.

My Sincere thanks to past and current students in the Górecki laboratory. Special thanks to Dr. Suresh Seethapathy for his continuous help at the beginning of my project.

No words can express my gratitude to my mother and brother in Egypt for all their support, patience and encouragement.

Finally, I would like to thank my wife Dr. Heba Shaaban not only for motivating me to start this interesting endeavor, but also for her continuous help, support and patience. Many thanks to my lovely kids; Ziad, Abdel-Rahman, Omar and Ruaa for their patience.

# Table of Contents

# List of Figures

# List of Tables

# Chapter 1

# Introduction[i]

Comprehensive two-dimensional gas chromatography (GC×GC) was first introduced over two decades ago. Currently, it is one of the most powerful and effective techniques for the characterization and analysis of a variety of complex mixtures. This introductory section provides a brief description of the technique in an effort to acquaint readers with the fundamentals and possible benefits of the technique as one of the most rapidly developing areas in separation science. In addition, the history, evolution and optimization aspects of GC×GC will be described.

Chromatography is the technique used most widely to separate and yield quantitative information about components of complex mixtures. Gas chromatography (GC) using modern capillary columns offers higher peak capacities than other chromatographic techniques. The overall resolving power of a single GC column can be described in terms of its peak capacity, [3] which is the maximum number of peaks that can be placed, side by side, into the available one-dimensional

[i] This chapter is partly based on the author's book chapter "History and evolution of GC×GC" [1] and the author's review "Optimization aspects of comprehensive two-dimensional gas chromatography (GC×GC)" [2]

separation space at a given resolution. [4] In order to resolve 98% of the components, the peak capacity must exceed the number of components by a factor of 100, [5] i.e. 100 ordered component peaks require a column of about 40,000 plates, whereas to resolve only 82 of 100 random component peaks requires ~ 4,000,000 plates. [5] In conventional one-dimensional gas chromatography (1D-GC), values of peak capacity approaching 1000 are very difficult to attain. One way to improve the separation power of a GC system is to subject the sample separated by a given GC column to an additional separation using a different separation mechanism. This is referred to as multidimensional separation, a method introduced more than 50 years ago. [6] In 1984 Giddings discussed at length the idea of subjecting a sample to multiple types of separation to get improved resolution and separation power. [7] He concluded that the best results are obtained when the two separation mechanisms are independent. However, within a class of similar compounds there is often correlation between the separation mechanisms, giving rise to diagonal lines on the retention plane. [7]

Multidimensional gas chromatography can be subdivided into two categories: heart-cut multidimensional gas chromatography (GC-GC), where a single fraction (or a few specific fractions at the most) of the first dimension ($^1$D) effluent are

introduced into the second dimension ($^2$D) for further separation, [8] and comprehensive multidimensional gas chromatography (GC×GC), where the entire sample (or at least a representative fraction of each sample component) eluting from the $^1$D is introduced into the $^2$D for further separation. [9]

While combining two (or more) different separation mechanisms is the best solution to improve resolution and separation power in chromatography, it is not always a trivial task. The idea can be implemented easily only in planar chromatography (e.g. TLC), where the chromatographic plate can be physically rotated by 90 ° after the first separation and then developed with a second, different solvent. For obvious reasons, such an approach is not practical in column chromatography (including GC×GC). The fundamental requirement of comprehensive two-dimensional separation is that components separated in the $^1$D must remain separated after passing through the $^2$D. This precludes the use of two columns connected directly in series for this purpose, as explained below. It was not until 1991 that Liu and Phillips realized the vision of Giddings and developed the first GC×GC system using a special modulator. [9]

## 1.1 Fundamentals of GC×GC

As mentioned above, there are two types of multidimensional gas chromatography: GC-GC and GC×GC. In GC-GC (Figure 1-1A), two different columns are used, but only a small portion of the material eluting from the $^{1}$D ("heart-cut") is introduced for further separation into the $^{2}$D. The number of heart-cuts can be increased provided that the time allowed for the separation of the cuts in the $^{2}$D is proportionally reduced (Figure 1-1B). When the number of heart-cuts gets high enough (and the time for their separation short enough), one accomplishes a comprehensive separation (Figure 1-1C), in which the entire sample (or a representative fraction of each sample component) is subjected to separation in both dimensions. Consequently, one can say that GC×GC is in essence an extension of conventional heart-cut GC. In true multidimensional separations, two different separation mechanisms should be applied to the entire sample to achieve separation orthogonality. [10, 11]

Figure 1-2 illustrates the basic layout of a GC×GC system used to accomplish this goal. The sample is first introduced and separated on the first capillary column. However, rather than being sent to the detector, the effluent is introduced into a second capillary column coated with a different stationary phase for further

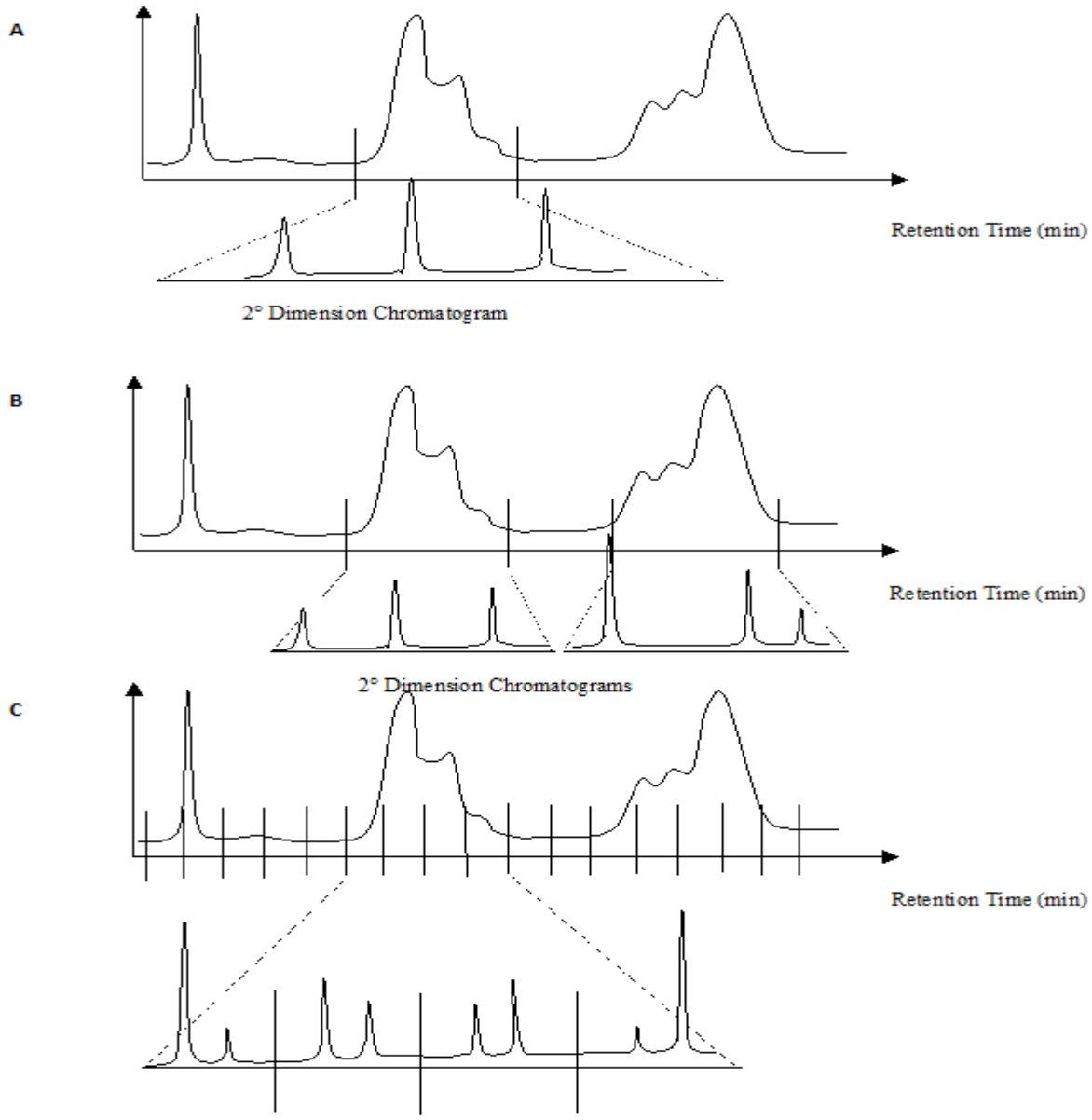


**Figure 1-1: The concept of multidimensional GC. (A) single heart-cut GC analysis, where a large portion of the effluent from the $^{1}$D column with coelutions is diverted to the $^{2}$D column and separated over an extended period of time. (B) dual heart-cut GC analysis, where two regions with coelutions are diverted to the $^{2}$D column, but with less time to perform each separation. (C) Comprehensive two-dimensional GC analysis occurs when the size of the sequential heart cuts is very short, as are the $^{2}$D chromatograms. [From [12]].**

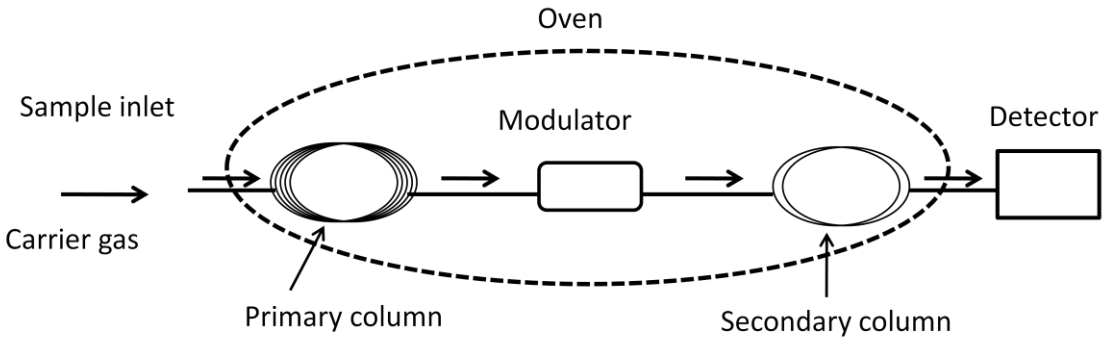


**Figure 1-2: Block diagram of a GC×GC system.**

separation. The two columns are connected through a special interface called a modulator. The $^{1}$D column typically contains non-polar stationary phase, therefore separation in this column is primarily based on analyte volatility (applies strictly to non-polar analytes only). The $^{2}$D column, which is much shorter and often narrower than the $^{1}$D one, is usually coated with a more polar stationary phase to achieve orthogonality (a more detailed discussion of the column combinations used in GC×GC is presented later in this Chapter). The separation in the $^{2}$D has to be extremely fast (a few seconds) to make sure that fractions of the $^{1}$D effluent are sampled frequently enough to preserve the separation accomplished in the $^{1}$D. The effluent from the $^{2}$D is directed to the detector.

## 1.2 Modulation

The modulator is arguably the most important component of any GC×GC system. Figure 1-3 explains the need for and the role of the modulator. Direct serial connection of two different columns without a modulator results in a one-dimensional separation because analytes separated in the $^{1}$D are not prevented from coelution at the exit of the $^{2}$D (Figure 1-3B). Their elution order might even be reversed (Figure 1-3C). The modulator allows the flow of the analytes from the $^{1}$D to the $^{2}$D to be controlled, which fundamentally changes the nature of the separation, as illustrated in Figure 1-3D-G. Following the same separation in the $^{1}$D

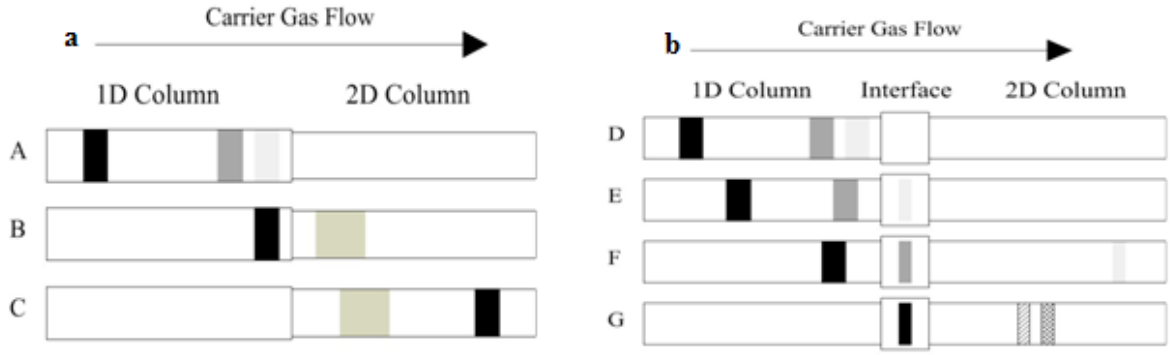


**Figure 1-3: (a) Without a modulator present between the primary and secondary columns, analytes separated in the $^{1}$D might coelute at the outlet of the $^{2}$D (A–C). (b) A modulator between the primary and the secondary columns prevents coelutions of previously separated analytes (see the text) [From [13]].**

(Figure 1-3D), the modulator traps and focuses the first band (light grey in Figure 1-3E), and then injects it into the $^{2}$D while collecting the following band (dark grey in Figure 1-3F). The dark grey band is injected into the $^{2}$D only after the light grey band had eluted from it. The dark grey band is then separated into two bands on the $^{2}$D, while the black band is collected by the modulator (Figure 1-3G). This sequence of events assures that separation achieved in the $^{1}$D column is preserved, and additional separation in the $^{2}$D is possible.

To sum up, the role of the modulator is to trap, refocus, and inject the $^{1}$D heart-cuts sequentially into the $^{2}$D (although it should be pointed out that instead of being trapped, the effluent from the $^{1}$D might also be sampled, as will be explained later in this Chapter). The time taken to complete a single cycle of events is called the modulation period. The preservation of the $^{1}$D separation can only be accomplished if every peak eluting from the $^{1}$D is sampled at least three times [14] (although 2.5 times has also been proposed as the optimal value) [15]. Thus, if e.g. a 12 s wide peak elutes from the $^{1}$D, the modulation period should be no longer than 4 s. Górecki et al. illustrated the effect of the length of the modulation period on the preservation of the $^{1}$D separation in their review in 2004. [12]

## 1.3 GC×GC data interpretation

A conventional 1D-GC chromatogram is a two-dimensional plot of detector signal intensity versus retention time. A GC×GC chromatogram, on the other hand, is a three-dimensional plot with two retention times and signal intensity as the axes. However, the detector positioned at the outlet of the $^{2}$D records only a continuous linear signal, being in fact a series of $^{2}$D chromatograms produced by each modulation cycle (Figure 1-4A). Interpretation of such a chromatogram is very difficult, especially considering that each component eluting from the $^{1}$D might be present in several secondary chromatograms. Consequently, the data has to be converted into a three-dimensional representation before it can be effectively analyzed. This task is handled by appropriate computer software. The construction of such a plot is illustrated in Figure 1-4. The software utilizes the times of injection of the fractions of the $^{1}$D effluent into the $^{2}$D ($t_1$, $t_2$ and $t_3$ in Figure 1-4) to "slice" the continuous chromatogram into the individual $^{2}$D chromatograms (Figure 1-4B). The times when the injection into the $^{2}$D took place provide the $^{1}$D retention times for all peaks eluting in a given modulation period. The $^{2}$D retention time of each peak is its absolute retention time minus the injection time for the modulation cycle. [16] As illustrated in Figure 1-4C, after arranging the individual $^{2}$D chromatograms side by side, the X-axis becomes the primary retention time, the Y-axis the secondary

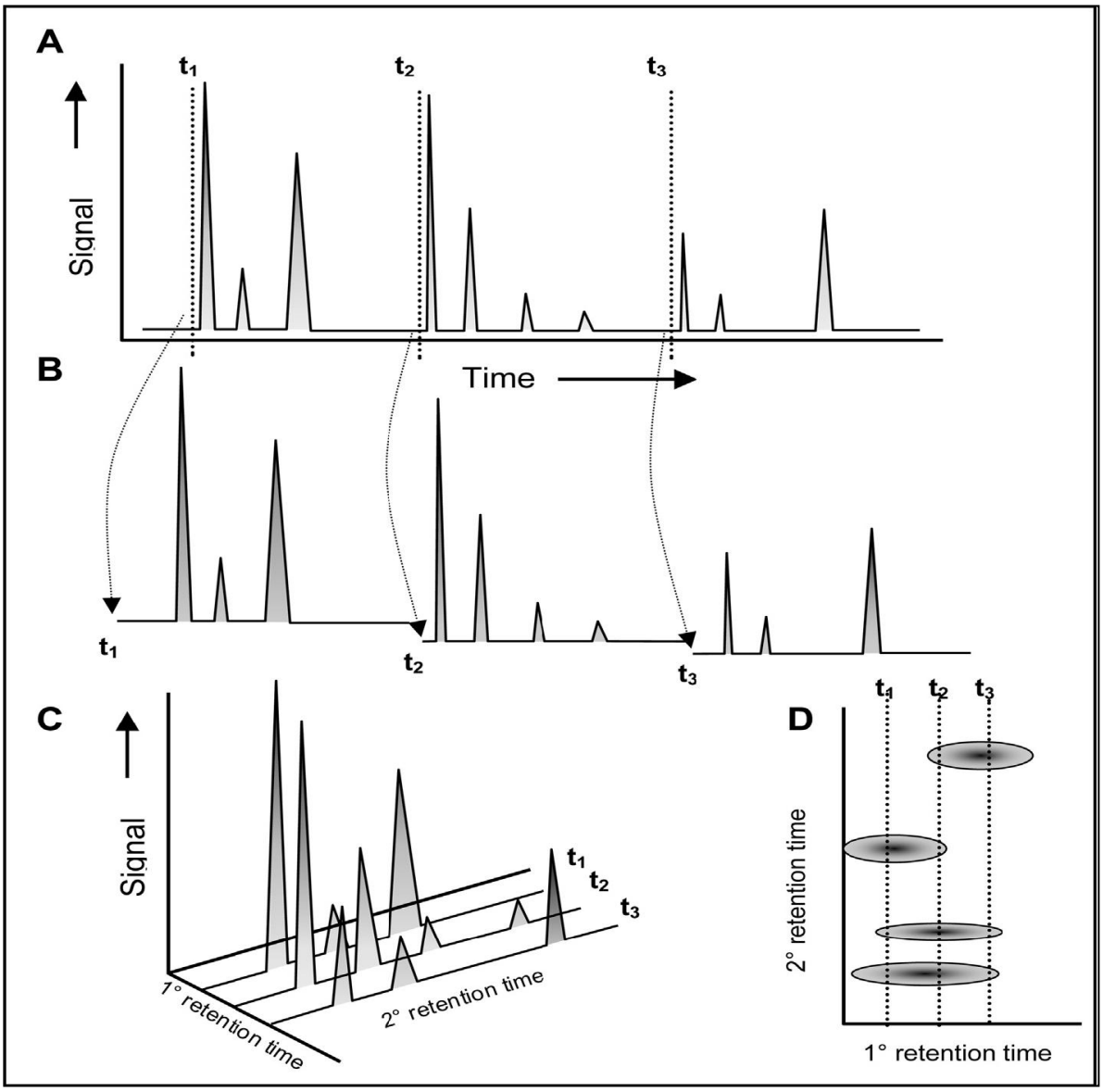


**Figure 1-4: The interpretation of GC×GC data and generation of contour plots. (A) The raw GC×GC chromatogram consisting of a series of short $^2$D chromatograms; $t_1$, $t_2$, and $t_3$ indicate the times when injections to the $^2$D column occurred. The computer uses these injection times to slice the original signal into a multitude of individual chromatograms (B). These are then aligned on a two-dimensional plane with primary retention and secondary retention as the X and Y axes, and signal intensity as the Z-axis (C). When viewed from above, the peaks appear as rings of contour lines or color-coded spots (D) [From[13]].**

retention time, and the Z-axis represents signal intensity. In such representation, $^{2}$D peaks of the same component appear in several consecutive "slices" with the same secondary retention times (recall that each $^{1}$D peak should be sampled at least three times, therefore component(s) of this peak might show up in several consecutive $^{2}$D chromatograms). The peaks of a given analyte observed in the individual secondary chromatograms are then merged into a single component peak. The approach described requires that the modulation periods are precisely known and reproducible, which can be accomplished using modern computer-controlled hardware.

Quantification of GC×GC data is similar to that encountered in 1D-GC, except that instead of integrating a single peak for a single analyte, multiple peaks for each analyte have to be taken into consideration. In the simplest approach, each peak in the 2D chromatogram is integrated separately, and the areas of the peaks belonging to the same analyte are summed. While different approaches to analyte quantitation in GC×GC have been proposed, the simple summation of the peak areas seems to work the best. [17] Quantitative methods employed in GC×GC were reviewed by Dallüge et al., [18] Górecki et al., [19] Adahchour et al. [20] and Amador-Muñz and Marriott. [21]

In the early GC×GC history, most research groups had to develop their own in-house written GC×GC analysis software. [22-25] These GC×GC data handling packages usually allowed visualization of the multidimensional data, data pre-processing, and (less often) peak detection and quantification. Harynuk et al. [16] demonstrated the steps of data manipulation that permit conversion of raw data to the contour plots generated in GC×GC. They explained the challenges associated with the accurate conversion of GC×GC data, based on their observations from developing GC×GC data analysis software. Reichenbach et al. at the University of Nebraska-Lincoln [26, 27] developed software called "GC Image" that produced background-free peaks in GC×GC chromatograms. The software was available for quantification purposes. The same group later developed software with added support for mass spectrometry (GC×GC-MS), 3D visualization, and many other features. [28] Techniques for peak alignment were also developed, which significantly improved comparative analysis of GC×GC data. [29] GC Image is commercially available from Zoex Corporation. [27]

Another GC×GC software package, HyperChrom, developed by Thermo Fisher Scientific, was paired with the TRACE GC×GC instrument sold by the same company. It has been used extensively by some researchers, e.g.[30, 31]

The leading GC×GC –MS software package, ChromaTOF, is available from LECO together with their Pegasus 4D GC×GC –TOFMS system. The software, which works also with FID data, incorporates perhaps the most sophisticated data processing capabilities for GC×GC.

## 1.4 GC×GC instrumentation

GC×GC utilizes much of the basic instrumentation used for 1D-GC. For example, injectors used in GC×GC play the same role as in 1D-GC. Consequently, injectors and injection techniques used for 1D-GC can in principle also be used for GC×GC analyses. The $^{1}$D column is usually long, with typical dimensions of 15 to 30 m × 0.25 mm. The stationary phase film thickness in the $^{1}$D is usually in the range of 0.25- 1.0 μm. These columns allow the generation of peaks with widths of 10–20 s, which are required for typical modulation periods (3 to 6 s). The $^{2}$D column has to be very short and efficient, as each individual separation in this column should be finished in a time shorter than the modulation period. Typical $^{2}$D column dimensions range from 0.5–1.5 m in length and 0.1-0.25 mm in diameter. The $^{1}$D columns are typically coated with non-polar stationary phases (although other options are explored increasingly often). With non-polar coating in the $^{1}$D, the $^{2}$D columns are usually coated with polar stationary phases (See section 1.7.4).

The two columns used in the GC×GC systems can be housed in one oven or a second optional oven can be used for the $^{2}$D column. In fact, most commercially available systems use two separate ovens. This option provides more flexibility in method development and allows better control over the $^{2}$D separation. In contrast, in most home-made GC×GC systems, both columns are housed in one oven to avoid making the system too complex. Satisfactory separations can usually be achieved with both setups.

The detectors used for 1D-GC can be used for GC×GC as well, but with an additional requirement that their data acquisition rates must be high. Peaks eluting from the $^{2}$D are typically very narrow, with widths of 100-500 ms at the base. [32-35] To get reliable and reproducible determination of a peak area, at least 10 data points should be collected along the peak profile. [22] Consequently, a detector that is capable of collecting data at a rate of at least 50 Hz is required. Thus far Flame Ionization Detectors (FID) have been the most popular choice in GC×GC, followed by mass spectrometers. Micro Electron Capture Detector (μ-ECD), [36, 37] Atomic Emission Detector (AED), [38] Nitrogen Chemiluminescence Detector (NCD), [39] Miniaturized Pulsed Discharge Detector [40] and Sulphur Chemiluminescence Detector (SCD) [41] have also been used for GC×GC work.

The most critical and important component of any GC×GC system is the modulator. Two main classes of modulators are being used: thermal modulators and flow modulators. Thermal modulators can be further sub-divided into heater-based (trapping at ambient temperature, including oven temperature), and cooling-based (trapping at sub-ambient temperature). The next section is a brief summary of the history of modulator design. For a more thorough discussion of interface technology, readers are advised to refer to the reviews by Górecki et al. [12], Bertsch et al. [17] and Adahchour et al. [20]

## 1.5 Thermal modulators

### 1.5.1 Heater-based modulators

Liu and Phillips introduced the first GC×GC modulator in 1991. [9] First designed as a single-stage sample introduction device in multiplex and high-speed GC, this simple device was applied to GC×GC with very little alteration to its original design.[42, 43] The interface (Figure 1-5) was constructed using the head of the non-polar $^{2}$D column (0.5 μm $d_f$) looped outside the GC oven at ambient temperature and coated with gold paint. The modulator length was 15 cm, divided equally between two stages. As effluent from the $^{1}$D column (A in Figure 1-5) entered the $^{2}$D

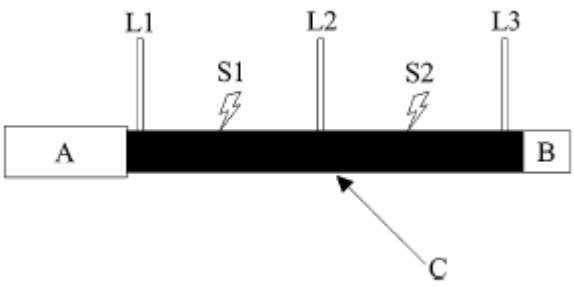


**Figure 1-5: The original thermal desorption modulator. The $^{1}$D column (A) is connected to the $^{2}$D column (B). Gold paint (C) is applied to the beginning segment of the $^{2}$D column. Electrical leads (L1, L2, L3) allow current to flow alternately between stage one (S1) and stage two (S2) during modulation. [Based on [9]]**

column (B in Figure 1-5), it would become trapped and focused by the stationary phase coating. Electrical current was then applied to the first stage of the trap (S1 in Figure 1-5) through leads L1 and L2 in Figure 1-5. This caused rapid heating of the gold paint layer (C in Figure 1-5), forcing analytes trapped within the capillary to partition into the carrier gas. Once in the carrier gas, the effluent was swept to the second stage (S2 in Figure 1-5) of the capillary, where it became trapped once again. At this time the first stage of the modulator had cooled and would continue its trapping function, as the second stage was pulsed through leads L2 and L3 in Figure 1-5, injecting the trapped components as a narrow band.

Although good results were obtained using those thermal modulators, [44-46] they appeared to have significant disadvantages, mostly due to the fact that the modulator capillaries and the paint coating were not very robust or reproducible. However, the early thermal modulators did demonstrate that GC×GC was a viable technique and formed the foundation for many modulators that followed. The idea of dual-stage modulation in GC×GC is used in almost all thermal modulators these days.

The first commercial modulator, the Rotating Thermal Modulator (RTM) (Figure 1-6), was also developed by Phillips et al. [47, 48] Briefly, a thick-film capillary housed in the GC oven was used to trap and focus the $^{1}$D effluent. Desorption of the trapped material and its re-injection into the $^{2}$D column were accomplished by the anticlockwise rotation of a slotted heater over the trapping capillary, heating it locally to a temperature higher by about 100 °C than the oven temperature. As the heater passed over the trap moving in the same direction as the carrier gas, any material sorbed by the stationary phase in the heated region partitioned back into the gas phase and was "swept" towards the end of the trap and focused into a narrow band before entering the second column as shown in Figure 1-6. This modulator worked satisfactorily in many different applications e.g. [22, 23, 48-50]. Dallüge

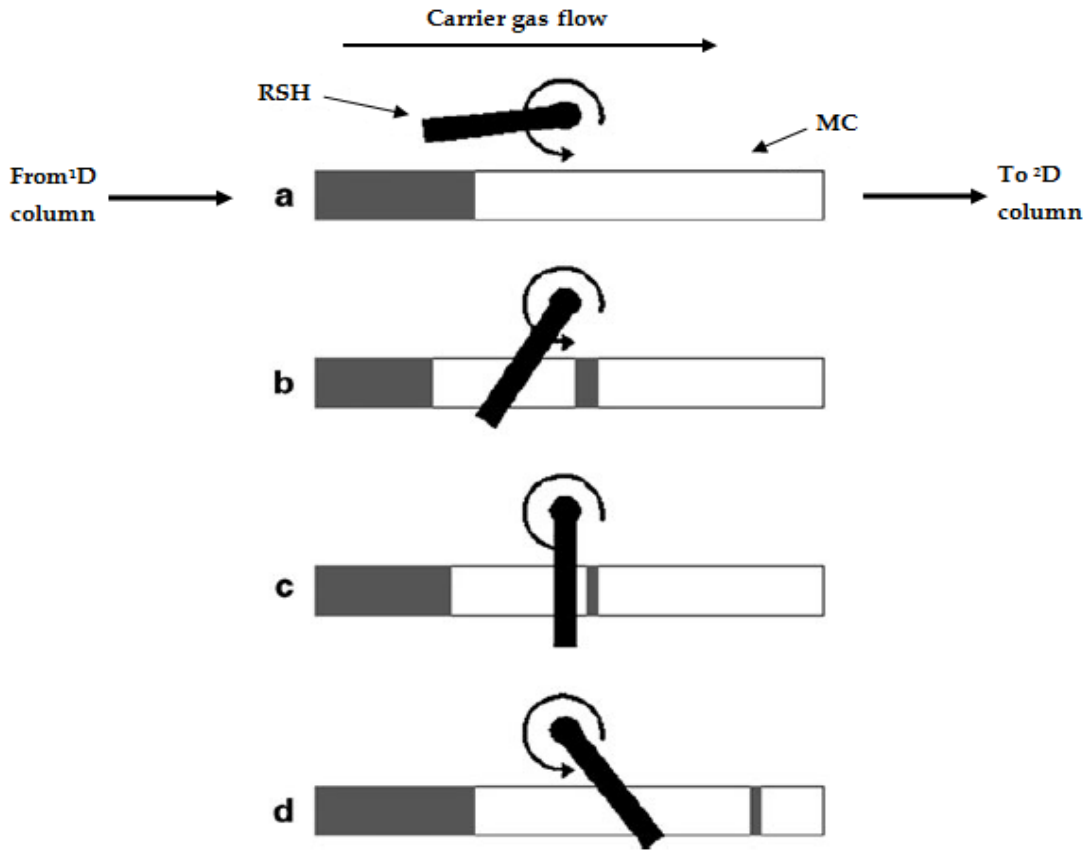


**Figure 1-6: The rotating thermal modulator. The rotating slot heater (RSH) periodically rotates anti-clockwise over the modulating capillary (MC) as four main functions occur: accumulation (a), cut (b), focus (c) and launch (d). [Based on [48]]**

et al. [18] stated that the use of the RTM was reported in approximately 30% of all articles on GC×GC published before 2003. However, the moving parts caused problems when the alignment of all the modulator parts was not perfect. In addition, the modulator was incapable of collecting volatile compounds at conventional oven temperatures, and the maximum oven temperature had to be

kept about 100 °C lower than the maximum operating temperature of the stationary phase in the modulator, which significantly limited the range of analyte volatilities. In the light of these disadvantages, the RTM concept was abandoned and the device is no longer commercially available.

Harynuk and Górecki [51] developed a different dual-stage thermal modulator based on the early concepts of Phillips et al. It was based on a pair of inline micro sorbent traps housed in deactivated Silcosteel capillaries that could be resistively heated in order to desorb and re-inject the trapped analytes. Very rapid heating was accomplished by means of capacitive discharge. This modulator design had no moving parts and much higher capacity for analyte trapping than the thick-film modulator capillaries used in other modulators. The main disadvantage was the limited thermal stability of the sorbent, which made the modulator poorly suitable for higher boiling compounds (similarly to other heated modulator designs).

Another heated modulator was developed by Burger et al. [52] This modulator used rapid resistive heating of consecutive segments of a stainless steel capillary housing a thick-film column inside, where the $^{1}$D effluent was trapped. The steel capillary had multiple electrical contacts that allowed small regions to be heated in sequence for brief periods of time to shuttle bands of analytes through the modulator, keeping

them focused. Lack of moving parts was the main advantage of this design, but it suffered from the same disadvantages as other heated modulators when it comes to the modulation of very volatile analytes (~$C_3$-$C_5$ range) and thermal stability of the coating. Today, the sweeper and/or related modulators are rarely used. Their low efficiency in trapping volatile compounds at conventional oven temperatures and the limited range of analyte volatilities were the main reasons why they were largely replaced by cryogenic modulators. One exception to this rule is the thermal modulator developed recently by Górecki and co-workers for the determination of the composition of the semi-volatile fraction of air particulate matter ($PM_{2.5}$) in the field using thermal desorption aerosol GC (2D-TAG) system. [53, 54] The design of this modulator was based on the original idea of Liu and Phillips, [9] except that deactivated stainless steel Silcosteel® capillary tubing was used for the modulator rather than painted fused-silica capillary. The tubing used for the modulator was either coated with a 1 μm layer of polydimethylsiloxane (PDMS) stationary phase, or just deactivated. The modulator was mounted outside the GC oven allowing for continuous forced air cooling. The effluent was trapped in the interface at ambient temperature. Desorption was performed through pulsed resistive heating of one segment of the trapping capillary using a capacitive discharge power supply, while the other segment was trapping and focusing another portion of the effluent. This

modulator proved to be robust, had no moving parts and did not require any consumables, making it suitable for an automated in-situ field instrument, as well as for laboratory work. Very recently, the same group introduced a modified version of the modulator using single-stage thermal modulation instead of dual-stage. Other modifications included the use of a Vortex cooler to allow cooling with sub-ambient temperature air at the beginning of the run and temperature programming of the cooling air. This system has been recently employed by Worton et al. to study in-situ speciated organic aerosols. [55]

### 1.5.2 Cooling-based modulators

This group of modulators can be further subdivided into cryogenic and cryogen-free modulators. The first cryogenic modulator, Longitudinally Modulated Cryogenic System (LMCS), was developed in Australia by Kinghorn and Marriott. [56] This modulator worked on a principle similar to that of the heated modulators. However, rather than trapping the effluent at the oven temperature and desorbing it by increasing the temperature above the oven temperature, trapping was performed at temperatures significantly below that of the GC oven, and re-injection was accomplished at oven temperature. Schematic diagram of the LMCS is presented in Figure 1-7 This design was based on the group's previous work on cryogenic

trapping of solutes as a means of narrowing the chromatographic bands to provide sharper elution profiles in GC.[57] Their first cryogenic trap was constructed from two steel tubes of differing lengths and inside diameters that formed a cavity; a cryogen could be pumped into and out of this cavity. The analytical GC column was placed within this trap approximately 40 cm from the detector. Liquid $CO_2$ was pumped through the trap while compounds of interest eluted. The flow of the cryogen was then shut off, allowing the cooled capillary segment to return to oven temperature, thereby releasing any trapped analytes as focused bands into the detector. It was found that GC analysis of *n*-alkanes ($C_{13}$–$C_{16}$) utilizing this trap produced greater sensitivity and lower detection limits than conventional GC. The main disadvantage was the time required for the capillary to reach temperatures high enough for effective desorption of trapped analytes. Their solution to this problem was to expose the portion of the capillary where components were trapped to the elevated temperatures of the GC oven, allowing desorption of analytes to occur while trapping continued upstream of the desorbed peak. In this way, the LMCS was born [58]. Modulation with this device was accomplished by moving the cryogenic trap longitudinally along the column towards the detector to trap components (a in Figure 1-7) or away from the detector to release them (b in Figure 1-7).

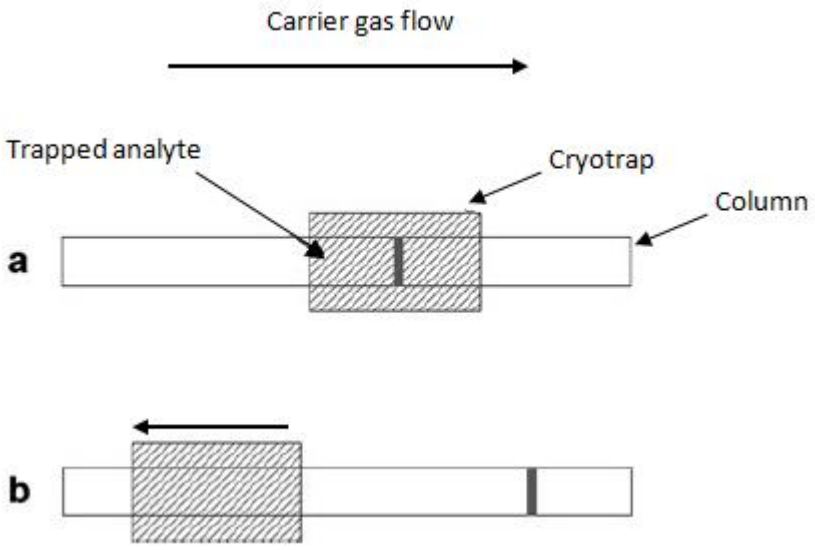


**Figure 1-7: The longitudinally modulated cryogenic system. Analytes travelling through the column become trapped in the segment of the column cooled by the cryotrap (a). Longitudinal movement of the cryotrap away from the detector releases the trapped segment as a narrow focused band (b). [Based on [58]]**

The cryogenic modulation introduced with LMCS offered significant advantages over heated modulation. First, the column segment used for analyte trapping needed only to be raised to the GC oven temperature for desorption, not to a temperature above the oven. Consequently, higher final oven temperatures could be used during separation compared to heated modulators. Second, the modulator was capable of trapping volatile analytes much more efficiently than heated modulators owing to the low trapping temperature.

On the other hand, there were also some limitations to this approach. The first was the use of the moving trap, which could damage the column in the worst case scenario or cause other problems. Another limitation was the use of liquid $CO_2$ as the cryogenic agent, which allowed the trap to be cooled to about -50 °C only. This temperature is not sufficiently low to trap highly volatile analytes (~ $C_3$-$C_4$ range). Generally speaking, though, cryogenic modulators had fewer limitations than heated modulators. Today, cryogenic modulators have replaced the latter almost completely.

The next goal in the development of cryogenic modulators was the elimination of moving parts inside the GC oven. The first modulator of this kind was reported by Ledford. [59] In this design, shown in Figure 1-8A, dual-stage modulation was accomplished with the use of two cold $CO_2$ jets ($C_1$ and $C_2$ in Figure 1-8A) for analyte trapping and focusing and two hot air jets ($H_1$ and $H_2$ in Figure 1-8A) for desorption. When the upstream cryojet ($C_1$) was turned on, the effluent from the $^1$D was trapped in the upstream position. Cryojet $C_1$ was then turned off and the upstream warm jet ($H_1$) was activated together with the downstream cryojet ($C_2$). The effluent collected at position $C_1$ along with any effluent that arrived at the trap while the warm jet ($H_1$) was on were then carried to the downstream cold spot ($C_2$), where they were re-

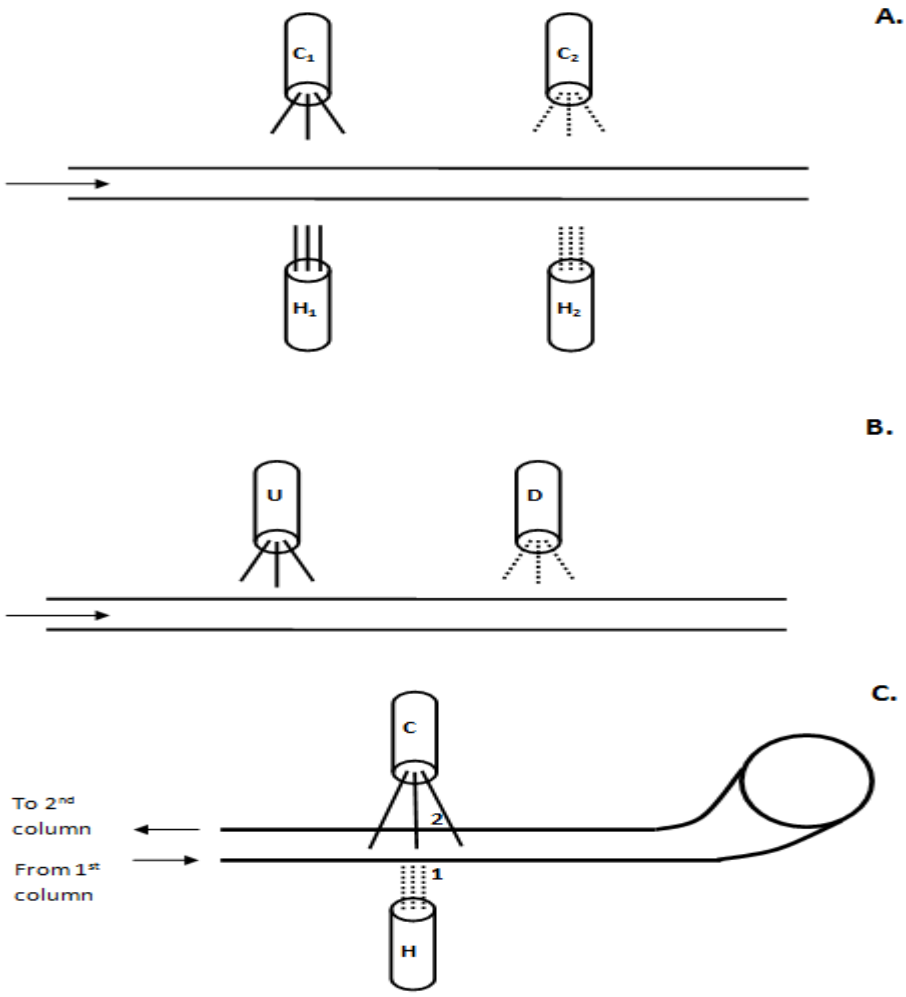


**Figure 1-8: Schematic diagrams of selected dual-stage cryogenic modulators. (A) Quad-jet cryogenic modulator developed by Ledford and Billesbach. (B) Dual-jet cryogenic modulator developed by Beens et al. (C) Single cryojet, dual-stage modulator with a delay loop. [From [19]]**

-focused. In the next part of the cycle, the upstream warm jet ($H_1$) was turned off and the upstream cryojet ($C_1$) was activated, while the opposite happened at the downstream position. This prevented analyte breakthrough when the downstream cryojet ($C_2$) was turned off and the downstream warm jet ($H_2$) was turned on to inject the narrow analyte band onto the $^2$D column. This modulator generally worked very well. Its main limitation was the somewhat complicated design including four jets that needed to be controlled in sequence. It did provide the basis for the design of most of the new cryogenic modulators that have been developed recently, however. A commercial version of this modulator utilizing liquid nitrogen as the cooling agent is now available on GC×GC instruments from the LECO Corporation.

Shortly after the quad-jet modulator was introduced, Harynuk and Górecki [51, 60] reported the development of another cryogenic modulator with no moving parts. The interface consisted of two empty deactivated Silcosteel® capillaries connected in series and mounted inside a cryochamber cooled with liquid nitrogen. In this modulator, trapping was performed through freezing rather than partitioning into the stationary phase as in other cryogenic modulator designs. Launching of the trapped analytes into the second column was accomplished through resistive

heating of the trap using an electrical pulse. This modulator was able to trap highly volatile analytes (including propane), which was one of its major advantages in addition to the ability to very precisely control the injection timing. The main drawback of this modulator were the occasional leaks on the seals between the Silcosteel® capillaries and the cryochamber, which led to the development of cold spots resulting in band broadening. [51, 60]

Utilizing liquid nitrogen instead of liquid $CO_2$ for analyte trapping via partitioning into the stationary phase allows much lower trapping temperatures, which makes modulation of highly volatile components possible. On the other hand, it also has some limitations. Liquid nitrogen is not easily available in all laboratories and requires bulky insulation to be transported through tubing. [32] Beens et al. simplified Ledford's quad-jet design by using two liquid $CO_2$ cryojets for trapping the analytes, which were then remobilized by the heat from the oven air. In this way, the two hot jets of the quad-jet design could be eliminated (Figure 1-8B). The commercial version of this modulator is offered on GC×GC instruments from Thermo Scientific. A further simplification of this modulator was introduced by Adahchour et al. [61] In this version only a single-jet was used to perform single-stage modulation (Figure 1-9).

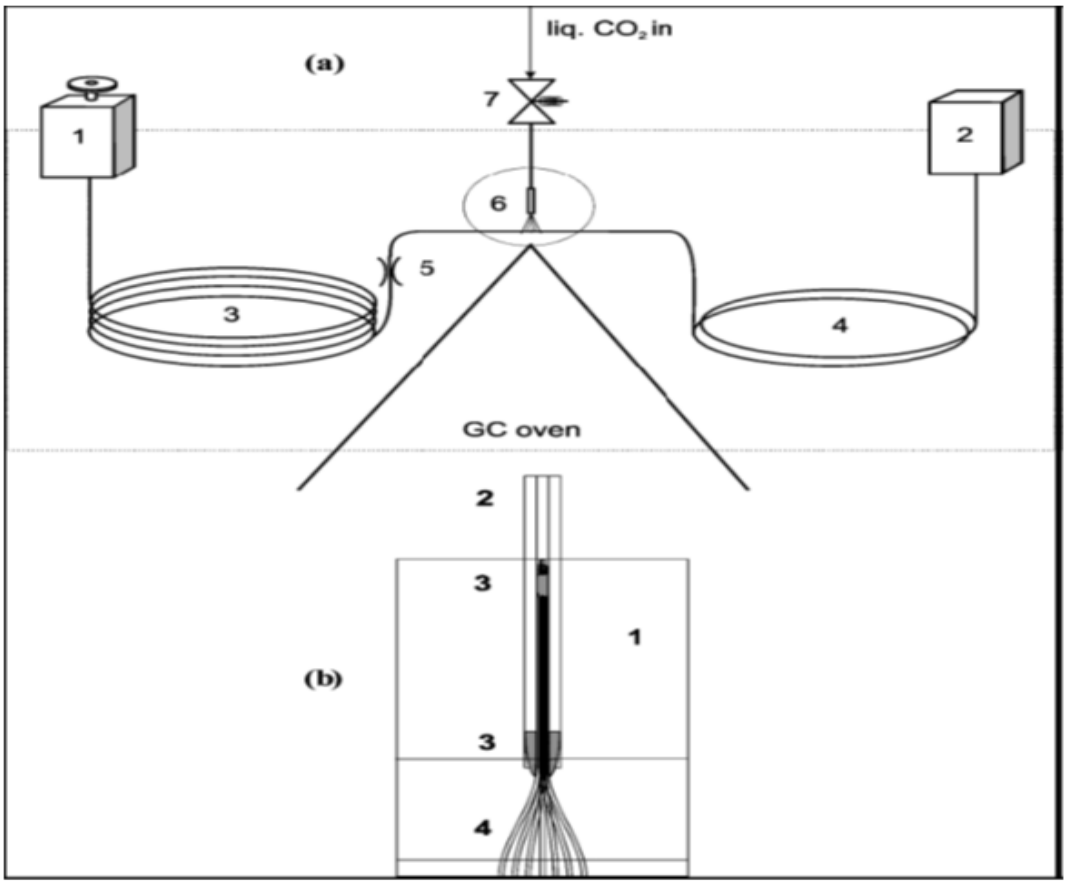


**Figure 1-9: (a) Schematic of the single-jet cryogenic modulator developed by Adahchour et al.: 1- injector, 2- detector, 3- $^1$D column, 4- $^2$D column, 5- column connection (press-fit), 6- $CO_2$ nozzle, 7- $CO_2$ valve. (b) $CO_2$ nozzle: 1- brass block, 2- stainless steel (SS) connecting capillary, 3- soldering, 4- seven SS spraying capillaries, 0.11 mm I.D. [From [61]].**

The primary advantage of this technique was the simplicity of the instrumentation and the decrease in $CO_2$ consumption by more than 37% with no significant effect on the modulation performance. [61] The disadvantage of this approach was that when using only one trapping zone, the timing of the jet and the tuning of the instrumental parameters had to be done very carefully so as to minimize

breakthrough from the $^{1}$D while the trap was hot. In another development, Ledford and co-workers simplified the concept of the original quad-jet, dual-stage modulator by introducing a single cryojet interface capable of dual-stage modulation with the use of a delay loop [62] (Figure 1-8C). In this design, gaseous nitrogen cooled with liquid nitrogen was used as the cryogenic agent. The single jet cooled two segments of a coiled trapping capillary simultaneously. The effluent from the $^{1}$D was first trapped at the upstream cold spot when the cryojet was turned on. Turning the hot jet on caused the cold spot to quickly warm up and launched the material collected there to the delay loop along with any breakthrough from the $^{1}$D. The hot jet was then turned off, which led to cooling of both cold spots so that the effluent from the primary column started to be collected again in the first (upstream) cold spot, while the material in the loop was re-trapped in the second (downstream) cold spot. When the hot jet was turned on again, material from the first cold spot was injected into the loop, while the band collected in the second cold spot was injected to the $^{2}$D. This modulator, available commercially from Zoex Corporation, represents one of the simplest dual-stage cryogenic designs. The main drawback of this modulator is that the length of the loop and the velocity of the carrier gas have to be carefully adjusted whenever the chromatographic conditions change. If the flow of the carrier gas is

not adjusted properly, the band travelling through the delay loop might not reach the trapping spot at a time when it is cold, and therefore it might not be refocused.

Harynuk and Górecki developed another modulator based on the idea of the dual-stage, single-jet modulation with a delay loop [25] (Figure 1-10). The main difference between this design and the design developed by Ledford et al. was that liquid nitrogen was used as a cryogen rather than cold nitrogen gas, thus highly volatile analytes (~$C_3$-$C_6$ range) could be efficiently trapped. In addition, trapping was performed in uncoated fused silica capillaries, thus eliminating potential problems occurring when coated capillaries were used for trapping (e.g. pre-separation of the analytes in the trap due to different times required to desorb the analytes from the stationary phase). In addition, the consumption of liquid nitrogen was decreased.

A rather different interface design was introduced by Górecki's group, which was based on stop-flow GC×GC. [63, 64] In this new design, the flow in the $^1$D was periodically stopped for short periods of time using a six-port valve, while supplying carrier gas to the $^2$D from an auxiliary source. Thus, the two columns were decoupled, which allowed for a longer period of time for the separation in the $^2$D. As a result, both columns could be operated simultaneously under optimal flow conditions and the second column did not necessarily had to be short and/or

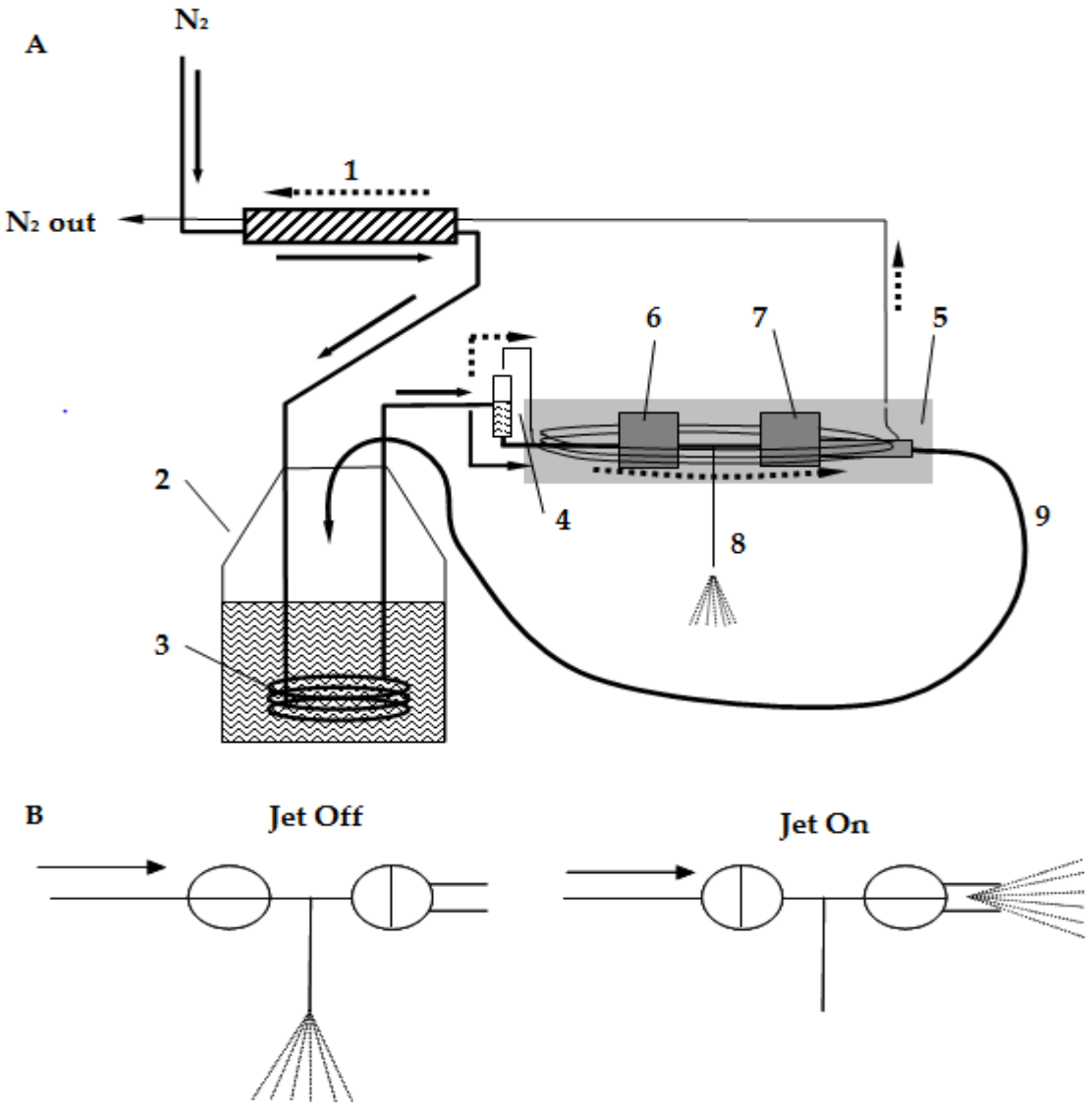


**Figure 1-10: (A) The cryogen supply system. Bold solid arrows denote the primary flow path of nitrogen from the high-pressure supply to the cryojet nozzle and back to the liquid nitrogen Dewar. Dashed arrows denote the secondary flow path of cold gaseous nitrogen and excess liquid nitrogen. (1) Heat exchanger; (2) Dewar with liquid nitrogen; (3) cooling coils; (4) phase separator; (5) modulator; (6) upstream solenoid valve; (7) downstream solenoid valve; (8) cryojet nozzle; (9) cryojet vent with liquid nitrogen return to the liquid nitrogen Dewar. (B) The two on/off solenoid valves controlling the flow of liquid nitrogen through the cryojet. The arrow denotes the direction of liquid nitrogen flow from the phase separator. [From [25]]**

narrow. The stop-flow interface was followed by the cryogenic modulator. The utilization of valves in this design had a number of drawbacks. High-temperature rotary valves did not last long when switched continuously. Pneumatic valves had low upper temperature limits. In addition, artifact peaks appeared in the $^{2}D$, as polymeric materials used in the valves tended to offgas at high temperatures. [34]

Libardoni et al. developed an air-cooled, resistively heated single-stage thermal modulator with no moving parts. [65] The modulator utilized refrigerated air for trapping and resistive heating for desorption. The main disadvantage was the single-stage design, which resulted in analyte breakthrough during the desorption cycle of the trap. The same group developed another modulator based on the same concept but using liquid ethylene glycol rather than air for cooling. [66] The most significant limitation in both designs was the higher trapping temperature (- 30 °C) relative to the temperatures attainable with liquefied gases used as cryogenic agents. As a result, both designs were incapable of trapping highly volatile analytes. On the other hand, they were characterized by very low operating costs. A cryogen-free modulator based on this research has been recently commercialized by the LECO Corporation.

A different cryogenic modulator was developed by Hyötyläinen et al. It was based on two-step cryogenic trapping with continuously delivered $CO_2$ and thermal desorption with electric heating. [67] In this design, two nozzles were mounted on a tube at an angle of 45 ° to each other. When the tube was rotated, liquid $CO_2$ from the nozzles would alternately hit a trapping capillary and create two trapping zones. The major problems with this design were the high consumption of $CO_2$ and the fact that occasional overheating tended to burn the stationary phase. The same group then simplified the design of this modulator to one that used a single $CO_2$ nozzle mounted on a disc that rotated by 180 ° back and forth to provide two spots on the column that were alternately cooled for trapping and focusing. [68] Recently, the same group developed a third version of the semi-rotating modulator to allow more reliable and rugged performance and operation. [69] In this version, a separate modulator control program was replaced with a pre-programmed microcontroller equipped with a 4-MHz quartz crystal to control the movement of the modulator, which led to improved repeatability of retention times. [69] In addition, the new version was simpler and lighter, and the modulator was easy to install in any commercial GC system.

Though the semi-rotating modulator was based on the same principle as that of any two-stage cryogenic modulator, the main advantage came from the fact that with the single jet rotating from one position to the other there was no need for valves to control the flow of the cryogen. Moreover, this design did not cause any risk of column breakage during modulation as was found with the rotating thermal modulator and the early implementations of LMCS. [12]

## 1.6 Flow modulators

The sometimes limited availability and large consumption of liquified gas cryogenic agents ($LCO_2$ and $LN_2$) were the main limitations of cryogenic modulation. In addition, instrument portability was very limited. This led to the parallel development of flow modulators requiring no consumables and assembled using inexpensive off-the-shelf components. Unlike thermal modulators which trap effluent from the $^1D$ using temperature differentials, flow modulators utilize pneumatic means to accomplish modulation of the $^1D$ effluent. There is one exception which utilizes both cryogens and valves to modulate chromatographic peaks.

### 1.6.1 Diaphragm valve modulators

The first flow modulator based on a fast switching diaphragm valve was developed by Bruckner et al. [70] Early flow modulators operated through the diversion of portions of the effluent exiting the $^{1}$D into the $^{2}$D. [71] In fact, a controversy developed initially among the GC×GC community whether such an approach really produced a comprehensive multidimensional separation considering that not all the sample was subjected to additional separation in the second dimension. Following extensive discussions at the First International Symposium on Comprehensive Multidimensional Gas Chromatography held in 2003 in Volendam (Holland), the community agreed that this was indeed the case, as the resulting chromatogram was representative of the entire sample. A significant limitation of the diaphragm valve-based modulator design was the low maximum operating temperature of the valve, which restricted the range of applications to compounds eluting from the GC oven at temperatures not exceeding the maximum operating temperature of the valve (~180 °C).

Hamilton et al.[72] developed a different flow modulator using a design similar to that of Bruckner et al. This valve modulation system utilized a rotary valve that transferred only small fractions of the $^{1}$D effluent to the $^{2}$D. In 2006, Mohler et al.

developed a diaphragm valve-based modulator (DVM) which accomplished total transfer of the compounds from the $^{1}$D to the $^{2}$D. [73] The design was based on a sample loop that was closed at one end during sampling, with the head pressure on the $^{1}$D higher than the head pressure on the $^{2}$D, ensuring compression instead of diffusion of the $^{1}$D effluent into the loop.

### 1.6.2 Differential flow modulation

Seeley et al. [71] first introduced differential flow modulation (DFM) in 2000. The design and function was based upon the DVM invented by Bruckner et al. [70] Unsatisfied with poor sample transfer between $^{1}$D and $^{2}$D, Seeley devised an interface capable of transferring significantly more of the $^{1}$D effluent into the $^{2}$D column. The design utilized a 6-port diaphragm valve with a similar configuration as the aforementioned authors, but featured the addition of a sample loop, thus making use of all six valve ports. The interface was kept outside of the oven and its temperature was maintained at 125 °C by block heaters. Effluent was transferred into and out of the interface by deactivated fused silica capillaries that were connected to the $^{1}$D and $^{2}$D columns with fused silica unions. The modulator had two main stages: collection and injection. During the collection stage, effluent from the $^{1}$D entered the valve and was directed to a deactivated stainless steel sample

loop measuring 10 cm in length by 0.51 mm I.D. Effluent would collect in this loop and be vented to the atmosphere once maximum volume had been reached. During the injection stage, the valve would be actuated, allowing a secondary flow of carrier gas to enter the sample loop and effectively sweep away the collected fraction into the $^{2}$D. The flow rate in the $^{2}$D column was 20 times higher than in the $^{1}$D column in order to produce compressed injection bands and allow fast separation. For a 1 s modulation cycle, the collection stage would last 0.8 s, and the injection stage 0.2 s. This improved version of Bruckner's DVM increased transfer efficiency of the $^{1}$D effluent to the $^{2}$D column to approximately 80%. The simple design and fast actuation speeds produced pulse widths similar to those described in cryogenic modulation studies. The system proved to be robust, but was still restricted by the maximum operating temperature of the diaphragm valve. [74] High flow rates in the second column also eliminated the possibility of using microbore columns, as very high head pressures would be required. [75] Because of the temperature limitations of the diaphragm valve design, steps were taken to increase its functionality at higher temperatures. Sinha et al. established that the valve temperature limitations were due to polymeric o-rings contained within the valve. Their solution was to mount the valve in such a way as to keep the o-rings outside of the oven, while the diaphragm and sample loop were kept inside. [76, 77] With the oven programmed to

250 °C, the sample loop was found to reach 247 °C, while the portion of the valve containing the o-rings maintained a temperature of approximately 180 °C. With the diaphragm valve components exposed to effluent now capable of reaching higher temperatures, the range of compounds this interface could effectively modulate had increased to include semi-volatiles. [77]

Although differential flow modulators had been improved, flow modulators were still inapplicable to the analysis of complex samples containing higher boiling point compounds (above 200 °C). These limitations would not plague those in the field for much longer, as Bueno and Seeley were developing a novel system that would see the removal of the diaphragm valve from the flow path.

### 1.6.3 Flow-switching modulator

Recognizing that the diaphragm valve was the major detriment to the differential flow system, Bueno and Seeley [75] devised a flow-switching system that featured no valves within the GC×GC oven, and used materials capable of handling a much wider range of temperatures than the problematic valve (Figure 1-11). Attached to the exit of the primary column was a T-union (T1 in Figure 1-11) that allowed carrier gas to travel either left or right through deactivated fused silica tubing to two additional T-unions (T2 and T3 in Figure 1-11). T2 and T3 were both connected to an

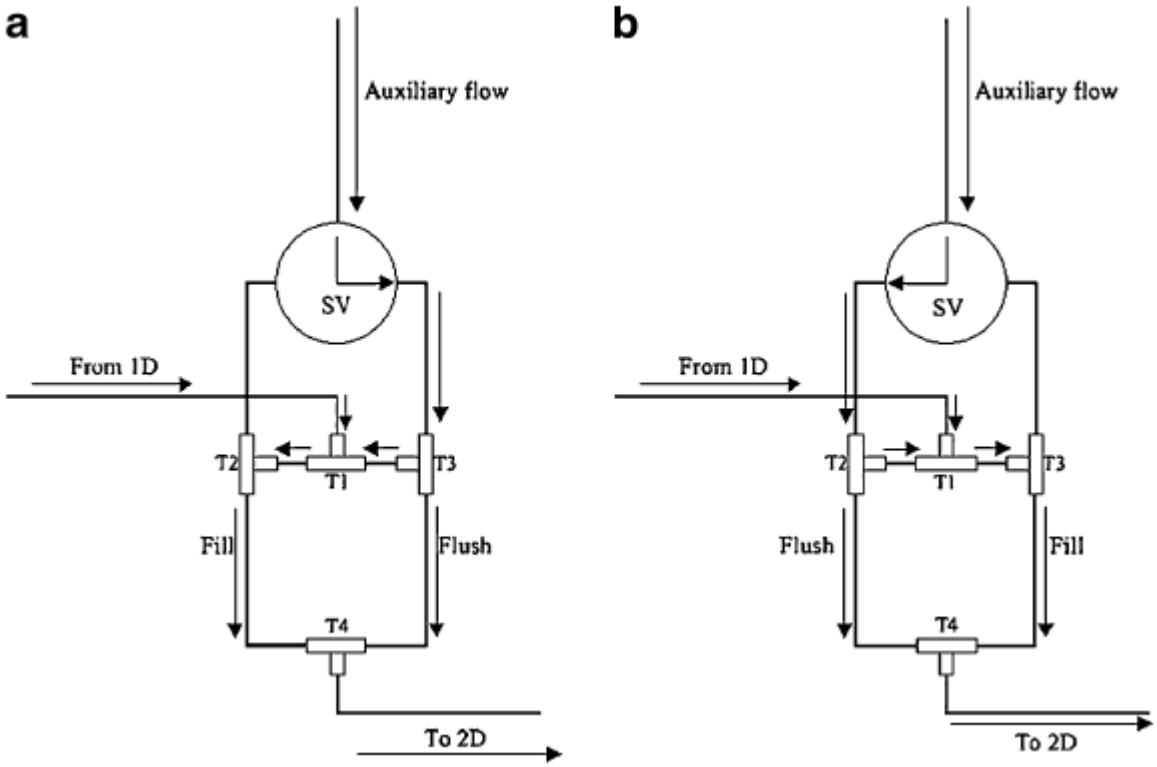


**Figure 1-11: The flow-switching modulator. (a) The capillary attached to T2 is filled with first-dimension effluent as the capillary attached to T3 is flushed to the $^{2}$D column. (b) Auxiliary flow is switched by the solenoid valve (SV) and the recently filled capillary is flushed into the $^{2}$D, allowing the alternate capillary to fill with the effluent. Arrows indicate the direction of gas flow. [Based on [78]]**

auxiliary gas supply at their top port, and to a sample loop at their bottom port. All connections between unions were made with deactivated fused silica tubing. The auxiliary gas supply was controlled by a three-port solenoid valve (SV in Figure 1-11) capable of directing gas flow to either T2 or T3. Both sample loops were connected at the bottom of the apparatus with another T-union (T4 in Figure 1-11),

whose bottom outlet was connected to the $^{2}$D. Effluent from the $^{1}$D would be directed to either the fill or the flush sample loop, depending on the direction of the auxiliary flow. This would allow one sample loop to fill with the effluent, while the other was flushed with auxiliary gas. As the sample loop reached its effluent capacity, the solenoid valve would be activated, switching flow to the opposite side of the interface, allowing the auxiliary gas to inject the contents of the recently filled sample loop into the $^{2}$D, while the now-flushed sample loop functioned as an effluent collector. The auxiliary gas flow valve would be switched at regular intervals to achieve consistent modulation throughout the chromatographic run. Differential flow was also featured in this design, with the ratio between the $^{1}$D and $^{2}$D flows fluctuating between 25 and 30 depending on the analysis. The authors successfully used the flow-switching system to analyse a mixture of VOCs, diesel fuel and aromatics in gasoline. [75, 78] Narrow injection bands were observed throughout the chromatographic run. Placement of the switching valve outside the oven and all components in contact with the effluent within the oven allowed this interface to expand its range of analytes to include less volatile species. Another advantage of this interface was the removal of a $^{1}$D effluent vent. This ensured 100% mass transfer from the $^{1}$D to the $^{2}$D, a significant improvement from the approximately 10% and 80% mass transfer of the previously introduced valve-based

modulators. [70, 79] The disadvantages of this system were mainly derived from its inflexibility. [80] Balancing gas flow rate with sample loop volume and modulation timing was a careful operation. If any single parameter was altered, the whole pneumatic system would have to be reevaluated and optimized, a rather tedious exercise. Modulation periods were also limited to around 2s, thereby forcing separations in the $^{2}$D to be very fast and perhaps not as effective as longer $^{2}$D separations.

Seeley et al. [81] later introduced an alternative form of the flow-switching modulator called the simple fluidic modulator. This interface featured $^{1}$D and $^{2}$D columns connected with two T unions, and a deactivated fused silica capillary in between (Figure 1-12). An auxiliary gas flow of 20 mL/min was introduced to the last port of the T-unions. Control of the auxiliary flow was accomplished by a three-port solenoid valve. A short segment of deactivated fused silica tubing was used to join the solenoid valve and the $^{1}$D column, whereas the $^{2}$D column was joined with a long segment. The modulator operated in two stages, fill and flush. During the fill stage, effluent from the $^{1}$D column would enter the sample loop for a desired period of time, while auxiliary gas flow moved through the $^{2}$D column T-union and into

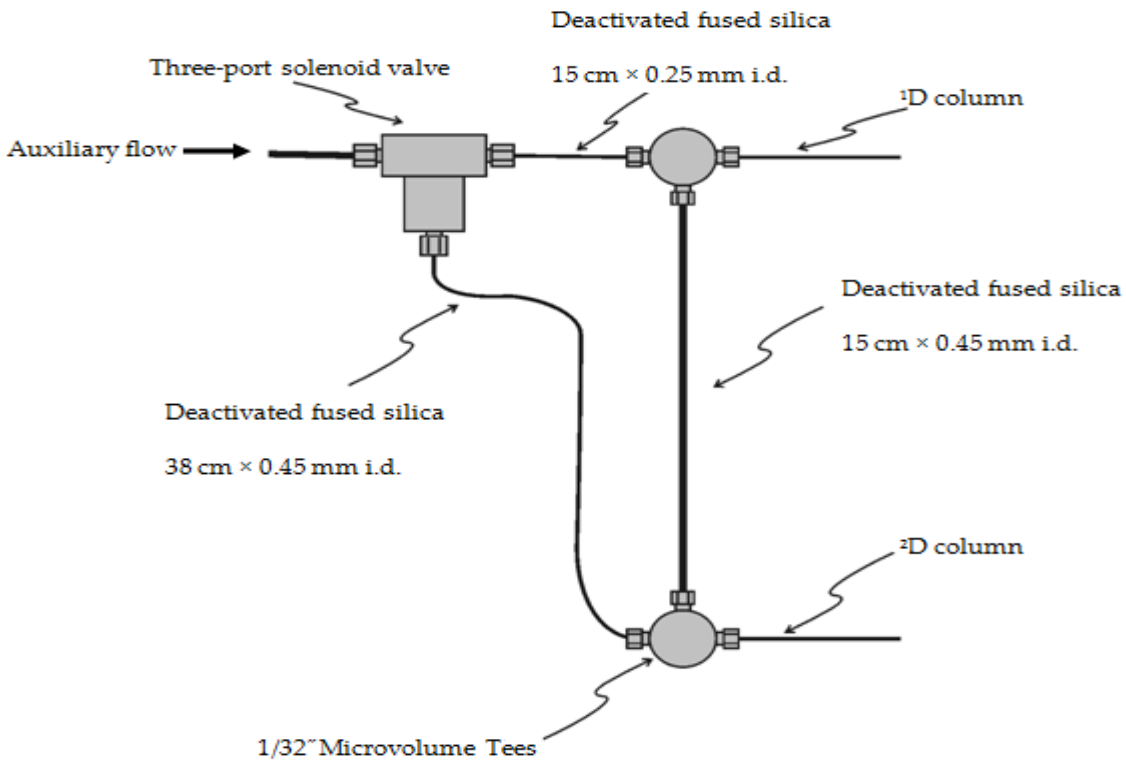


**Figure 1-12: Schematic of Seeley's fluidic modulator. [From[81]]**

the ²D column. The second stage began when the solenoid valve was actuated, forcing auxiliary gas flow in the opposite direction through the primary column T union. The significantly higher flow rate of the auxiliary gas temporarily stopped the flow of effluent from the ¹D, and quickly flushed the sample loop into the ²D. Each stage would alternate to effectively sample ¹D peaks. Seeley et al. [81] used this modulator to analyse a sample of gasoline and obtained results of the same quality as those achieved by the previously described flow-switching interfaces. In later years, this method was investigated and modified further by Poliak et al. [82, 83] to

become what is now known as the pulsed-flow modulator. In 2007, Agilent Technologies introduced a flow modulator based on Seeley's et al. design (the only commercially-available flow modulator GC×GC system), constructed using capillary flow technology (CFT). [84]

In 2008, Wang introduced a flow modulator that used two four-port rotary valves fitted with two sample loops. [85] Wang tested this device by analysing samples of naphtha, diesel, fatty acid methyl esters (FAMEs) and polychlorinated biphenyls (PCBs). [85] Performance equivalent to that of thermal modulators was observed, and 100% transfer of the effluent from the primary column to the secondary column was achieved. The valves used were capable of withstanding temperatures of up to 350 °C, allowing a wide range of analyses to be performed with this device. On the other hand, it was not clear if the modulator was effective with more modest auxiliary flows (~20 mL/min) typical for differential flow GC×GC.

## 1.7 Optimization aspects of GC×GC

The hardware setup of a GC×GC system is quite simple and can be built on any commercially available GC instrument. However, GC×GC method optimization is far more complicated than that in 1D-GC. Typically, a non-polar column is used in the $^{1}$D and a short polar column is used in the $^{2}$D. The next step is to select a

temperature program, carrier gas flow rate, and modulation period that allows all peaks to be sampled at least 2.5 – 3 times. [14, 15] In this conventional approach to optimization, the two dimensions are treated somewhat independently. Though this approach has been popular with GC×GC users for a long time, it is not a standardized procedure and the conditions do not always provide the optimum GC×GC separation. Harynuk and Górecki [86] pointed out that the outcomes of separations optimized using this non-standardized procedure often seemed far from optimal. For example, when chromatograms obtained using a 0.1 mm I.D. column in the $^{2}$D were compared with those obtained using a 0.25 mm I.D. column, the $^{2}$D peak widths for major components were often significantly larger when using the 0.1 mm column, with the remaining conditions being similar. [86] The authors attributed this to overloading of the narrow-bore column in the $^{2}$D. Therefore, it is quite obvious that GC×GC method optimization is not straightforward, which is probably one of the reasons for the still somewhat limited usage of the technique. Figure 1-13 illustrates the complex interplay between different parameters in GC×GC separations. [86] It shows for example that increasing the oven temperature programming rate causes the elution temperature of an analyte to increase, while the $^{1}$D peak width and the analysis time decrease. Increasing the inlet pressure has

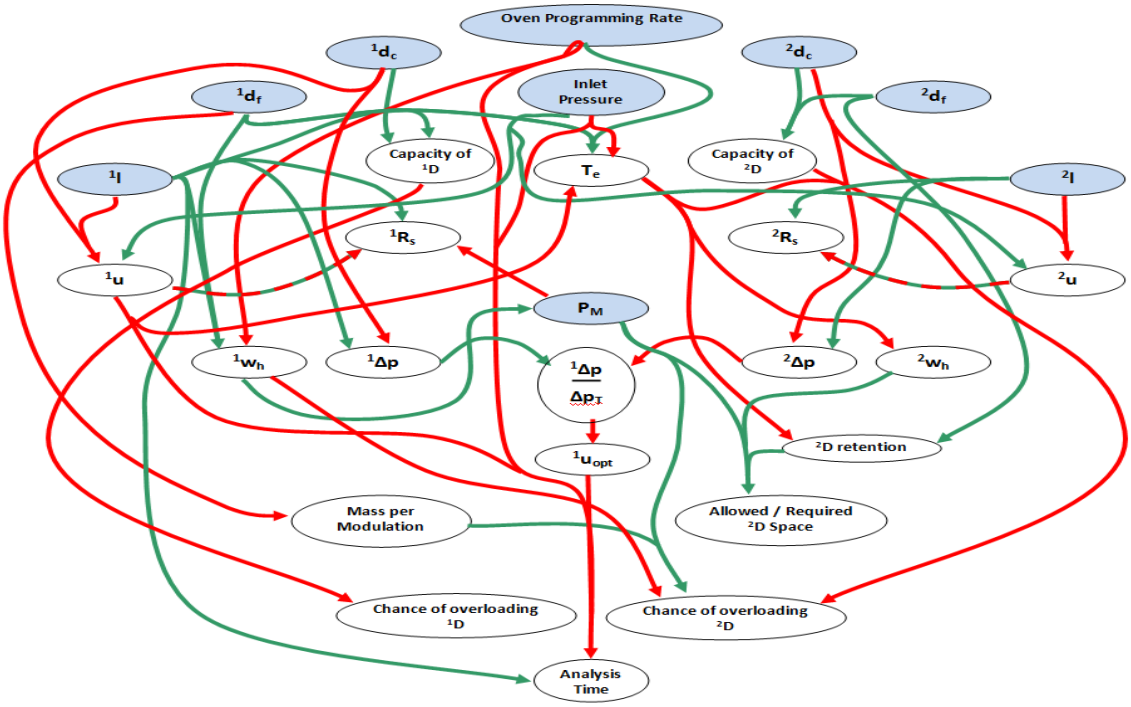


**Figure 1-13: Interplay of parameters in GC×GC separations. Individual parameters indicated by ovals, with instrumental parameters that are directly controllable by the chromatographer shown in blue. Green arrows point to parameters whose values increase as the input parameter value increases; red arrows indicate opposite influences (the value of the parameter decreases as the value of the input parameter increases), red/green dashed arrows indicate uncertain influences. The relationships shown in the diagram are valid when only one instrumental parameter is changed at a time, with the rest held constant. For example, increasing the oven temperature programming rate causes the elution temperature of an analyte to increase (as illustrated by the green arrow), while the first dimension peak width and the analysis time decrease (as illustrated by the red arrows). Increasing the inlet pressure has the opposite effect on the elution temperature (as illustrated by the red arrow), while the analysis time decreases as well (red arrow). Other relationships can be studied in a similar way.**

Symbols: $^1d_c$ : $^1$D column diameter, $^2d_c$ : $^2$D column diameter, $^1d_f$ :$^1$D column film thickness, $^2d_f$ : $^2$D column film thickness, $^1l$ :$^1$D column length, $^2l$ :$^2$D column length, $T_e$: elution temperature, $^1u$: $^1$D column linear velocity, $^2u$ : $^2$D column linear velocity, $^1w_h$: $^1$D peak width, $^2w_h$: $^2$D peak width, $^1\Delta p$: pressure drop in the $^1$D, $^2\Delta p$: pressure drop in the $^2$D, $^1\Delta p/\Delta p_T$: pressure drop in the $^1$D compared to the total pressure drop, $^1R_S$ : $^1$D resolution, $^2R_S$ : $^2$D resolution, $^1u_{opt:}$ $^1$D column optimal linear velocity. (Adapted from [86]).

the opposite effect on the elution temperature, while the analysis time decreases as well.

Method optimization in GC×GC is mainly devoted to maximizing separation power and sensitivity. The main operational conditions that must be optimized are the modulation parameters, stationary phase chemistries, column dimensions, carrier gas flow, temperature programs and detector settings.

### 1.7.1 Modulation parameters

The modulation process requires careful optimization for optimum performance. The main optimization parameters for thermal modulators are the modulation period or frequency, modulation temperature and stationary phase thickness. Flow modulators have fewer tunable modulation parameters and are generally more difficult to optimize due to their principle of operation and hardware restrictions.

### 1.7.2 Modulation period or frequency

The modulation period ($P_M$) must be sufficiently short to preserve $^1$D separation, which requires every peak eluting from $^1$D column to be sampled at least 2.5-3 times.[14, 15]

Figure 1-14 illustrates the effect of the $P_M$ on the preservation of a hypothetical $^1$D separation. $^1$D peaks with widths of 24 s are shown in A. The resolution obtained in

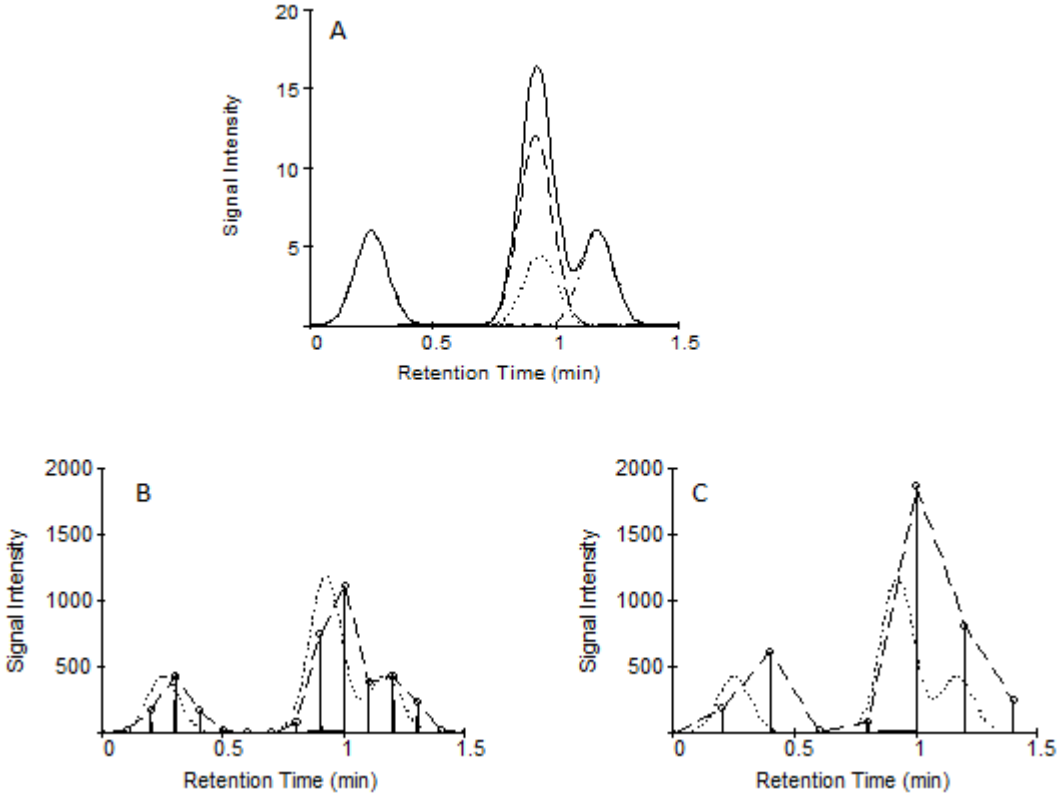


**Figure 1-14: The effect of modulation period on the preservation of the $^{1}$D separation. (A) a hypothetical $^{1}$D column separation with four components (each shown in dotted lines), each peak having a base width of 24 s. (B) injection pulses presented to the $^{2}$D column using 6 s modulation period. (C) injection pulses presented to the $^{2}$D column using 12 s modulation period. Peak widths for all injection pulses are 180 ms at the base. The original primary separation is plotted as a solid line, and magnified 72x (dotted line) in each of the panes with modulation to facilitate visual comparisons. The reconstructed primary dimension chromatogram is plotted as a dashed line. [From [12]].**

the $^{1}$D is preserved reasonably well when a modulation period of 6 s is used, as shown by the reconstructed $^{1}$D chromatogram in B. In this case, the $^{1}$D peaks are sampled up to 4 times across their profiles. With a 12 s modulation period (2 samples per peak), the partial separation between the second and third peak is lost (Figure 1-14C). [12]

Figure 1-15 shows the experimental verification of the effect of $P_M$ on the GC×GC separation of two selected polycyclic aromatic hydrocarbons (PAHs), indeno[1,2,3-c,d] pyrene (1) and dibenzo [a,h] anthracene (2). The separation was accomplished using a DB-5 × BPX-50 column combination under similar chromatographic conditions, but using different modulation periods. A quad-jet dual-stage modulator

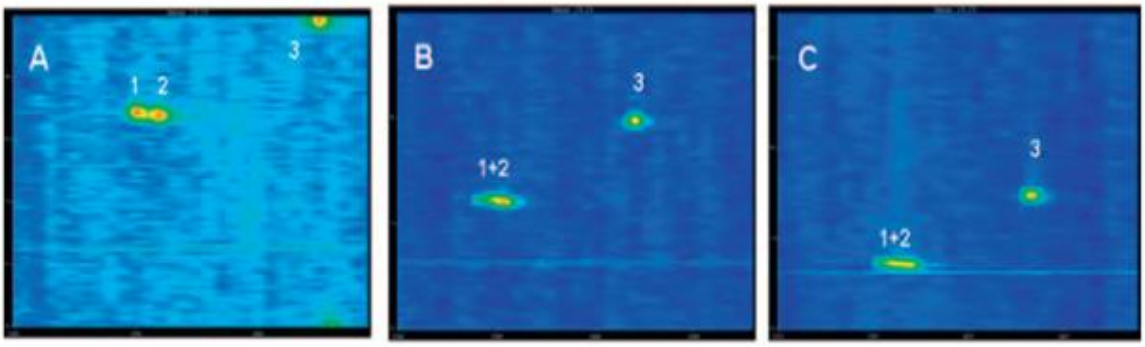


**Figure 1-15: Reconstructed GC×GC – TOF MS contour plots (m/z 276 + 278) obtained for (1) indeno[1,2,3 – cd]pyrene, (2) dibenzo[a,h]anthracene, and (3) benzo[ghi]perylene using a $P_M$ of (A) 5 s, (B) 6 S, and (C) 7 s. All other experimental parameters were kept constant throughout the study. [From [87]].**

was used with a hot jet pulse of 600 ms in all instances. [87] As shown in Figure 1-15A, both analytes had the same retention times on the $^{2}$D column; however, they were separated to some extent on the $^{1}$D column. The separation of the two compounds was well preserved using a modulation period of 5 s (four modulations per $^{1}$D peak), as the two compounds yielded two separate spots. The separation deteriorated somewhat when using a modulation period of 6 s (Figure 1-15B), and was lost completely with a modulation period of 7 s (Figure 1-15C).

The major drawback of shortening the modulation period is the potential "wraparound" of analytes that are strongly retained in the second dimension. Wraparound occurs when the $^{2}$D retention of an analyte becomes longer than the modulation period, which causes some or all of this analyte to elute during the successive modulation cycle(s). This disturbs the structure of the chromatogram and might make its interpretation difficult. An example of a partially wrapped around peak is shown in Figure 1-15A (analyte 3). Wraparound is problematic, especially when it leads to coelutions with analytes eluting in the following modulation cycle(s). It should be noted, however, that wraparound might be acceptable as long as peaks wrap around into the empty region of the separation space below the dead time, in which case they do not disturb the structure of the 2D chromatogram.

Modern flow modulators (differential flow modulators) [71, 82, 83] present a different set of challenges. These devices are gaining in popularity due to their relatively low cost. These systems typically utilize a modulation period of around 2 s and extremely high flow rate in the $^{2}$D column (20 – 30 ml/min). Needless to say, the optimization of this system can be rather complicated. [88] Variation of the modulation period can be accomplished, but only by varying the flow of the carrier gas in the $^{1}$D column. This is due to the fixed volume of the effluent collection channel(s). Carrier gas flow from the modulation valve must remain very fast to produce an analyte plug in the $^{2}$D column of appropriately small width, as well as to ensure that all analytes exit the $^{2}$D column quickly. When optimized, this style of modulation has been shown to perform similarly to cryogenic systems. [89] However, the inability of this system to be easily paired with mass spectrometry presents a significant obstacle if compound identification is required.

### 1.7.3 Modulation temperature

To accomplish effective thermal modulation, the modulator must generate sharp and symmetrical injection bands at the head of the $^{2}$D column for all analytes. Cooling-based modulators trap volatile compounds through cooling of a region of a column placed in the trap using various cooling mechanisms. On the other hand,

heater-based modulators trap and focus the analytes in a thick film of stationary phase at ambient or GC oven temperature (phase-ratio focusing). This increases the component retention factor ($k$) and retards its travel. [35] Desorption is accomplished in both cases by application of high temperature to rapidly flush the focused zone out of the modulator region and deliver it to the $^{2}$D column. Therefore, trapping and desorption temperature control is important to get effective modulation.

#### 1.7.3.1 Thermal modulators

##### *1.7.3.1.1 Cryogen-free modulators*

Since trapping at GC oven temperature limits the range of analyte volatilities and does not work effectively for highly volatile compounds, trapping at lower temperatures has been explored in recent years. [54, 65, 90]

Górecki et al. described a new, consumable-free dual stage thermal modulator based on a modified Silcosteel capillary, [54] described in section 1.5.1. Compared to earlier attempts at using stainless steel capillaries for thermal modulation, the authors were able to dramatically improve the capabilities of the device through optimization in several key areas. To eliminate the effect of potential cold spots within the trap, stationary phase coating within the capillary was selectively removed to yield two small lengths of coating within each of the two trapping

stages. The volatility range of the analytes could be adjusted by using stationary phases of different thicknesses, with the 1μm thick phase offering the widest range. Application of a Vortex cooler capable of supplying air at temperatures as low as -20 °C allowed trapping of volatile analytes and reduced the cooling times of the modulator. Temperature programming of the cooling air was accomplished by routing the Vortex cooler air supply lines through the GC oven. This allowed the modulator temperature to increase as the oven temperature increased. The most recent optimization made to this system has been the switch from dual stage to single stage modulation.

#### *1.7.3.1.2 Cryogenic modulators*

##### *1.7.3.1.2.1 Longitudinally modulated cryogenic system*

The LMCS interface was discussed before. Even though trapping temperatures in the LMCS were much lower than with heater-based modulators, very volatile compounds (~ $C_3$-$C_4$ range) still could not be trapped efficiently with this device. Conversely, excessively low trapping temperatures might retard analyte desorption, especially with high-boiling point analytes. This issue may be solved by optimization of modulation parameters such as the trap temperature, desorption time, and/or stationary phase thickness. [91]

As the trap temperature had a major influence on the $^{2}$D peak profiles, the design of the LMCS was further improved to feature more efficient cryogenic trap temperature control. [91] The optimum peak widths in both dimensions were obtained when the temperature difference between the trap and the oven ($\Delta T$) was ~70 °C . When $\Delta T$ was small (~ 20 °C), the analytes were not effectively trapped. However, when the trap temperature was too low ($\Delta T$ = 130 - 220 °C), the analytes were not completely desorbed and they were released from the trap during subsequent modulation cycles. As a result, both the $^{1}$D retention times and peak widths increased. [91]

***1.7.3.1.2.2 Gas jet cryogenic modulators***

Temperature is used in all cryogenic modulators with gas jet design [32, 92, 93] to perform three main functions for modulation: [94] (1) efficient trapping and focusing of the $^{1}$D effluent; (2) rapid release and injection of the trapped bands onto the $^{2}$D column, and (3) rapid return to trapping conditions. The cold region temperature must be low enough to trap and focus the analyte bands. At the same time, it should not be excessively low, as this increases coolant consumption and might retard analyte band desorption. [91] Once the analyte bands are trapped, the cold region must then be heated rapidly to a temperature permitting remobilization of the trapped

bands (i.e. trapped compounds should have a retention factor on the trapping capillary of zero). [94]

The first modulator of this type was reported in 2000 by Ledford, [59] which was discussed in detail earlier in the text. In this type of device, modulation occurs in a segment of the $^{2}$D column. Trapping in the stationary phase might result in problems such as pre-separation of the analytes in the trap due to different times required to desorb the analytes from the stationary phase, which changes with changing modulator temperature. In addition, modulator temperature offset (the difference between the hot jet temperature and the oven temperature) might affect the $^{2}$D retention times because part of the $^{2}$D column is enclosed within the modulator assembly. Consequently, the modulator temperature offset affects the average $^{2}$D column temperature, which in turn affects $^{2}$D retention times. This is illustrated in the contour chromatograms in Figure 1-16. [95] A modulator offset of 80 °C relative to the $^{1}$D column in Figure 1-16D caused a change not only in the peak shapes, but also in the $^{2}$D retention times. Most importantly, relative retention of some analytes was also affected.

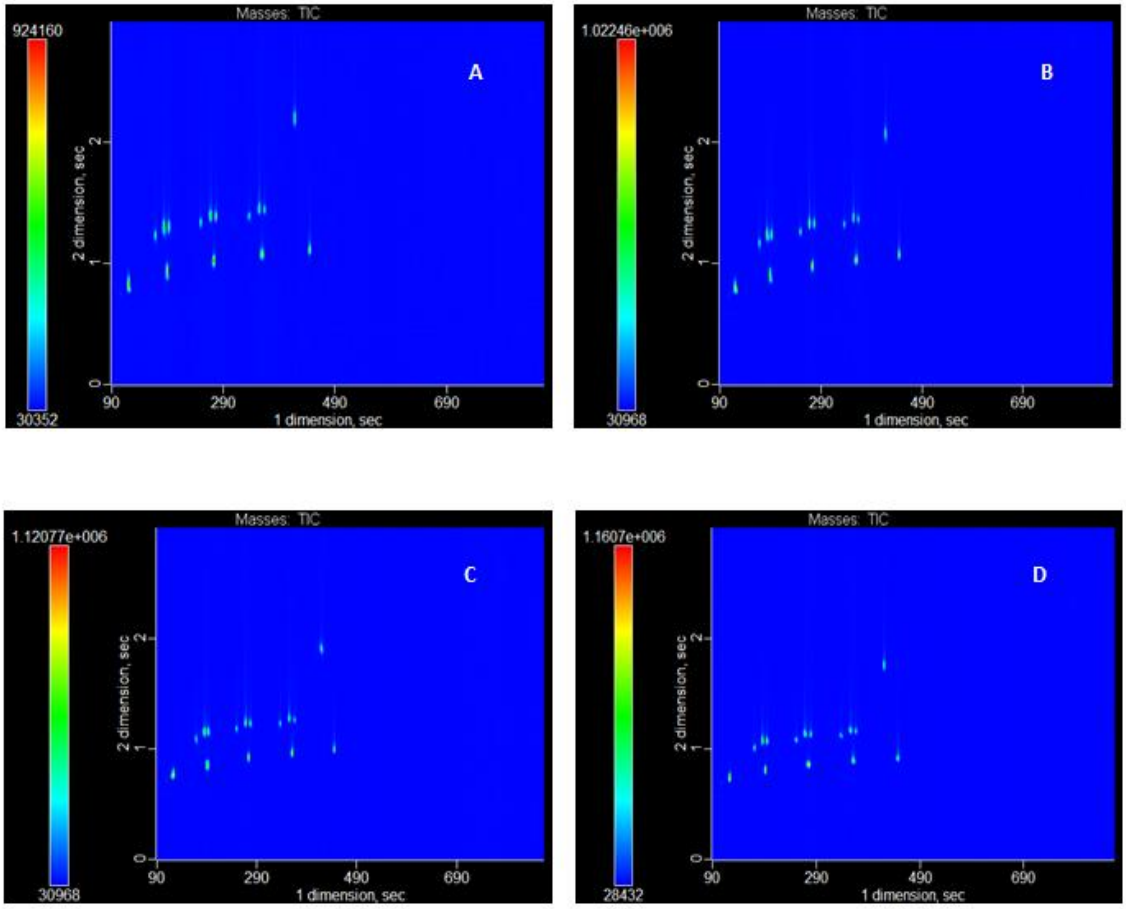


**Figure 1-16: GC × GC contour plot chromatograms of Dimandja mixture using different modulator temperature offsets relative to the primary oven A: 10° C, B: 12° C, C: 40° C and D: 80° C. [From [95]]**

*1.7.3.1.2.3 Gas jet cryogenic modulators with a delay loop*

The temperature requirements of this type of modulators were investigated in details by Gaines and Frysinger. [94] The authors found that the cold spot had to be 120 to 140 °C colder than the elution temperature to achieve efficient trapping. This temperature differential could be easily achieved when using liquid nitrogen ($LN_2$) as the coolant in the heat exchanger Dewar, allowing compounds from $C_4$ to $C_{40}$ to be properly modulated. As the number of carbon atoms increased from $C_4$ to $C_{40}$, the $LN_2$ flow required for optimum modulation had to be decreased from 15.5 to 1.5 standard L/min (SLPM). When other coolants were used in the heat exchanger Dewar, such as ice water at 0.4 °C, only compounds from the $C_{18}$ to $C_{40}$ range were properly trapped. When room temperature air at 20.7 °C was used as the coolant, compounds from $C_{20}$ to $C_{40}$ were properly trapped. Desorption temperatures approximately 40 °C above the elution temperature were sufficient to provide effective reinjection onto the $^2$D column. When the trapping temperature was too low, the hot jet was incapable of reinjecting the trapped analyte bands effectively. This is illustrated in Figure 1-17, which shows the $C_{24}$ to $C_{36}$ part of GC×GC separation of two crude oil samples under otherwise identical conditions except the cold jet flow. A constant cold jet flow of 17.0 SPLM was used in (a), and

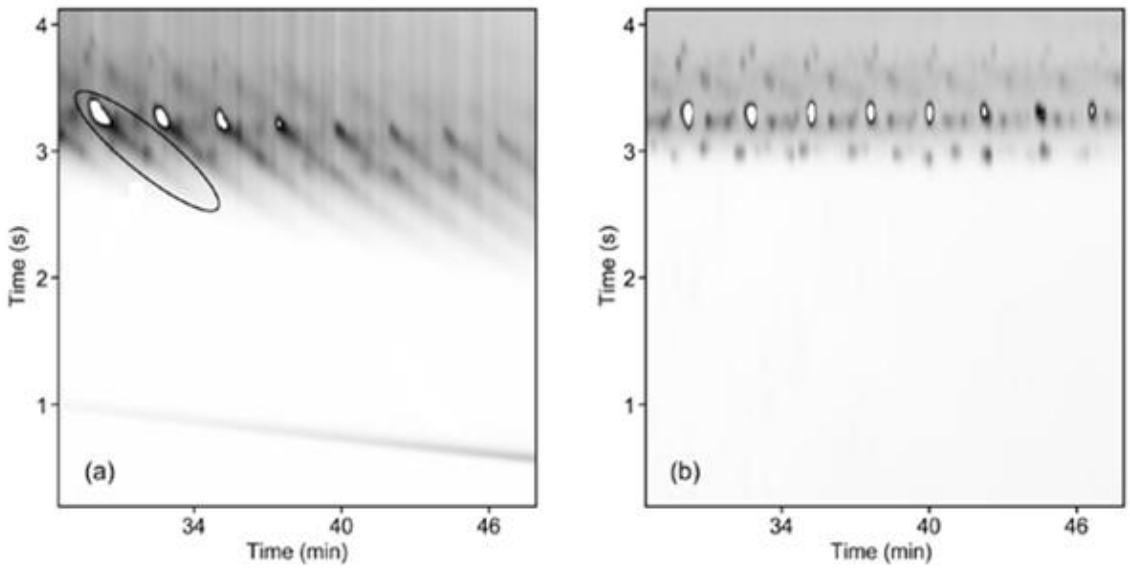


**Figure 1-17: The $C_{24}$ – $C_{36}$ portion of a crude oil GC × GC chromatogram showing effect of excessive cold jet flow on modulation. (a) constant 17.0 SLPM cold jet flow, and (b) programmed cold jet flow. [From [94]].**

programmed flow in (b). Under high cooling gas flow conditions (a), the trapping temperature was too low and analyte bands were not desorbed efficiently, generating broad and tailing peaks. Under programmed coolant flow, the trapping temperature was higher, thus the hot jet was able to reinject the trapped bands more effectively, producing narrow peaks.

Another parameter that needs to be optimized carefully for this kind of modulators is the length of the delay loop. The typical length of the loop is approximately 1 m. [25] If the loop is too short, the band travelling through the delay loop might not reach the second trapping spot at a time when it is cold, and may

therefore not be refocused, allowing breakthrough to occur. Conversely, if the loop is too long, multiple injections from the first cold spot could be present within the loop simultaneously. This increases the probability of running into breakthrough problems when the modulation period is changed, and can even cause an increase of the apparent primary retention times, which could be problematic for the identification of the components of complex mixtures. [96] Overall, it should be kept in mind that the length of the loop might need to be adjusted every time the GC×GC parameters (especially carrier gas flow rate and modulation period) are changed. A model for GC×GC systems using a loop modulator was developed to determine the optimum length of the loop capillary. [96]

### 1.7.4 Column combinations

Although the modulator is the key to successful GC×GC separations, the chromatographic columns play the most significant role in any GC separation. Simply installing the modulator between two columns does not guarantee a good GC×GC separation. Consequently, column combination optimization, including stationary phase chemistry, column dimensions and film thickness, is required to accomplish efficient GC×GC separation.

### 1.7.4.1 Stationary phase chemistry

The most important aim of an optimized GC×GC separation is the maximum use of the 2D separation space. The structured order separation is important only when analyzing samples that contain structurally related compounds such as homologues or isomers (e.g. petrochemical or FAME samples). Nevertheless, many of the published GC×GC chromatograms showed low exploitation of the separation space. For example, Figure 1-18A illustrates GC×GC chromatogram of the cod oil FAMEs. Even though the chromatogram is well structured, only 22.3% of the entire 2D space is used. [97] According to the authors of this contribution, this could be due to two main reasons: (1) partial correlation between the two dimensions, (2) non-optimized $^{2}$D column conditions. Therefore, GC×GC stationary phase optimization is required to achieve an effective separation, in particular for highly complex samples. Unfortunately, in most cases optimal column combinations are still decided through trial-and-error testing. The majority of applications in GC×GC have used a non-polar $^{1}$D column (100% dimethyl polysiloxane or 5% diphenyl/95% dimethyl polysiloxane) connected to a more polar $^{2}$D column (e.g. polyethylene glycol, 50% phenyl/50% methyl polysiloxane, etc.). [18, 98] With such column combinations, analytes are separated primarily according to their vapor pressures in $^{1}$D (especially the non-polar ones), and according to their polarity in $^{2}$D. This means that two

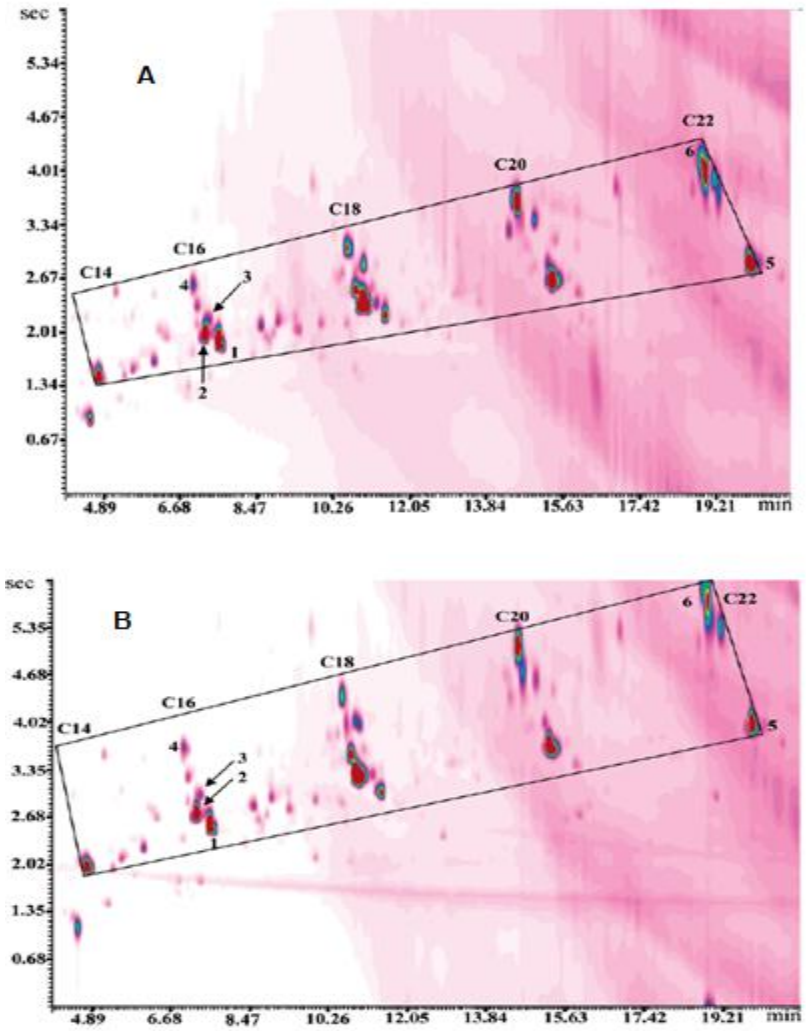


**Figure 1-18: Conventional GC×GC chromatogram of cod liver oil FAMEs (A) and Split flow GC×GC chromatogram of cod liver oil FAMEs (B) (See later in the text). [From [97]].**

different separation mechanisms are involved (i.e. orthogonality). There are, however, numerous applications in which the columns are used in the reverse order, i.e. a more polar column in $^{1}$D and a less polar one in $^{2}$D (e.g. [99-102]). The higher is the orthogonality between the $^{1}$D and $^{2}$D columns, the better is the separation. [63, 103] It should be emphasized that orthogonality is not a goal in itself. The success or failure of any separation is always decided by sufficient separation of the target analytes. In the past over twenty years, dozens of GC×GC stationary phase combinations have been evaluated. Representative examples of the combinations are presented in Table 1-1.

Ryan et al. [104] studied how selectivity tuning of the $^{1}$D column polarity affected the separation achieved. This study was mainly aimed at predicting GC×GC peak positions in the 2D separation space. The $^{1}$D column polarity was systematically varied by combining different lengths of polar and low polarity columns while keeping the total column length constant. The resulting $^{1}$D column was then coupled to both polar and non-polar $^{2}$D columns. Figure 1-19 and Figure 1-20 show the GC×GC 2D contour plots of a 17-component standard mixture obtained from coupling of columns A-E (Table 1-2) with the polar polyethylene glycol phase and low-polarity 5% phenyl methyl polysilphenylene siloxane phase $^{2}$D columns, BP20

**Table 1-1: Representative examples of GC×GC column combinations**

| $^{1}$D (length m × I.D. μm) | $^{2}$D (length m × I.D. μm) | Analyte/sample | Reference examples |
|---|---|---|---|
| Poly(ethylene glycol) (21 m × 250 μm) | 100% Polydimethylsiloxane (PDMS) (1 m × 100 μm) | A hydrocarbon mixture and a coal liquids sample | [9] |
| (SolGel + poly(ethylene glycol)) composite phase (SolGel-WAX (30 m × 250 μm) | 5% Phenyl polysilphenylene siloxane (1 m × 100 μm) | Roasted coffee bean volatiles | [105] |
| Poly(ethylene glycol) (30 m × 250 μm) | 5% Phenyl polysilphenylene siloxane (1 m × 100 μm) | Lipids and roasted coffee bean volatiles | [106, 107] |
| Polyethylene glycol (TPA-treated) (30 m × 250 μm) | 35% Phenyl-polysilphenylenesiloxane (1 m × 100 μm) | Food analysis | [108] |
| (5%-Phenyl)(1%-Vinyl)-methylpolysiloxane (2 m × 100 μm) | 14% Cyanopropylphenyl) methylpolysiloxane (0.5 m × 100 μm) | Test mixtures | [18, 109] |
| 100% PDMS (30 m × 250 μm) | (SolGel + Poly(ethylene glycol)) composite phase (SolGel-WAX (1.5 m × 250 μm) | Volatile components of Pinotage wines | [98] |
| 100% PDMS (50 m × 530 μm) | 50% Phenyl-polysilphenylene siloxane (2.2 m × 150 μm) | Volatile organic compounds in urban air | [110] |
| 100% Cyclodextrin directly bonded to PDMS (10 m × 100 μm) | (50% Liquid crystal / 50% dimethyl) siloxane column (1 m × 100 μm) | PCBs in environmental samples | [111] |
| 100% PDMS (1 m × 100 μm) | 14% Cyanopropylphenyl) methylpolysiloxane (2 m × 100 μm) | Essential oils | [112] |
| Polyethylene glycol (60 m × 250 μm) | (14%-Cyanopropyl-phenyl)-methylpolysiloxane (3 m × 100 μm) | Cigarette smoke condensates | [10, 113, 114] |

| | | | |
|---|---|---|---|
| Poly(5%-phenyl–95%-methyl)siloxane phase (40 m × 100 μm) | 1,12-Di (tripropylphosphonium) dodecane bis (trifluoromethanesulfonyl)<br><br>imide (3 m × 100 μm) | PCBs | [115] |
| Poly(methyltrifluoropropyl siloxane) (30 m × 250 μm) | Poly(dimethyldiphenylsiloxane) (5 m × 250 μm) | Trace biodiesel in petroleum-based fuel | [116] |

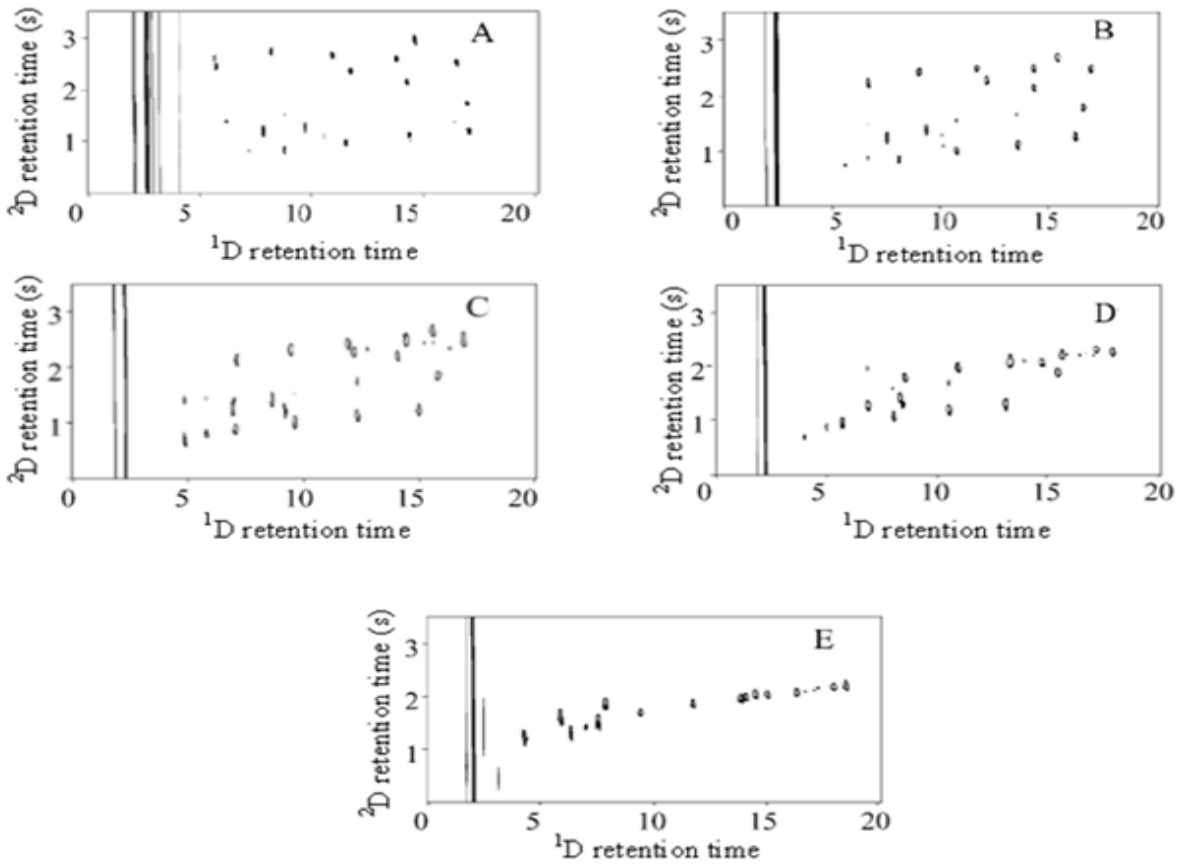


**Figure 1-19: 2D contour plots for different $^1$D columns coupled with a BP20 $^2$D column. Parts (A – E) correspond to column designation according to $^1$D columns shown in Table 1-2. [From [104]].**

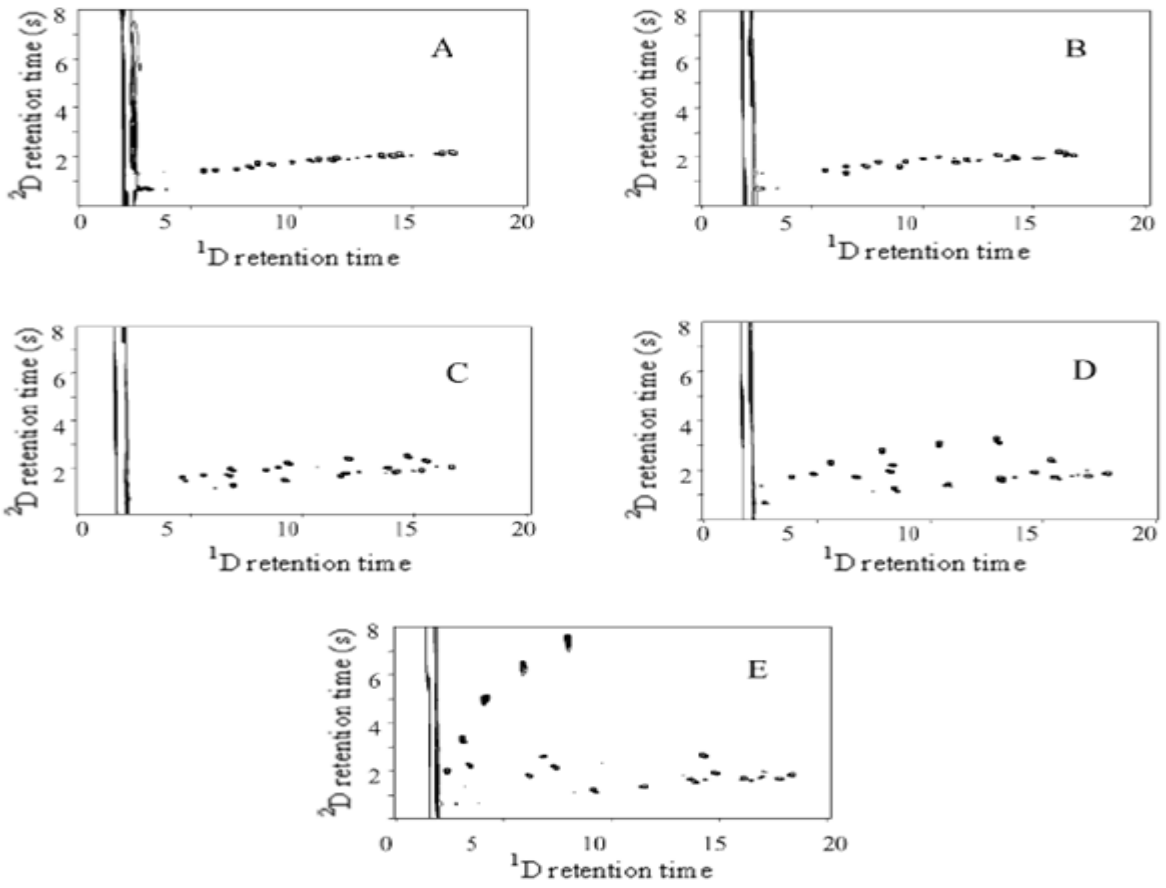


**Figure 1-20: 2D contour plots for different [1]D columns coupled with a BPX5 [2]D column. Parts (A – E) correspond to column designation according to [1]D columns shown in Table 1-2. [From [104]].**

**Table 1-2: Combined-polarity columns used in the $^{1}D$** [104]

| $^{1}D$ | Length of BPX5 column* | Length of BP20 column* |
|---|---|---|
| A | 20 | 0 |
| B | 15 | 5 |
| C | 10 | 10 |
| D | 5 | 15 |
| E | 0 | 20 |

* each column is 0.25 mm I.D. and 0.25 μm $d_f$.

and BPX5, respectively. Maximal use of the 2D separation space was achieved when the two columns were most disparate (Figure 1-19A and Figure 1-20E). As the polarity of the $^{1}D$ column approached that of the $^{2}D$ column, the separation space utilization was significantly reduced (see Figure 1-19) until nearly all analytes were arranged diagonally in the separation space (Figure 1-19E), indicating almost complete lack of two-dimensional separation. This occurred when the $^{1}D$ column was 100% BP20, i.e. the same as the $^{2}D$ column. The same result was obtained when a 100% BPX5 column A was coupled to the same column in the second dimension (Figure 1-20A). A similar study was performed by Cordero et al., but in that case the influence of selectivity tuning of the $^{2}D$ column on the GC×GC separation was studied. [102, 104] The results showed that using a non-polar stationary phase in the $^{1}D$ provided the most orthogonal systems. Using a polar stationary phase in $^{1}D$ tends to

decrease the separation space even when a correct orthogonal phase is used in $^{2}$D. [102, 104]

Ionic liquids (ILs) stationary phases can be tailored to have different degrees of polarity. They have the following characteristics: (1) high affinity towards dipolar solutes and solutes that can serve as hydrogen bond acids, [117] (2) unique selectivity towards non-polar solutes such as alkanes and alkenes, similar to low-polarity stationary phases such as dimethylsiloxanes, [118, 119] and (3) high temperature stability (for example, partially cross linked ILs can withstand up to 350 °C, [119] compared to majority of conventional polar stationary phases which cannot be used above 280 °C). Seeley et al. [120] used a high-temperature phosphonium IL column in $^{1}$D in combination with a conventional non-polar (5% diphenyl / 95% dimethyl siloxane) $^{2}$D column. The selectivity of IL column was compared with selectivities of polyethylene glycol and 50% phenyl / 50% methyl polysiloxane. The IL stationary phase tested showed strong interactions with hydrogen bonding and dipolar compounds. In addition, it displayed a unique selectivity towards low polarity hydrocarbons such as acyclic and cyclic alkanes and monounsaturated alkenes. In another study, a triflate (trifluoromethylsolfonate) IL column was used in the $^{2}$D of a non-polar × IL setup, and evaluated in the separation of 32 compounds exemplifying

varying chemical properties. [121] In particular, focus was placed on the separation of four phosphorus-oxygen containing compounds found in the 32 compound mixture. The performance of this setup was compared to a setup containing a conventional polyethylene glycol column in the $^{2}$D. The authors found the triflate IL column demonstrated superior selectivity towards phosphorus-oxygen containing compounds compared to the polyethylene column.

#### *1.7.4.1.1 Predictive modeling for GC×GC separation and stationary phase selectivity optimization*

Without a mathematical model, both the separation optimization and the selection of optimal stationary phases can be very time consuming. Therefore, a good predictive model for a range of analytes on a range of stationary phases would greatly increase the ease of the optimization process. Some researchers tried to develop predictive modeling to help optimize GC×GC separations and stationary phases selectivity. Some of these models were based on either Kovats indices [122, 123] or on the calculation of retention indices based on GC×GC retention data. [124] Dorman and coworkers developed a computer model to predict and optimize separations for GC×GC. [125] Their approach used calculated thermodynamic retention indices. The model simulates GC×GC separations as a function of the many variables involved. Adjusted retention time of each analyte on each stationary phase under two

different temperature programs is used as the input data. The model can then optimize variables for GC×GC separations.

Recently, Harynuk et al. developed a thermodynamic parameter model to predict retention times of compounds on different stationary phases and in different carrier gases. [126, 127] The authors mentioned that if the thermodynamics can be modeled precisely, then the retention time of an analyte can be predicted directly, independently of the operating conditions. In practice, though, properties such as the retention index can vary with temperature and temperature programming rate. Seeley et al. developed a solvation parameter model [128] to predict relative retention of compounds in GC×GC chromatograms. Most recently, the same group used that model to screen 50 stationary phases to find the best GC×GC stationary phase combination that allows organic esters such as FAMEs to be fully separated from petroleum hydrocarbons. [116] The model was able to correctly predict that poly(methyltrifluoropropyl siloxane) (fairly polar) in combination with poly(dimethyldiphenylsiloxane) (semi-polar) allowed full separation of FAMEs from the hydrocarbons. The interesting finding of this study is that this stationary phase combination goes against the "conventional wisdom" that the best GC×GC separations are obtained when polarity difference between the two dimensions is

maximized. The authors concluded that it is better to choose stationary phases that can best exploit the solubility characteristics differences of the analytes and the sample matrix.

### 1.7.4.2 Column dimensions

The typical dimensions of the $^{1}$D and $^{2}$D columns were mentioned before. Adahchour et al. reported the use of a 0.5 m × 0.05 mm I.D. column with a film thickness of 0.05 μm in the $^{2}$D instead of the more usual 0.1 mm I.D. columns with film thickness of 0.1 μm. [129] The design provided ultra-fast $^{2}$D separation, i.e. the analysis time was reduced by more than three-fold without sacrificing resolution. However, the column was very prone to overloading, and such columns are not easily available.

In theory, short, narrow bore columns with thin films of stationary phase should always provide the most efficient separation. In GC×GC, however, problems arise when the $^{2}$D column becomes overloaded, [130] as discussed earlier in section 1.7. Harynuk et al. studied the effect of the $^{1}$D column film thickness on the GC×GC separation. [131] Four 30 m × 0.25 mm non-polar $^{1}$D columns with film thicknesses of 0.1, 0.25, 0.5 and 1 μm were tested. Two polar columns (1 m × 0.1 mm × 0.1 μm $d_f$ and 1 m × 0.25 mm × 0.15 μm $d_f$) were used as the $^{2}$D columns. The authors

concluded that when speed of the separation is prioritized over high resolution, thin-film $^{1}$D columns and narrow-bore $^{2}$D columns might be optimal. However, when high resolution is desired, thicker film (i.e. 0.25 or 0.5 μm) $^{1}$D columns and larger diameter (i.e. 150 μm I.D.) $^{2}$D columns could be a better combination. [131]

#### 1.7.4.3 Carrier gas linear velocities

The majority of GC×GC separations in the literature are derived from previously optimized 1D-GC methods, especially with respect to the carrier gas flow rates. However, when the internal diameter of the $^{2}$D column is smaller than that of the $^{1}$D column, carrier gas pressure in the latter is considerably higher than in 1D-GC separations. As a result, the diffusion coefficients, and consequently the optimum velocity in the $^{1}$D column are far lower than in 1D-GC. Beens et al. [132] illustrated this in 2005 and developed software to assist in the optimization of carrier gas flow rates and column dimensions selection. The software developed was used to calculate the separation parameters of different GC×GC sets of column dimensions (15 m × 0.25 mm I.D. × 0.25 μm) × (1.5 m × 0.1 mm I.D. × 0.1 μm). From the results dipected in Figure 1-21, it can be concluded that: (1) the optima for both columns are at widely different linear velocities, (2) the optimum of the $^{1}$D column is at a relatively low

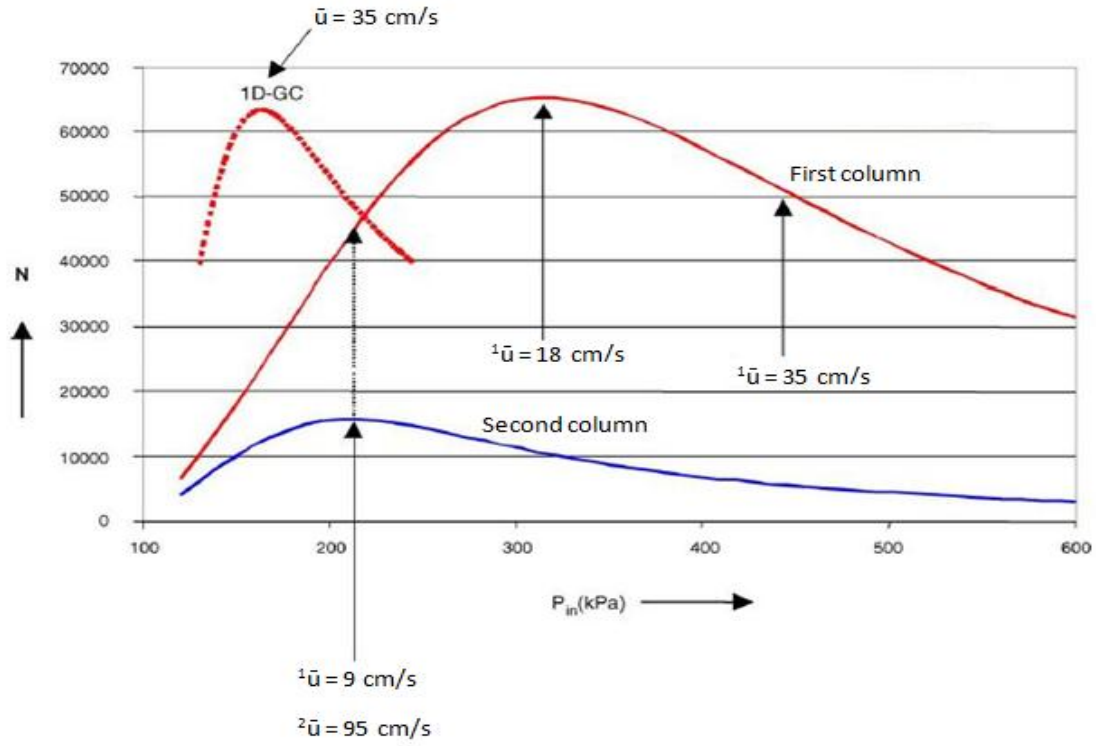


**Figure 1-21: Plate number (N) versus inlet pressure ($P_{in}$) for (15 m × 0.25 mm × 0.25 μm) × (1.5 m × 0.1 mm × 0.1 μm) columns. The dotted line is the curve for the first column when used as a 1D-GC column [From [132] ].**

linear velocity. Therefore a compromise has to be found for an optimum use of the GC×GC separation power. One approach is to operate the $^{1}$D at its optimum; however, the cost is lower plate number of the $^{2}$D column, albeit with the necessary speed. On the other hand, if one prefers to operate the $^{2}$D column at its optimum, the cost is not only low $^{1}$D plate number, but also a long analysis time. The authors concluded that it is advisable to operate both $^{1}$D and $^{2}$D columns close to their optimum flow rates, which can be achieved by using two columns with the same

internal diameter. Based on both this study and the Harynuk et al. [133] study of overloading mentioned in Section 1.7, the use of narrow-bore $^{2}$D columns might be far from optimal unless special precautions are taken, as described later in this section.

Tranchida et al. in 2007 [97] presented various options for carrier gas velocity optimization in GC×GC: (1) to reduce the head pressure, thus the linear velocities in both dimensions; this causes retention times to increase, $^{1}$D resolution to decrease and elution temperatures to increase; (2) to use a longer $^{2}$D column; this increases the $^{2}$D retention times and leads to degradation of the separation obtained in the $^{1}$D column because of the need to use longer modulation periods; and (3) to use a wider-bore (0.15 - 0.18 mm I.D.) $^{2}$D column; this might enable the operation of both dimensions under near-optimal velocities. An alternative option described in detail by the authors was the use of a flow splitter prior to the modulator, which can be called "split flow" GC×GC. The idea of splitting the flow was originally used by Phillips, [9, 44] where a T-union was used to connect the two analytical columns, thus enabling the diversion of about a third of the $^{1}$D column flow. The split flow GC×GC system by Tranchida et al. (Figure 1-22) enabled independent adjustment of the carrier gas linear velocities in both dimensions. A 30 m × 0.25 mm I.D. $^{1}$D column

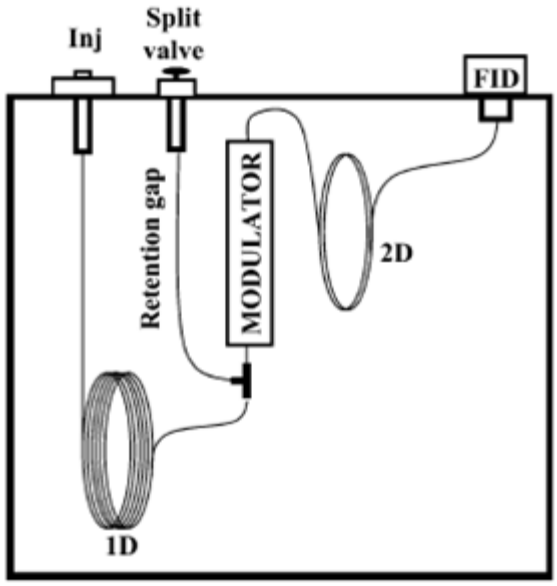


**Figure 1-22: Scheme of the split flow GC×GC setup developed by Tranchida et al. [From [97]].**

was connected to a 1 m × 0.10 mm I.D. $^{2}$D column and a 0.3 m × 0.10 mm I.D. uncoated capillary segment through a Y press fit. [97] The $^{2}$D column was passed through the cryogenic modulator, while the uncoated capillary was connected to a manual split valve. This design enabled optimization of the $^{2}$D gas flow simply by adjusting the split valve. The design was tested in the analysis of cod liver oil FAMEs and the results were compared to the results obtained from a conventional GC×GC system under the same temperature program and at an average $^{1}$D linear velocity of ~ 35 cm/s. Figure 1-18A illustrates the conventional GC×GC chromatogram obtained when the split valve was closed. The authors calculated the

$^{1}$D and $^{2}$D columns linear velocities as 35.3 and 333.2 cm/s, respectively, which was close to optimum in the $^{1}$D and far from optimum in the $^{2}$D. Although the chromatogram was well-structured (the $C_{14}$ – $C_{22}$ group-type patterns are evident), there was a large unexploited 2D space. The width of the $C_{16}$ group along the y-axis (i.e. the difference between the first and last-eluting peaks, 1 and 4) was 0.688 s, while the $C_{22}$ group width was 1.176 s. Meanwhile, there was partial coelution of peaks 2 and 3. By adjusting the split valve, the $^{2}$D linear velocity could be regulated and linear velocities of 35.4 and 213.5 cm/s were obtained for $^{1}$D and $^{2}$D, respectively. The GC×GC chromatogram obtained from this application is shown in Figure 1-18B. The structure of the chromatogram was maintained, while the $C_{16}$ and $C_{22}$ groups widths increased to 1.104 s (+60%) and 1.728 s (+47%), respectively. In addition, peaks 2 and 3 were well separated (Figure 1-23) and the occupied separation space in the chromatogram increased from ~22.3% to ~32%. The same group used split flow GC×GC design for the optimization of $^{2}$D separation using a 50 μm column in $^{2}$D and a twin-oven for the analysis of some complex samples such as roasted Arabica coffee volatiles [134] and a diesel sample. [135]

Another approach to optimized linear velocities in both dimensions was based on stop-flow GC×GC, [63, 64] discussed earlier in the text. In this design, the flow was

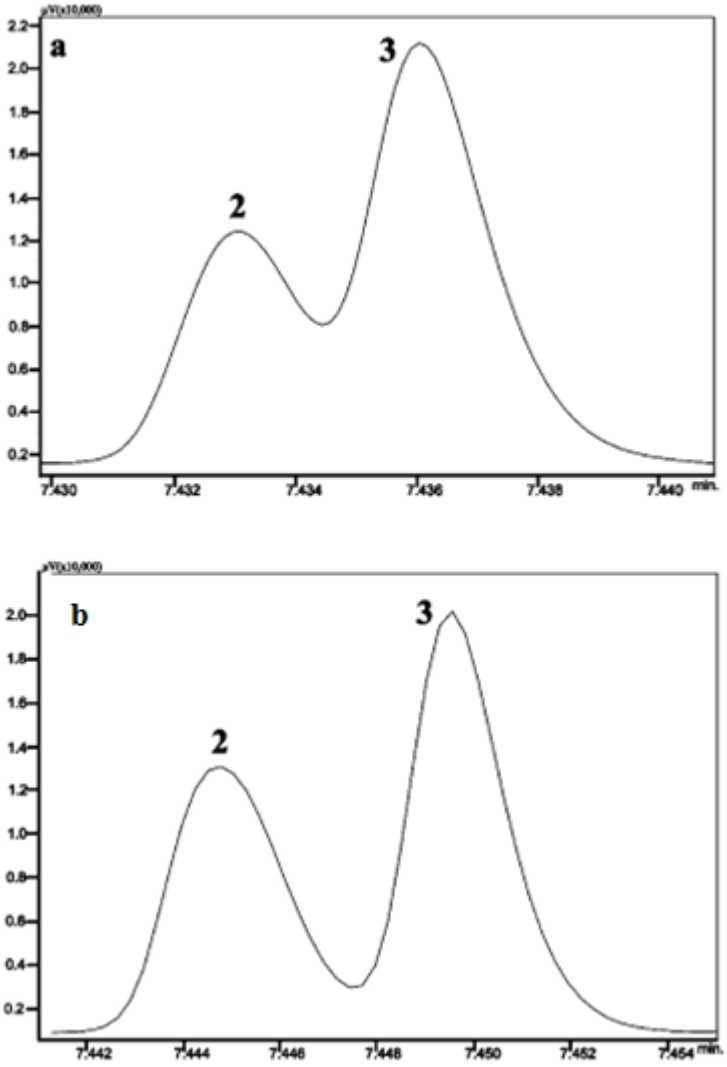


**Figure 1-23: Single modulation raw GC×GC chromatogram expansions relative to conventional (a), and 35:65 split flow (b) applications for compounds 2 and 3 [From [97]].**

stopped in the $^{1}$D for short periods of time through a six-port valve. The carrier gas was supplied to the $^{2}$D column from an auxiliary source. Periodically stopping the flow in the $^{1}$D allowed for longer separation in the $^{2}$D without the need to increase the length of the modulation period in $^{1}$D, thus preserving the separation accomplished in the $^{1}$D. In this system, the $^{1}$D and $^{2}$D columns could be operated simultaneously under optimal flow conditions and the $^{2}$D column did not necessarily have to be short and/or narrow. The stop-flow interface was followed by the cryogenic modulator.

### 1.7.5 Temperature programming

Temperature program optimization is an important factor that influences any GC×GC separation. The occupation of the 2D separation space can be increased by tuning and optimizing the temperature programming rate. [11, 97] Figure 1-24A shows the distribution of the analytes around a diagonal when both dimensions are operated isothermally. [11] In this case analyte volatility is the main determinant of retention, thus the retention times in both dimensions are correlated. Keeping the $^{1}$D isothermal while increasing the $^{2}$D temperature linearly causes the low-boiling point analytes eluting early from the $^{1}$D to be launched into the $^{2}$D column at lower $^{2}$D temperature. On the contrary, high-boiling point analytes are launched into the $^{2}$D

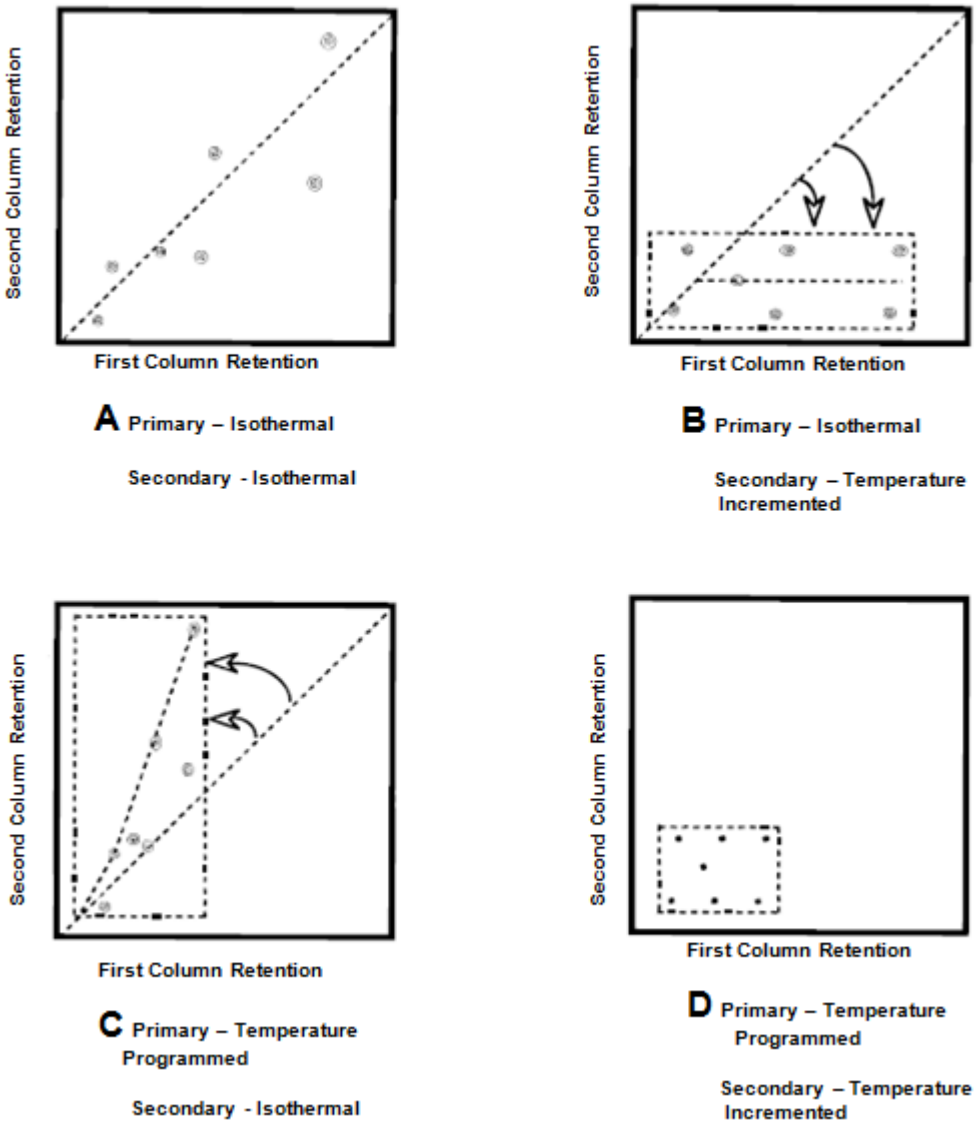


**Figure 1-24: Simulated GC×GC chromatogram showing the influence of temperature on sample retention. [Based on [11]].**

column at higher $^{2}D$ temperature. Therefore, the $^{2}D$ temperature increase compensates for the decrease in sample volatility. This rotates the diagonal in Figure 1-24A into a horizontal in Figure 1-24B. In Figure 1-24C, the $^{1}D$ temperature is increased linearly, while $^{2}D$ is kept isothermal. The diagonal in Figure 1-24A was curved upward. By increasing the temperature linearly in both dimensions, the retention times in both dimensions became independent. Thus the peaks were well distributed within a smaller area and the retention times in both dimensions were independent of each other (Figure 1-24D). [11] This simulation was close to the practical results obtained by Venkatramani et al. [11] It is important to mention that GC×GC designs use either a single oven or two independent ovens. The latter increases the flexibility of the system. Using a single oven has two main limitations: (1) the maximum operating temperature is limited by the maximum temperature of the less thermally stable column, and (2) the $^{2}D$ analysis temperatures are dependent on the $^{1}D$ elution temperature. [1] Generally, the temperature-programming rate in GC×GC should be rather slow, i.e. only 1 - 5 °C/min, to produce relatively broad peaks in the $^{1}D$ thus allowing the required 2.5 – 3 fold modulation of each peak. However, excessively slow temperature rates can adversely affect sensitivity and/or

cause wraparound. [1] When two independent ovens are used, the $^2$D column is usually programmed at the same rate, but with 20 - 30 °C offset from the $^1$D rate.

### 1.7.6 Detection Parameters

The detector is another important component of a GC×GC system. GC×GC separation produces peak widths of 100-500 ms at the base. [32-35] Very fast GC×GC using narrow-bore 50 μm I.D. $^2$D columns may produce peaks on the order of 25 ms wide. [1, 129, 136] To get reliable and reproducible determination of a peak area, at least 10 data points should be collected along the peak (width at the baseline $w_b = 4\delta$), which is about three data points per peak standard deviation. [22] Consequently, a detector that is capable of collecting data at a rate of at least 50 Hz is required. Therefore, the detector used in GC×GC separation must be characterized by high acquisition speed, in addition to low internal volumes and low time constants. [13, 129, 136, 137] Thus far FID have been the most popular choice in GC×GC, followed by time-of-flight mass spectrometers. Nevertheless, alternative element-selective detectors such as μECD, NCD, SCD, NPD, ADE and miniaturized pulsed discharge detector (MPDD) have also been used for some GC×GC applications. Examples of GC×GC applications using element-selective detectors are summarized in Table 1-3.

**Table 1-3: Various selected GC×GC applications in the literature using element-selective detectors**

| Detector | Analyte/sample | References (examples) |
|---|---|---|
| μECD | Pesticides in sediments | 138-140 |
| | PCBs/OCs/CBz in soils, sediments and sludges | 141, 142 |
| | Dioxins and dioxin-like PCBs in food and feed | 143 |
| | Chiral toxaphenes typically found in real-life samples | 144 |
| | Polybrominated diphenyl ethers | 145 |
| | Polychlorinated dibenzo-p-dioxins, dibenzofurans and PCBs in food | 36, 146 |
| | Chiral PCBs in food | 36 |
| | PCBs in Baltic grey seals | 147 |
| | Toxaphene | 148 |
| | Polychlorinated dibenzo-p-dioxins, polychlorinated dibenzofurans and PCAs in a cod liver extract and a standard mixture | 149 |
| NPD | Nitrogen-containing compounds in Brazilian heavy gas oil | 150 |

| | | |
|---|---|---|
| | Volatile fraction of creosote-treated railway wood sleepers | [151] |
| | Nanoparticles in roadside atmosphere | [152] |
| | methoxypyrazines in coffee headspace | [153] |
| | Fungicide residues in vegetable samples | [154] |
| | Methoxypyrazines in wine | [155] |
| SCD | Sulfur-containing compounds in straight run diesel oil | [156] |
| | Sulfur-containing compounds in heavy petroleum cuts | [157] |
| | Sulfur-containing compounds in middle distillates | [158] |
| | Sulfur-containing compounds in crude oils | [41] |
| | Sulfur compounds in diesel oils | [159] |
| | Sulfur-containing compounds in diesel | [160] |
| AED | Sulfur-containing compounds in crude oil | |
| MPDD | Pyrolysis gasoline (cracked naphtha) and pyrolysis of a polyethylene copolymer | [40] |

#### 1.7.6.1 Flame Ionization Detector

FID offers acquisition rates up to 500 Hz, [161] which is fast enough for the detection of the very narrow GC×GC peaks eluting from $^{2}$D columns. [10, 93, 162] Owing to this, FID was the first detector applied to GC×GC. [9] Not only is the FID acquisition rate high, but sensitivity is also reasonably good in the low pg $s^{-1}$ of carbon range, and the linear dynamic range is very broad (up to seven orders of magnitude). The FID is also extremely robust, user friendly, reliable and stable. [137] Lack of selectivity and structural information are this detector's major drawbacks.

#### 1.7.6.2 Mass Spectrometric Detectors

One of the most powerful detectors for GC×GC is the mass spectrometer. Mass-spectrometric (MS) detectors are capable of structure identification, which adds an additional dimension to the system. The first combination of a mass spectrometer with a GC×GC system was reported in 1999. [50] The use of MS detection in GC×GC is mainly limited by the data acquisition speed that can be accomplished with this detector. Time-of-flight (TOF), and to a lesser extent quadrupole MS detectors are the most commonly used with GC×GC. [163] In recent years, high resolution TOF instruments have also been employed.

*1.7.6.2.1 Quadrupole MS*

Despite the slow scan speed of the quadrupole (qMS) of 2.43 full-scan spectra/s, Frysinger and Gains were able to use it with GC×GC to analyze marine diesel fuel. [50] It was necessary to slow down the GC×GC analysis speed to get $^{2}$D peak widths of at least 1 s. Even under these conditions, the 1 s-wide peaks were severely undersampled. Although the number of data points collected per peak was not enough for correct peak reconstruction or quantification, it allowed for acceptable peak identification. Three years later, Shellie and Marriott [164] used qMS in selected ion monitoring (SIM) mode, with data acquisition rate of 8.33 Hz for enantiomer separation by GC×GC. The authors made use of the vacuum outlet conditions, which promote increased diffusion coefficients and higher component volatility. In 2003, the same group used GC×GC- qMS for the analysis of ginseng volatiles. [162] To achieve a high scan rate (20 Hz), a reduced mass range of 41 – 228.5 m/z was used. Four data points per peak were collected, and the authors reported that it was sufficient for identification purposes. The first example of using qMS for quantitation purposes in combination with GC×GC was reported by Debonneville and Chaintreau. [165] The authors used the qMS in the SIM mode to achieve an acquisition rate of 30.7 Hz which was reported to be sufficient for the purpose of quantitation. Such an acquisition frequency is still insufficient for correct

reconstruction of narrower GC×GC peaks (e.g. 80 – 200 ms). Moreover, SIM mode is efficient only for target analysis. An interesting study about the principles, practicability, and potential of rapid-scanning qMS in GC×GC separations was conducted by Adahchour et al. [166] In this study, the performance of a rapid-scanning generation of qMS (Shimadzu QP2010) was studied for both qualitative and quantitative purposes. This detector has a scan speed of up to 10,000 amu/s and can reach the 50 Hz data acquisition frequency required for GC×GC using a restricted mass range of 95 amu. The authors reported that the minimum number of data points required for reliable quantitation was seven. This number of data points was collected at acquisition rate of 33 Hz and a mass range of up to 200 amu. If a wider mass range was desired, a time-scheduled option with mass windows on the order of 50 – 100 amu could be used without significant deterioration of the analytical performance. The authors concluded that for applications with fairly limited mass range (e.g. 100 – 200 amu), a rapid-scanning qMS becomes the best alternative to TOF-MS. However, for complex samples and non target analysis with a wide mass range, TOF-MS is superior. Recently, Purcaro et al. reported a study that focused on the evaluation of a rapid-scanning qMS instrument (Shimadzu QP2010-Ultra) in combination with GC×GC [163]. The detector is characterized by a 20,000 amu/s scan speed and a 50 Hz scan frequency using a 290 amu mass range (40 – 330 m/z). The

performance of the system was evaluated by analyzing perfume allergens. This research was the first reported study of true full-scan quantification using a standard GC×GC setup with qMS. The authors reported that more than 15 data points per peak were collected, enabling reliable peak reconstruction.

#### *1.7.6.2.2 Time-of-Flight MS (TOFMS)*

TOFMS is characterized mainly by its ability to produce a complete spectrum for every pulse of ions from the ion source in an extremely short time. TOF-MS fast data acquisition rate (up to 500 spectra per second [167]), allows up to 50 acquisitions per 100 ms peak, which is more than enough for reliable reconstruction and quantitation of the peak. Van Deursen et al. reported the first use of TOFMS with GC×GC [168] in 2000. To limit the size of the data files created (which was the main problem at the time) and to get enough data points with good sensitivity, a 50 Hz acquisition rate was used. In 2003, LECO Corp.® introduced a complete GC×GC–TOFMS instrument with fully integrated software for system control and data processing. [100, 163, 169] Since then, because of the increasing need for analyte identification, and due to complexity of most samples analyzed by GC×GC, TOF MS has been continuously gaining popularity and is considered the preferred GC×GC detector. It has been reported that over 200 papers had been published in the field of GC×GC-MS during

the 1999 – 2010 (June) period. More than 80% of them used TOF-MS, and about 16% used qMS. [170]

#### *1.7.6.2.3 High Resolution Time-of-Flight MS (HRTOF-MS)*

In recent years, HRTOF-MS has been paired with GC×GC separation techniques. These detection systems typically operate with much lower data acquisition rates (20-25 Hz) and narrower dynamic range. However, sensitivity is much greater than with q-MS and unit resolution TOF-MS systems, allowing the generation of highly detailed 2D chromatograms. [171] The ability to accurately calculate elemental composition from precisely determined molecular ion masses is another valuable feature. Even at lower than preferred data acquisition rates, HRTOF-MS has the potential to be an extremely valuable tool in new chemical discovery and detailed group type analysis of very complex samples. Researchers have been successfully using GC×GC-HRTOF-MS for some time now to study the composition of a variety of complex samples. [152, 171-178]

## 1.8 Scope of the thesis

In the following chapters, the results of research on advances in GC×GC fundamentals, instrumentation and applications will be presented, starting with fundamentals and instrumentation, followed by the applications. The first project

was devoted to the study of sensitivity enhancement of GC×GC compared to 1D-GC. In the next chapter, a new single-stage cryogenic modulator was developed. The device rivals the performance of the commercially available cryogenic modulators while being much simpler and consuming significantly less cryogens. Further chapters present various applications of GC×GC to demonstrate the advantages of the technique such as enhanced sensitivity and high separation power. This included utilizing the technique for the analysis and characterization of highly challenging natural products including South African wines and blue honeysuckle berries. One of the most interesting applications included the use of the GC×GC separation power to study the effect of malolactic fermentation on the aroma of South African Pinotage wines during vinification.

It is worth pointing out here that the order of the chapters is not necessarily the same as the order in which the experimental work was performed. The first experiments were the sensitivity comparison study followed by the analysis of wines and blue honeysuckle berries using a dual-stage delay loop cryogenic modulator developed previously in our group. Because of the challenging design of this modulator, many problems appeared related to the need of careful adjustment between the loop length and the carrier gas velocity whenever the chromatographic

conditions were changed. This was a tedious process which became the trigger to start working on the interesting project of developing a simple single-stage cryogenic modulator to overcome these problems. This was accomplished as presented in Chapter 3.

# Chapter 2

# Sensitivity of Comprehensive Two-Dimensional Gas Chromatography (GC×GC) versus One-Dimensional Gas Chromatography (1D-GC)[i]

In spite of the maturing status of GC×GC, little attention has been devoted in the literature to quantitative evaluation of the technique, and to quantitative comparison of these systems with their 1D (one-dimensional) counterparts. Moreover, there are still some outstanding issues that spark discussions and controversy. One of them is the sensitivity enhancement in GC×GC separations compared to conventional 1D separations.

Cooling-based modulators collect the effluent fractions at sub-oven temperatures and re-inject them in the form of a very narrow pulse when the temperature of the modulator is increased. This increases the signal-to-noise ratio owing to the analyte band compression. Increasing the frequency of the chemical signal entering a detector is an excellent way to enhance the signal-to-noise ratio. [179] Phillips and Liu used thermal desorption modulation between the outlet of the column and the inlet

[i] This chapter is based on the author's paper "Sensitivity of comprehensive two-dimensional gas chromatography (GC×GC) versus one dimensional gas chromatography (1D-GC)" (at the final stages of submission to Journal of Separation Science).

of the detector to enhance chromatographic sensitivity and signal-to-noise ratio. An increase by a factor of ten was observed. [45] Kinghorn and Marriott used LMCS for the same purpose, i.e. signal-to-noise enhancement in capillary gas chromatography. An increase of signal-to-noise ratio by a factor of ten was also reported. [180, 181] The increase in peak amplitude using GC×GC in comparison with a single column has been qualitatively discussed by DeGeus. [182] Habram and Welsch reported a 10 to 27 times increase in the signal-to-noise ratio through modulation. [183] Lee et al. proposed a theoretical model for simple calculation of sensitivity enhancement in GC×GC over 1D separation. [184] Contrary to that, a paper published in Journal of Chromatography A in 2003 [15] claimed that there is no increase in the sensitivity of GC×GC over 1D-GC and claimed "(…) addition of the second dimension does not change the system MDC (minimum detectable concentration) for any solute that is sufficiently separated in one-dimensional GC and in GC×GC and has the same retention in both cases." The author mentioned that the detector electronic noise is the main contributor in the determination of MDC, and this noise cannot be reduced below a certain level limited by the white noise. [15]

In a GC system, under controlled conditions, the noise consists primarily of the sum of two slowly varying components: a steady-state standing-current offset (GC

detector noise) [26] and "chemical" or "chromatographic" noise, which includes temperature-induced column-bleed, solvent tail, etc. The main aim of the work in this chapter was to compare the sensitivity in GC×GC and 1D-GC, using EPA-recommended methodology [185] for the determination of limits of detection (LODs) for both techniques, to study the effect of noise on the sensitivity of the method and to determine major noise contributors (electronic noise, chromatographic noise, etc.).

## 2.1 Experimental

### 2.1.1 Instrumental parameters

The GC×GC system consisted of an Agilent 6890 GC (Agilent Technologies, Palo Alto, CA, USA) equipped with a single jet, liquid nitrogen cryogenic modulator, coupled to a Pegasus III time-of-flight mass spectrometer and an FID detector (LECO Corp., St. Joseph, MI). [25] The column set consisted of a 30 m × 0.25 mm I.D. × 1.00 μm $d_f$ VF-1MS (Varian, Mississauga, ON) as a primary column coupled to a 1.5 m × 0.25 mm I.D. × 0.25 μm $d_f$ SolGel-Wax phase second dimension column (SGE, Austin, TX). Different modulation periods of 2, 4, 6 and 8 s were used with the cryogenic trap cooled to –196 °C using liquid nitrogen. The separation was performed using the following temperature program: initial temperature 50 °C, kept for 0.2 min, ramped at 4 °C/min to 150 °C (Mixture 1); and initial temperature 40 °C,

kept for 0.2 min, ramped at 30 °C/min to 240 °C, then ramped at 4 °C/min to 280 °C and held for 3 min (Mixture 2). The injector was operated at 280 °C and 1 μL injections were performed in the pulsed splitless mode, with a splitless time of 1 min. Helium was used as the carrier gas at a constant flow of 1.4 mL/min for TOF MS and 1.6 mL/min for the FID. The MS transfer line was maintained at 250 °C. Ions in the mass range 35 - 400 amu were acquired at a rate of 100 spectra/s. The ion source temperature was 225 °C and the detector voltage was set to -1800 V. FID detection was performed at 350 °C, with data collected at 100 Hz. Three different types of inlet ferrules were used: 100% graphite ferrules (with Mixture 1); Vespel/graphite and SilTite ferrules (with Mixture 2).

### 2.1.2 Chemicals and stock solutions

Two mixtures were used for this study. Mixture 1 consisted of *n*-nonane (*n*-$C_9$), *n*-decane (*n*-$C_{10}$), *n*-dodecane (*n*-$C_{12}$) and 3-octanol dissolved in *n*-hexane (freshly distilled before use). Mixture 2 was composed of *n*-eicosane (*n*-$C_{20}$), *n*-docosane (*n*-$C_{22}$), *n*-tetracosane (*n*-$C_{24}$) and pyrene in $CS_2$. Hexane and all the standards were obtained from Sigma–Aldrich (Mississauga, ON, Canada). $CS_2$ was obtained from Fisher Scientific (Toronto, Canada). Helium (99.999% purity) was delivered by Praxair (Mississauga, ON, Canada).

Stock solutions of *n*-$C_9$, *n*-$C_{10}$, *n*-$C_{12}$ and 3-octanol were prepared in *n*-hexane at a concentration of 1 mg/mL; *n*-$C_{20}$, *n*-$C_{22}$, *n*-$C_{24}$ and pyrene were prepared in $CS_2$ at the same concentration. The concentrations used with TOF MS and FID (Table 2-1) were prepared by dilution of the appropriate volumes into *n*-hexane and $CS_2$.

### 2.1.3 Method detection limit calculation

The EPA approach as defined in the U.S. EPA Electronic Code of Federal Regulations [185] was used for the calculation of LODs. The EPA method detection limit approach utilizes a single-concentration design estimator. The first step is to determine an estimate of the detection limit (EDL). An EDL is defined as a concentration value which maintains an instrument signal-to-noise ratio in the range of 2.5-5. The EDL is then used to choose the concentration at which standards should be prepared. The EPA recommends using a concentration that is between 1 and 5 times the EDL. Eight aliquots of the sample concentration (Table 2-1) were prepared and the standard deviations for the peak height of replicate measurements were calculated. The LOD was calculated as follows:

$$LOD = t_{n-1,1-\alpha=0.99} \times S$$

Where; $LOD$ is the limit of detection, $t_{n-1,1-\propto=0.99}$ is the Student's t value appropriate for a 99% confidence level and a standard deviation estimate with *n*-1 degrees of

**Table 2-1: Sample concentrations used in LOD determination**

| Compound | | TOF MS concentration (μg/L) | | | | | | FID concentration (μg/L) | | | | | |
|---|---|---|---|---|---|---|---|---|---|---|---|---|---|
| | | 100% Graphite ferrules | | Vespel/Graphite ferrules | | SilTite ferrules | | 100% Graphite ferrules | | Vespel/Graphite ferrules | | SilTite ferrules | |
| | | 1D | GC×GC | 1D | GC×GC | 1D | GC×GC | 1D | GC×GC | 1D | GC×GC | 1D | GC×GC |
| Mixture 1 | ***n*-C$_9$** | 80 | 5 | - | - | - | - | 80 | 5 | - | - | - | - |
| | ***n*-C$_{10}$** | 80 | 5 | - | - | - | - | 80 | 5 | - | - | - | - |
| | ***n*-C$_{12}$** | 80 | 5 | - | - | - | - | 80 | 5 | - | - | - | - |
| | **3-octanol** | 500 | 40 | - | - | - | - | 500 | 50 | - | - | - | - |
| Mixture 2 | ***n*-C$_{20}$** | - | - | 100 | 7 | 100 | 7 | - | - | 70 | 7 | 70 | 7 |
| | ***n*-C$_{22}$** | - | - | 100 | 7 | 100 | 7 | - | - | 70 | 7 | 70 | 7 |
| | ***n*-C$_{24}$** | - | - | 100 | 7 | 100 | 7 | - | - | 70 | 7 | 70 | 7 |
| | **Pyrene** | - | - | 150 | 15 | 150 | 15 | - | - | 150 | 15 | 150 | 15 |

freedom, and *S* is the standard deviation of the replicate analyses. In this study, the LODs were estimated using the highest second-dimension peak for a given analyte, because at or close to the LOD only this peak would be visible in most cases.

## 2.2 Results and discussion

***"Chemical" or "chromatographic" noise***

The "chemical" or "chromatographic" noise in GC might result from a number of sources, such as the solvent tail and the column bleed. In this study, the solvent tail was created by using 100% graphite ferrules for the inlet. These ferrules are porous, thus they can interact with the solvent causing tailing and can become a constant source of contamination (graphite acts as a "chemical sponge" causing a near-continuous release of solvent during the run). Mixture 2 was composed of high boiling-point analytes that eluted with the column bleed at the end of the run. Vespel/graphite and SilTite inlet ferrules were used with Mixture 2. In order to compare the sensitivity between 1D-GC and GC×GC, the two mixtures were analyzed using both approaches applying the EPA-recommended method to calculate the LODs. The limits of detection for TOF MS were calculated using unique masses for each analyte to enhance the sensitivity. For *n*-$C_9$, *n*-$C_{10}$, *n*-$C_{12}$ the m/z was 71; m/z 83 was selected for 3-octanol, 57 for *n*-$C_{20}$, *n*-$C_{22}$, *n*-$C_{24}$ and 202 for pyrene.

Figure 2-1a shows the 1D-GC total ion current (TIC) traces of 5 and 80 μg/L of *n*-$C_9$, *n*-$C_{10}$ and *n*-$C_{12}$. Even using the extracted ion chromatogram at m/z 71, the analytes were not detected at 5 μg/L concentration levels within the high background noise levels of the solvent tail (Figure 2-1B). However, in GC×GC the analytes were detected at the 5 μg/L concentration levels. The main reason was that the analytes were separated from the high background noise. This is illustrated in Figure 2-2, where the small *n*-$C_9$ peak was separated from the solvent tail. This was obvious in the LOD values shown in Table 2-2. The same scenario applied to the FID. However, FID is a non-selective detector. Thus the advantage of selectivity and sensitivity enhancement through using extracted ions with MS is lost. Therefore, chromatographic separation is very important. This is illustrated in Figure 2-3, where *n*-$C_9$ small peak is also separated from the solvent tail.

The second type of chemical noise is the temperature-induced column bleed. Figure 2-4(top) demonstrates the TIC trace of 100 μg/L of *n*-$C_{20}$, *n*-$C_{22}$ and *n*-$C_{24}$ using 1D-GC. No distinct peaks of the analytes could be observed within this high

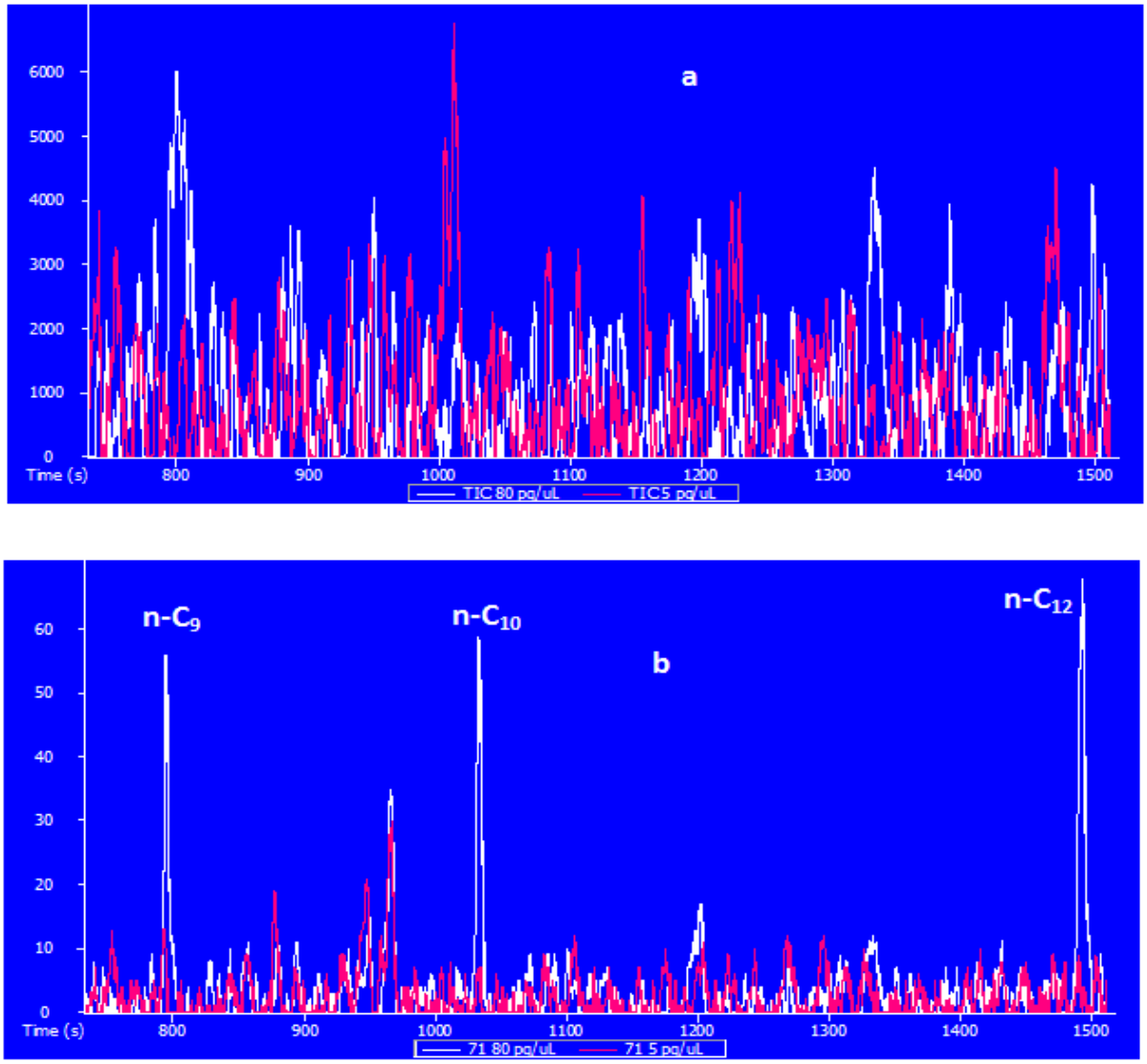


**Figure 2-1: (a) TIC of *n*-C9, *n*-C10, *n*-C12 (5 µg/L, red and 80 µg/L, white) using 1D-GC TOFMS separation. (b) m/z 71 chromatogram of *n*-C9, *n*-C10, *n*-C12 (5 µg/L, red and 80 µg/L, white) using 1D-GC TOFMS.**

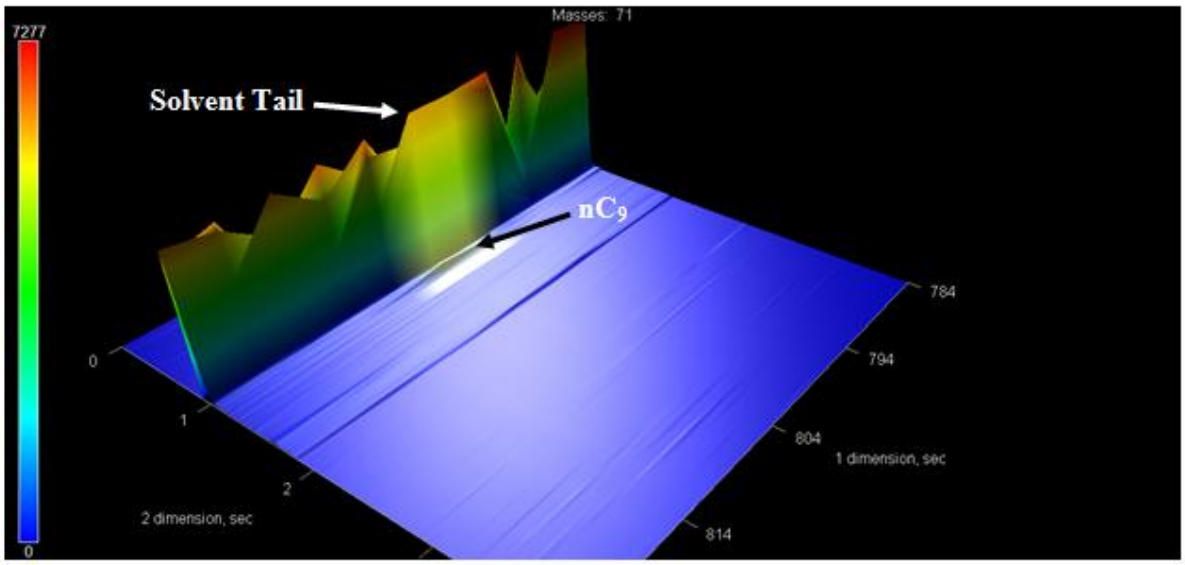


**Figure 2-2: GC×GC TOF MS separation of 5 μg/L n-$C_9$ peak from the solvent tail (4 s modulation, m/z 71).**

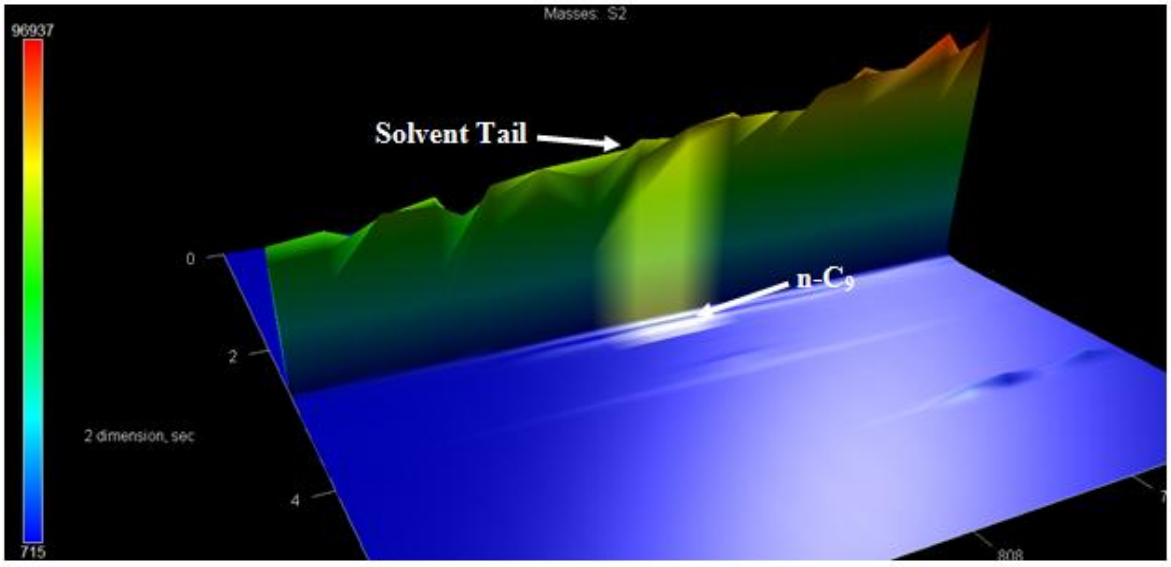


**Figure 2-3: GC×GC FID separation of 5 μg/L n-$C_9$ peak from the solvent tail (6 s modulation).**

**Table 2-2: LOD values of 1D-GC TOF MS, 1D-GC FID, GC×GC-TOFMS and GC×GC-FID using 100% graphite inlet ferrules**

| | GC×GC TOFMS (LOD μg/L) | | | | | GC×GC FID (LOD μg/L) | | | | |
|---|---|---|---|---|---|---|---|---|---|---|
| | **1D** | **2 s Modulation** | **4 s Modulation** | **6 s modulation** | **8 s Modulation** | **1D** | **2 s Modulation** | **4 s Modulation** | **6 s modulation** | **8 s Modulation** |
| ***n*-$C_9$** | 21.5 | 2.7 | 2.6 | 2.4 | 1.6 | 21 | 1.7 | 1.7 | 1.4 | 1.2 |
| ***n*-$C_{10}$** | 20.4 | 3.8 | 2.7 | 1.7 | 1.6 | 23.4 | 2.9 | 2.9 | 2.7 | 2.5 |
| ***n*-$C_{12}$** | 22.3 | 2.5 | 1.9 | 1.9 | 1.8 | 20.4 | 1.4 | 1.3 | 1.2 | 1.1 |
| **3-oct*** | 74.1 | 9.8 | 8.4 | 8.4 | 7.9 | 54.1 | 9.8 | 8.3 | 8.1 | 7.4 |

* 3-octanol

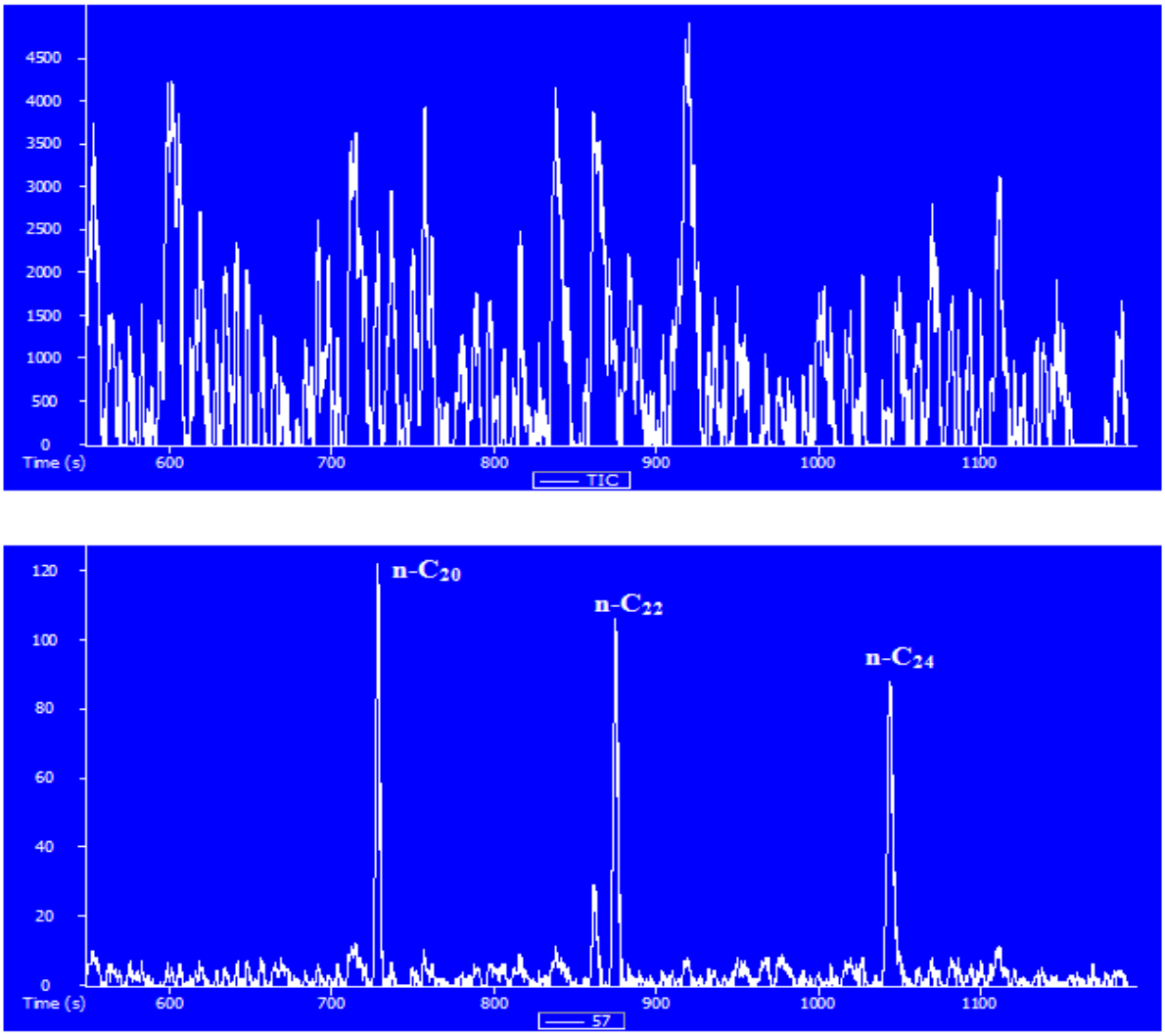


**Figure 2-4: (top) TIC of 100 µg/L *n*-C20, *n*-C22 and *n*-C24; (bottom) m/z 57 chromatogram of 100 µg/L *n*-C20, *n*-C22 and *n*-C24 using 1D-GC.**

background noise. One of the main advantages of TOFMS is its selectivity. Therefore, by selecting the unique masses of the analytes, their peaks could be detected (Figure 2-4 bottom). Despite of this selectivity of the MS, LODs of 1D-GC were still higher than these of GC×GC (Table 2-3) because of lack of band compression in the former.

Selective detector is an advantage in chromatography; however, not all laboratories can afford TOFMS. In such cases sensitivity is highly affected by the chromatographic separation efficiency. The analyte peaks of *n*-$C_{20}$, *n*-$C_{22}$ and *n*-$C_{24}$ could be effeciently separated from the column bleed using GC×GC and detected using FID with much lower LODs than in 1D-GC (Figure 2-5 and Table 2-4). The effect of chromatographic separation can be clearly shown and explained in the separation of pyrene in Mixture 2 from the column bleed. In Figure 2-6, pyrene peak was wrapped around when 2 s modulation period was used in GC×GC and coeluted with the column bleed noise. The selectivity of the TOFMS could solve this problem by quantitation at m/z 202, the unique mass of pyrene. Its LOD was calculated and it was still much better than in 1D-GC (Table 2-3). However, with the FID, pyrene peak could not be separated from the noise (Figure 2-7). Therefore, LODs of pyrene at 2 and 4 s modulation could not be calculated. The only solution to this

**Table 2-3: LOD values of 1D-GC TOFMS and GC×GC-TOFMS using vespel/graphite and SilTite inlet ferrules**

| | Vespel/Graphite ferrules (LOD μg/L) | | | | | SilTite ferrules (LOD μg/L) | | | | |
|---|---|---|---|---|---|---|---|---|---|---|
| | **1D** | **2 s Modulation** | **4 s Modulation** | **6 s modulation** | **8 s Modulation** | **1D** | **2 s Modulation** | **4 s Modulation** | **6 s modulation** | **8 s Modulation** |
| ***n*-$C_{20}$** | 22.3 | 3.4 | 3.2 | 3.1 | 2.4 | 22.8 | 3.7 | 3.3 | 3.2 | 2.5 |
| ***n*-$C_{22}$** | 24.4 | 4.3 | 4.1 | 4 | 1.8 | 22.6 | 4.3 | 3.8 | 3.6 | 3.3 |
| ***n*-$C_{24}$** | 23.1 | 3.4 | 3.3 | 3.1 | 2.9 | 22.5 | 4.1 | 4.1 | 3.6 | 3.3 |
| **PYN*** | 62 | 9.4 | 8.7 | 8.2 | 6.5 | 55.6 | 9.8 | 9.1 | 7.9 | 6.1 |

* Pyrene

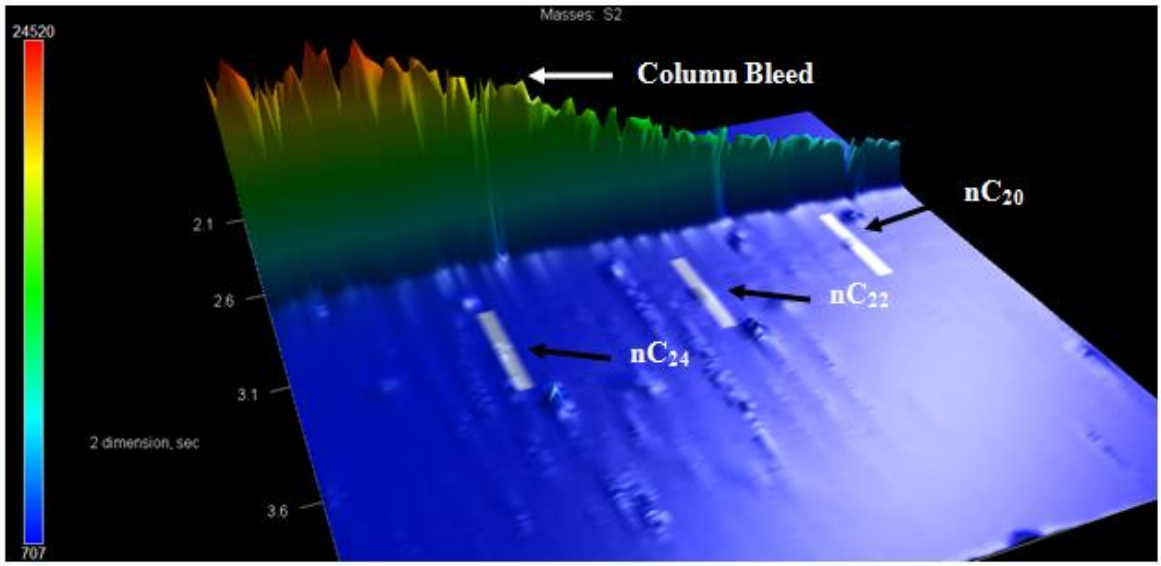


**Figure 2-5: GC×GC-FID separation of *n*-$C_{20}$, *n*-$C_{22}$ and *n*-$C_{24}$ from column bleed (6 s modulation).**

**Table 2-4: LOD values of 1D-GC FID and GC×GC-FID using vespel/graphite and SilTite inlet ferrules**

| | Vespel/Graphite ferrules (LOD μg/L) | | | | | SilTite ferrules (LOD μg/L) | | | | |
|---|---|---|---|---|---|---|---|---|---|---|
| | **1D** | **2 s Modulation** | **4 s Modulation** | **6 s modulation** | **8 s Modulation** | **1D** | **2 s Modulation** | **4 s Modulation** | **6 s modulation** | **8 s Modulation** |
| ***n*-$C_{20}$** | 29.9 | 3.1 | 2.5 | 2.2 | 2.1 | 27.9 | 3.2 | 3.1 | 3 | 2.8 |
| ***n*-$C_{22}$** | 24.7 | 3.2 | 2.8 | 2.5 | 2.2 | 22.5 | 4.1 | 4 | 3.7 | 3.3 |
| ***n*-$C_{24}$** | 31.8 | 3.4 | 2.4 | 2.1 | 2 | 22.3 | 3.6 | 3.2 | 3.1 | 3 |
| **PYN*** | 63.7 | - | - | 10 | 6.6 | 52.9 | - | - | 10.8 | 7.7 |

* Pyrene

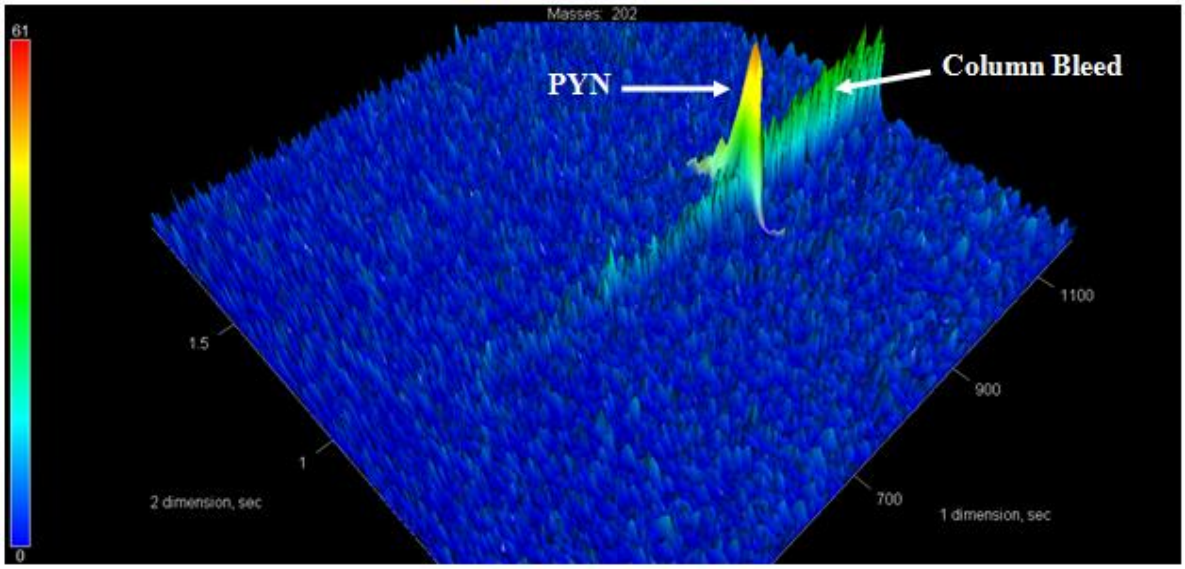


**Figure 2-6: GC×GC-TOFMS separation of 15 μg/L pyrene (PYN), 2 s modulation (m/z 202).**

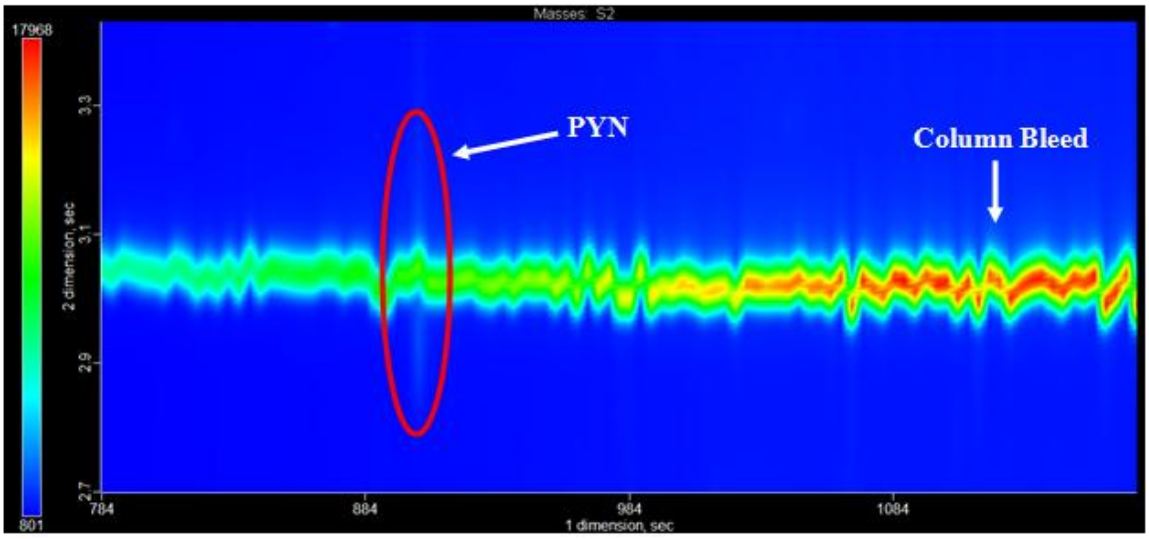


**Figure 2-7: Contour plot of GC×GC-FID separation of 150 μg/L pyrene (PYN), 4 s modulation.**

problem is the chromatographic separation of the pyrene peak from the column bleed, which can be achieved with GC×GC, but not with 1D-GC. This is illustrated in Figure 2-8, where pyrene peak was completely separated from the column bleed by increasing the modulation period to 6 s, and could be detected with low LODs (Table 2-4).

The results shown in Table 2-2, Table 2-3 and Table 2-4 show that LODs increased with the increase in the number of modulations per peak (i.e. the highest LODs were with 2 s modulation periods and the lowest LODs were with 8 s modulation periods). The results show that a 6 to 18 fold (for GC×GC-FID) and 6 to 13 fold (for GC×GC-TOFMS) increase in sensitivity can be achieved when the analyte is

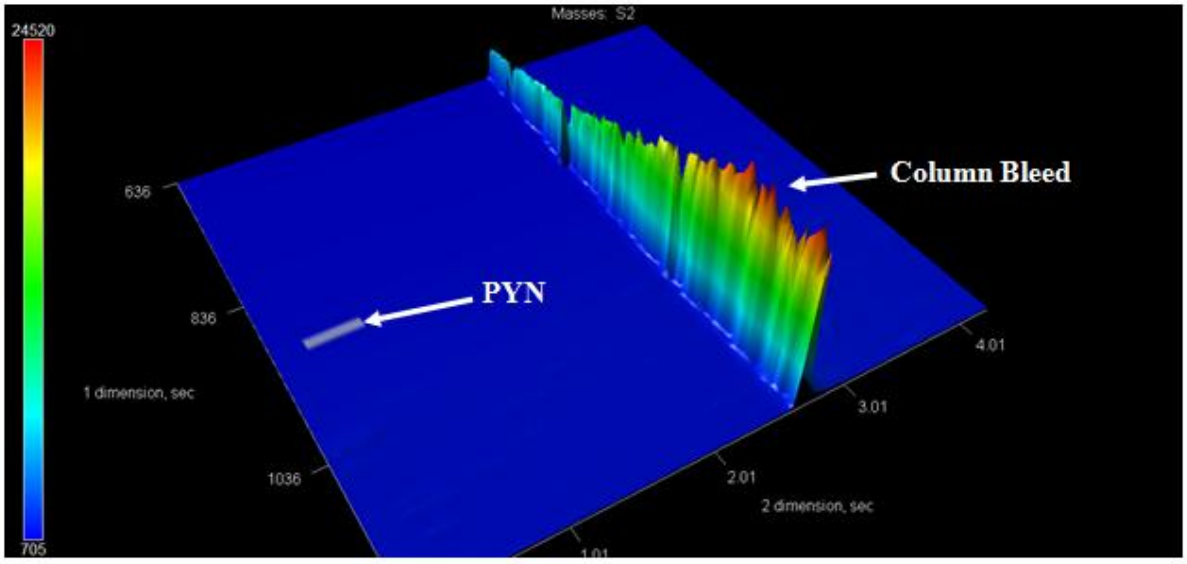


**Figure 2-8: GC×GC FID separation of 15 μg/L pyrene (PYN), 6 s modulation.**

modulated into one (or maybe two) second dimension peaks (i.e. 8 s modulation). When the peaks were modulated three to four times (as in 2 s modulation), sensitivity improvement of 5 to 14 (for FID) and 5 to 9 fold (for TOFMS) was achieved. This is because the peak height in the second dimension decreased with increasing modulation frequency. Nevertheless, LODs were still very good and better than those of 1D-GC.

The results for 3-octanol and pyrene indicated that sensitivity enhancement strongly depended on the second dimension retention time of the analyte. Since the separation in the second dimension was almost isothermal, the increased retention

time of both 3-octanol and pyrene resulted in broader peaks, and thus in lower sensitivity gain compared to earlier eluting analytes.

As it was mentioned by Blumberg, [15] the noise in a GC system is composed of several types, such as detector and chemical noise. Detector noise is limited by the white noise, [186] therefore it cannot be reduced below a certain limit. However, in reality it is the chemical noise that is the major contributor to the overall noise in any GC system. When the magnitude of the analyte peak becomes comparable to that of the background noise, the analyte peaks of interest begin to merge with the noise and can no longer be distinguished unless they can be chromatographically separated from that noise. Therefore, the practical limit in sensitivity is usually imposed by the chemical or chromatographic noise rather than the inherent sensitivity of the detector. The ability of GC×GC to separate the analytes from themselves and from the chromatographic noise is of utmost importance with complex mixtures. 1D-GC LOD is directly influenced by any closely eluting interfering compounds or noise, and in this case, GC×GC LOD enhancement becomes greater.

## 2.3 Conclusions

The sensitivity of GC×GC was compared to that of 1D-GC. GC×GC (using 8 s modulation period) offered at least an order of magnitude (average) improvement in

LOD. Electronic noise cannot be reduced below a certain limit, thus it is a limiting factor of the sensitivity. However, this is not the case when chromatographic or chemical noise is the main contributor to overall noise. In such a case chromatographic separation strongly affects the LOD. The ability of GC×GC to produce peak isolation with true baseline is of significant importance with complex mixtures. LOD in 1D-GC is directly affected by any closely eluting interferents (e.g. other analytes, column bleed, solvent tail, etc.), and in this case GC×GC can significantly enhance the sensitivity.

# Chapter 3

# Development and Design of a New Single-Stage Cryogenic Modulator[i]

GC×GC modulator designs can be classified into two main groups; thermal and flow modulators, as described in Chapter 1. One of the main advantages of thermal modulators is enhanced sensitivity due to analyte refocusing. Most of the currently used flow modulators utilize pneumatic devices [71] that use sample loops and valves to collect the primary column effluent and inject it into the secondary column. While cost-effective flow modulators are gaining popularity, their optimization is rather complicated. When optimized, this style of modulation has been shown to perform similarly to cryogenic systems. [158] However, the inability of such systems to be easily paired with mass spectrometry presents a significant problem if compound identification is required. The description of flow modulator operation was presented in Chapter 1.

In thermal modulation, analytes may be trapped and modulated in a single point, then reinjected directly into the secondary column (single-stage modulation). The

[i] This chapter is based on the author's article "Development and design of a new single-stage cryogenic modulator for comprehensive two-dimensional gas chromatography (GC×GC)" to be submitted to Analytical Chemistry. The author presented this work at the 9th GC×GC sypmosium at Riva del Garda, Italy, May 27 to June 1, 2012 and won the "Best Innovative Poster Presentation" award.

modulated peak may go through the trapping point with a portion of the next un-modulated peak, causing peak-shape irregularities and broad injection bands. This is called breakthrough, which is considered the major drawback of single-stage modulation. To solve the problems associated with the single-stage design, dual-stage design was introduced. In this design, the primary column effluent collected in the first stage is thermally released with any potential breakthrough into a second trapping stage for additional focusing before being injected into the second column. All commercial modulators use the dual-stage design these days.

Although this design solves or minimizes the breakthrough problem, it suffers from several drawbacks. For example, the quad-jet design is quite complicated. Even though the development of the delay loop modulator solved that problem and made the design simpler, it introduced new issues. In particular, the length of the loop and the velocity of the carrier gas have to be carefully adjusted whenever the chromatographic conditions change. If the flow of the carrier gas is not adjusted properly, the band travelling through the delay loop might not reach the trapping spot at a time when it is cold, and therefore it might not be refocused.

With this in mind, It was hypothesized that the GC×GC field required a high performance liquid $N_2$-based cryogenic modulator with simpler design. It was found

in the literature that some research groups tried to achieve that goal through the development of modulator designs based on the first developed concept of the single-stage design. These designs and trials were discussed in Chapter 1, section 1.5.2. Thus, a project was started to develop such a simple and highly efficient modulator.

## 3.1 Experimental

### 3.1.1 Apparatus

A model 6890 gas chromatograph (Agilent Technologies, Mississauga, ON, Canada) equipped with a split/splitless injector and flame ionization detector (FID) was used. The GC was controlled and data was collected using LECO's ChromaTOF software (LECO Corp., St. Joseph, MI, USA, version 3.25). Data was processed using ChromaTOF version 4.41. The GC oven door was replaced with a window made of heat-resistant glass attached to a piece of sheet metal to help observe the modulator behavior while the system was running. The door interlock was defeated with a small magnet. The primary column, 30 m × 0.25 mm × 1.0 μm VF1-MS (Varian, Mississauga, ON, Canada) was coupled to 0.8 m × 0.25 mm × 0.25 μm SolGel-Wax phase second dimension column (SGE, Austin, TX, USA).

### 3.1.2 Liquid $N_2$ Delivery System

Figure 3-1 illustrates a diagram of the cryogen supply system. The custom-built cryogen system used a high-pressure (22 psi) liquid $N_2$ Dewar (Praxair Canada Inc., Mississauga, ON, Canada). A cryogenic valve (Asco Valve Canada, Brantford, Ontario, Canada) was used to control the flow of liquid $N_2$ out of the cooling jet. The design details will be described in the next section.

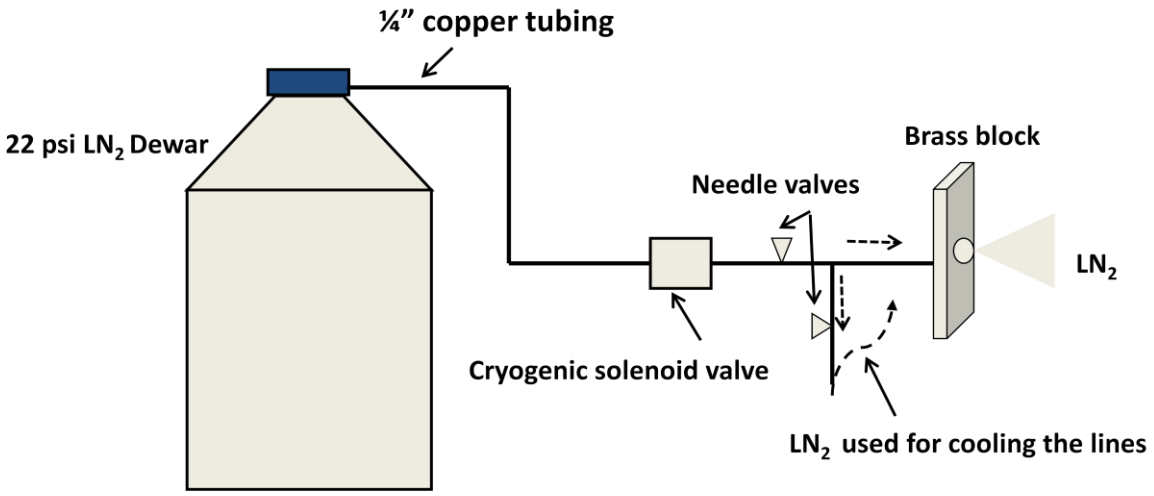


**Figure 3-1: Liquid $N_2$ supply system.**

### 3.1.3 Modulator design

A detailed depiction of the modulator design is shown in Figure 3-2. The modulator capillary was 10 cm × 0.32 mm deactivated fused silica tubing (Agilent Technologies, Mississauga, ON, Canada). The capillary was held in place and stretched between two 1/16 in. Swagelok tees mounted on the plate with custom-built clips. Nuts with graphite/vespel ferrules were used to accommodate the capillary and seal the ports of the Swagelok tees. The restriction in the trap was made in the form of a 3-4 mm plug of compressed fused silica wool (Restek Corp., Bellefonte, PA, USA) and quartz fiber filter (F & J Specialty Products Inc., Ocala, FL, USA) placed in the middle of the deactivated fused silica capillary using

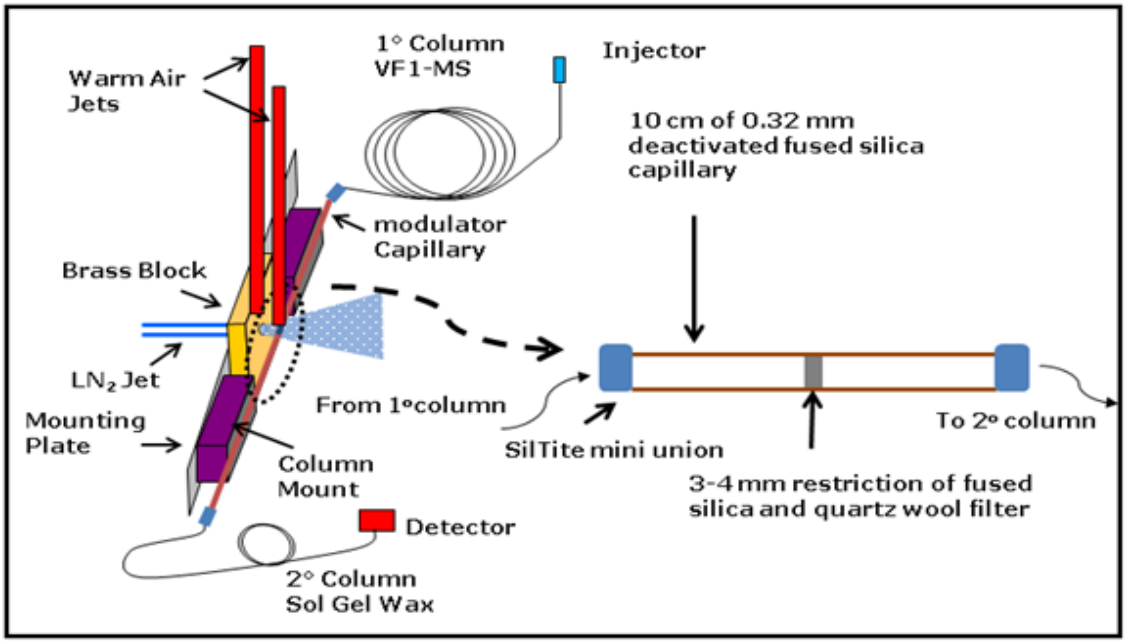


**Figure 3-2: Schematic diagram of the modulator design.**

a fused silica optical fiber (Polymicro Technologies, Phoenix, AZ, USA). All column connections were made using SilTite mini unions (SGE, Austin, TX, USA).

The $LN_2$ sprayed was collected through a 1/2 in. O.D. brass tube, mounted inside the oven facing the cryojet outlet and bent at $90^o$ angle. The collected $LN_2$ was directed out of the oven through its floor to avoid any possible effect of $LN_2$ on oven temperature.

### 3.1.4 Materials and procedures

A linear *n*-alkane test mixture consisting of *n*-pentane through *n*-tetracosane in $CS_2$ was prepared for testing of the modulator. The linear alkanes and $CS_2$ were obtained from Sigma-Aldrich (St. Louis, MO, USA). Regular unleaded gasoline and diesel fuel samples were obtained from a local gas station. Diesel fuel was diluted 1:10 in $CS_2$. A commercial Grob mixture (composed of 12 components including *n*-decane , *n*-undecane, 2,3-butanediol, dicyclohexylamine , 2,6-dimethylaniline, 2,6-dimethylphenol, 2-ethylhexanoic acid, nonanal, 1-octanol, methyl decanoate, methyl undecanoate and methyl dodecanoate dissolved in methylene chloride) was obtained from Restek Corporation (Bellefonte, PA, USA). Dimandja mixture components (*n*-octane, *n*-nonane, *n*-decane, *n*-undecane, *n*-dodecane, 1-hexanol, 1-heptanol, 1-octanol, 2-heptanone, 2-octanone, 2-nonanone, heptanal, nonanal, octanal and 2,6-dimethylaniline) were dissolved in *n*-hexane. They were all obtained

from Sigma-Aldrich (St. Louis, MO, USA). For studies of the modulator performance (analyzing the *n*-alkane mixture), the second column was replaced by an 80 cm segment of 0.25 mm ID deactivated fused silica capillary.

For the analysis of the alkane test mixture and diesel fuel sample, the temperature program started at 40 °C for 0.2 min, then was ramped to 280 °C at a rate of 6 °C/min, with a final hold time of 4 min. For gasoline, the final temperature of the oven program was changed to 220 °C, the rate was 4 °C/min, and the final hold time was 10 min. For the Grob mixture, the final temperature was changed to 225 °C, the rate was 10 °C/min and the final hold time was 1 min. For the Dimandja mixture, the oven was ramped to 180 °C at a rate of 10 °C/min, with no hold time.

The inlet temperature was 250 °C. It was operated in the split mode (1 μl split 100:1 for the alkane mixture and the Dimandja mixture; 0.2 μl split 50:1 for gasoline; and 1 μl split 50:1 for the Grob mixture and the diesel sample). The carrier gas was helium, delivered at a constant average velocity of 40 cm/s. The FID detector was operated at 320 °C and 100 Hz.

## 3.2 Results and discussion

### 3.2.1 Development of the cryogen supply system

The single-stage cryogenic modulator developed uses $LN_2$ as the cryogen to trap the analytes in an uncoated fused silica capillary with a restriction in the middle. $LN_2$ was used as the cryogen because $LCO_2$ or cooled $N_2$ gas are not capable of producing temperatures low enough to achieve trapping in uncoated capillaries. On the other hand, using $LN_2$ as the cryogen has some drawbacks. The entire system must be kept at a very low temperature to keep the cryogen in liquid phase, which is not the case when using $LCO_2$ that can be kept in the liquid state at room temperature under sufficient pressure. $LN_2$ consumption was an important factor that was kept in mind, thus one of the main objectives was to develop a system that reduced the $LN_2$ consumption and capable of delivering $LN_2$ to the jet reliably.

The system developed is shown in Figure 3-1. $LN_2$ was supplied directly from a high pressure (22 psi) $LN_2$ Dewar through 1/4 in. O.D. copper tubing. $LN_2$ flow was turned on and off through a two-way solenoid valve and was expelled through the cryojet made of 10 cm, 1/4 in. O.D. copper tubing welded into a 6 mm thick brass bracket. Copper tubing with 1/4 in. O.D. was used because smaller diameter tubing had too large a surface area which led to rapid boiling and evaporation of $LN_2$. On

the other hand, using larger diameter tubing caused the $LN_2$ to be expelled from the croyjet at very high flow rate, which caused overcooling of the trap. Therefore, a needle valve was mounted in the path of the flow right after the solenoid valve, thus the flow could be reduced. Though the needle valve helped reduce the $LN_2$ flow, the cooling was still excessive. Thus, a 1/4 in T was connected to the needle valve to split the flow and another needle valve was mounted to control the $LN_2$ flow going to the cryojet (Figure 3-1). The excess $LN_2$ coming through the second needle valve was directed through 1/4 in. O.D. copper tubing wrapped tightly around the solenoid, needle valves and connectors in the interface, thus continuously cooling the entire interface and carrying away the excess heat produced by the solenoid valve from the main $LN_2$ delivery path. All lines were thermally insulated.

The configuration described above was capable of delivering $LN_2$ to the cryojet efficiently. In addition, the consumption of $LN_2$ was significantly reduced to ~ 30 L per day versus 50 to 100 L per day for the commercially available cryogenic modulators. [62] This consumption could most likely be reduced even further by the use of better thermal insulation for the connection lines and the valves.

### 3.2.2 Development of warm air jets

Though the trapping capillary would heat up quite quickly in the oven on its own without any additional warm air jets, the heating timing was not reproducible. Consequently, a warm jet was mounted approximately 5 mm above the trapping capillary to blow compressed air at oven temperature towards the middle of the capillary. Though this helped somewhat, the desorption was still irreproducible. Therefore, a rope heater (FGR-030, OMEGA Engineering Limited, Laval (Quebec), Canada) was wrapped around the warm air jet coil to help heat the air inside. A temperature controller (CN742, OMEGA Engineering Limited, Laval (Quebec), Canada) was used to control the warm air jet temperature. A temperature offset was controlled through connecting two k-type thermocouples (5TC-GG-K-20-36, OMEGA Engineering Limited, Laval, Quebec, Canada) differentially to the temperature controller with one of the thermocouples spot welded to the warm air jet coil (kept inside the GC oven) and the other one connected to the GC oven itself. To help prevent the build-up of ice on the cryojet nozzle, another warm air jet was mounted to blow compressed air at oven temperature across the face of the cryojet nozzle when the cold jet was off (Figure 3-3). The flow of compressed air through the two warm air jets was controlled in such a way that the flow would turn on

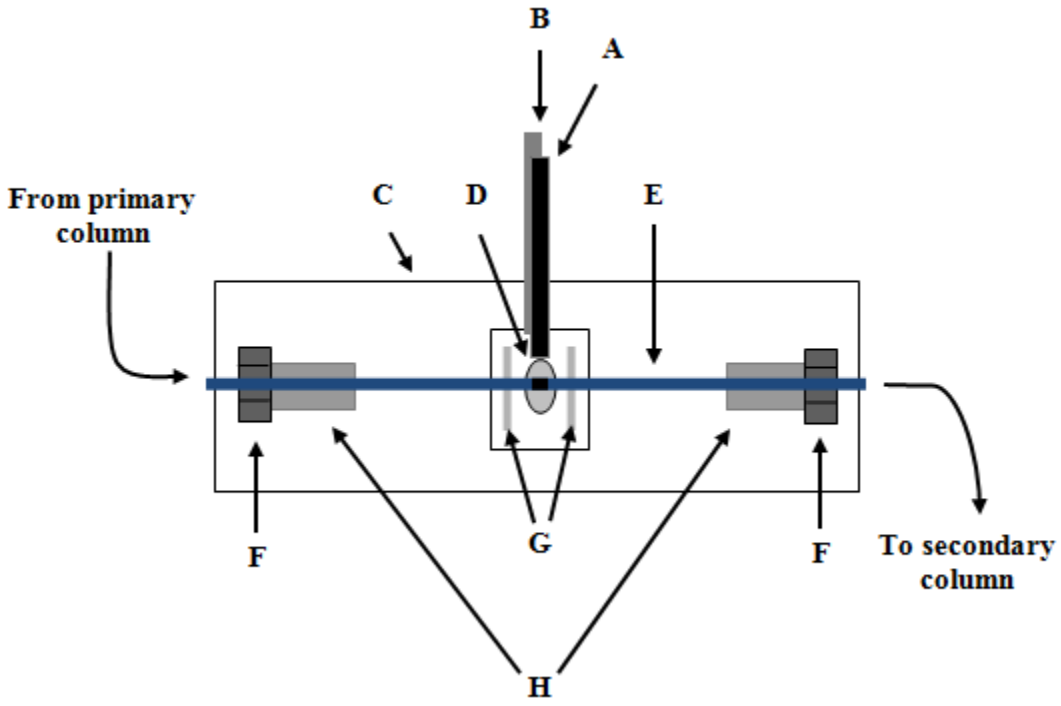


**Figure 3-3: Front view of the cryojet mount. (A) Warm air jet for desorption; (B) Warm air jet blowing across the cryojet nozzle to prevent ice build-up; (C) Mounting plate; (D) Brass block with cryojet nozzle; (E) Deactivated fused silica capillary with the trapping plug packed in the middle; (F) Nuts with vespel/graphite ferrules; (G) Jet alignment slots and screws; (H) 1/16″ Swagelok tees.**

when the cryojet was off, and then off for trapping when the cryojet was on. The warm air supply is shown in Figure 3-4.

### 3.2.3 Trapping capillary

Initially a segment of deactivated fused silica capillary, 0.1 mm I.D., was used as the single-stage trap and connected to the primary and the secondary column. Even

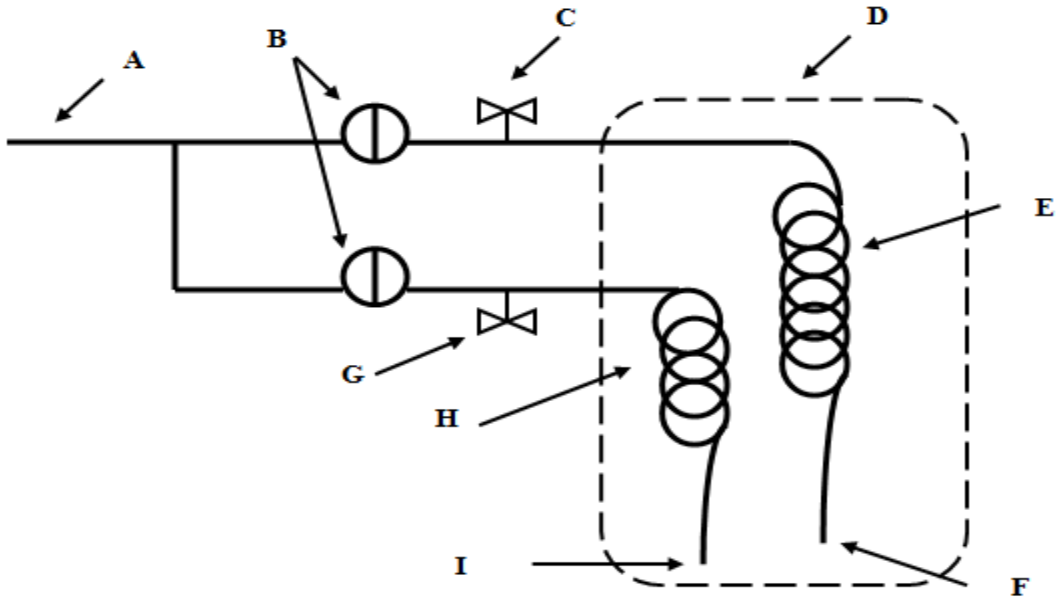


**Figure 3-4: Warm air supply system. (A) 80 psi nitrogen; (B) Solenoid valves controlled electrically through the modulator electrical box (turned on when the cryojet is off); (C) Needle valve for desorption jet regulation; (D) GC oven; (E) Desorption jet coil with the rope heater wrapped around; (F) Flow towards trapping capillary for desorption; (G) Needle valve for cryojet defrost jet regulation; (H) Cryojet defrost jet coil; (I) Flow towards the cryojet nozzle.**

though using $LN_2$ as the cryogen achieved trapping temperature low enough to trap all of the analytes, breakthrough was observed (Figure 3-5). This was mainly attributed to the fact that radial diffusion was too slow for analytes near the centre of the column to reach the walls of the capillary while they travelled through the relatively short distance that was cooled by the jet (~ 5 - 7 mm), and trapping could occur only when a collision with the wall took place. More importantly, the trapping

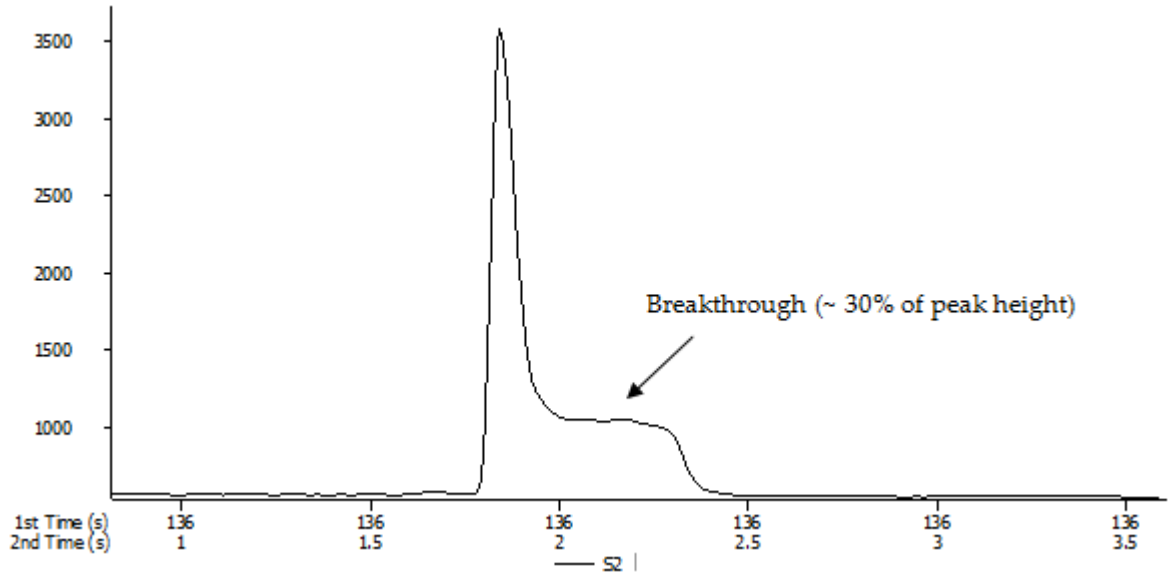


**Figure 3-5: *n*-pentane peak modulation using 100 μm I.D. deactivated fused silica capillary showing characteristic chair-shape peak due to breakthrough (~ 30% of peak height).**

position did not constitute sufficient restriction to carrier gas flow. The idea to overcome this problem was to produce a significant restriction to the carrier gas flow through the incorporation of a small plug composed of compressed fused silica wool and quartz fiber filter (~ 3 - 4 mm) in the centre of the capillary. This plug provided increased surface area for the analytes passing through the trap without significantly increasing its thermal mass. In addition, it provided a significant restriction to the carrier gas flow when the trapping capillary was at the oven temperature. This was due to the increase in the carrier gas viscosity with increasing temperature. At the very low trapping temperature, the viscosity of the carrier gas

decreased so low that the plug offered a negligible resistance to the flow of the carrier gas.

While viscosity of liquids decreases with increasing temperature, viscosity of gases increases with increasing temperature. As a gas is heated, the movement of gas molecules increases, thus increasing the probability that one gas molecule will collide with another gas molecule. In other words, increasing gas temperature causes the gas molecules to collide more often. This increases the gas viscosity because the transfer of momentum between stationary and moving molecules is what causes gas viscosity.

The big challenge in this project was in the construction of the trap inside the capillary regarding the packing procedure and keeping the plug in place without being dislodged by the flow of the carrier gas. A 0.53 mm I.D. deactivated fused silica capillary was used initially with two short supporting segments of 0.32 mm I.D. deactivated fused silica capillaries whose polyimide coating was removed and deactivated to make sure that there were no active sites. The deactivation and removal of the polyimide coating of these segments was performed by heating at 150 °C in conc. $H_2SO_4$ for 15 min. These support segments helped keep the plug in place without moving down with the carrier gas flow. Metal wires were used as

packing rods. Unfortunately, this was not very successful as during the packing procedure, the fused silica capillary was scratched on the inside, making it too fragile. Even when it did not break, the presence of the supporting segments inside the capillary caused mechanical difficulties during the connection of the trapping capillary with the primary and secondary columns. When construction was successful, the trap did not last for a long time before it broke. Nevertheless, the results obtained from these runs were promising with peak widths at half height of 116, 107 and 106 ms for *n*-$C_5$, *n*-$C_{12}$ and *n*-$C_{19}$ peaks, respectively (Figure 3-6). Thus, smaller inner diameter fused silica capillaries were used such as 0.32 mm and 0.25 mm I.D. Better results were obtained (Table 3-1) but similar problems remained. Therefore, it was tried to keep the plug in place without the use of the supporting capillaries, but the plug moved in the stream of the flow of the carrier gas.

A further attempt was to construct the trap within a 0.25 mm I.D. Silcosteel capillary that was tapered in the middle. The plug was packed within the capillary with no difficulty. Due to the high thermal mass of this capillary, however, the heating and cooling were not fast enough, which resulted in multiple peaks for the same analyte (Figure 3-7).

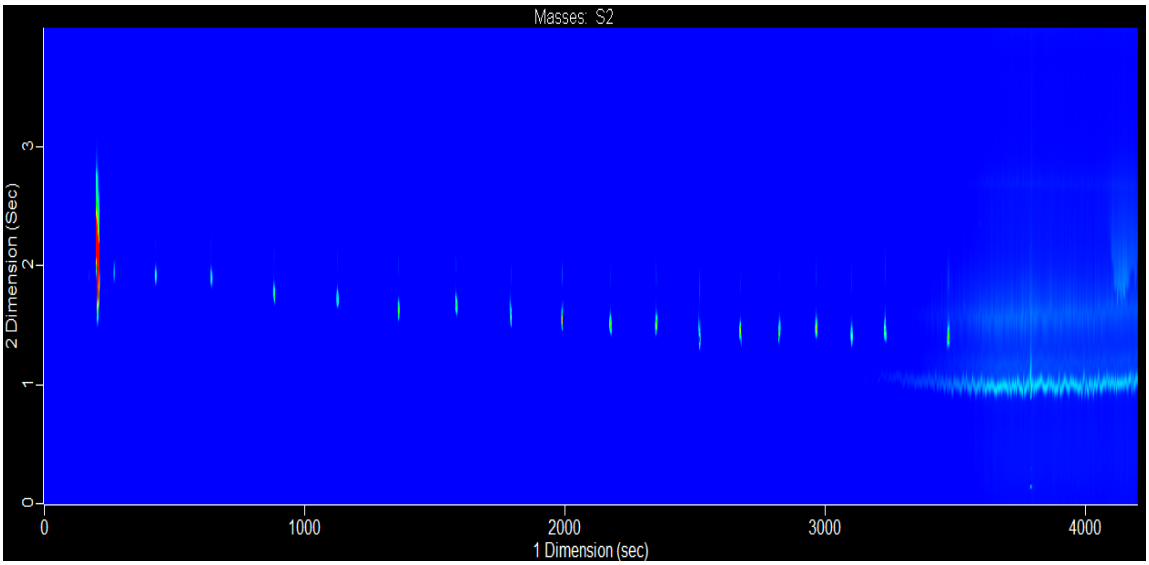


**Figure 3-6: 2D chromatogram of *n*-$C_5$ to *n*-$C_{24}$ alkanes in $CS_2$ using 0.53 mm I.D. deactivated fused silica capillary with two short supporting segments of 0.32 mm I.D. deactivated fused silica capillary to keep the plug in place.**

**Table 3-1: Peak widths at half height of *n*-alkanes using different trapping capillaries with fused silica restriction inside**

| Trapping capillary | Alkane (peak width at half height) | | |
|---|---|---|---|
| | ***n*-$C_5$** | ***n*-$C_{12}$** | ***n*-$C_{19}$** |
| 0.53 mm I.D. fused silica (with inside supporting capillaries) | 116 | 107 | 106 |
| 0.25 mm I.D. Silcosteel capillary | 50 | 86 | 588 |
| Press-fit union | 115 | 117 | 407 |
| 0.32 mm I.D. fused silica | 35 | 40 | 51 |
| 0.25 mm I.D. fused silica | 35 | 41 | 50 |

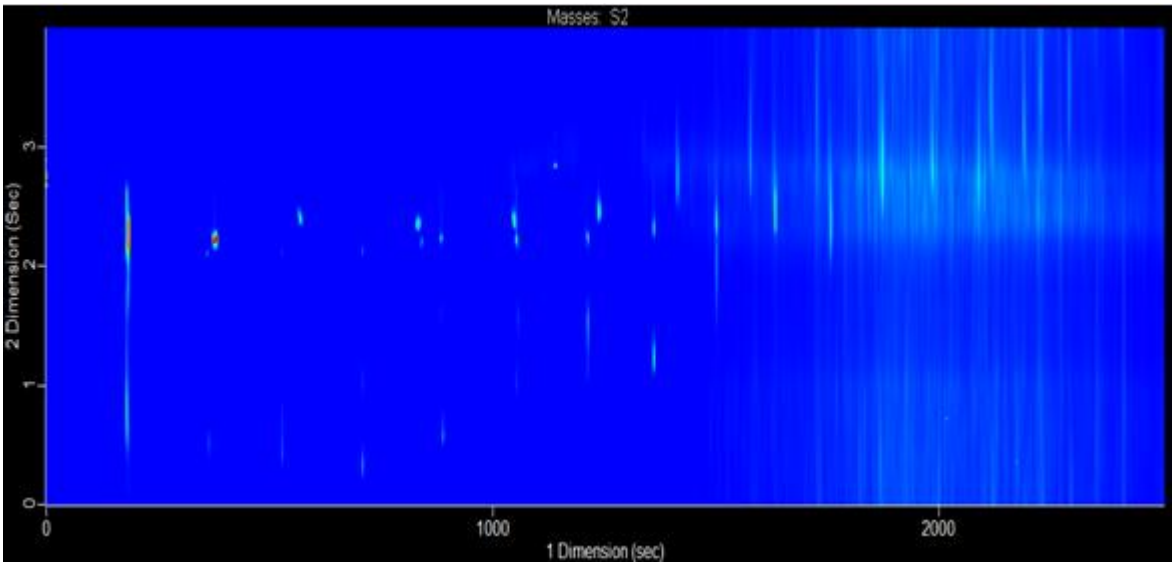


**Figure 3-7: 2D chromatogram of *n*-$C_5$ to *n*-$C_{24}$ alkanes in $CS_2$ using 0.25 mm I.D. Silcosteel capillary with fused silica wool restriction inside.**

Another attempt was performed using a press-fit connection with the restriction plug packed in the middle and the two columns connected to it. This configuration provided better results than the Silcosteel capillary (Figure 3-8), but because of the thick walls of these connections broader peaks were produced due to slower cooling and heating rates (Table 3-1). Therefore, It was decided to use fused silica as it achieved the best results. Packing this time was accomplished using an optical fiber (0.27 mm O.D.) obtained from Polymicro Technologies, which helped not to scratch the inside of the capillary. Meanwhile, the plug was kept and sintered in place by

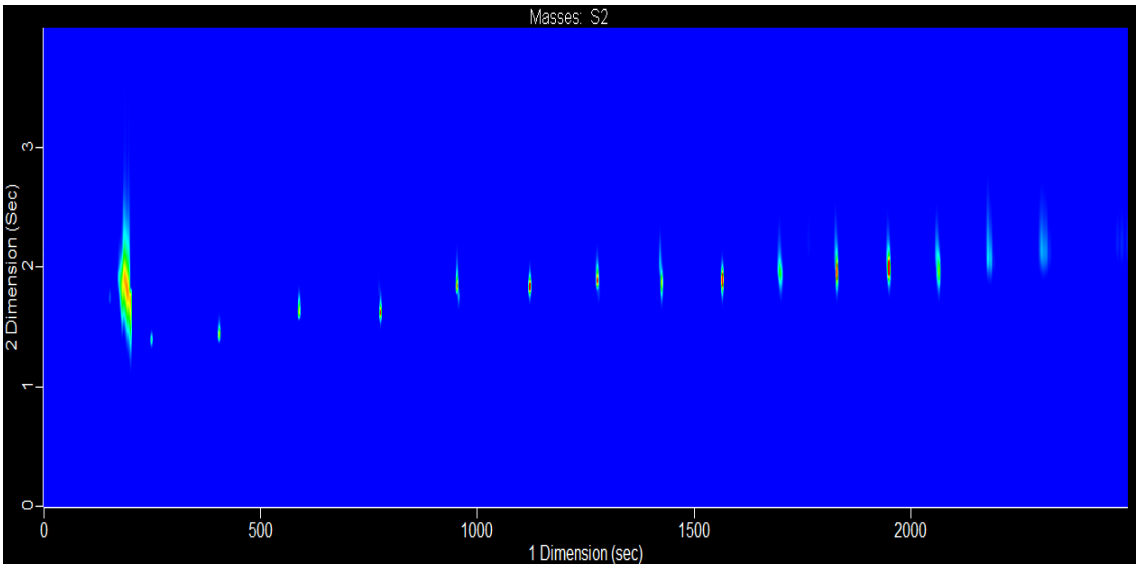


**Figure 3-8: 2D chromatogram of *n*-$C_5$ to *n*-$C_{24}$ alkanes in $CS_2$ using press-fit union connection.**

passing the portion of the capillary containing the plug through Ronson TechTorch® flame (Ronson Corp., Mississauga, Ontario, Canada) twice. This helped solve the construction problem of the trap. Peak widths of 35, 40 and 51 ms at half height were obtained for *n*-$C_5$, *n*-$C_{12}$ and *n*-$C_{19}$ peaks, respectively (Table 3-1).

Once the trapping capillary was constructed, the effect of the restriction plug on the flow of the carrier gas was tested experimentally. One end of the trapping capillary was connected to the primary column outlet, and the other end was connected to a flow meter. Various inlet pressures were applied and the flow through the capillary was measured when the $LN_2$ was off. Then the flow was

measured again when the $LN_2$ jet was on. When the $LN_2$ jet was on, the flow of the carrier gas was much higher than the flow when $LN_2$ jet was off. Once the $LN_2$ flow was reactivated, the carrier gas flow immediately increased again. (Table 3-2)

The thermal characteristics of the 0.25 mm I.D. fused silica capillary was studied. [25] Heating and cooling of the capillary was reproducible. The capillary reached 90% of the oven temperature in about 250 ms and reached 90% of the final trapping temperature in about 200 ms.

**Table 3-2: Effect of temperature on carrier gas flow through the 0.32 mm ID deactivated fused silica capillary with fused silica wool plug.**

| Inlet pressure (psi) | Flow (ml/min) at 30 °C | |
|---|---|---|
| | $LN_2$ jet off | $LN_2$ jet on |
| 9 | 0.2 | 1.4 |
| 12 | 0.2 | 1.6 |
| 25 | 0.9 | 5.9 |
| 33 | 1.3 | 8.4 |

### 3.2.4 Modulator performance

#### 3.2.4.1 Propane modulation

For initial testing of the interface, propane from a continuous source (a hand-held torch) was injected with the oven isothermal at 40 °C using 4 s modulation period and 0.8 s hot pulse time. The negative peaks in Figure 3-9 illustrate the modulation of the carrier gas flow i.e. the significant decrease in the carrier gas flow due to increasing viscosity when the carrier gas temperature was increased. FID is a mass-

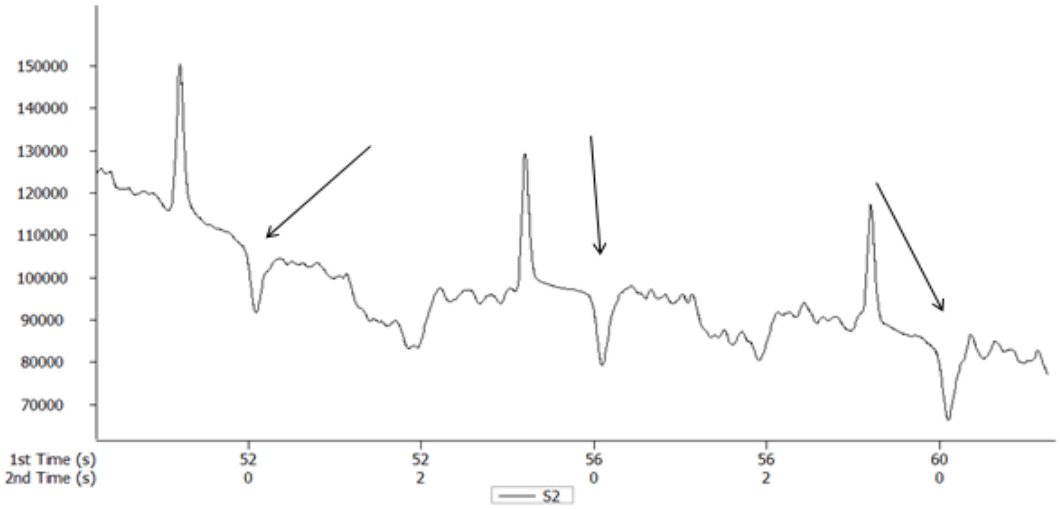


**Figure 3-9: Performance testing of the modulator with propane showing changes in carrier gas flow. The negative peaks indicates the significant decrease in the carrier gas flow.**

-sensitive detector, therefore the peak area depends on the absolute amount of propane arriving at the detector. When the carrier gas temperature was increased, the viscosity increased as well, and the flow of the carrier gas was significantly reduced by the fused silica wool plug at the trapping capillary. The mass of propane reaching the detector was significantly decreased creating these negative peaks. The positive peaks show the powerful trapping capabilities of the developed modulator to trap and modulate propane ($C_3$) without tailing or breakthrough.

#### 3.2.4.2 Performance testing with test mixtures

To test the developed interface with a broader range of compounds, a mixture of *n*-$C_5$ to *n*-$C_{24}$ in $CS_2$ was analyzed with a modulation period of 4 s. The performance of the interface can be assessed through the peak shapes and widths. Figure 3-10 A presents a 2D chromatogram of *n*-$C_5$ to *n*-$C_{24}$ alkanes in $CS_2$ showing very sharp peaks. Peak widths of 60 and 65 ms at the base were obtained with practically no breakthrough (Figure 3-10B and C). Figure 3-10 D and E show a closer view of *n*-$C_5$, $CS_2$ and *n*-$C_6$ peaks with efficient trapping and modulation of the volatile injection solvent ($CS_2$) (will be discussed later).

The interface developed was also tested in the analysis of a commercial Grob mixture sample, which contained various classes of organic components including

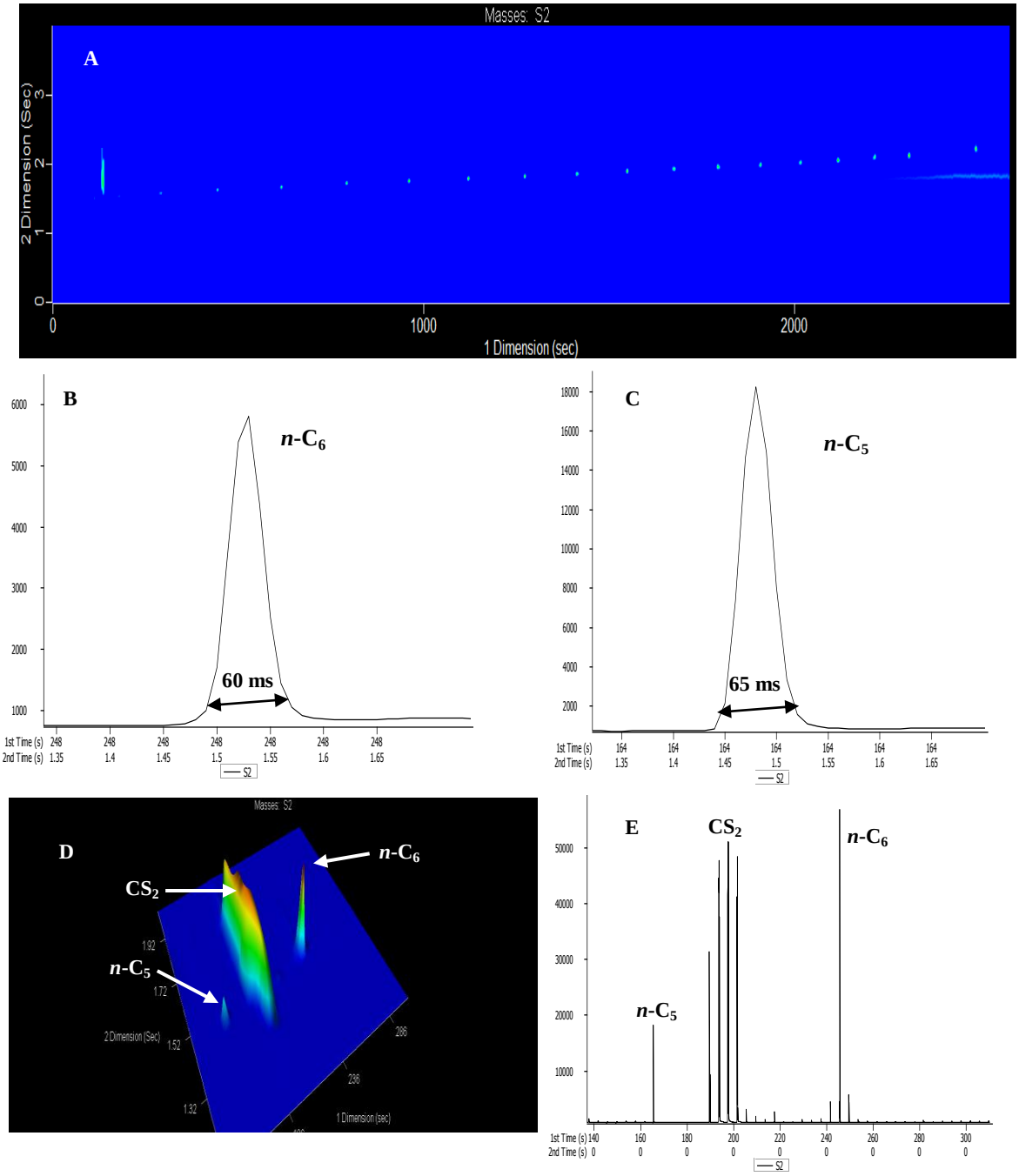


**Figure 3-10: Analysis of *n*-alkane mixture (*n*-$C_5$ to *n*-$C_{24}$ in $CS_2$). 2D contour plot (A). Close up view of hexane (B) and pentane (C) peaks showing practically no breakthrough. *n*-$C_5$, $CS_2$ and *n*-$C_6$ surface plot (D) and raw chromatogram (E).**

hydrocarbons, esters, aldehydes, acids, bases and alcohols to test the performance of the modulator in trapping a wide range of different polarity components. Figure 3-11 shows a 2D contour plot chromatogram of the mixture. For clarity of presentation, the solvent peak (methylene chloride), which was perfectly trapped (will be discussed later), was removed from the display. All 12 peaks were very sharp with no tailing or breakthrough even for analytes that are known to be problematic in their chromatographic separation, such as acids, amines and diols.

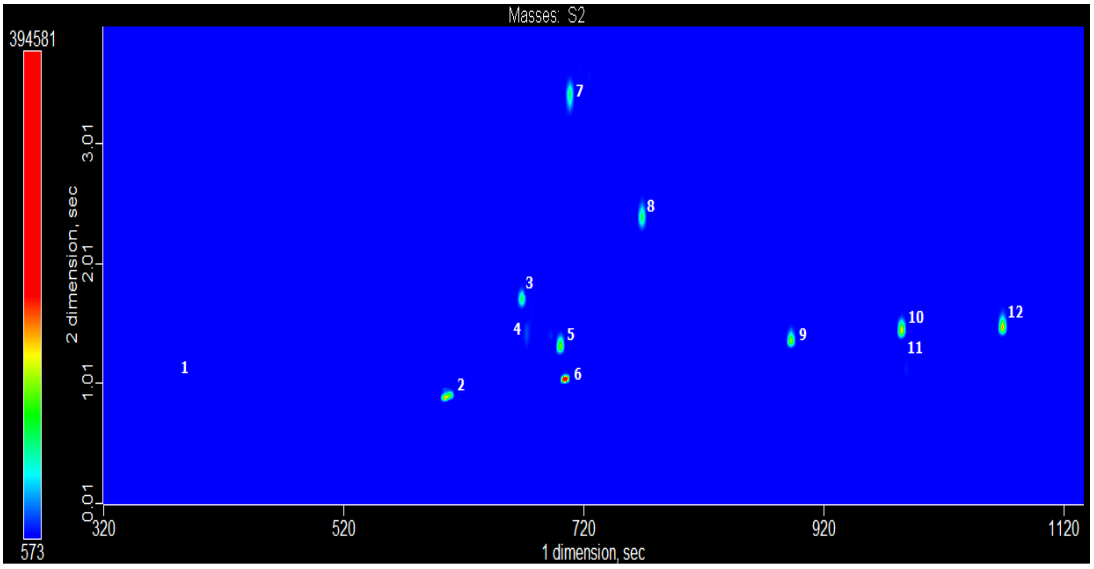


**Figure 3-11: GC×GC chromatogram of the Grob mixture. Compound identification: (1) 2,3-butanediol; (2) n-decane; (3) 1-octanol; (4) 2-ethylhexanoic acid; (5) nonanal; (6) n-undecane; (7) 2,6-dimethylphenol; (8) 2,6-dimethylaniline; (9) methyl decanoate; (10) dicyclohexylamine; (11) methyl undecanoate; (12) methyl dodecanoate.**

The Dimandja mixture was analyzed as well to test the performance of the modulator in trapping components with a wide range of polarities. As can be seen in Figure 3-12, the 15 components of the Dimandja mixture were efficiently modulated showing sharp peaks with no tailing or breakthrough. The *n*-hexane solvent peak (which was perfectly trapped) was removed from the display for clarity.

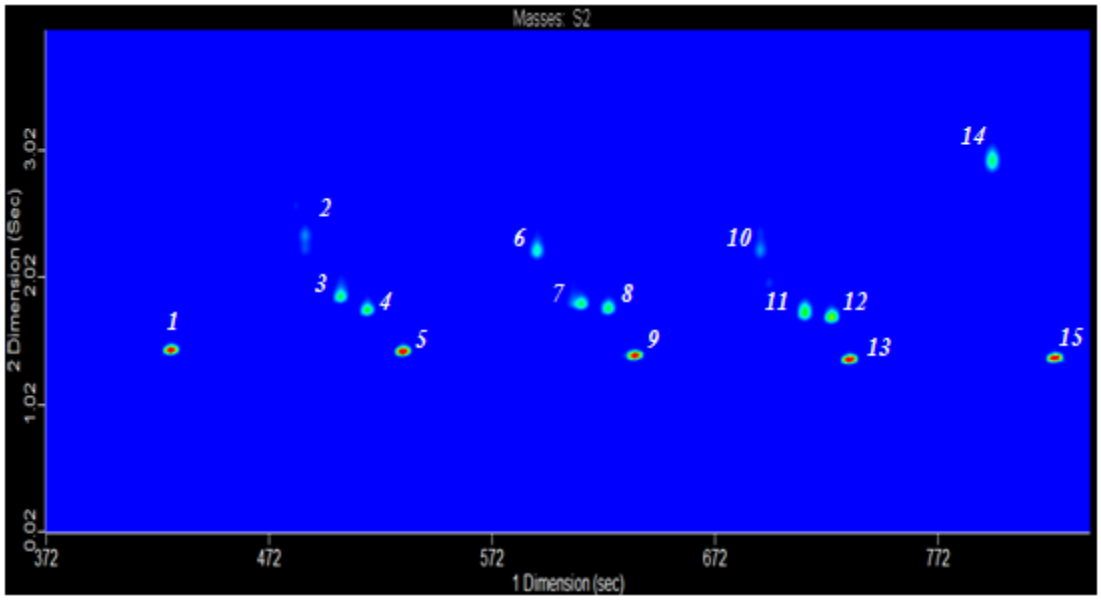


**Figure 3-12: GC×GC chromatogram of the Dimandja mixture. Compound identification: (1) *n*-C$_8$; (2) 1-hexanol; (3) 2-heptanone; (4) heptanal; (5) *n*-C$_9$; (6) 1- heptanol; (7) 2- octanone; (8) octanal; (9) *n*-C$_{10}$; (10) 1- octanol; (11) 2- octanone; (12) octanal; (13) *n*-C$_{11}$; (14) 2,6- dimethylaniline; (15) *n*-C$_{12}$.**

### 3.2.4.3 Solvent trapping and modulation

One of the most interesting and impressive results obtained during the development of this interface was the capability to perfectly trap and modulate the volatile injection solvents. As can be seen in Figure 3-10 D and E, the solvent peak of $CS_2$ was perfectly trapped and modulated without any tailing or breakthrough. Figure 3-13 shows the perfect trapping and modulation of methylene chloride peak (Grob mixture solvent). To the best of our knowledge, none of the commercially available or commonly used thermal modulators is capable of efficient trapping and modulating volatile injection solvents. This is very important when some of the analytes of interest elute close to the solvent peak, thus permitting their detection and quantification precisely.

### 3.2.4.4 Performance testing with real samples

The interface developed was tested in the analysis of regular unleaded gasoline. Numerous chromatograms have been published in the literature using different GC×GC interfaces. [23, 25, 187, 188] Gasoline is a useful sample to compare interface performance to that of other interfaces. Figure 3-14 shows a GC×GC chromatogram of regular gasoline obtained with the newly developed single-stage modulator. Good peak shapes with no tailing or breakthrough for any peak, especially those

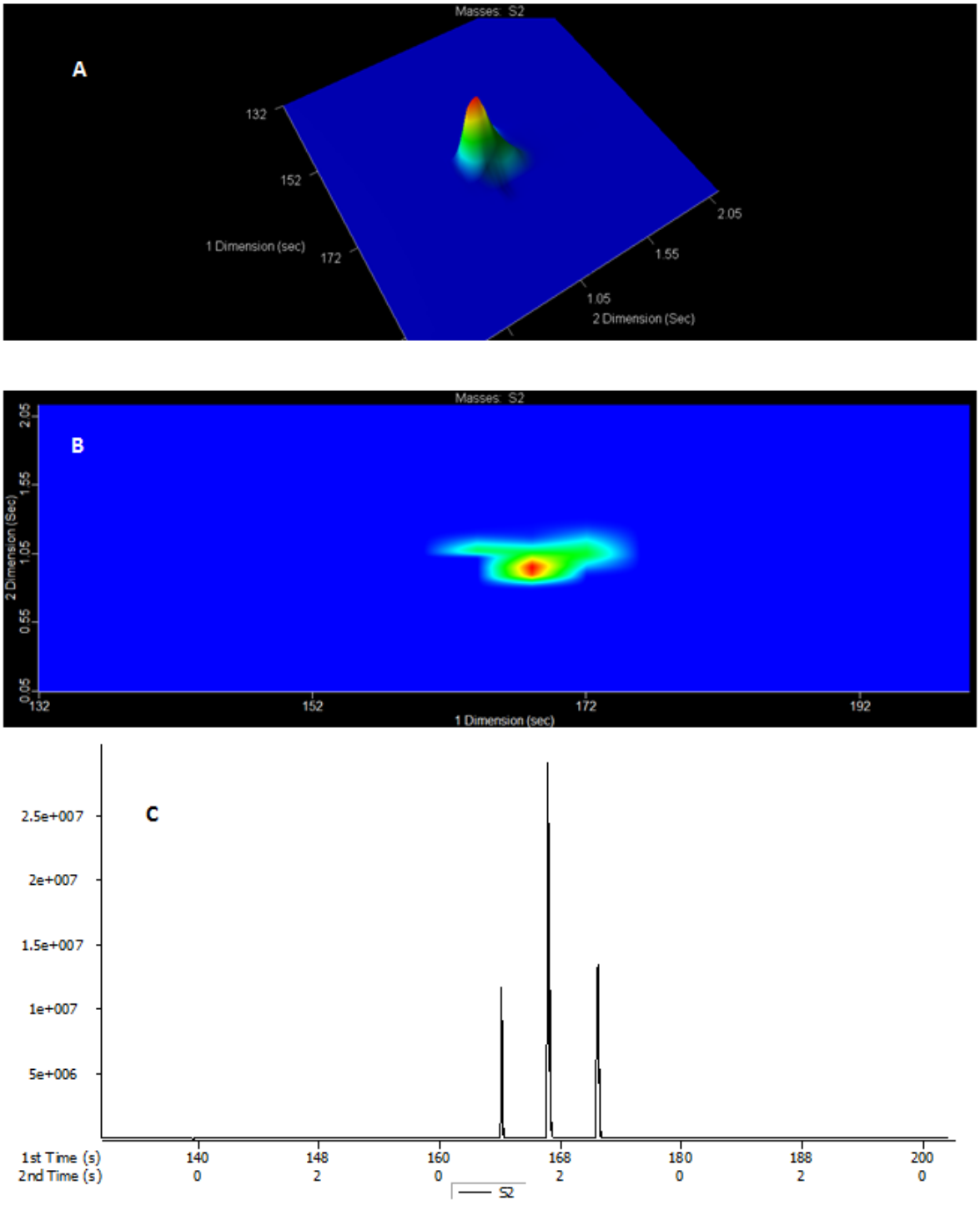


**Figure 3-13: Methylene chloride (Grob mixture solvent) trapping and modulation. (A) Surface plot; (B) Contour plot; (C) Raw GC×GC trace.**

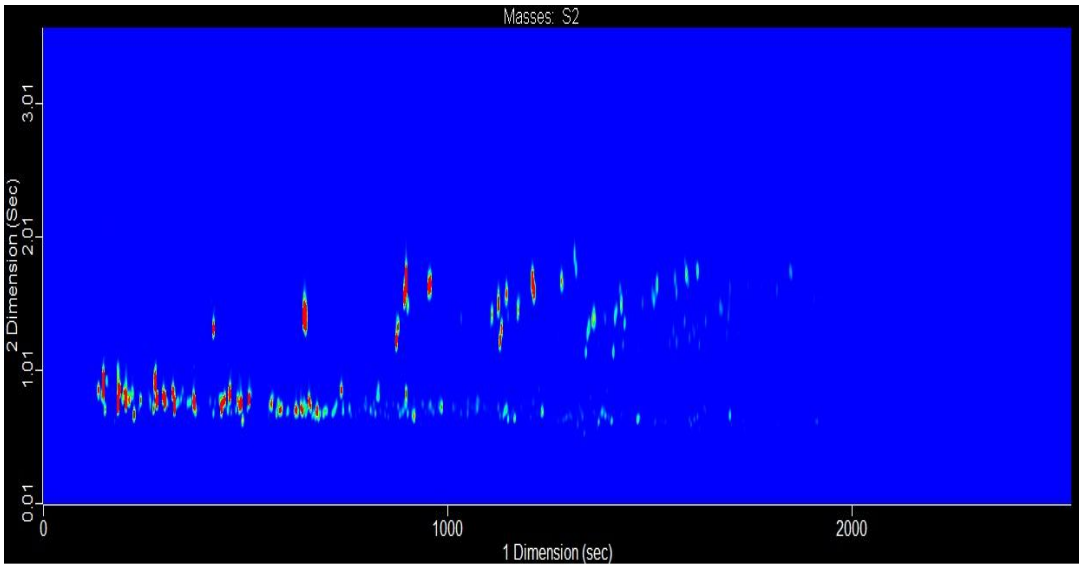


**Figure 3-14: GC×GC contour plot chromatogram of regular gasoline.**

eluting at the beginning of the chromatogram, were observed.

Figure 3-15 shows the GC×GC chromatogram of a diesel fuel sample. The chromatogram presents sharp peaks with no tailing or breakthrough and shows distinct bands of analytes grouped by specific chemical characteristics.

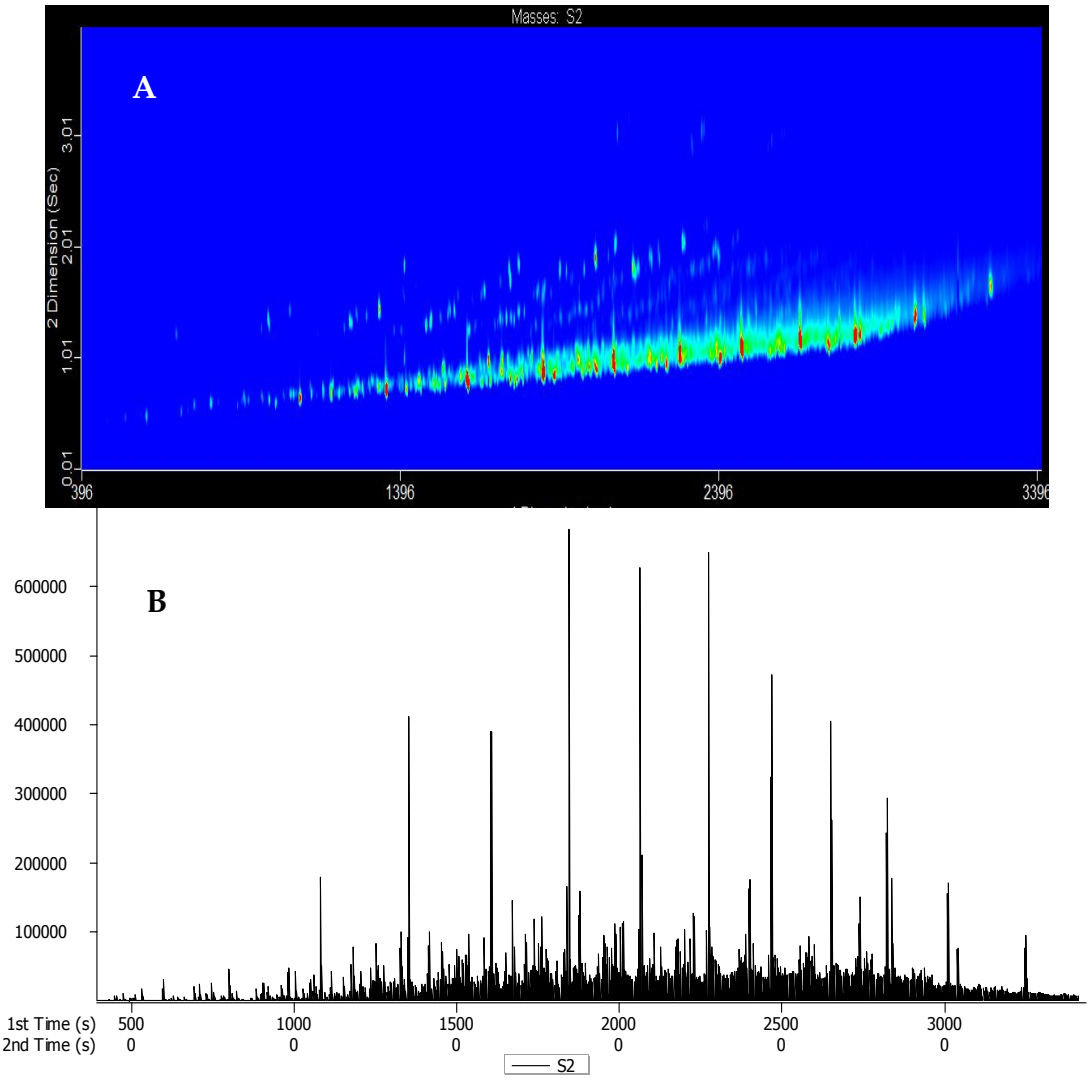


**Figure 3-15: GC×GC chromatogram of diesel fuel sample: (A) 2D contour plot; (B) raw GC×GC trace.**

## 3.3 Conclusions

Single-stage modulation is a viable alternative to more complicated dual-stage designs. Band breakthrough during injection can be prevented by using changes in carrier gas viscosity with temperature to reduce the carrier gas flow during desorption. In addition, the newly developed $LN_2$ delivery system reduces the $LN_2$ consumption. Very sharp peaks with no tailing or breakthrough were obtained; even the volatile injection solvents were perfectly trapped and modulated.

# Chapter 4

# Characterization of Volatile Components of Pinotage Wines Using Comprehensive Two-Dimensional Gas Chromatography Coupled to Time-of-Flight Mass Spectrometry (GC×GC-TOFMS)[i]

As discussed in Chapter 1, GC×GC is a powerful separation technique, especially when it is coupled with TOFMS . In the next chapters, the applications of this technique in the analysis of some highly challenging matrices such as natural products including South African wine and Polish honeysuckle berries will be presented.

The aroma of wine is an essential characteristic in product evaluation and therefore plays an important role in consumer preference. Wine aroma is determined by the combined effects of several hundreds of chemically diverse volatile compounds.[189] Numerous odor-active compounds already exist in the grape; still, many more are produced during fermentation and maturation.[190] Their

[i] This chapter is based on the author's paper " Characterization of volatile components of Pinotage wines using comprehensive two-dimensional gas chromatography coupled to time-of-flight mass spectromery (GC×GC-TOFMS)". [98]
Data analysis was spearheaded at the University of Stellenbosch; however, it was also done by the author independently.

combined influence contributes to the character of wine and distinguishes one wine from another. Pinotage is a unique South African red wine cultivar cross-bred from Pinot Noir and Cinsaut varieties in mid 1920s. It is known for its distinctive fruity character.[191, 192] In order to characterize the unique qualities of Pinotage wines, elucidation of the compounds that contribute to the aroma and flavor of this variety is important.

Wine volatiles are commonly analyzed using GC. Since these compounds may exist at widely varying concentrations, ranging from ng/L to per cent level, proper sample preparation prior to GC analysis is essential. Common sample preparation techniques include liquid-liquid extraction (LLE)[193] and solid phase extraction (SPE); [194] solid phase microextraction (SPME) [189] and stir bar sorptive extraction (SBSE) [195, 196] have also been successfully applied for these analyses. Nevertheless, despite extensive research, universal sample preparation and analysis techniques suitable for the analysis of compounds with varying physicochemical properties from a complex matrix such as wine remain a challenge.

Due to the complexity of wine volatile fractions, identification and quantitation of its constituents (especially minor ones) using conventional one-dimensional chromatography is hampered by frequent co-elutions, even when using high-efficiency capillary columns, selective stationary phases and programmed oven

temperature conditions. GC×GC is a much more powerful technique for the analysis of complex volatile fractions. Therefore we were approached by colleagues at the University of Stellenbosch, South Africa to perform this analysis using GC×GC. This technique has been successfully applied to the analysis of flavor compounds in different food matrices such as cheese, [197] pepper,[198] oil,[199] sour cream,[200] coffee beans,[201] honey,[200] fish,[202] etc. Ryan et al. [155] used GC×GC in combination with nitrogen phosphorus detection and TOFMS for the identification of methoxypyrazines in Sauvignon Blanc wine. Other authors [203, 204] applied GC×GC for the analysis of grape volatiles. The combination of GC×GC with TOFMS adds an extra dimension of information in terms of full mass spectral data acquisition and mass spectral continuity, which permits the deconvolution of spectra for co-eluting peaks.[204, 205]

To date, few literature reports have dealt with Pinotage volatiles. Limited qualitative and quantitative data pertaining mainly to the major volatiles common to most wines have been reported. [195, 196, 206, 207] In the present work the volatile constituents of nine young Pinotage wine samples of 2006 vintage determined by GC×GC-TOFMS is reported. Initial results were limited to those compounds extracted using a generic HS-SPME method and previously identified in wine and wine-related samples. Further research into potential changes in Pinotage aroma

due to malolactic fermentation during vinification will be reported in Chapter 5. To the best of our knowledge, no in-depth study on Pinotage volatile composition has been reported to date.

## 4.1 Experimental

### 4.1.1 Instrumentation

The GC×GC system consisted of an Agilent 6890 GC (Agilent Technologies, Palo Alto, CA, USA) equipped with a single jet, liquid nitrogen cryogenic modulator and coupled to a Pegasus III time-of-flight mass spectrometer (LECO Corp., St. Joseph, MI). [25] The column set consisted of a 30 m × 0.25 mm I.D. × 1.00 μm $d_f$ VF-1 (Varian, Mississauga, ON) as a primary column coupled to a 1.5 m × 0.25 mm I.D. × 0.25 μm $d_f$ SolGel-Wax phase second dimension column (SGE, Austin, TX). A modulation period of 4 s was used with the cryogenic trap cooled to –196 °C using liquid nitrogen. The separation was performed using the following temperature program: initial temperature 40 °C, kept for 0.2 min, ramped at 3 °C/min to 225 °C and held for 10 min. The injector was operated at 275 °C in the splitless mode, with a splitless time of 2 min. Hydrogen was used as carrier gas at a constant flow of 0.8 mL/min and an initial inlet pressure of 18.2 psi. The transfer line was maintained at 250 °C.

Ions in the mass range 35 - 250 amu were acquired at a rate of 50 spectra/s. The ion source temperature was 225 °C and the detector voltage was set to -1595 V.

### 4.1.2 Samples, chemicals and materials

A total of 9 young Pinotage wines from 2006 vintage were obtained from the South African Young Wine Show. Each wine was from a different producer and geographical origin in South Africa. The wines were transferred under argon to completely filled amber vials and shipped to the University of Waterloo (ON, Canada) for analysis. NaCl (ACS grade) was obtained from EMD Chemicals (Gibbstown, NJ.), while $C_6$ to $C_{18}$ *n*-alkanes (99%) used for linear retention index determination were from Sigma-Aldrich (St. Louis, MO). A carboxen/polydimethylsiloxane (CAR/PDMS, 75 μm) SPME fiber was used (Supelco, Belletonte, PA). Water for blank determinations was purified using Barnstead Nanopure water purification system (Thermo Scientific, Mississauga, ON).

### 4.1.3 Sample preparation

Sample preparation was based on a slightly modified method described by Setkova et al.[208] Ten milliliter aliquots of the samples were transferred to 20 mL crimp-top headspace vials. Five gram aliquots of ACS grade sodium chloride, pre-baked at 250 °C and cooled to room temperature before use, were added to the vials

together with PTFE-coated stir-bars. The vials were then sealed immediately with PTFE-lined septa and aluminum crimp-top caps using a hand crimper. The resulting solutions were maintained at a temperature of 23 °C in a water bath before sampling. SPME in the headspace mode was performed for ten minutes with stirring at 500 rpm, followed by desorption of the fiber in the GC split/splitless injector port at 275 °C for 5 min. After the analysis, selected SPME fibers were desorbed again for 5 min at 275 °C in the injector port. No sample carryover was observed, but fiber blanks showed the presence of petroleum hydrocarbons, most likely picked from laboratory air. System blanks were run daily prior to sample analysis to confirm cleanliness of the system. All analyses were performed in duplicate.

**4.1.4 Data analysis**

Data processing was performed automatically using the peak detection algorithm of the ChromaTOF software (LECO Corp. version 2.22). Compounds were identified using authentic standards (when available), while for the rest tentative identification was based on mass spectra comparison with NIST 05 and Wiley 275 libraries. A series of *n*-alkanes ($C_6$ -$C_{18}$) were also analyzed to establish $^1$D retention indices ($RI_1$) for each peak. Experimental retention indices ($RI_{exp.}$) were calculated according to [209] and compared to literature values ($RI_{lit.}$) for identification purposes. A

chromatographic blank run with the fiber was performed and necessary corrections were applied for the compounds observed in the samples.

## 4.2 Results and discussion

To date, very few studies on the volatile composition of Pinotage have been reported. [195, 196] These studies exclusively used conventional capillary GC on polar (wax) phases and at most ~40 compounds have been identified and quantified. Advanced chromatographic techniques are required for the detailed investigation of the volatile composition of Pinotage wines, in order to benefit local producers. Taking this into account, GC×GC-TOFMS was used in the current investigation for the purpose of in-depth characterization of Pinotage volatiles. In addition to the significantly enhanced resolving power of this technique, it also offers improved signal to noise ratios, as explained in Chapter 2, and the power of spectral deconvolution using TOFMS.

In complex matrices such as wine, containing a large number of volatiles of wide-ranging physicochemical properties, frequent co-elutions are observed on any single stationary phase. This limitation is overcome in GC×GC by subjecting the sample to separation based on two different mechanisms, e.g. vapor pressures in $^{1}$D and polarity in $^{2}$D. Figure 4-1 illustrates the benefits of this approach for wine analysis.

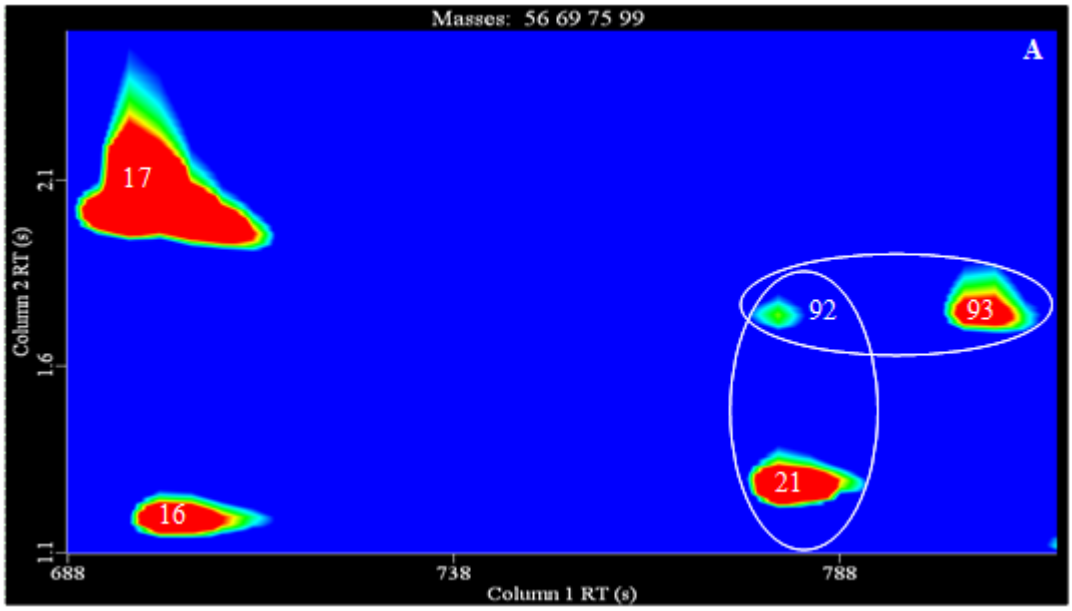


**Figure 4-1: Extracted ion chromatograms illustrating the separation of butyl acetate (16), ethyl-S-lactate (17), 2-butenoic acid, ethyl ester, (E)- (21), 4-methyl-1-pentanol (92) and 3-methyl-1-pentanol (93). For detailed compound identification, refer to Table 4-1.**

Here butyl acetate (**16**) and ethyl-S-lactate (**17**) co-elute in the $^{1}$D due to their similar boiling points, but are separated based on differences in polarity in the $^{2}$D. Similarly, the ethyl ester of *trans*-2-butenoic acid (**21**) and 4-methyl-1-pentanol (**92**) are separated according to differences in polarity. On the other hand, 4- (**92**) and 3-methyl pentanol (**93**), which have similar retention times in the $^{2}$D, are separated on the non-polar column in the $^{1}$D. Figure 4-1 illustrates excellent performance of the system: peak widths in the $^{2}$D were smaller than 100 ms for many analytes. Even the somewhat tailing peak of 3-methyl pentanol (**93**) was less than 200 ms wide at the

base. All $^{1}$D peaks were sampled at least three times across their profiles, which assured that $^{1}$D separation was preserved. The slight tailing seen for peak (**17)** in Figure 4-1 was also observed for other compounds of high polarity present at high levels. Tailing in the $^{1}$D was related to the incompatibility of the polar compounds with the non-polar stationary phase used in $^{1}$D. Tailing in the second dimension was mainly related to modulator overloading with high concentration analytes. Owing to the relatively large diameter of the $^{2}$D column (0.25 mm) and the correspondingly higher amount of the stationary phase compared to a comparable 0.1 mm I.D. column, overloading of the $^{2}$D column was observed much less frequently than is typical for 0.1 mm I.D. columns. [133]

A relatively generic HS-SPME method was used to extract the volatiles for the analysis. An SPME fiber coated with Carboxen adsorbent kept in place by polydimethylsiloxane binder (CAR/PDMS) was selected for the study as this fiber was previously reported to have good enrichment for wine volatiles.[210] The chromatographic method proved sufficiently reproducible, as evidenced by generally negligible retention time variations for analytes detected in multiple samples. These variations are shown in Table 4-1 as the number of modulation period(s) (NMP) in the $^{1}$D and standard deviation (SD) in the $^{2}$D. In addition, the

method was shown to be suitably sensitive to allow the identification of various trace-level compounds such as methoxy pyrazines.

Considering that this investigation was the first step in comprehensive screening of Pinotage volatiles, the signal to noise ratio (S/N) used during data processing was varied to also include minor peaks. Due to a lack of authentic standards for numerous compounds, tentative identification for those compounds lacking standards was based in the first instance on a comparison of the deconvoluted mass spectra with NIST 05 and Wiley 275 spectral libraries, performed using ChromaTOF software with a match value of 70% as a minimum requirement. In addition, linear retention indices (LRI) were experimentally determined [209] in the first dimension using a homologous series of *n*-alkanes and were compared with literature values. The retention indices were calculated from the retention times of the *n*-alkanes bracketing a given analyte in the modulated chromatogram. In a properly optimized GC×GC separation, each peak eluting from the $^{1}$D column is sampled at least three times, which leads to the same analyte showing in several consecutive $^{2}$D chromatograms ("slices"). To calculate the RIs, the averaged $^{1}$D retention time was used for each compound. A maximal absolute retention index difference of 30 compared to literature values was used as the selection criterion in this study.

Deviation of this magnitude was considered reasonable taking into account that the literature values were determined using one-dimensional systems.

The results presented in Table 4-1 demonstrate that the position of a compound in the two dimensional separation space was reproducible. Hence, the presence of certain compounds could be established based on positive identification of the same compounds in other samples, through the correspondence of the retention times in both dimensions. However, often these tentative identifications were rejected due to low mass spectral match quality (see for example Figure 4-3). In addition, it should be noted that many peaks detected with good spectral matches were excluded from the results presented here because there were no other means to confirm their identity. More than 200 volatile compounds presented in Table 4-1 were identified (positively or tentatively) in the nine samples using authentic standards (when available), mass spectra and linear retention indices as outlined previously. A detailed rationalization of the different classes of compounds identified, focusing on those that may contribute to wine aroma, is given below.

**Table 4-1: Volatile compounds identified in Pinotage wines using HS-SPME-GC×GC-TOFMS.**

| No. | Compounds | RT1(s) ± NMP[a] | Average RT2 (s) ± SD[b] | Similarity[c] | Reverse[d] | $LRI_{cal.}$[e] | $LRI_{lit.}$[f] | Wines[g] |
|---|---|---|---|---|---|---|---|---|
| | **Esters** | | | | | | | |
| 1 | Formic acid, ethyl ester (ethyl formate)[h] | 168 ± 0 | 1.04 ± 0.03 | 893 | 893 | < 600[j] | 495 | 1, 3, 6, 7 |
| 2 | Acetic acid, methyl ester (methyl acetate) | 188 ± 2 | 1.06 ± 0.02 | 975 | 975 | < 600[j] | 513 | 1-9 |
| 3 | Acetic acid, ethyl ester (ethyl acetate)[h] | 264 ± 1 | 1.18 ± 0.11 | 952 | 952 | 612 | 611 | 1-9 |
| 4 | Acetic acid, 1-methylethyl ester (isopropyl acetate) | 344 ± 0 | 1.09 ± 0.01 | 756 | 793 | 652 | 653 | 2, 3 |
| 5 | Formic acid, butyl ester (butyl formate) | 400 | 1.6 | 777 | 777 | 680 | 696 | 6 |
| 6 | Acetic acid, 2-propenyl ester (2-propenyl acetate) | 408 | 1.08 | 749 | 800 | 684 | 675 | 2 |
| 7 | Propanoic acid, ethyl ester (ethyl propanoate) | 448 ± 2 | 1.16 ± 0.03 | 957 | 957 | 688 | 688 | 1-9 |
| 8 | Acetic acid, propyl ester (propyl acetate) | 452 ± 1 | 1.12 ± 0.07 | 943 | 943 | 705 | 707 | 2, 3, 5, 8, 9 |
| 9 | Propanoic acid, 2-methyl-, ethyl ester (ethyl isobutyrate)[h] | 556 ± 0 | 1.16 ± 0.04 | 931 | 931 | 745 | 745 | 1-9 |
| 10 | Acetic acid, 2-methylpropyl ester (isobutyl acetate) | 592 ± 1 | 1.20 ± 0.04 | 970 | 970 | 759 | 758 | 1-9 |
| 11 | 1-Butanol, 3-methyl-, formate (isoamyl formate) | 636 ± 0 | 1.20 ± 0.04 | 815 | 815 | 777 | 775 | 2, 4, 6 |

| | | | | | | | | |
|---|---|---|---|---|---|---|---|---|
| 12 | Pyruvic acid, ethyl ester (ethyl pyruvate) | 644 ± 1 | 1.76 ± 0.05 | 954 | 954 | 780 | 785 | 1-9 |
| 13 | Butanoic acid, ethyl ester (ethyl butyrate)[h] | 664 ± 0 | 1.21 ± 0.03 | 954 | 954 | 788 | 787 | 1-9 |
| 14 | Butanoic acid, 1-methylethyl ester (isopropyl butyrate) | 672 | 1.52 | 725 | 737 | 791 | 716 | 2 |
| 15 | Propanoic acid, propyl ester (propyl propanoate) | 692 | 1.16 | 744 | 772 | 798 | 796 | 5 |
| 16 | Acetic acid, butyl ester (Butyl acetate) | 700 ± 2 | 1.23 ± 0.03 | 927 | 927 | 801 | 800 | 1-9 |
| 17 | Propanoic acid, 2-hydroxy-, ethyl ester, (S)- ( ethyl-S-lactate) | 700 ± 2 | 2.06 ± 0.04 | 988 | 988 | 799 | 800 | 1-9 |
| 18 | Propanoic acid, 2-hydroxy-, ethyl ester (Ethyl lactate) | 724 ± 3 | 2.13 ± 0.10 | 985 | 985 | 807 | 806 | 1-9 |
| 19 | Formic acid, pentyl ester (pentyl formate) | 744 ± 2 | 1.46 ± 0.04 | 808 | 858 | 815 | 810 | 1, 4, 5, 6, 8 |
| 20 | Butanoic acid, 2-propenyl ester (allyl butyrate) | 772 | 1.28 | 806 | 832 | 825 | 850 | 7 |
| 21 | 2-Butenoic acid, ethyl ester, (E)- (*trans*-ethyl 2-butenoate)[h] | 780 ± 0 | 1.32 ± 0.06 | 938 | 938 | 827 | 827 | 1, 2, 4, 6, 7, 9 |
| 22 | Butanoic acid, 2-methyl-, ethyl ester (ethyl 2-methylbutanoate)[h] | 816 ± 1 | 1.17 ± 0.05 | 947 | 947 | 839 | 839 | 1, 5, 7, 9 |
| 23 | Acetic acid, methoxy-, ethyl ester (ethyl methoxyacetate)[i] | 820 | 1.86 | 727 | 748 | 840 | - | 6 |
| 24 | Butanoic acid, 3-methyl-, ethyl ester | 820 ± 1 | 1.17 ± 0.04 | 916 | 916 | 840 | 840 | 1-9 |

| | | | | | | | | |
|---|---|---|---|---|---|---|---|---|
| | (ethyl isovalerate) | | | | | | | |
| 25 | Propanoic acid, 2-hydroxy-, 1-methylethyl ester, (S)-((S)-isopropyl lactate)[i] | 832 | 2.84 | 851 | 876 | 844 | - | 5 |
| 26 | 1-Butanol, 3-methyl-, acetate (isoamyl acetate)[h] | 892 ± 2 | 1.27 ± 0.06 | 942 | 953 | 862 | 861 | 1-9 |
| 27 | 4-Pentenyl acetate | 916 | 1.26 | 803 | 869 | 871 | 861 | 1 |
| 28 | Pentanoic acid, ethyl ester (ethyl pentanoate)[h] | 964 ± 0 | 1.20 ± 0.06 | 776 | 776 | 887 | 887 | 1, 6, 7, 9 |
| 29 | Acetic acid, pentyl ester (pentyl acetate) | 996 ± 2 | 1.25 ± 0.08 | 913 | 913 | 887 | 887 | 1, 4, 5, 6, 7, 8, 9 |
| 30 | 1-Butanol, 2-methyl-, acetate (2-methylbutyl acetate) | 1004 ± 2 | 1.24 ± 0.11 | 850 | 873 | 866 | 868 | 1, 5, 6, 7 |
| 31 | Hexanoic acid, methyl ester (methyl hexanoate) | 1040 ± 0 | 1.29 ± 0.09 | 934 | 934 | 911 | 913 | 1, 2, 5, 6, 7, 8, 9 |
| 32 | Butanoic acid, 3-hydroxy-, ethyl ester (ethyl 3-hydroxybutyrate) | 1060 | 2.28 | 917 | 917 | 918 | 947 | 1 |
| 33 | 2-Butanone, 4-hydroxy-, acetate | 1084 | 1.16 | 723 | 794 | 925 | 921 | 9 |
| 34 | Pentanoic acid, 4-methyl-, ethyl ester (ethyl 4-methylpentanoate) | 1172 | 1.20 | 734 | 788 | 953 | 951 | 6 |
| 35 | Butanoic acid, 2-hydroxy-3-methyl-, ethyl ester (ethyl 2-hydroxyisovalerate) | 1180 ± 0 | 1.63 ± 0.01 | 745 | 760 | 955 | 968* | 6, 9 |

| | | | | | | | | |
|---|---|---|---|---|---|---|---|---|
| 36 | Propanoic acid, 2-hydroxy-, 2-methylpropyl ester | 1180 | 1.76 | 803 | 803 | 955 | 983 | 6 |
| 37 | Propanoic acid, 2-hydroxy-, butyl ester (butyl lactate)[i] | 1180 ± 0 | 1.75 ± 0.07 | 907 | 919 | 955 | - | 1, 9 |
| 38 | 1-Butanol, 3-methyl-, propanoate (isoamyl propanoate) | 1184 ± 0 | 1.24 ± 0.07 | 834 | 858 | 956 | 954 | 1, 2, 4, 5, 8 |
| 39 | Hexanoic acid, ethyl ester (ethyl hexanoate)[h] | 1276 ± 0 | 1.22 ± 0.04 | 950 | 950 | 985 | 985 | 1-9 |
| 40 | 3-Hexen-1-ol, acetate, (E)- | 1300 ± 0 | 1.31 ± 0.10 | 856 | 856 | 993 | 996 | 1, 5, 6 |
| 41 | Acetic acid, hexyl ester (hexyl acetate)[h] | 1320 ± 0 | 1.24 ± 0.05 | 959 | 959 | 999 | 999 | 1-9 |
| 42 | Propanoic acid, 2-methyl-, 2-methylbutyl ester (2-methylbutyl isobutyrate) | 1328 ± 0 | 1.16 ± 0.06 | 901 | 908 | 1001 | 1002 | 5, 6, 9 |
| 43 | Ethyl 2-hexenoate | 1408 ± 0 | 1.32 ± 0.05 | 832 | 832 | 1027 | 1026 | 1, 6, 7, 9 |
| 44 | Butanoic acid, 3-methylbutyl ester (isoamyl butyrate) | 1460 ± 0 | 1.21 ± 0.03 | 860 | 892 | 1043 | 1044 | 1, 2, 5, 6, 7, 9 |
| 45 | Pentanoic acid, 2-hydroxy-4-methyl-, ethyl ester | 1468 ± 0 | 1.65 ± 0.05 | 841 | 852 | 1046 | 1060* | 1, 5 |
| 46 | Propanoic acid, 2-hydroxy-, 3-methylbutyl ester (isoamyl lactate) | 1504 ± 1 | 1.66 ± 0.04 | 881 | 881 | 1057 | 1082 | 1, 6, 9 |
| 47 | Butanedioic acid, ethyl methyl ester | 1576 | 1.82 | 737 | 864 | 1080 | 1070 | 6 |
| 48 | Hexanoic acid, propyl ester (propyl hexanoate) | 1580 ± 0 | 1.24 ± 0.04 | 772 | 815 | 1081 | 1081 | 5, 6 |

| | | | | | | | | |
|---|---|---|---|---|---|---|---|---|
| 49 | Heptanoic acid, ethyl ester (ethyl heptanoate) | 1592 ± 0 | 1.23 ± 0.05 | 924 | 924 | 1084 | 1084 | 1, 2, 5, 7, 9 |
| 50 | Butanoic acid, 3-methyl-, pentyl ester (n-amyl isovalerate) | 1620 ± 0 | 1.15 ± 0.01 | 816 | 859 | 1094 | 1093 | 1, 6 |
| 51 | Acetic acid, heptyl ester (heptyl acetate) | 1632 ± 0 | 1.21 ± 0.04 | 912 | 912 | 1098 | 1096 | 1, 5, 6, 7 |
| 52 | octanoic acid, methyl ester (methyl octanoate) | 1672 ± 0 | 1.26 ± 0.04 | 912 | 912 | 1111 | 1111 | 1, 2, 5, 6, 7, 8, 9 |
| 53 | Butanedioic acid, diethyl ester (diethyl succinate)[h] | 1804 ± 1 | 1.60 ± 0.05 | 970 | 970 | 1153 | 1149 | 1-9 |
| 54 | Benzoic acid, ethyl ester (ethyl benzoate)[h] | 1812 | 1.60 | 711 | 748 | 1157 | 1157 | 5 |
| 55 | octanoic acid, ethyl ester (ethyl octanoate)[h] | 1892 ± 0 | 1.19 ± 0.03 | 927 | 927 | 1184 | 1184 | 1-9 |
| 56 | Benzoic acid, 2-hydroxy-, methyl ester (methyl salicylate) | 1896 ± 0 | 1.81 ± 0.01 | 878 | 878 | 1185 | 1183 | 2, 9 |
| 57 | Propanedioic acid, oxo-, diethyl ester (diethyl oxomalonate) | 1944 | 1.56 | 806 | 806 | 1202 | 1188 | 6 |
| 58 | Benzeneacetic acid, ethyl ester (ethyl phenylacetate)[h] | 2012 ± 0 | 1.77 ± 0.07 | 867 | 932 | 1225 | 1224 | 1, 5 |
| 59 | Hexanoic acid, 3-methylbutyl ester (isoamyl hexanoate) | 2044 ± 0 | 1.17 ± 0.05 | 940 | 940 | 1238 | 1238 | 1, 2, 5, 6, 7, 9 |
| 60 | Acetic acid, 2-phenylethyl ester (2-phenylethyl acetate)[h] | 2048 ± 0 | 1.72 ± 0.07 | 915 | 941 | 1239 | 1244 | 1, 2, 3, 4, 5, 6, 7, 9 |

| | | | | | | | | |
|---|---|---|---|---|---|---|---|---|
| 61 | Nonanoic acid, ethyl ester (ethyl nonanoate)[h] | 2176 ± 0 | 1.21 ± 0.04 | 889 | 889 | 1286 | 1288 | 6, 9 |
| 62 | Ethyl 9-decenoate | 2416 ± 0 | 1.22 ± 0.03 | 787 | 830 | 1374 | 1371 | 6, 9 |
| 63 | Decanoic acid, ethyl ester (ethyl decanoate)[h] | 2444 ± 0 | 1.16 ± 0.02 | 921 | 921 | 1384 | 1382 | 1-9 |
| 64 | octanoic acid, 3-methylbutyl ester (isoamyl octanoate) | 2576 ± 0 | 1.15 ± 0.06 | 846 | 846 | 1436 | 1435 | 1, 5, 6 |
| 65 | Butanoic acid, 2-phenylethyl ester (2-phenylethyl butyrate) | 2744 | 2.44 | 824 | 824 | 1505 | 1491* | 2 |
| 66 | Dodecanoic acid, ethyl ester (ethyl dodecanoate) | 2936 ± 0 | 1.17 ± 0.02 | 846 | 846 | 1584 | 1583 | 1, 5, 6, 7, 9 |
| 67 | Benzoic acid, 4-hydroxy-, n-heptyl ester (heptyl 4-hydroxy benzoate) | 3764 | 3.38 | 789 | 789 | 1891 | 1877 | 1 |
| | | | | | | | | |
| | **Alcohols** | | | | | | | |
| 68 | Ethyl alcohol[h] | 132 ± 0 | 1.55 ± 0.15 | 965 | 965 | < 600[j] | 416 | 1-9 |
| 69 | 2-Propanol | 196 ± 0 | 1.41 ± 0.01 | 881 | 916 | < 600[j] | 500 | 3, 6, 8 |
| 70 | 2-Propenol | 208 ± 0 | 1.75 ± 0.01 | 913 | 913 | < 600[j] | 549 | 8, 9 |
| 71 | 1-Propanol[h] | 224 ± 1 | 1.48 ± 0.04 | 966 | 966 | < 600[j] | 548 | 1-9 |
| 72 | 2-Butanol | 252 | 1.36 | 887 | 887 | 606 | 581 | 4 |
| 73 | 2-Butanol (isomer) | 256 ± 0 | 1.39 ± 0.04 | 925 | 925 | 608 | 585 | 4, 8, 9 |
| 74 | 1-Propanol, 2-methyl- (isobutanol)[h] | 292 ± 0 | 1.56 ± 0.02 | 925 | 925 | 626 | 626 | 1-9 |

| | | | | | | | | |
|---|---|---|---|---|---|---|---|---|
| 75 | 1-Butanol[h] | 352 ± 0 | 1.66 ± 0.03 | 928 | 928 | 656 | 655 | 1-9 |
| 76 | 1-Penten-3-ol | 384 ± 0 | 1.65 ± 0.01 | 848 | 906 | 672 | 672 | 2, 6, 9 |
| 77 | 2-Pentanol | 420 ± 0 | 1.51 ± 0.03 | 903 | 903 | 690 | 691 | 2, 4, 5, 7, 9 |
| 78 | 3-Pentanol | 424 ± 0 | 1.47 ± 0.04 | 948 | 948 | 692 | 693 | 1-9 |
| 79 | 2-pentanol (isomer) | 424 | 1.5 | 848 | 848 | 692 | 681 | 1 |
| 80 | 4-Penten-2-ol | 420 | 1.34 | 815 | 948 | 690 | 662 | 8 |
| 81 | 3-Buten-1-ol, 3-methyl- | 492 ± 0 | 1.92 ± 0.04 | 949 | 949 | 720 | 717 | 1, 2, 5, 6, 7, 8, 9 |
| 82 | 1-Butanol, 3-methyl- (isoamyl alcohol)[h] | 500 ± 2 | 1.78 ± 0.14 | 946 | 946 | 723 | 724 | 1-9 |
| 83 | 1-Butanol, 2-methyl- (active amyl alcohol)[h] | 516 ± 1 | 1.80 ± 0.06 | 928 | 928 | 730 | 728 | 1-8 |
| 84 | 1-Pentanol (amyl alcohol) | 592 ± 1 | 1.69 ± 0.11 | 912 | 928 | 759 | 760 | 1-9 |
| 85 | 2-Penten-1-ol, (E)- | 596 | 2.18 | 780 | 839 | 761 | 760 | 4 |
| 86 | 2,3-Butanediol | 600 ± 0 | 1.48 ± 0.02 | 912 | 912 | 762 | 743 | 1, 2, 4, 5, 6, 7, 9 |
| 87 | 2-Buten-1-ol, 2-methyl- | 600 ± 0 | 2.23 ± 0.01 | 820 | 840 | 763 | 762 | 5, 9 |
| 88 | 2,3-Butanediol (isomer) | 628 ± 1 | 2.33 ± 0.07 | 909 | 909 | 773 | 768 | 1, 2, 3, 4, 5, 6, 7, 9 |
| 89 | 2-Pentanol, 3-methyl- | 692 | 2.10 | 807 | 807 | 798 | 797 | 6 |
| 90 | 2-Hexanol | 736 ± 0 | 2.03 ± 0.10 | 823 | 859 | 813 | 795 | 2, 6 |
| 91 | 1-Propanol, 3-ethoxy- | 772 | 2.04 | 919 | 919 | 825 | 837 | 1 |
| 92 | 4-Methyl-1-pentanol | 780 ± 0 | 1.84 ± 0.06 | 915 | 915 | 826 | 821 | 1-9 |

| | | | | | | | | |
|---|---|---|---|---|---|---|---|---|
| 93 | 3-Methyl-1-pentanol | 808 ± 0 | 1.84 ± 0.06 | 903 | 903 | 835 | 829 | 1-9 |
| 94 | 3-Hexen-1-ol, (E)- | 820 ± 0 | 1.98 ± 0.04 | 916 | 916 | 840 | 840 | 1, 3, 6, 9 |
| 95 | 3-Hexen-1-ol, (Z)-[h] | 832 ± 0 | 2.14 ± 0.07 | 934 | 934 | 846 | 846 | 1, 2, 5, 6, 9 |
| 96 | 2-Hexen-1-ol, (E)- | 864 | 2.24 | 793 | 812 | 855 | 854 | 9 |
| 97 | 1-Hexanol[h] | 876 ± 0 | 1.81 ± 0.04 | 919 | 919 | 858 | 858 | 1-9 |
| 98 | 2-Heptanol | 972 ± 0 | 1.64 ± 0.07 | 916 | 916 | 890 | 889 | 1, 2, 4, 5, 9 |
| 99 | 1-Heptanol | 1196 ± 0 | 1.78 ± 0.07 | 904 | 904 | 960 | 960 | 1, 2, 3, 4, 5, 6, 7, 9 |
| 100 | 2-Hepten-1-ol, (E)- | 1228 | 1.68 | 731 | 778 | 970 | 968 | 6 |
| 101 | 5-Hepten-2-ol, 6-methyl- | 1268 | 1.64 | 775 | 794 | 983 | 974 | 1 |
| 102 | 2-octanol[h] | 1296 | 1.54 | 848 | 848 | 991 | 992 | 1 |
| 103 | Isooctanol | 1368 ± 0 | 1.68 ± 0.00 | 845 | 845 | 1014 | 995 | 2, 9 |
| 104 | 2,6-Dimethyl-4-heptanol[i] | 1468 ± 0 | 1.62 ± 0.03 | 842 | 869 | 1046 | - | 6, 9 |
| 105 | 1-octanol | 1516 ± 0 | 1.68 ± 0.07 | 888 | 888 | 1061 | 1061 | 1, 2, 5, 6, 7 |
| 106 | 2-Phenylethyl alcohol[h] | 1636 ± 0 | 3.28 ± 0.07 | 947 | 947 | 1098 | 1098 | 1-9 |
| 107 | 1-Nonanol | 1828 | 1.56 | 877 | 894 | 1163 | 1163 | 1 |
| | | | | | | | | |
| | **Aldehydes** | | | | | | | |
| 108 | Acetaldehyde | 120 ± 1 | 1.00 ± 0.02 | 992 | 992 | < 600[j] | 372 | 1-9 |
| 109 | Propanal | 152 ± 2 | 1.04 ± 0.03 | 941 | 983 | < 600[j] | 461 | 1-9 |
| 110 | 2-Propenal (acrolein) | 156 ± 1 | 1.05 ± 0.07 | 971 | 971 | < 600[j] | 463 | 2, 4, 5, 8, 9 |
| 111 | 2-Methyl-propanal (isobutanal) | 208 ± 0 | 1.06 ± 0.02 | 804 | 804 | < 600[j] | 538 | 2, 3, 7 |

| | | | | | | | | |
|---|---|---|---|---|---|---|---|---|
| 112 | 2-Methyl-2-propenal (isobutenal) | 216 ± 1 | 1.12 ± 0.02 | 824 | 872 | < 600[j] | 553 | 3, 5, 7 |
| 113 | Butanal (butyraldehyde)[h] | 240 ± 0 | 1.08 ± 0.03 | 784 | 784 | 600 | 600 | 3, 5 |
| 114 | Methylglyoxal (pyruvaldehyde) | 308 | 1.44 | 915 | 945 | 634 | 644 | 8 |
| 115 | 3-Methyl-butanal (isovaleraldehyde) | 332 ± 0 | 1.17 ± 0.02 | 955 | 955 | 646 | 645 | 1-9 |
| 116 | 2-Methyl-butanal | 384 ± 0 | 1.08 ± 0.03 | 752 | 752 | 668 | 665 | 3, 4 |
| 117 | Pentanal (valeraldehyde) | 416 ± 1 | 1.09 ± 0.03 | 830 | 866 | 688 | 687 | 1-8 |
| 118 | 2-Methyl-2-butenal (E)- | 512 ± 2 | 1.38 ± 0.07 | 887 | 938 | 727 | 724 | 1, 2, 5 |
| 119 | 2-Methyl-2-butenal (2,3-dimethylacrolein) | 520 ± 0 | 1.38 ± 0.02 | 918 | 918 | 731 | 730 | 3, 4, 8 |
| 120 | 2-Pentenal, (E)- | 544 | 1.32 | 712 | 723 | 741 | 743 | 1 |
| 121 | Hexanal[h] | 652 ± 1 | 1.26 ± 0.05 | 892 | 892 | 783 | 784 | 1-9 |
| 122 | 3-Hexenal, (Z)- | 780 ± 1 | 1.45 ± 0.01 | 755 | 804 | 829 | 834 | 2, 3, 4 |
| 123 | Heptanal | 960 | 1.24 | 799 | 799 | 886 | 885 | 1 |
| 124 | Benzaldehyde[h] | 1140 ± 0 | 2.20 ± 0.12 | 956 | 956 | 943 | 942 | 1-7 |
| 125 | octanal | 1284 ± 0 | 1.28 ± 0.06 | 853 | 871 | 988 | 988 | 1, 2, 3, 8, 9 |
| 126 | Benzeneacetaldehyde (phenylacetaldehyde) | 1392 ± 0 | 2.21 ± 0.08 | 952 | 952 | 1022 | 1022 | 1-9 |
| 127 | Nonanal[h] | 1604 | 1.34 | 849 | 849 | 1089 | 1088 | 5 |
| 128 | 2-Nonenal, (Z)- | 1628 | 1.02 | 752 | 760 | 1096 | 1098 | 5 |
| 129 | Decanal[h] | 1916 | 1.26 | 799 | 816 | 1192 | 1192 | 9 |
| | | | | | | | | |
| | **Ketones** | | | | | | | |

| | | | | | | | | |
|---|---|---|---|---|---|---|---|---|
| 130 | 2,3-Butanedione | 228 | 1.10 | 959 | 959 | < 600[j] | 586 | 6 |
| 131 | 2-Propanone, 1-hydroxy- (acetol) | 292 | 1.34 | 829 | 829 | 626 | 625 | 2 |
| 132 | 2-Butanone, 3-methyl- | 384 ± 0 | 1.22 ± 0.04 | 924 | 949 | 672 | 677 | 1, 5, 6, 7 |
| 133 | 2,3-Pentanedione | 392 ± 0 | 1.34 ± 0.00 | 867 | 885 | 676 | 676 | 3, 5, 6 |
| 134 | 2-Pentanone[h] | 396 ± 1 | 1.27 ± 0.03 | 860 | 860 | 677 | 680 | 1, 3, 6, 7 |
| 135 | 3-Pentanone | 412 ± 2 | 1.19 ± 0.03 | 920 | 954 | 684 | 683 | 1, 2, 5, 6, 8 |
| 136 | 2-Butanone, 3-hydroxy- (acetoin) | 416 ± 1 | 2.33 ± 0.02 | 884 | 884 | 688 | 687 | 2, 3, 6, 7 |
| 137 | 3-Penten-2-one | 488 ± 1 | 1.49 ± 0.04 | 961 | 961 | 719 | 719 | 1, 3, 4, 5, 6, 7, 8, 9 |
| 138 | Cyclopentanone | 540 | 1.34 | 790 | 829 | 739 | 747 | 4 |
| 139 | 3-octanone | 1236 ± 0 | 1.28 ± 0.05 | 924 | 924 | 972 | 973 | 1, 5, 6, 7, 9 |
| 140 | 2-octanone | 1244 | 1.24 | 922 | 922 | 975 | 976 | 1 |
| 141 | 4-Heptanone, 2,6-dimethyl- | 1196 | 1.16 | 772 | 806 | 960 | 962 | 4 |
| 142 | Cyclohexanone, 2,2,6-trimethyl- | 1404 ± 0 | 1.23 ± 0.01 | 842 | 842 | 1025 | 1022 | 1, 6, 9 |
| 143 | Acetophenone[h] | 1476 ± 0 | 2.15 ± 0.05 | 830 | 830 | 1048 | 1048 | 1, 2, 5, 6 |
| 144 | 2-Nonen-4-one | 1504 | 1.14 | 797 | 797 | 1057 | 1065 | 8 |
| 145 | 2-Nonanone | 1568 ± 0 | 1.34 ± 0.00 | 894 | 894 | 1077 | 1078 | 6, 9 |
| | | | | | | | | |
| | **Acids** | | | | | | | |
| 146 | Formic acid | 132 ± 0 | 2.11 ± 0.04 | 905 | 905 | < 600[j] | 512 | 1, 7 |
| 147 | Acetic acid[h] | 260 ± 0 | 3.36 ± 0.10 | 965 | 965 | 610 | 610 | 1-9 |
| 148 | Propanoic acid, 2-methyl- (isobutyric | 580 ± 0 | 3.06 ± 0.07 | 892 | 892 | 755 | 753 | 1, 5, 6, 7, 9 |

| | | | | | | | | |
|---|---|---|---|---|---|---|---|---|
| | acid)[h] | | | | | | | |
| 149 | Acetic acid, methoxy- (methoxyacetic acid) | 628 ± 1 | 3.76 ± 0.00 | 993 | 993 | 772 | 752 | 2, 5 |
| 150 | Acetic acid, hydroxy- (glycolic acid) | 816 ± 2 | 1.96 ± 0.08 | 980 | 980 | 841 | 819 | 3, 8, 9 |
| 151 | Propanoic acid, 2-hydroxy- (lactic acid) | 816 | 2.04 | 959 | 997 | 839 | 838 | 5 |
| 152 | Butanoic acid, 3-methyl- (isovaleric acid)[h] | 816 ± 0 | 2.85 ± 0.09 | 900 | 900 | 839 | 840 | 1, 4, 5, 6, 7, 9 |
| 153 | Hexanoic acid[h] | 1236 ± 1 | 1.93 ± 0.17 | 921 | 921 | 973 | 971 | 1, 2, 5, 6, 7, 9 |
| | | | | | | | | |
| | **Acetals** | | | | | | | |
| 154 | 1,1-Diethoxyethane (acetal) | 492 ± 0 | 1.07 ± 0.04 | 811 | 830 | 720 | 718 | 1, 3, 4, 5 |
| 155 | 2,4,5-Trimethyl-1,3-dioxolane | 540 ± 2 | 1.17 ± 0.04 | 914 | 914 | 741 | 761 | 1-9 |
| 156 | 1,1-Diethoxy-2-methylpropane (propane, 1,1-diethoxy-2-methyl-) | 860 ± 0 | 1.12 ± 0.03 | 891 | 891 | 853 | 859 (29)* | 1, 2, 3, 5, 6 |
| 157 | 1,1-Diethoxy-2-methylbutane (butane, 1,1-diethoxy-3-methyl-) | 1152 ± 0 | 1.10 ± 0.05 | 736 | 761 | 948 | 952* | 1, 5, 6 |
| 158 | 1-(1-Ethoxyethoxy)pentane (pentane, 1-(1-ethoxyethoxy)-) | 1212 | 1.16 | 745 | 762 | 965 | 970* | 5 |
| 159 | 1,1-Diethoxypentane (pentane, 1,1-diethoxy-) | 1316 | 1.30 | 740 | 740 | 998 | 995* | 1 |
| | | | | | | | | |

| | | | | | | | | |
|---|---|---|---|---|---|---|---|---|
| | **Furans and Lactones** | | | | | | | |
| 160 | Furan | 164 | 1.02 | 726 | 935 | < 600[j] | 492 | 5 |
| 161 | Furan, 2,5-dimethyl- | 444 ± 0 | 1.13 ± 0.01 | 810 | 877 | 702 | 700 | 1, 9 |
| 162 | 2-Furancarboxaldehyde (furfural)[h] | 728 ± 0 | 3.17 ± 0.07 | 901 | 915 | 810 | 810 | 1, 2, 3, 5, 6 |
| 163 | 2-Acetylfuran (acetylfuran) | 896 ± 1 | 1.10 ± 0.03 | 807 | 938 | 866 | 870 | 2, 8 |
| 164 | 2(3H)-Furanone, dihydro- (γ-butyrolactone) | 920 ± 2 | 0.19 ± 0.09 | 941 | 941 | 873 | 871 | 1-9 |
| 165 | 2(3H)-Furanone, dihydro-5-methyl- γ-pentalactone) | 1056 | 3.26 | 874 | 874 | 916 | 914 | 5 |
| 166 | 2(3H)-Furanone, dihydro-3,5-dimethyl- | 1144 ± 2 | 1.26 ± 0.03 | 779 | 813 | 946 | 947 | 5, 7 |
| 167 | Ethyl 2-furoate | 1424 ± 0 | 2.02 ± 0.00 | 828 | 877 | 1032 | 1009 | 1, 6 |
| | | | | | | | | |
| | **Sulphur containing compounds** | | | | | | | |
| 168 | Sulphur dioxide[i] | 100 ± 1 | 1.10 ± 0.05 | 967 | 967 | < 600[j] | - | 1-9 |
| 169 | Dimethyl sulphide | 176 ± 0 | 1.00 ± 0.02 | 864 | 914 | < 600[j] | 493 | 1, 2, 3, 5 |
| 170 | Methyl thiolacetate | 408 ± 0 | 1.26 ± 0.04 | 923 | 923 | 684 | 683 | 4, 5, 6 |
| 171 | Ethyl thiolacetate | 580 | 1.30 | 782 | 803 | 755 | 749 | 6 |
| 172 | Thiophene, 2-methyl- | 620 ± 0 | 1.33 ± 0.05 | 818 | 834 | 770 | 770 | 1, 6, 7, 8, 9 |
| | | | | | | | | |
| | **Nitrogen containing compounds** | | | | | | | |
| 173 | 2-Methylpropylamine (isobutylamine) | 216 ± 0 | 1.06 ± 0.00 | 779 | 882 | < 600[j] | 588 | 8 |
| 174 | 2-Butanamine, 2-methyl-[i] | 300 | 1.02 | 761 | 785 | 630 | - | 8 |

| | | | | | | | | |
|---|---|---|---|---|---|---|---|---|
| 175 | Pyrrolidine | 936 | 1.04 | 791 | 888 | 706 | 695 | 1 |
| 176 | 2-Methoxy-3-(1-methylethyl)- Pyrazine [2-Methoxy-3-isopropylpyrazine (IPMP)][h] | 1564 | 1.18 | 902 | 902 | 1082 | 1081 | 9 |
| 177 | 2-Methoxy-3-(1-methylpropyl)- Pyrazine [ 2-Methoxy-3-sec-butylpyrazine (SBMP)][h] | 1892 | 2.58 | 735 | 735 | 1184 | 1159 | 9 |
| 178 | 2-Methoxy-3-(2-methylpropyl)- Pyrazine [ 2-Methoxy-3-isobutylpyrazine (IBMP)][h] | 1972 | 1.25 | 671 | 671 | 1210 | 1211 | 9 |
| | | | | | | | | |
| | **Terpenes** | | | | | | | |
| 179 | Cumene | 1068 ± 0 | 1.18 ± 0.04 | 962 | 962 | 920 | 916 | 1-9 |
| 180 | Isocumene | 1164 ± 0 | 1.21 ± 0.06 | 964 | 964 | 950 | 949 | 1, 2, 4, 5, 6, 7, 8, 9 |
| 181 | 1-Methyl-4-(1-methylethylidene)- cyclohexane [4(8)-p-menthene] | 1288 | 1.04 | 705 | 861 | 989 | 998 | 9 |
| 182 | 2-Methyl-5-(1-methylethyl)-1,3- cyclohexadiene ($\alpha$-Phellandrene) | 1312 | 1.08 | 708 | 708 | 996 | 996 | 2 |
| 183 | 1,4-Epoxy-p-Menthane (isocineole) | 1364 ± 0 | 1.11 ± 0.01 | 755 | 887 | 1013 | 1011 | 6, 9 |
| 184 | *o*-Cymene | 1392 ± 0 | 1.18 ± 0.05 | 963 | 963 | 1022 | 1022 | 1-9 |
| 185 | 1-Methyl-4-(1 methylethenyl)- | 1420 ± 0 | 1.13 ± 0.04 | 911 | 915 | 1030 | 1028 | 1, 2, 4, 5, 7, |

| | | | | | | | | |
|---|---|---|---|---|---|---|---|---|
| | cyclohexene (limonene)[h] | | | | | | | 9 |
| 186 | 1,8-Epoxy-p-menthane (eucalyptol) | 1424 ± 0 | 1.09 ± 0.03 | 814 | 814 | 1030 | 1030 | 4, 6, 9 |
| 187 | 3,5,5-Trimethyl-2-cyclohexen-1-one (isophoron) | 1480 | 1.32 | 734 | 758 | 1049 | 1074 | 6 |
| 188 | 1-Methyl-4-(1-methylethyl)- 1,3-cyclohexadiene (α-Terpinene) | 1508 | 1.12 | 745 | 789 | 1058 | 1040 | 7 |
| 189 | 5-Ethenyltetrahydro-α,α,5-trimethyl-*cis*-2-furanmethanol [linalool oxide, (Z)-][h] | 1536 | 1.36 | 866 | 866 | 1067 | 1067 | 9 |
| 190 | 1,3,3-Trimethylbicyclo[2.2.1]heptan-2-one (fenchon)[h] | 1580 | 1.30 | 876 | 876 | 1081 | 1080 | 3 |
| 191 | 5-Ethenyltetrahydro-α,α,5-trimethyl-*trans*-2-furanmethanol (linalool oxide, (E)-) | 1580 | 1.38 | 839 | 839 | 1081 | 1081 | 9 |
| 192 | 1-Methyl-4-(1-methylethylidene)-1-cyclohexene (terpinolen) | 1608 | 1.12 | 797 | 806 | 1090 | 1089 | 9 |
| 193 | 3,7-Dimethyl-1,6-octadien-3-ol (linalool)[h] | 1612 ± 0 | 1.51 ± 0.06 | 783 | 796 | 1091 | 1091 | 1, 6, 7 |
| 194 | 2,6,6-Trimethylbicyclo[3.1.1]heptan-3-ol (isopinocampheol) | 1612 | 1.52 | 728 | 728 | 1091 | 1120 | 5 |
| 195 | α,α,4-Trimethyl- cyclohexanemethanol, (p-menthan-8-ol) | 1768 | 1.48 | 755 | 780 | 1143 | 1162** | 9 |
| 196 | 1,6-octadien-3-ol, 3,7-dimethyl-, formate | 1844 ± 0 | 1.09 ± 0.04 | 747 | 747 | 1168 | 1170 | 6, 9 |

| | | | | | | | | |
|---|---|---|---|---|---|---|---|---|
| | (linalool formate) | | | | | | | |
| 197 | 4-Methyl-1-(1-methylethyl)-3-cyclohexen-1-ol (4-terpineol) | 1868 | 1.44 | 762 | 762 | 1176 | 1175 | 9 |
| 198 | α,α,4-Trimethyl-3-cyclohexene-1-methanol (α-terpineol)[h] | 1900 ± 0 | 1.60 ± 0.04 | 907 | 909 | 1187 | 1185 | 1, 2, 5, 6, 7, 8, 9 |
| 199 | 3-Cyclohexen-1-ol, 4-methyl-1-(1-methylethyl) acetate (4 -terpineol acetate) | 2116 ± 1 | 1.19 ± 0.03 | 911 | 911 | 1264 | 1270 | 1, 2, 4, 5, 6, 7, 8, 9 |
| 200 | 1,1,6-Trimethyl-1,2-dihydro-naphthalene (TDN) | 2372 ± 0 | 1.30 ± 0.04 | 808 | 827 | 1358 | 1336 | 1, 6, 9 |
| 201 | 1,1,6-Trimethyl-1,2,3,4-tetrahydro-naphthalene (TTN) | 2384 ± 0 | 1.22 ± 0.05 | 811 | 834 | 1362 | 1340 | 1, 6, 9 |
| 202 | 2-Buten-1-one, 1-(2,6,6-trimethyl-1,3-cyclohexadien-1-yl)-, (E)- (⍟-Damascenone) | 2432 ± 0 | 1.38 ± 0.02 | 790 | 844 | 1380 | 1373 | 1, 7, 9 |
| | | | | | | | | |
| | **Volatile phenols** | | | | | | | |
| 203 | 2,4-Bis(1,1-dimethylethyl)-phenol | 2748 | 2.04 | 779 | 779 | 1506 | 1502 | 6 |
| 204 | Butylated hydroxytoluene (BHT)[h] | 2756 ± 0 | 1.26 ± 0.02 | 861 | 869 | 1510 | 1505 | 1, 5, 6, 7, 9 |
| | | | | | | | | |
| | **Pyrans** | | | | | | | |

| | | | | | | | | |
|---|---|---|---|---|---|---|---|---|
| 205 | 2H-Pyran-2-one, tetrahydro- | 992 | 1.34 | 761 | 774 | 896 | 910 | 8 |
| 206 | 2H-Pyran, 2-ethenyltetrahydro-2,6,6-trimethyl- | 1232 ± 0 | 1.09 ± 0.04 | 803 | 803 | 971 | 960 | 6, 7, 8, 9 |

[a] $RT_1$(s) ± NMP: $^1D$ retention times with the variation in modulation period (MP) amongst the samples where a compound was detected.

[b] SD: Standard deviation of $^2D$ retention times amongst the samples where a compound was detected.

[c] Forward similarity (value out of 1000).

[d] Reverse similarity (value out of 1000).

[e] $LRI_{cal}$: linear retention indices experimentally determined.

[f] $LRI_{lit.}$: linear retention indices obtained from literature (NIST, 05; [211]).

[g] Wines: the wine samples in which the compound has been identified (numbers 1,2,3...9 are codes given to the nine Pinotage wine samples consecutively).

[h] Compound identity confirmed using authentic standards.

[i] Identification was based only on mass spectra from the NIST 05 library.

[j] $LRI_{cal.}$ < 600 estimated since $C_6$ was the lowest *n*-alkane analyzed.

[*] $LRI_{lit.}$: LRI obtained from a column with (5%-Phenyl)-methylpolysiloxane stationary phase. [212-214]

[**] $LRI_{lit.}$: LRI obtained under isothermal conditions.

### 4.2.1 Esters

Esters are abundant wine volatiles produced during fermentation and through esterification occurring during wine ageing. Young Pinotage wines are characterized by relatively high concentrations of esters. [192] Amongst the nine samples analyzed, 67 esters were detected. Of these, 17 were positively identified using authentic standards (indicated by superscript ''h'' in Table 4-1). Most ethyl and acetate esters were mainly separated in the $^{1}$D and displayed very similar and rather low $^{2}$D retention times (RTs). In contrast, hydroxyl substituted esters such as ethyl lactate (see Figure 4-1) tended to be more retained in the second dimension. Similarly, ethyl esters of di-acids and aromatic esters had longer $^{2}$D RTs due to their higher polarity.

Esters previously reported in Pinotage wines included ethyl acetate (**3**), -butyrate (**13**), -lactate (**18**), -isovalerate (**24**), -hexanoate (**39**), -octanoate (**55**), -phenylacetate (**58**), -9-decenoate (**62**), - decanoate (**63**) and dodecanoate (**66**), as well as isoamyl acetate (**26**), hexyl acetate (**41**), diethyl succinate (**53**) and 2-phenylethyl acetate (**60**). [195, 196, 206] These esters were common to most of the wines analyzed. Isoamyl acetate was reported to be an impact odorant characteristic of the Pinotage varietal. [192] This compound was detected at relatively high levels in all wines. According to Ferreira et al., [215] ethyl esters of hexanoic (**39**) and octanoic acids (**55**), which have low odor thresholds of 5 and 14 μg/L, respectively, are important aroma constituents.

Minor concentrations of other carboxylic acids and alcohols produced during fermentation may lead to the production of esters capable of contributing to wine aroma. For instance, ethyl esters of 2-methyl- (**22**) and 3-methylbutyric acids (**24**) were reported to play a role in the aroma of a wine.[216] Other naturally rare ethyl esters which may have some impact on the wine aroma include ethyl 2-, 3- and 4-methylpentanoate and ethyl cyclohexanoate, [217] which reveal pleasant strawberry/liquorice-like odors. The concentrations of these esters tend to increase with wine age due to slow esterification of their corresponding acids formed during fermentation. However, only one of the four esters, ethyl 4- methylpentanoate, can be found in young wines at low levels. [217] Indeed, only ethyl-4-methylpentanoate (**34**) was detected in one of the nine wines analyzed here. Allyl butyrate (**20**) and ethyl methoxyacetate (**23**), both identified tentatively, have previously been reported in Moutai Chinese liquor,[218] and pentyl formate (also identified tentatively) (**19**) in grape brandy.[219] No literature reports demonstrating the occurrence of these compounds in wine could be found.

### 4.2.2 Alcohols

Alcohols were the second largest group of identified volatiles, amounting to a total of 40 compounds in all nine wines. The identity of 10 of these was confirmed

using authentic standards. Unlike most esters, the alcohols reported here showed varying retention times in both dimensions (Table 4-1). Alcohols such as isoamyl alcohol (**82**) showed noticeable tailing and even wraparound, which could be attributed to their high concentrations and polarities. Ethanol masked a number of minor compounds due to its high concentration. Figure 4-2 depicts some of the aliphatic alcohols identified in Pinotage wines.

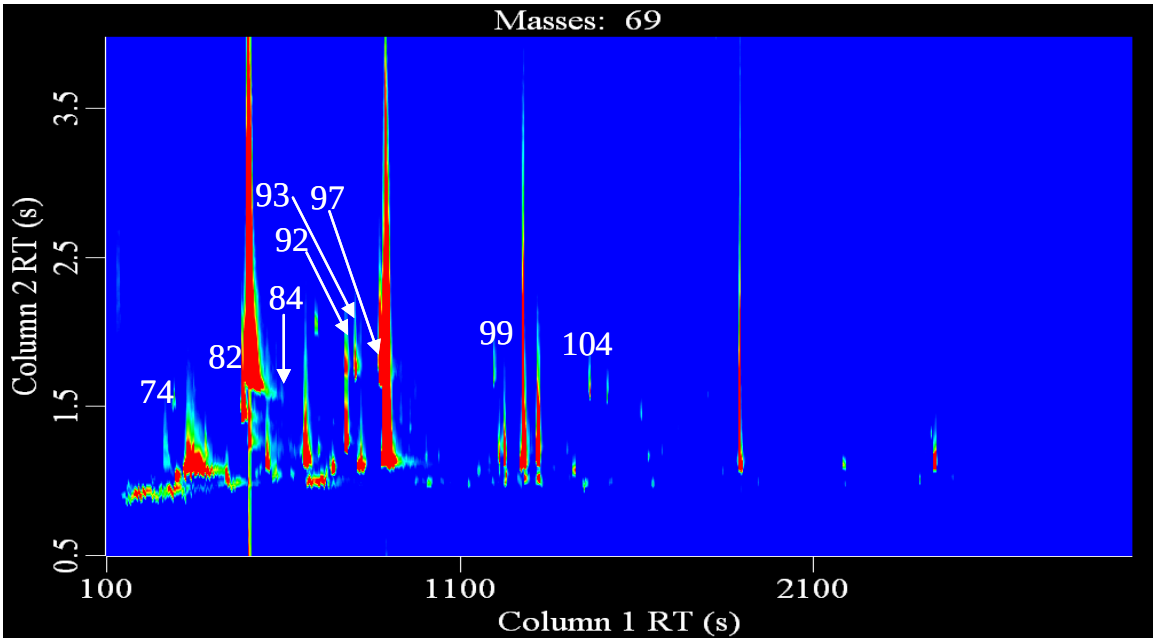


**Figure 4-2: Extracted ion contour plot depicting selected alcohols in a Pinotage wine. Peak numbers correspond to Table 4-1.**

Alcohols are produced as secondary metabolic products of yeast.[220] Di-alcohols such as butanediol (**86** and **88**) are produced from carbohydrates.[221] Isoamyl alcohol (**82**) and 2-phenylethyl alcohol (**106**) have odor thresholds of 30 and 14 mg/L, respectively, in red wine.[215] As these compounds usually occur at levels above their odor thresholds, they are important odorants in wine, and have previously been identified in Pinotage wines. [195, 196] Isobutanol (**74**), 1-butanol (**75**), 1-pentanol (**84**), 1-hexanol (**97**) and 1-octanol (**105**) have also been reported in Pinotage. [195, 196, 206] With the exception of 1-octanol, which was identified in only five wines, all these alcohols were detected in each of the nine samples. 2-Hepten-1-ol, (E) (**100**; identified tentatively) has been previously reported in grape brandy, [219] but to the best of our knowledge, this is the first evidence of its occurrence in wine.

### 4.2.3 Carbonyls

Aldehydes and ketones are highly volatile constituents of alcoholic beverages. In the present study 22 aldehydes and 16 ketones were reported. Most aldehydes were retained somewhat stronger than ketones in the $^{2}$D. Hydroxy-substituted (acetoin, **136**) and aromatic carbonyls (benzaldehyde **124**, benzeneacetaldehyde, **126** and acetophenone, **143**) showed longer retention times in the $^{2}$D, as expected. Aldehydes and ketones are believed to result from the direct oxidation of their corresponding

alcohols and fatty acids, respectively.[222] Other authors suggested that carbonyls result from the degradation of amino acids and sugars.[223]

Amongst the carbonyls, acetaldehyde (**108**, odour threshold of 500 mg/L) [224] is a major component and generally represents more than 90% of the total aldehyde content in wine. Benzeneacetaldehyde (**126**) has been described as contributing a honey odor above its odor threshold level of 1 mg/L. [222] This compound was identified in each of the nine wine samples. In addition, a significant number of unsaturated aldehydes were identified as well. For instance, acrolein (2-propenal, **110**), which is known for its pungent odor and peppery smell, was identified in five of the nine wine samples. This compound may be produced by bacteria from glycerol. [225] In addition to the mono-keto group, $C_4$ and $C_5$ di-ketones were identified in a few samples. These di-ketones are formed in wine by oxidative decarboxylation of 2-acetolactate. [225] Acetoin and 2-octanone have been reported previously in Pinotage wines. [195, 196] Isobutenal (2-methyl-2-propenal, **112**) and 3-octanone (**139**), both identified tentatively, have only been reported before in grape brandy [219] and grape juice, [226] respectively.

### 4.2.4 Acids

Generally speaking few acids were identified using the current analytical method. This was most likely related to the low sample/ headspace and headspace/fibre partition coefficients of these ionizable species. [196] Typically, acids showed high retention in the $^{2}D$, and in fact some of these highly polar compounds showed tailing and wraparound due to their high polarity (for example acetic acid). Acetic acid is known to contribute a vinegar odor,[227] and was the dominant acid (based on peak area), in agreement with a previous report. [196] Of the eight acids identified in the current study, five: formic acid (**146**), acetic acid (**147**), isobutyric acid (**148**), isovaleric acid (**152**) and hexanoic acid (**153**) have been reported previously in Pinotage wines. [195, 196, 206] Isovaleric acid is known as a very powerful contributor to wine flavor. [215] Further optimization of the method and the sample preparation procedure in particular, is required for the detailed study of the acid content of Pinotage wines.

### 4.2.5 Acetals

Acetals comprise both cyclic and acyclic di-oxo-compounds, and are produced in wine as secondary products during maturation. Câmara et. al.[228] reported the formation of different heterocyclic acetals from acetaldehyde and glycerol via

acetalization. Of the six acetals reported, 2,4,5-trimethyl- 1,3-dioxolane (**155**) was identified in all wines with a good match factor (Table 4-1).

### 4.2.6 Furans and Lactones

The furan-related compounds identified here were unsaturated heterocyclic compounds with a five-membered ring as a basic structure and have been identified in a wide range of foodstuffs (including wine) in both desirable and undesirable circumstances. In the present report, a total of eight different compounds categorized under this group and including esters, aldehydes, ketones and lactones were detected (Table 4-1). Some furan derivatives are believed to be sourced from wood cooperage.[229] Furfural (**162**) is one of the many aldehydes that is released to the wine from wood and has previously been reported in Pinotage wine. [195, 196] The level of furfural can increase after drying or seasoning of the wood, mainly when high temperatures are used. [230] It has also been suggested that the release of furfural into wine increases significantly with toasting levels. [231] This increase may have an important sensory impact. According to Spillman et al., [232] the amount of furfural and other aldehydes sourced from wood decreases during ageing due to biological reduction in the course of both alcoholic and malolactic fermentation to form the corresponding alcohols. γ-Butyrolactone (**164**) was identified in all wines with

greater than 90% match factor. For the rest of the furans identified, some discrepancies amongst the samples were observed, which could be due to differences in maturation practices as outlined above.

### 4.2.7 Sulphur compounds

Volatile sulphur compounds play a remarkable role in the aroma of food and beverages, even when present at low concentrations. These compounds can be produced through either enzymatic processes in yeast, or non-enzymatic processes through different chemical, photochemical or thermal reactions during winemaking and storage. [233] Five low molecular weight sulphur compounds have been detected in Pinotage. Amongst the identified compounds, sulphur dioxide ($SO_2$, **168**), commonly used to prevent undesired microbiological growth, [234] was detected in all samples. Sulphides and thiols that have a negative impact on wine odor are divided into light (boiling point < 90 °C) and heavy (boiling point > 90 °C) compounds based on their olfactory contribution to wine aroma. Dimethyl sulphide (DMS, **169**) is reported to contribute positively to wine bouquet. DMS is characterized by quince or/and truffle odour and has a perception threshold of 5 μg/L. This compound is synthesized by yeast from cysteine. The concentration of DMS depends on grape variety and can vary during ageing. [233, 235]

### 4.2.8 Nitrogen containing compounds

Nitrogen in wine is sourced from the degradation of amino acids and is used for the synthesis of other nitrogen compounds by yeast cells. [236] The best known volatile nitrogen compounds in wine are 3-alkyl-2-methoxypyrazines, which are commonly present in Sauvignon Blanc and Cabernet Sauvignon grape varieties. Methoxypyrazines are nitrogenated heterocycles produced by the metabolism of amino acids.[237] In the current study three methoxypyrazines were detected: 2-methoxy-3-isopropylpyrazine (IPMP, **176**), 2-methoxy-3-sec-butylpyrazine (SBMP, **177**) and 2-methoxy-3-isobutylpyrazine (IBMP, **178**). Note that IBMP is included in Table 4-1 despite the fact that the match factor for this compound was less than the requisite 70%, as its identity was confirmed using an authentic standard. The levels of IBMP in red wine exceeded those of the other two compounds by a factor 10, and since similar extraction efficiencies are expected for all three methoxypyrazines, it is likely that the poor match factor for IBMP may be ascribed to co-elution.

Methoxypyrazines are characterized by very low perception thresholds of 1–2 ng/L and 15 ng/L in white and red wines, respectively. These compounds are well-known for their contribution to vegetative, herbaceous, green bell and pepper character of wines. [155, 237] At the time of performing the experiments of this chapter there were no reports in the literature on the presence of methoxypyrazines in

Pinotage wines. This has changed with the publication of the paper by Alberts et al. in 2009. [238] Although no quantification was performed in the current study, it is known that the levels of IBMP commonly vary between 0.4 and 10 ng/L in red wines, while SBMP and IPMP are typically below 10% of these levels. This indicates that the analytical method used here was capable of ultra-trace level determination of some compounds.

### 4.2.9 Terpenes

Terpenes are important varietal aroma compounds that are biosynthesized from acetyl-coenzyme A (CoA). Various types of monoterpene compounds have been reported in grapes including hydrocarbons and oxygen-containing compounds, such as monoterpenols, monoterpendiols and monoterpenes. [239] A large proportion of terpenes (~ 90%) are present as nonvolatile glycosides in the grape, which can be hydrolyzed (enzymatically or chemically) to the corresponding free forms during fermentation and ageing. [240] Moreover, during wine processing and ageing changes in concentration and the formation of new compounds can take place due to acid-catalyzed rearrangements. [240, 241]

In the current study 24 terpenes have been identified (positively or tentatively), most of them being present in one to three samples. Exceptions are terpene

hydrocarbons including cumene (**179**), isocumene (**180**), o-cymene (**184**) and limonene (**185**), as well as an alcohol, a-terpineol (**198**) and an ester, 4-terpineol acetate (**199**), which were positively identified in more than six wines. A very similar terpene profile to that reported for grapes using GCxGC–TOFMS [204] was obtained in the present study. Moreover, terpene profiles and levels were found to vary significantly between different samples. Figure 4-3 presents a comparison between

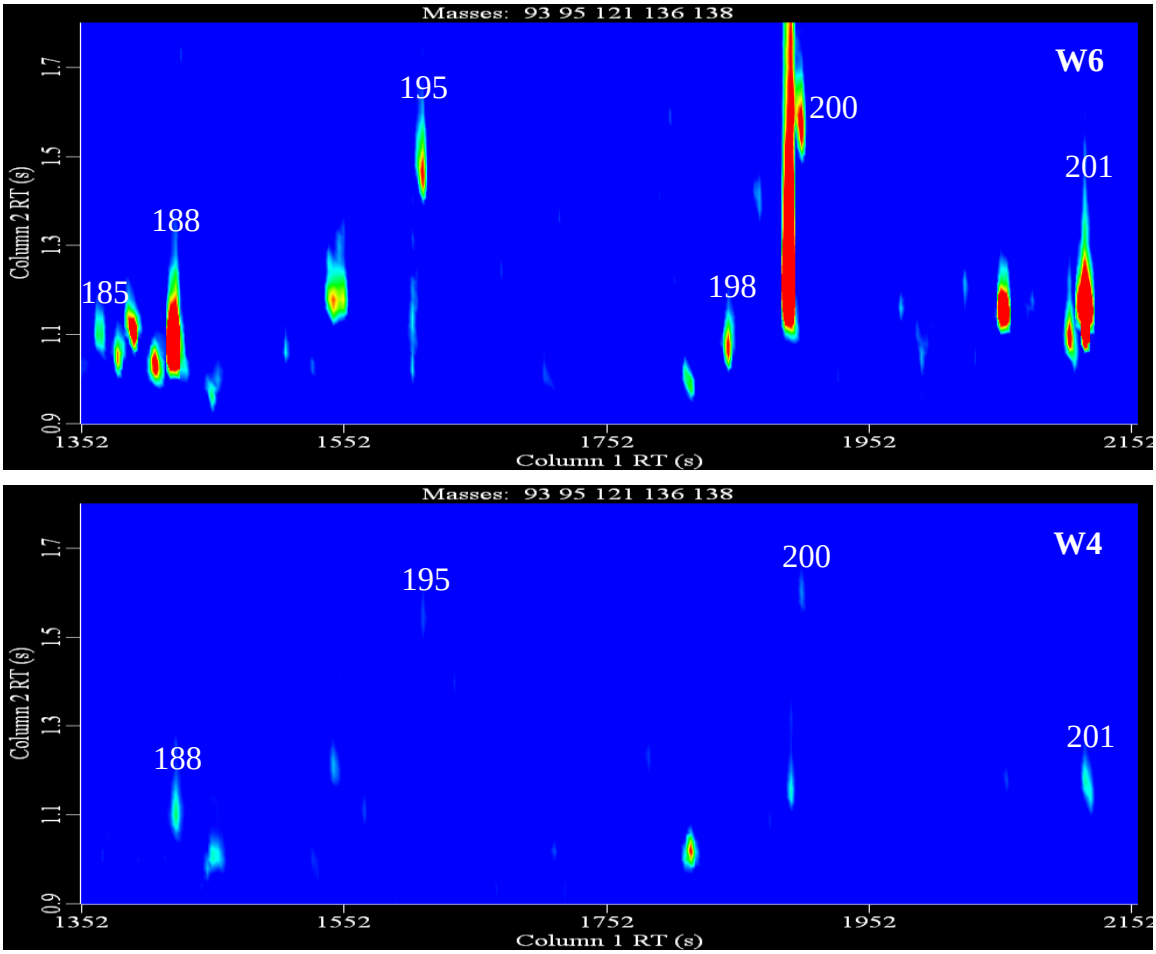


**Figure 4-3: Comparison of terpene profiles between two different Pinotage wines (W4 and W6). Peak numbers correspond to Table 4-1.**

terpene profiles for two different Pinotage wines. Two compounds – isocineole (**183**) and linalool formate (**196**) were not detected at all in sample W4. Note that only eucalyptol (**186**) and 4-terpineol acetate (**199**) were tentatively identified in this sample using our criteria, since the match factors for linalool (**193**) and a-terpineol (**198**) were below 70%.

The characteristic varietal terpene composition may be influenced to some extent by geographical origin. For instance, a comparison of Riesling wines in cooler (Germany) and in warmer (South Africa) climates have shown very similar monoterpene profiles, but the levels were lower in the warmer climate wines.[242] However, variations due to climatic differences are expected to be less significant for the samples analyzed here, and the differences in terpene content between these samples can more likely be ascribed to variations in fermentation conditions. [240, 241]

The monoterpene alcohols linalool (**193**) and $\alpha$-terpineol (**198**) are known for floral aroma properties and are important impact odorants. The odor perception thresholds of these compounds range from 50 to 400 μg/L. Monoterpene hydrocarbons such as aphellandrene (**182**), limonene (**185**), $\alpha$-terpinene (**188**) and terpinolen (**192**), as well as several monoterpene ketones and esters were also detected. Three norisoprenoid derivatives, 1,1,6-trimethyl-1,2- dihydro-naphthalene (TDN, **200**), 1,1,6-trimethyl-1,2,3,4-tetrahydro- naphthalene (TTN, **201**) and β-

damascenone (**202**) were also tentatively identified. These compounds are characterized by high RTs in the first dimension, due to relatively low vapour pressures. These $C_{13}$ norisoprenoid derivatives can be formed in grapes or/ and wine due to degradation of $C_{40}$ terpenes like carotenoids. TDN may be responsible for a kerosene or petrol odor in some wines and has a sensory threshold of 20 μg/L. The concentration of this compound increases significantly during bottle ageing. [237, 242, 243] β-Damascenone is an influential contributor to wine aroma and is believed to be present in all grape varieties. [215, 224, 237] This compound is characterized by a complex tropical fruit aroma and has an odor threshold of 50 ng/L.

Fenchon (**190**) and p-menthan-8-ol (**195**) were previously reported in grape, [219] but this is the first report of these compounds in wine. Fenchon was positively identified by an authentic standard, while p-menthan-8-ol was identified tentatively.

### 4.2.10 Hydrocarbons

In this study, over 20 hydrocarbons (not listed in Table 4-1) were detected. The sources of these hydrocarbons were most probably from the laboratory air, as most of them were also detected in blank analyses. It is also worth noting that the sample preparation procedure used favored the extraction of these molecules, even if they were present at very low concentrations. Most of these hydrocarbons have been

identified previously in wine and in cork stoppers.[244] Aromatic hydrocarbons have previously been detected in wine, where their presence is chiefly associated with contamination arising from petroleum-derived products.[245] Jordão et al.[246] also reported the presence of aromatic hydrocarbons in oak-wood.

### 4.2.11 Volatile phenols

Although the sample preparation method employed here hardly revealed high-boiling compounds like volatile phenols, 2,4-Bis(1,1- dimethylethyl)-phenol (**203**) and butylated hydroxytoluene (BHT, **204**) were detected in one and five samples, respectively. The source of these two compounds in wine is unclear, although plastic containers (plastic cap inserts were used for transport of the wine samples) have been reported as possible sources of BHT in wine.[247]

### 4.2.12 Pyrans

Pyran-related compounds have a six-membered ring as a basic chemical structure. In the current study two pyrans: 2H-pyran-2- one, tetrahydro- (**205**) and 2H-pyran, 2 ethenyltetrahydro-2,6,6- trimethyl- (**206**), were detected.

## 4.3 Conclusions

The methodology applied proved successful for the most detailed screening of volatile compounds in Pinotage wines reported to date. This is largely due to the

intrinsically high resolving power and sensitivity of GC×GC coupled to TOFMS. The proposed method was also found to be reproducible, but the time and labor intensive nature of data interpretation seems to preclude its usage in routine analysis for now. In total, 206 volatile compounds belonging to various chemical classes were identified (positively or tentatively). Many of the compounds were common to all samples, while others were uniquely identified in only a few, possibly reflecting differences in viticultural and winemaking practices. Differences may also be ascribed to the presence of co-eluting compounds and the low levels of occurrence, both of which make accurate identification difficult.

Several limitations were encountered in the methodology applied. First, the high level of ethanol, acetaldehyde, acetic acid and certain esters and alcohols masked a potentially large number of minor compounds and hampered their identification, even with the deconvolution software. Secondly, less volatile, highly polar and large molecular weight compounds such as acids, volatile phenols, lactones, etc., which could contribute significantly to wine flavor, were not detected. This was likely related to the sample preparation technique used, which favored the extraction of nonpolar and highly volatile compounds. While less volatile compounds might also be effectively extracted by the Carboxen coating used, they are notoriously difficult to desorb from the fiber. Despite these drawbacks, the methodology proved suitable

for the screening of a large number of wine volatiles. Future work will focus on the development of more selective sample preparation procedures to allow the detection of particular classes of minor wine volatiles.

It should be pointed out that all the compounds reported in this paper have previously been identified in wine or related products, although most of them are identified for the first time in Pinotage wine. Many compounds reported here may potentially contribute to the unique aroma of wine of this cultivar, notably sulphur compounds, terpenes and methoxypyrazines. These results therefore represent a valuable contribution to the knowledge of this uniquely South African cultivar and might eventually be used to improve winemaking practices for the production of Pinotage wines.

# Chapter 5

# Investigation of the Volatile Composition of Pinotage Wines Fermented with Different Malolactic Starter Cultures Using Comprehensive Two-Dimensional Gas Chromatography Coupled to Time-of-Flight Mass Spectrometry[i]

Malolactic fermentation (MLF) is an important part of the vinification process of especially red wines. During MLF, lactic acid bacteria (LAB) facilitate the conversion of harsh tasting malic acid to milder lactic acid. The resultant reduction in acidity and increase in pH improves the "mouth feel" of the wine. [249] Furthermore, the reduction of malic acid enhances the biological stability of the wine. [250, 251]

Besides deacidification of wine, MLF also results in the production of volatile metabolites as well as the modification of aroma compounds and flavor precursors originating from grapes and alcoholic fermentation, thereby influencing aroma of the final wine. [252] As a result, MLF offers winemakers an opportunity to modify the sensory properties of their wine. It has been shown that LAB metabolism can have

[i] This chapter is based on the author's paper " Investigation of the volatile composition of Pinotage wines fermented with different malolactic starter cultures using comprehensive two-dimensional gas chromatography coupled to time-of-flight mass spectrometry (GC×GC-TOF-MS)". [248]
Data analysis was spearheaded at the University of Stellenbosch, however it was also done by the author independently.

an impact on the concentrations of different wine volatiles, including esters, [253] alcohols, [253] volatile phenols, [254] terpenoids, [255, 256] and sulphur compounds. [257] The interaction of MLF bacteria with wine chemical constituents, however, depends on the wine type, the grape variety, [258, 259] the prevailing physicochemical factors and bacterial strain used to induce MLF. [252, 254, 260-264] As a result of the low pH, high alcohol concentration and low nutrient levels associated with the wine matrix, only four lactic acid bacteria species are known to be able to survive in wine. Three of the four, *Lactobacillus*, *Leuconostoc* and *Pediococcus*, are usually responsible for wine spoilage, whereas *Oenococcus oeni* is the preferred species for MLF. [251, 265]

Previous research on the aroma modification of wine as a function of MLF was mainly focused on diacetyl (2,3-butanedione). This compound, in addition to acetic acid, acetoin, 2,3-pentanedione and 2,3-butanediol, is formed through citric acid metabolism by LAB and is one of the most important aroma compounds formed during MLF.[258, 266] Whereas diacetyl has a characteristic buttery aroma at higher concentrations, it can contribute to nutty and toasty aromas at lower concentrations.[250, 250, 252, 253] The sensory impact and methods for diacetyl management in wine have been comprehensively studied [253, 267, 268] and reviewed by several authors.[250, 258, 266, 269, 270]

In addition to an increase of buttery aroma, other alterations of aroma, such as the reduction of vegetative, green aromas or changes in perceived fruitiness, have been reported.[252, 271] The reasons for these alterations of wine aroma are still not fully understood, as only limited research has focused on the changes of volatile composition as a function of MLF. Levels of wine esters have been shown to vary following MLF, with some authors reporting increased, [254, 262, 263, 272] but others lower, concentrations for these compounds. [260] Acetaldehyde, which can contribute together with hexanal, cis-hexen-3-al, and trans-hexen-2-al to green, grassy, and vegetative aromas in wine, has been shown to be present at lower levels following MLF.[273] The levels of several alcohols have also been shown to increase during MLF.[261, 262, 264, 272] Monoterpenes, norisoprenoids, hydrocarbons, and phenolic compounds can be released from their odorless glycoconjugated precursors by either acid or enzymatic hydrolysis. During alcoholic fermentation yeast provide glycosidases. [274] Although similar enzyme activity for *O. oeni* has been demonstrated[250, 275, 276], a decrease of some of these compounds has been reported following MLF. [254, 262] It is clear that MLF does affect the aroma profile of wine, although a detailed description of this alteration in terms of chemical changes induced by MLF is still lacking.

GC is the method of choice for the analysis of wine volatiles and has also been used for the investigation of the impact of MLF on wine volatile composition.[254, 263, 277] Conventional GC methods do, however, display some limitations regarding selectivity and resolving power (peak capacity), especially when applied to the analysis of very complex mixtures such as wine. GC×GC provides much higher resolution due to the combination of orthogonal separations using columns with different stationary phase properties.[12, 278] The enhanced peak capacity, improved sensitivity, and structured retention patterns for compounds with similar chemical characteristics[12] make GC×GC a powerful tool for screening of the volatile composition of food products, as has been demonstrated for hazelnut and coffee,[279, 280] fruits,[281] olive oil,[282] Cachaca, [213] and wine.[98, 283-286] Schmarr et al.[284] used GC×GC-qMS to investigate the changes in volatile composition occurring due to micro-oxygenation of red wines. Robinson et al.[286] recently reported an untargeted method employing headspace solid phase microextraction in combination with GC×GC coupled to time-of-flight mass spectrometry (HS-SPME-GC×GC-TOFMS) to investigate the influence of yeast strain, canopy management, and field site on the volatile composition of Cabernet Sauvignon wines.

Previous research on the effect of MLF on volatiles in Pinotage wines[287, 288] utilized 1D-GC with FID and MS detection. This approach did demonstrate some limitations associated with 1D-GC: primarily, the compounds identified and quantified were limited to those that can be separated on a single column and accurately quantified using these detectors. These compounds corresponded to major volatiles such as esters, alcohols, and acids, as well as carbonyl compounds, which have previously been shown to undergo changes in concentrations as a result of MLF.

The relatively limited knowledge on the chemical changes induced in wine by MLF, which may be ascribed in part to the lack of relevant analytical data, clearly highlights the need for new methods of in-depth, comprehensive chemical profiling, as well as the importance of identifying impact odorants associated with MLF. This is especially true for Pinotage wines. Relatively little is currently known with regard to the effect of MLF on Pinotage volatile composition.

In light of the above, and after performing in-depth qualitative analysis of volatiles in Pinotage wines in Chapter 4, our colleagues at Stellenbosch University, South Africa, approached us to exploit the benefits of GC×GC-TOFMS for the in-depth qualitative and quantitative analysis of volatiles in Pinotage wines subjected to MLF. To study differences in volatile composition as a function of MLF conditions, wines

produced under controlled conditions with different *O. oeni* starter cultures[287, 288] were analyzed by GC×GC-TOFMS, and data were analyzed statistically to investigate the main effects.

## 5.1 Experimental

### 5.1.1 Bacterial starter cultures

The three commercial starter cultures used in this study were Viniflora oenos (O) and Viniflora CH16 (C), both from CHR Hansen (Hørsholm, Denmark), and Lalvin VP41 (V), from Lallemand (Stellenbosch, South Africa). All starter cultures were kindly donated by Lallemand and CHR Hansen.

### 5.1.2 Wine samples

Wine samples were prepared by our colleagues at Stellenbosch University in South Africa. Pinotage wine samples from the 2009 harvest were obtained from an earlier study,[288] in which the impact of different MLF *O. oeni* starter cultures on wine aroma was assessed. Grapes were crushed and destemmed, and 30 mg/L of sulphur dioxide was added. Alcoholic fermentation was conducted at 25 °C with the commercial yeast WE372 (Anchor Technologies, South Africa). Punchdowns of the cap were done frequently. After pressing (at 2 °Brix), the wine was divided into

different lots to produce triplicate biological repeats of the control wines (in which MLF was prevented through the addition of 0.25 g/L of lysozyme to the juice to inhibit LAB growth), and the wines were produced using three different MLF starter cultures. Malolactic fermentations were performed in triplicate at 20 °C and were considered to be complete when the concentration of malic acid was below 0.3 g/L. The wines inoculated with starter cultures C and V completed MLF within 9 days, whereas those inoculated with starter culture O completed MLF within 12 days. All wines were racked from the lees, $SO_2$ levels were adjusted to 50 mg/L, and the wines were stored at 0 °C for 2 weeks for cold stabilization before they were bottled as described before.[288] All control and MLF wines were analyzed by GC×GC-TOFMS after 8 months of storage at 15 °C.

### 5.1.3 Chemicals and materials

A series of $C_6$ to $C_{18}$ *n*-alkanes for the determination of linear retention indices were obtained from Sigma-Aldrich (St. Louis, MO). NaCl (ACS grade) was obtained from EMD Chemicals (Gibbstown, NJ). Volatile standards (See later in Table 5-1) were purchased from Sigma-Aldrich, Fluka (Zwijndrecht, Netherlands), Riedel-de Haën (Steinheim, Germany) and Merck (Darmstadt, Germany). For headspace solid

phase microextraction (HS-SPME), a divinylbenzene/carboxen/polydimethylsiloxane (DVB/CAR/PDMS) 50/30 μm fiber was used (Supelco, Bellefonte, PA).

### 5.1.4 Sample preparation

HS-SPME sampling was carried out as follows: 5 mL of the wine sample (pH adjusted to 3 using hydrochloric acid) was transferred to a 20 mL headspace crimp-top vial and spiked with 0.3 mg/L 2-pentanone as internal standard. Three grams of sodium chloride (preheated to 250 °C and cooled to room temperature) were added to the vial together with a PTFE-coated stir bar, and the vial was capped immediately using a PTFE-lined septum and aluminum cap. The resulting saturated solutions were maintained with stirring at a temperature of 23 °C in a water bath before sampling. Each wine sample was submitted to HS-SPME sampling with stirring at 500 rpm for 5 and 30 min, respectively. Fiber blank and column blank analyses were carried out regularly to confirm that no sample carry-over occurred. Some hydrocarbons observed in the fiber blanks originated from the laboratory air. All chromatographic analyses were performed in duplicate.

### 5.1.5 Chromatographic conditions

The same instrumentation and columns used in Chapter 4 were used. The oven temperature program was as follows: initial temperature, 40 °C; kept for 0.2 min;

ramped at 3 °C/min to 170 °C and then at 10 °C/min to 250 °C; and held for 5 min. Thermal desorption and injection were performed using a split-splitless injector, operated at 260 °C in the splitless mode, with a splitless time of 3 min. Helium was used as the carrier gas at a constant flow of 1.5 mL/min. The transfer line between the GC and the MS was maintained at 250 °C. Mass spectral acquisition was carried out in the mass range 35-450 amu at a rate of 100 spectra per second (ionization energy 70 eV). The ion source temperature was 225 °C, and the detector voltage was set to -1750 V. For initial data processing the automatic peak detection algorithm of the ChromaTOF software (LECO Corp., version 2.22) was used. Positive identification was performed by analysis of authentic standards. The remaining peaks were tentatively identified on the basis of mass spectral comparison with the NIST 08 library. Using a series of *n*-alkanes, $^{1}$D retention indices ($LRI_{calcd}$) for each peak were automatically calculated by the ChromaTOF software. Experimental retention indices ($LRI_{calcd}$) were compared to literature values ($LRI_{lit.}$) to confirm tentative peak identification based on the mass spectra.

### 5.1.6 Statistical analysis

Analysis of variance (ANOVA) and Fisher's least significant difference (LSD) test were carried out using Statistica v10 (StatSoft, Inc., Tulsa, OK) to determine

significant differences in sample means based on the 95% confidence level. For multivariate analysis, the BiplotGUI package[289] of the open source software R (version 2.12.1)[290] was used. Peak area ratios of analytes relative to the internal standard were mean-centered and autoscaled prior to construction of principal component analysis (PCA) biplots in R.

## 5.2 Results and discussion

### 5.2.1 HS-SPME-GC×GC-TOFMS analysis of volatile composition

Wine contains a large number of diverse volatiles ranging widely in concentration, which makes analysis by 1D-GC, where sample components are typically separated by a single retention mechanism, challenging. To study both major volatiles and trace-level components in wine as a function of MLF, multiple analytical methods are often required[287, 288] to provide accurate quantitative data for a relatively limited number of compounds. To overcome these challenges, GC×GC was used in the current study. GC×GC has been shown to be a particularly powerful separation method for the analysis of complex mixtures of volatiles, including wine. [98, 155, 283-286]

However, despite the enhanced selectivity and sensitivity of GC×GC, sample preparation remains a crucial part of the analytical procedure, especially when complex samples such as red wine are analyzed. When wine aroma is profiled, both

minor and major compounds are of interest. Typically, extraction methods are optimized to provide either maximum sensitivity for trace level compounds (for example, by removal of major volatiles that would otherwise obscure the analysis of minor constituents) or for analyses of major compounds (these methods do not provide the sensitivity required for low-level analytes). When SPME is used for screening of both major and minor compounds, overloading sometimes occurs in 1D-GC, but is even more prevalent in GC×GC (especially in the $^{2}$D) because of refocusing of the bands in the cryogenic modulator. When excessive amounts of analytes are introduced into the GC×GC system, three phenomena combine to make accurate quantitation unreliable, if not impossible: the capacity of the modulator might be exceeded, which typically leads to significant injection band broadening and irregular injection band shapes; the $^{2}$D column might be overloaded, which leads to distorted peaks; and finally, the linear dynamic range of the detector might be exceeded, which is particularly important when TOFMS is used at high data acquisition rates. For these reasons, in the current work every sample was analyzed using two different sets of HS-SPME conditions. To extract the maximum amount of minor compounds, a 30 min extraction time was used. This time allowed the minor components to equilibrate with the fiber, thus maximizing the sensitivity. However, the major components overloaded the system under such conditions, which made

their quantitation impossible. To overcome this problem, a 5 min extraction time was also used. The amounts of major components extracted under such conditions were significantly reduced, which eliminated overloading of the system and allowed accurate quantification of such compounds.

It should be noted, nevertheless, that the selective nature of HS-SPME does influence the compounds extracted from the wine matrix. This form of sample preparation is favorable for the more volatile wine constituents, but may not necessarily be suited to the analysis of higher-boiling compounds such as some terpenoids,[283] for which alternative methods such as solid phase extraction (SPE) are better suited.

Figure 5-1 presents contour plots obtained for the HS-SPME-GC×GC-TOFMS analysis of the control and the three MLF Pinotage wines. Note that whereas some differences in the volatile profiles of the four wines are evident from this figure, the z-axis scale obscures further significant differences in the levels of minor constituents.

The orthogonal column configuration used in this study was a nonpolar polydimethylsiloxane column in the $^{1}$D providing separation mainly according to boiling point of the analytes and a polar polyethylene glycol column in

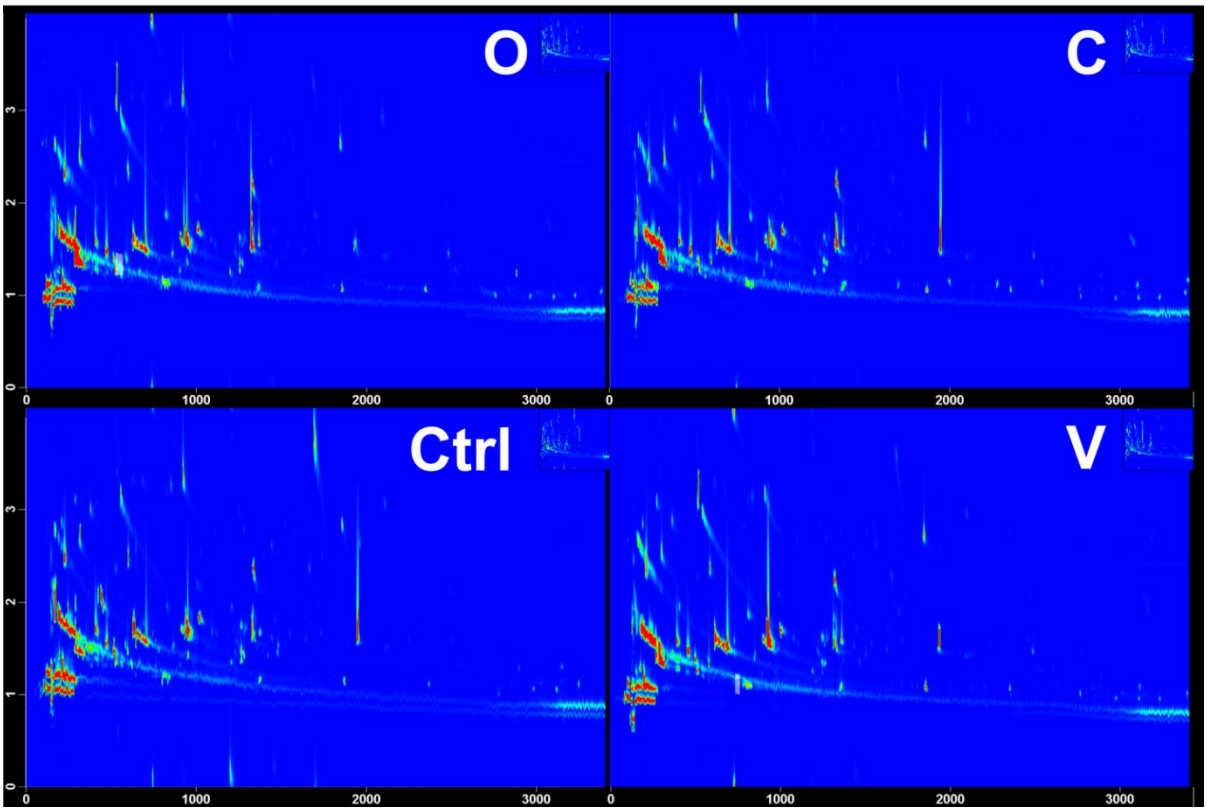


**Figure 5-1: Analytical ion chromatograms (AICs) obtained for the control and the three MLF wines fermented with *O. oeni* starter cultures Viniflora oenos (O), Viniflora CH16 (C) and Lalvin VP41 (V) using HS-SPME-GC×GC-TOFMS (5 min extraction). The sums of unique ions (see Table 5-1) were used to generate the AICs.**

the $^{2}$D providing separation based on differences in polarity. Therefore, more polar compounds were strongly retained in the $^{2}$D, even leading to wraparound for compounds such as ethyl-S-lactate and, to a larger extent, the volatile acids. In general, these results are in agreement with those of previous studies utilizing the "normal" (i.e. apolar × polar) column configuration for the GC×GC analysis of wine

volatiles.[98, 285, 287] Schmarr et al.[284] used a reversed, polar × apolar, column combination for wine analysis, although significant breakthrough in the $^{2}$D was reported under these conditions, resulting in multiple peaks being detected for numerous compounds.

The experimental setup used here provided a significant improvement in the resolution of wine volatiles compared to conventional 1D-GC. This is illustrated for a selected group of compounds in Figure 5-2. Linalool and 2-nonanol, as well as

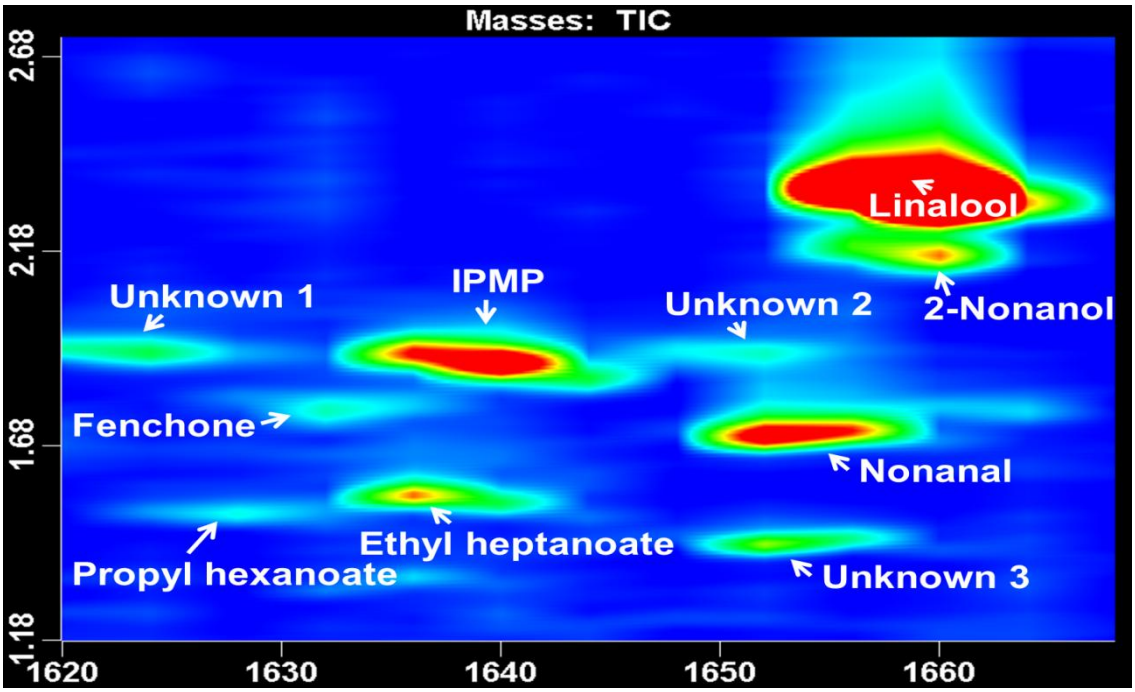


**Figure 5-2: Total ion chromatogram of a wine fermented with starter culture O presenting the separation of selected volatiles by HS-SPME-GC×GC-TOFMS (30 min SPME extraction time).**

2-methoxy-3 isopropylpyrazine (IPMP) and ethyl heptanoate, can be seen to coelute in the $^{1}$D because of their similar boiling points, but are separated in the $^{2}$D due to differences in their polarity. The same is the case for nonanal and the unidentified compounds labeled unknowns 2 and 3. On the other hand, nonanal and fenchone, as well as IPMP and unknown 1, are separated in the $^{1}$D due to different boiling points, but coelute in the $^{2}$D because of their similar polarities. Clearly, coelution would inevitably occur in routine 1D-GC screening methods utilizing a single stationary phase (typically polar) not optimized for separation of specific compounds.

Another benefit of GC×GC compared to 1D-GC is the enhanced sensitivity, resulting from the refocusing of analytes in the modulator. This leads to narrower peaks and therefore larger signal-to-noise ratios in the $^{2}$D. [12] Excellent peak widths in the range of 100 ms for most analytes can be observed in Figure 5-2. Moreover, typical levels of IPMP in Pinotage are ~ 1 ng/L,[238] which served to highlight the excellent sensitivity of the HS-SPME-GC×GC-TOFMS method for selected trace-level compounds.

Identification of the majority of peaks was based on comparison of deconvoluted mass spectra with the NIST 08 spectral library using ChromaTOF software, employing a minimum match factor of 70% as criterion. Furthermore, linear

retention indices (LRI) were calculated using a homologous series of *n*-alkanes and compared with literature values. With the fact that literature LRI values were determined by means of 1D-GC taken into account, a relatively large maximum absolute difference of 30 between literature values and the experimental LRI values was used as criterion. In this manner, a total of 79 compounds were tentatively identified. In addition, authentic standards were used to positively confirm the identity of a further 36 compounds (Table 5-1).

Because the goal of this work was to investigate differences in the levels of individual volatile compounds between wines as a function of MLF, special care was taken with the identification of compounds based on the above-mentioned criteria. Compound identification was therefore confirmed manually in each instance. Although this conservative approach is necessarily time-consuming and resulted in a reduction in the number of compounds identified using an automated ChromaTOF search, we found this step to be essential to minimize the risk of possible incorrect identification and to improve statistical analysis and data interpretation. This explains the relatively low number of tentatively identified compounds reported in this study compared to previous reports utilizing GC×GC

**Table 5-1: Compounds Identified and Quantified in Pinotage Wine Samples by HS-SPME-GC×GC-TOFMS[a]**

| No | Compound | 1 | 1D RT | 2D RT | MS match[b] | $LRI_{calc}$[c] | $LRI_{lit}$[d] | Unique mass | Ctrl[h] av ± SD | 2 | V[h] av ± SD | 3 | O[h] av ± SD | 4 | C[h] av ± SD | 5 |
|---|---|---|---|---|---|---|---|---|---|---|---|---|---|---|---|---|
| | **Esters** | | | | | | | | | | | | | | | |
| 1 | Formic acid, ethyl ester (Ethyl formate) | e,f | 184 | 1.34 | 969 | 508 | 530 | 45 | 0.1548 ± 0.010 | a | 0.1649 ± 0.021 | a | 0.2117 ± 0.032 | b | 0.2289 ± 0.045 | b |
| 2 | Acetic acid, methyl ester (Methyl acetate) | f | 192 | 1.38 | 952 | 516 | 506 | 43 | 0.1629 ± 0.011 | a | 0.2537 ± 0.054 | b | 0.3129 ± 0.022 | bc | 0.3339 ± 0.047 | c |
| 3 | Ethyl acetate | e | 280 | 1.44 | 980 | 600 | 596 | 43 | not quantified | | | | | | | |
| 4 | Propanoic acid, ethyl ester (Ethyl propanoate) | f | 464 | 1.52 | 953 | 700 | 680 | 57 | 2.4040 ± 0.109 | a | 3.7544 ± 0.553 | b | 3.7631 ± 0.338 | b | 4.3243 ± 0.331 | c |
| 5 | Acetic acid, propyl ester (Propyl acetate) | f | 468 | 1.58 | 952 | 702 | 698 | 43 | 0.4509 ± 0.028 | a | 1.5736 ± 0.356 | b | 1.7971 ± 0.170 | bc | 1.9623 ± 0.237 | c |
| 6 | Propanoic acid, 2-methyl-, ethyl ester (Ethyl isobutyrate) | e,f | 588 | 1.44 | 920 | 746 | 743 | 71 | 0.4740 ± 0.044 | a | 0.7433 ± 0.094 | b | 0.7402 ± 0.087 | b | 0.7974 ± 0.102 | b |
| 7 | Acetic acid, 2-methylpropyl ester (Isobutyl acetate) | | 624 | 1.54 | 939 | 760 | 767 | 56 | not quantified | | | | | | | |
| 8 | 1-Butanol, 3-methyl-, formate (Isoamyl formate) | g | 672 | 1.73 | 789 | 778 | 777 | 55 | 0.0401 ± 0.005 | n.s. | 0.0375 ± 0.005 | n.s. | 0.0429 ± 0.007 | n.s. | 0.0434 ± 0.005 | n.s. |
| 9 | Propanoic acid, 2-hydroxy-, ethyl ester (Ethyl lactate) | | 676 | 0.68 | 716 | 779 | 787 | 45 | not quantified | | | | | | | |
| 10 | Butanoic acid, ethyl ester (Ethyl butyrate) | e,f | 704 | 1.54 | 867 | 790 | 778 | 91 | 5.2829 ± 0.254 | a | 15.2660 ± 4.514 | b | 15.4990 ± 3.532 | b | 15.5027 ± 2.708 | b |
| 11 | Propanoic acid, 2-hydroxy-, ethyl ester, (S) (Ethyl-S-lactate) | e,f | 736 | 0.12 | 984 | 801 | 800 | 45 | 0.0869 ± 0.006 | a | 0.4533 ± 0.061 | b | 0.4814 ± 0.027 | b | 0.5326 ± 0.047 | c |
| 12 | Acetic acid, butyl ester (Butyl acetate) | f | 736 | 1.61 | 955 | 801 | 805 | 43 | 0.0769 ± 0.010 | a | 0.2384 ± 0.046 | b | 0.2785 ± 0.030 | bc | 0.2891 ± 0.054 | c |

| | | | | | | | | | | | | | | | | |
|---|---|---|---|---|---|---|---|---|---|---|---|---|---|---|---|---|
| 13 | 2-Butenoic acid, ethyl ester (Ethyl 2-butenoate) | *f* | 820 | 1.95 | 939 | 828 | 819 | 69 | 0.2864 ± 0.011 | a | 1.1222 ± 0.258 | b | 1.3006 ± 0.102 | b | 1.3367 ± 0.135 | b |
| 14 | Butanoic acid, 2-methyl-, ethyl ester (Ethyl 2-methylbutanoate) | *e,f* | 856 | 1.49 | 950 | 840 | 829 | 102 | 0.1007 ± 0.007 | a | 0.1882 ± 0.013 | b | 0.2666 ± 0.003 | c | 0.2042 ± 0.008 | b |
| 15 | Butanoic acid, 3-methyl-, ethyl ester (Ethyl isovalerate) | *f* | 860 | 1.5 | 920 | 841 | 824 | 88 | 0.1975 ± 0.006 | a | 0.3005 ± 0.016 | b | 0.2999 ± 0.018 | b | 0.3484 ± 0.006 | c |
| 16 | 1-Butanol, 3-methyl-, acetate (Isoamyl acetate) | | 928 | 1.62 | 925 | 863 | 856 | 43 | not quantified | | | | | | | |
| 17 | 1-Butanol, 2-methyl-, acetate (2-Methylbutyl acetate) | | 936 | 1.61 | 935 | 866 | 868 | 43 | not quantified | | | | | | | |
| 18 | Pentanoic acid, ethyl ester (Ethyl pentanoate) | *e,g* | 1004 | 1.57 | 913 | 887 | 881 | 88 | 0.0339 ± 0.003 | a | 0.0553 ± 0.012 | b | 0.0588 ± 0.010 | b | 0.0659 ± 0.008 | b |
| 19 | Hexanoic acid, methyl ester (Methyl hexanoate) | *f* | 1084 | 1.66 | 922 | 913 | 903 | 74 | 0.1522 ± 0.008 | a | 0.1041 ± 0.009 | c | 0.1003 ± 0.008 | c | 0.1171 ± 0.009 | b |
| 20 | Butanoic acid, 3-hydroxy-, ethyl ester (Ethyl 3-hydroxybutyrate) | | 1108 | 0.6 | 939 | 920 | 949 | 43 | not quantified | | | | | | | |
| 21 | 1-Butanol, 3-methyl-, propanoate (Isoamyl propanoate) | *g* | 1228 | 1.52 | 874 | 958 | 948 | 57 | 0.0240 ± 0.003 | a | 0.0382 ± 0.008 | ab | 0.0489 ± 0.011 | b | 0.0524 ± 0.005 | b |
| 22 | Hex-5-enoic acid, ethyl ester | *e,g* | 1276 | 1.76 | 930 | 973 | 965 | 60 | 0.0320 ± 0.002 | a | 0.0558 ± 0.011 | c | 0.0672 ± 0.010 | bc | 0.0725 ± 0.004 | b |
| 23 | Butanoic acid, butyl ester (Butyl butyrate) | | 1312 | 1.53 | 942 | 984 | 978 | 71 | not quantified | | | | | | | |
| 24 | Hexanoic acid, ethyl ester (Ethyl hexanoate) | *e* | 1320 | 1.57 | 947 | 986 | 976 | 88 | not quantified | | | | | | | |

| | | | | | | | | | | | | | | | | |
|---|---|---|---|---|---|---|---|---|---|---|---|---|---|---|---|---|
| 25 | 3-Hexen-1-ol, acetate, (E)- | | 1332 | 1.81 | 719 | 990 | 983 | 82 | not quantified | | | | | | | |
| 26 | 3-Hexenoic acid, ethyl ester (Ethyl-3-hexenoate) | | 1336 | 1.78 | 819 | 991 | 986 | 68 | not quantified | | | | | | | |
| 27 | 3-Hexen-1-ol, acetate, (Z)- | | 1344 | 1.83 | 898 | 994 | 987 | 67 | not quantified | | | | | | | |
| 28 | Acetic acid, hexyl ester (Hexyl acetate) | e,f | 1364 | 1.62 | 957 | 1000 | 990 | 43 | 0.5141 ± 0.023 | a | 1.1137 ± 0.242 | b | 1.1633 ± 0.095 | b | 1.2256 ± 0.225 | b |
| 29 | Heptanoic acid, methyl ester (Methyl heptanoate) | | 1404 | 1.64 | 937 | 1013 | 1005 | 74 | not quantified | | | | | | | |
| 30 | Ethyl 2-hexenoate | f | 1452 | 1.79 | 957 | 1028 | 1023 | 97 | 0.0742 ± 0.008 | a | 0.1211 ± 0.013 | b | 0.1297 ± 0.007 | b | 0.1454 ± 0.030 | c |
| 31 | Hexanoic acid, 2-ethyl-, methyl ester (Ethyl 2-ethylhexanoate) | | 1472 | 1.49 | 922 | 1035 | 1024 | 87 | not quantified | | | | | | | |
| 32 | Propanedioic acid, diethyl ester (Diethyl malonate) | | 1504 | 3.11 | 899 | 1046 | 1038 | 115 | not quantified | | | | | | | |
| 33 | Butanoic acid, 3-methylbutyl ester (Isoamyl butyrate) | | 1508 | 1.45 | 942 | 1046 | 1041 | 71 | not quantified | | | | | | | |
| 34 | Pentanoic acid, 2-hydroxy-4-methyl-, ethyl ester | g | 1512 | 2.77 | 848 | 1048 | 1043 | 69 | 0.0861 ± 0.012 | a | 0.1013 ± 0.011 | ab | 0.1131 ± 0.014 | b | 0.1197 ± 0.020 | b |
| 35 | Propanoic acid, 2-hydroxy-, 3-methylbutyl ester (Isoamyl lactate) | g | 1548 | 2.87 | 837 | 1060 | 1047 | 45 | 0.0250 ± 0.005 | a | 0.0897 ± 0.022 | bc | 0.0695 ± 0.010 | c | 0.0918 ± 0.022 | b |
| 36 | Butanedioic acid, ethyl methyl ester | | 1624 | 3.21 | 915 | 1084 | 1070 | 115 | not quantified | | | | | | | |
| 37 | Hexanoic acid, propyl ester (Propyl hexanoate) | f | 1628 | 1.5 | 934 | 1085 | 1079 | 61 | 0.0215 ± 0.002 | a | 0.0309 ± 0.002 | b | 0.0320 ± 0.003 | bc | 0.0327 ± 0.004 | c |
| 38 | Heptanoic acid, ethyl ester (Etyhl heptanoate) | f | 1636 | 1.55 | 935 | 1087 | 1083 | 88 | 0.0753 ± 0.004 | n.s. | 0.0763 ± 0.006 | n.s. | 0.0809 ± 0.005 | n.s. | 0.0830 ± 0.009 | n.s. |

| | | | | | | | | | | | | | | | | |
|---|---|---|---|---|---|---|---|---|---|---|---|---|---|---|---|---|
| 39 | octanoic acid, methyl ester (Methyl octanoate) | f | 1720 | 1.62 | 942 | 1115 | 1108 | 74 | 0.0811 ± 0.010 | a | 0.0638 ± 0.003 | b | 0.0608 ± 0.005 | b | 0.0555 ± 0.023 | b |
| 40 | Hexanoic acid, 2-methylpropyl ester (Isobutyl hexanoate) | | 1804 | 1.41 | 840 | 1143 | 1152 | 99 | not quantified | | | | | | | |
| 41 | Butanedioic acid, diethyl ester (Diethyl succinate) | e,f | 1844 | 2.77 | 968 | 1157 | 1151 | 101 | 2.0866 ± 0.177 | a | 3.0600 ± 0.228 | b | 3.0860 ± 0.195 | b | 3.2183 ± 0.051 | b |
| 42 | octanoic acid, ethyl ester (Ethyl octanoate) | e | 1936 | 1.55 | 926 | 1187 | 1175 | 88 | not quantified | | | | | | | |
| 43 | Methyl salicylate | g | 1944 | 3.2 | 776 | 1190 | 1176 | 120 | 0.0253 ± 0.003 | ac | 0.0141 ± 0.003 | b | 0.0227 ±0.004 | c | 0.0267 ±0.004 | ab |
| 44 | Benzeneacetic acid, ethyl ester (Ethyl phenylacetate) | e,g | 2060 | 2.85 | 951 | 1231 | 1211 | 91 | 0.0647 ± 0.007 | a | 0.0328 ± 0.003 | b | 0.0364 ± 0.007 | b | 0.0397 ± 0.007 | b |
| 45 | Acetic acid, 2-phenylethyl ester (2-Phenylethyl acetate) | e,f | 2092 | 3.01 | 932 | 1243 | 1224 | 104 | 0.4673 ± 0.137 | n.s. | 0.4264 ± 0.061 | n.s. | 0.4316 ± 0.088 | n.s. | 0.4353 ± 0.106 | n.s. |
| 46 | Hexanoic acid, 3-methylbutyl ester (Isopentyl hexanoate) | | 2092 | 1.46 | 966 | 1242 | 1253 | 70 | not quantified | | | | | | | |
| 47 | Hexanoic acid, 2-methylbutyl ester (2-Methylbutyl hexanoate) | | 2104 | 1.44 | 922 | 1247 | 1236 | 99 | not quantified | | | | | | | |
| 48 | Nonanoic acid, ethyl ester (Ethyl nonanoate) | e,g | 2220 | 1.48 | 912 | 1289 | 1288 | 88 | 0.0161 ± 0.003 | a | 0.0253 ± 0.007 | b | 0.0269 ± 0.006 | b | 0.0322 ± 0.006 | b |
| 49 | Ethyl 9-decenoate | g | 2460 | 1.61 | 891 | 1379 | 1357 | 55 | 0.0262 ± 0.008 | a | 0.0462 ± 0.012 | b | 0.0478 ± 0.009 | b | 0.0605 ± 0.014 | b |
| 50 | Decanoic acid, ethyl ester (Ethyl decanoate) | e,f | 2488 | 1.47 | 918 | 1390 | 1367 | 88 | 0.1109 ± 0.010 | a | 0.2975 ± 0.026 | b | 0.3276 ± 0.027 | b | 0.3116 ± 0.034 | b |
| | **Alcohols** | | | | | | | | | | | | | | | |
| 51 | 1-Propanol | f | 220 | 2.31 | 962 | 544 | 524 | 59 | 3.3180 ± 0.267 | a | 4.7332 ± 0.592 | b | 5.5978 ± 0.352 | c | 5.2694 ± 0.657 | c |

| | | | | | | | | | | | | | | | | |
|---|---|---|---|---|---|---|---|---|---|---|---|---|---|---|---|---|
| 52 | 1-Propanol, 2-methyl- (isobutanol) | e,f | 312 | 2.65 | 825 | 618 | 625 | 74 | 0.9690 ± 0.135 | a | 1.5934 ± 0.146 | b | 1.8160 ± 0.141 | bc | 1.9612 ± 0.125 | c |
| 53 | 1-Butanol | e,f | 376 | 2.93 | 955 | 653 | 660 | 56 | 0.6411 ± 0.066 | a | 0.8428 ± 0.066 | b | 0.9640 ± 0.060 | c | 0.9102 ± 0.090 | c |
| 54 | 3-Buten-1-ol, 3-methyl- | | 520 | 3.78 | 923 | 722 | 728 | 39 | not quantified | | | | | | | |
| 55 | 1-Butanol, 3-methyl- (Isoamyl alcohol) | e | 524 | 3.17 | 965 | 723 | 718 | 55 | not quantified | | | | | | | |
| 56 | 2-Pentanol, 4-methyl- | f | 592 | 2.43 | 906 | 748 | 760 | 45 | 0.6999 ± 0.076 | n.s. | 0.6518 ± 0.048 | n.s. | 0.6128 ± 0.051 | n.s. | 0.6899 ± 0.033 | n.s. |
| 57 | 1-Pentanol (Amyl alcohol) | f | 616 | 3.23 | 935 | 758 | 744 | 42 | 0.0711 ± 0.018 | a | 0.1189 ± 0.017 | b | 0.1248 ± 0.006 | bc | 0.1360 ± 0.028 | c |
| 58 | 2,3-Butanediol | | 644 | 2.48 | 945 | 768 | 748 | 45 | not quantified | | | | | | | |
| 59 | 1-Pentanol, 4-methyl- (isohexanol) | f | 820 | 3.11 | 947 | 829 | 851 | 56 | 0.1327 ± 0.011 | n.s. | 0.1399 ± 0.016 | n.s. | 0.1555 ± 0.007 | n.s. | 0.1564 ± 0.017 | n.s. |
| 60 | 1-Pentanol, 3-methyl- (3-methylpentanol) | f | 844 | 3.18 | 929 | 837 | 854 | 56 | 0.3140 ± 0.027 | n.s. | 0.3014 ± 0.022 | n.s. | 0.3287 ± 0.030 | n.s. | 0.3270 ± 0.029 | n.s. |
| 61 | 1-Hexanol | e,f | 916 | 3.17 | 940 | 860 | 852 | 56 | 5.1824 ± 0.042 | a | 4.5378 ± 0.161 | b | 4.2983 ± 0.027 | c | 4.3190 ± 0.029 | c |
| 62 | 2-Heptanol | g | 1016 | 2.45 | 894 | 891 | 877 | 45 | 0.0201 ± 0.003 | n.s. | 0.0182 ± 0.001 | n.s. | 0.0184 ± 0.002 | n.s. | 0.0212 ± 0.002 | n.s. |
| 63 | 1-Heptanol | f | 1240 | 2.96 | 973 | 962 | 952 | 56 | 0.1981 ± 0.027 | a | 0.1080 ± 0.017 | b | 0.0973 ± 0.012 | b | 0.0973 ± 0.018 | b |
| 64 | 1-octen-3-ol | e,f | 1272 | 2.76 | 882 | 972 | 959 | 57 | 0.0951 ± 0.011 | a | 0.0561 ± 0.004 | b | 0.0625 ± 0.009 | bc | 0.0638 ± 0.010 | c |
| 65 | 2-octanol, (R)- | e | 1340 | 2.35 | 942 | 993 | 985 | 45 | not quantified | | | | | | | |
| 66 | 1-octanol | f | 1564 | 2.71 | 931 | 1065 | 1054 | 55 | 0.1082 ± 0.009 | n.s. | 0.0901 ± 0.021 | n.s. | 0.0909 ± 0.013 | n.s. | 0.0803 ± 0.027 | n.s. |
| 67 | 2-Nonanol | | 1660 | 2.17 | 948 | 1095 | 1084 | 45 | not quantified | | | | | | | |
| 68 | Phenylethyl Alcohol | e | 1684 | 3.71 | 954 | 1104 | 1082 | 91 | not quantified | | | | | | | |
| | **Ketones** | | | | | | | | | | | | | | | |
| 69 | 2,3-Butanedione (Diacetyl) | | 244 | 1.88 | 988 | 566 | 558 | 43 | 0.1766 ± 0.003 | a | 0.2064 ± 0.006 | b | 0.3755 ± 0.013 | c | 0.2511 ± 0.006 | d |
| 70 | 2-Butanone | g | 256 | 1.47 | 949 | 577 | 582 | 72 | 0.0267 ± 0.004 | a | 0.0121 ± 0.001 | b | 0.0145 ± 0.005 | b | 0.0161 ± 0.005 | b |
| 71 | 2,3-Pentanedione | e,g | 416 | 2.06 | 970 | 674 | 660 | 57 | 0.3459 ± 0.022 | a | 0.1058 ± 0.017 | b | 0.0972 ± 0.007 | b | 0.1114 ± 0.007 | b |
| 72 | 3-Penten-2-one | f | 520 | 2.31 | 937 | 721 | 697 | 69 | 0.2566 ± 0.026 | a | 0.1226 ± 0.037 | b | 0.2934 ± 0.032 | a | 0.3175 ± 0.016 | a |
| 73 | Methyl Isobutyl Ketone | | 528 | 1.59 | 882 | 724 | 730 | 58 | not quantified | | | | | | | |

| | | | | | | | | | | | | | | | | |
|---|---|---|---|---|---|---|---|---|---|---|---|---|---|---|---|---|
| 74 | 2,3-Pentanedione, 4-methyl- | | 640 | 2.05 | 945 | 766 | 763 | 71 | not quantified | | | | | | | |
| 75 | 2-Heptanone | *g* | 964 | 1.81 | 950 | 875 | 871 | 58 | 0.0405 ± 0.002 | a | 0.0184 ± 0.002 | b | 0.0103 ± 0.002 | c | 0.0159 ± 0.003 | bc |
| 76 | 1-octen-3-one | | 1248 | 1.92 | 911 | 964 | 956 | 55 | not quantified | | | | | | | |
| 77 | 3-octanone | *f* | 1280 | 1.67 | 953 | 974 | 963 | 57 | 0.3742 ± 0.052 | n.s. | 0.3030 ± 0.024 | ns | 0.3279 ± 0.136 | n.s. | 0.2973 ± 0.039 | n.s. |
| 78 | Acetophenone | *e* | 1528 | 3.87 | 901 | 1054 | 1049 | 77 | not quantified | | | | | | | |
| 79 | 2-Pentanone | | 404 | 1.65 | 935 | 668 | 651 | 43 | not quantified | | | | | | | |
| | **Aldehydes** | | | | | | | | | | | | | | | |
| 80 | 2-Propenal (Acrolein) | | 160 | 1.33 | 976 | 485 | 470 | 56 | | | | | | | | |
| 81 | Propanal, 2-methyl- (isobutanal) | *g* | 216 | 1.26 | 929 | 539 | 532 | 41 | 0.0504 ± 0.002 | ab | 0.0379 ± 0.009 | a | 0.0662 ± 0.016 | b | 0.0617 ± 0.016 | b |
| 82 | Butanal | *g* | 252 | 1.4 | 854 | 573 | 575 | 72 | 0.0138 ± 0.001 | n.s. | 0.0134 ± 0.003 | n.s. | 0.0130 ± 0.002 | n.s. | 0.0106 ± 0.001 | n.s. |
| 83 | Butanal, 3-methyl- (isopentanal) | *f* | 344 | 1.49 | 938 | 635 | 628 | 58 | 0.4486 ± 0.089 | n.s. | 0.4286 ± 0.026 | n.s. | 0.5130 ± 0.051 | n.s. | 0.5260 ± 0.024 | n.s. |
| 84 | Butanal, 2-methyl- (2-methylbutanal) | | 364 | 1.44 | 905 | 646 | 632 | 58 | not quantified | | | | | | | |
| 85 | Hexanal | *e,g* | 684 | 1.73 | 916 | 782 | 769 | 56 | 0.0348 ± 0.002 | a | 0.0209 ± 0.001 | b | 0.0199 ± 0.003 | b | 0.0179 ± 0.002 | c |
| 86 | Benzaldehyde | *e* | 1188 | 0.1 | 914 | 945 | 927 | 77 | not quantified | | | | | | | |
| 87 | octanal | | 1332 | 1.8 | 804 | 990 | 982 | 82 | not quantified | | | | | | | |
| 88 | Benzeneacetaldehyde (Phenylacetaldehyde) | *f* | 1444 | 0.3 | 954 | 1025 | 1012 | 91 | 0.2474 ± 0.010 | a | 0.1948 ± 0.013 | b | 0.1819 ± 0.021 | b | 0.1854 ± 0.029 | b |
| 89 | Nonanal | *e,g* | 1652 | 1.71 | 938 | 1093 | 1081 | 57 | 0.0853 ± 0.017 | n.s. | 0.0505 ± 0.009 | n.s. | 0.0616 ± 0.012 | n.s. | 0.0760 ± 0.019 | ns |
| 90 | Decanal | *e,g* | 1964 | 1.68 | 926 | 1196 | 1183 | 57 | 0.0217 ± 0.005 | n.s. | 0.0192 ± 0.005 | n.s. | 0.0227 ± 0.004 | n.s. | 0.0264 ± 0.007 | ns |
| | **Acids** | | | | | | | | | | | | | | | |
| 91 | Butanoic acid | | 696 | 1.17 | 724 | 787 | 780 | 60 | not quantified | | | | | | | |
| 92 | Hexanoic acid | | 1300 | 2.09 | 944 | 980 | 973 | 45 | not quantified | | | | | | | |
| 93 | octanoic Acid | | 1884 | 1.52 | 926 | 1170 | 1154 | 60 | not quantified | | | | | | | |
| | **Acetals** | | | | | | | | | | | | | | | |

| | | | | | | | | | | | | | | | | |
|---|---|---|---|---|---|---|---|---|---|---|---|---|---|---|---|---|
| 94 | 1,3-Dioxolane, 2,4,5-trimethyl- | | 508 | 1.42 | 717 | 944 | 711 | 43 | | | | | not quantified | | | |
| | **Furans** | | | | | | | | | | | | | | | |
| 95 | Furan, 2,5-dimethyl- | | 468 | 1.44 | 880 | 702 | 696 | 96 | | | | | not quantified | | | |
| 96 | 2-Furancarboxaldehyde (Furfural) | | 772 | 2.76 | 940 | 813 | 794 | 95 | | | | | not quantified | | | |
| | **Nitrogen containing compounds** | | | | | | | | | | | | | | | |
| 97 | Pyrazine, 2-methoxy-3-(1-methylethyl)- [2-Methoxy-3-isopropylpyrazine (IPMP)] | *e* | 1640 | 1.84 | 739 | 1089 | 1080 | 137 | | | | | not quantified | | | |
| 98 | Pyrazine, 2-methoxy-3-(1-methylpropyl)- [2-Methoxy-3-sec-butylpyrazine (SBMP)] | *e* | 1880 | 1.77 | 803 | 1168 | 1151 | 138 | | | | | not quantified | | | |
| | **Compounds with terpenoid character and others** | | | | | | | | | | | | | | | |
| 99 | Benzene, (1-methylethyl)- [Cumene] | | 1112 | 1.59 | 915 | 921 | 907 | 105 | | | | | not quantified | | | |
| 100 | Benzene, propyl- ) [Isocumene] | | 1208 | 1.63 | 945 | 951 | 934 | 91 | | | | | not quantified | | | |
| 101 | Camphene | | 1224 | 1.27 | 950 | 956 | 958 | 91 | | | | | not quantified | | | |
| 102 | 4-Heptanone, 2,6-dimethyl- | | 1240 | 1.48 | 878 | 961 | 951 | 56 | | | | | not quantified | | | |
| 103 | 5-Hepten-2-one, 6-methyl- | *g* | 1272 | 2.04 | 901 | 972 | 938 | 43 | 0.0334 ± 0.003 | a | 0.0029 ± 0.000 | b | 0.0038 ± 0.001 | b | 0.0036 ± 0.000 | b |
| 104 | 5-Hepten-2-ol, 6-methyl- | *g* | 1312 | 2.73 | 889 | 984 | 976 | 95 | 0.0246 ± 0.004 | ab | 0.0229 ± 0.003 | b | 0.0142 ± 0.002 | c | 0.0275 ± 0.004 | ab |
| 105 | 1,3-Cyclohexadiene, 2-methyl-5-(1-methylethyl)- [α-Phellandrene] | | 1388 | 1.4 | 863 | 1008 | 1007 | 93 | | | | | not quantified | | | |

| | | | | | | | | | | | | | | | | |
|---|---|---|---|---|---|---|---|---|---|---|---|---|---|---|---|---|
| 106 | 1,6-octadiene, 7-methyl-3-methylene- [ß-Myrcene] | | 1332 | 1.41 | 878 | 990 | 979 | 93 | not quantified | | | | | | | |
| 107 | Cyclohexene, 1-methyl-4-(1-methylethenyl)- [α-Limonene] | *e,g* | 1468 | 1.36 | 922 | 1033 | 1019 | 93 | 0.4025 ± 0.061 | a | 0.1729 ± 0.042 | b | 0.1374 ± 0.036 | b | 0.1749 ± 0.034 | b |
| 108 | Benzene, butyl- | | 1540 | 1.61 | 896 | 1057 | 1036 | 91 | not quantified | | | | | | | |
| 109 | Bicyclo[2.2.1]heptan-2-one, 1,3,3-trimethyl- [Fenchone] | *e* | 1632 | 1.79 | 888 | 1086 | 1097 | 81 | not quantified | | | | | | | |
| 110 | 1,6-octadien-3-ol, 3,7-dimethyl- [β-Linalool] | *e,f* | 1660 | 2.31 | 834 | 1095 | 1081 | 71 | 0.1197 ± 0.021 | a | 0.0840 ± 0.008 | b | 0.0686 ± 0.013 | b | 0.0669 ± 0.011 | b |
| 111 | 4-Methyl-2-(2-methyl-1-propenyl)tetrahydro-2H-pyran [trans-Rose oxide] | | 1700 | 1.53 | 867 | 1108 | 1107 | 139 | not quantified | | | | | | | |
| 112 | Bicyclo[2.2.1]heptan-2-ol, 1,3,3-trimethyl- [Fenchol] | | 1728 | 2.43 | 855 | 1118 | 1099 | 81 | not quantified | | | | | | | |
| 113 | Bicyclo[2.2.1]heptan-2-one, 1,7,7-trimethyl-, (1S)- [L-Camphor] | | 1804 | 1.99 | 919 | 1143 | 1148 | 95 | not quantified | | | | | | | |
| 114 | 3-Cyclohexene-1-methanol, à,à4-trimethyl- [α-Terpineol] | *e* | 1948 | 2.58 | 927 | 1191 | 1172 | 93 | not quantified | | | | | | | |
| 115 | 6-octen-1-ol, 3,7-dimethyl-, [β-Citronellol] | *e,g* | 2040 | 2.67 | 880 | 1224 | 1208 | 41 | 0.0968 ± 0.015 | a | 0.0656 ± 0.011 | b | 0.0622 ± 0.016 | b | 0.0757 ± 0.007 | ab |

[a] Letters in rows indicate significant differences ($p < 0.05$) in the sample means for triplicate biological repeats; and n.s. means there is no significant difference in these samlpe means. [b] Mass spectra similarity, value out of 1000. [c] $LRI_{calcd}$, experimentally determined linear retention indices. [d] $LRI_{lit.}$, linear retention indices reported from the literature.[291, 292] [e] Identification confirmed by authentic standard. [f] Compounds quantified in injection with 5 min HS-SPME sampling. [g] Compounds quantified in injection with 30 min HS-SPME sampling. [h] Values are peak areas relative to internal standard.

that were focused on screening of wine volatiles, e.g. the one described in the previous chapter.

Table 5-1 provides a summary of all compounds identified using this strategy in the wine samples. Compounds identified included esters, alcohols, ketones, aldehydes, acids, acetals, furans, nitrogen-containing compounds, and compounds with terpenoid character. They represent mainly grape- and fermentation-derived wine volatiles, which are typically extracted using HS-SPME methods.[293]

For semi-quantification purposes, peak area ratios of the identified compounds were calculated relative to 2-pentanone, the internal standard. This approach allowed relative quantification of compounds and consequently allowed comparison between the different treatments. To ensure the quality of peak integration, the peak table obtained from the automatic peak detection algorithm of the ChromaTOF software was manually reintegrated. The biggest problem with quantitation in GC×GC is the correct assignment of individual peak "slices" to a given compound. Random fluctuations in the modulation process might cause small shifts in the $^{2}$D retention times, which might trigger the software to assume that the peak had finished eluting and to integrate subsequent slices as separate peak(s). Manual integration involved careful assignment of each individual slice to a peak based on its retention time and mass spectrum. The actual $^{2}$D peaks were integrated

using automated algorithms. This step was necessitated by the fact that very high relative standard deviations (RSDs) between repeat injections were obtained when only automated integration was applied. High RSDs would have rendered quantitative comparison of different wine samples using statistical methods impossible. Despite reintegration, accurate quantification of the remaining compounds was not possible, in part due to tailing in the $^{2}$D, which negatively affected the standard deviations.

Compared to previous studies utilizing 1D-GC on the same wines,[287, 288] GC×GC-TOF-MS offered several benefits. First, a relatively wide range of compounds could be identified and/or quantified accurately using HS-SPME. For 1D-GC, liquid-liquid extraction in combination with FID may be used for the analysis of major compounds such as esters, alcohols, acids, and fatty acids, whereas HS-SPME with MS detection in selected ion monitoring (SIM) mode is required to quantify selected carbonyls in the same wines. [287, 288] All of these compounds, and a significant number of additional volatiles, were successfully analyzed in a single GC×GC-TOFMS analysis in this study. Second, the increased resolving power of GC×GC combined with the power of deconvolution of the TOFMS mass spectra allowed for the identification, and in some instances quantification, of a much larger number of

compounds in a single analysis. For example, more minor esters and compounds with terpenoid character were identified in the current study. Also, high-quality quantitative data could be obtained for more compounds in a single analysis, although this came at the price of much more intensive data analysis. Finally, the inherent sensitivity and wide dynamic range of GC×GC-TOFMS allowed the identification of major as well as minor compounds in a single analysis. For example, in the current study numerous compounds present at low levels (µg/L and lower) in wine were successfully identified. These include some of the terpenoids and methoxypyrazines, compounds for which analysis by 1D-GC often requires dedicated sample preparation and selective detection techniques.

All of these benefits allowed to report more qualitative and quantitative data in a single study and, therefore, provided a significant step forward in studying in detail the chemical changes resulting from MLF using different starter cultures, as discussed in the following section.

### 5.2.2 Statistical analysis *(Analysis of variance)*

Comparison of means by ANOVA and LSD testing showed significant differences in the levels of 47 of 60 quantified compounds (Table 5-1) between the four treatments (the control and three MLF wines). As one biological repeat of the wines

fermented with starter culture C was identified as an outlier in initial PCA and ANOVA analyses, both injections of this repeat were excluded from further data analysis.

For all three starter cultures, most of the 30 quantified esters increased after MLF. Levels of methyl hexanoate (**19**; numbers refer to compounds in Table 5-1), methyl octanoate (**39**), and ethyl phenylacetate (**44**), although, tended to decrease following MLF, whereas 2-phenylethyl acetate (**45**), ethyl heptanoate (**38**), and isoamyl formate (**8**) showed no significant difference compared to the control wines. The general increase in the levels of esters following MLF agrees with the results of other authors,[254, 262, 264, 288, 294] albeit some esters behaved differently (for instance, Ugliano and Moio[254] reported an increase in the levels of 2-phenylethyl acetate (**45**) and Bartowsky et al.[294] reported a general decrease of acetates).

Except for diacetyl (**69**), which originates from the citric acid metabolism of LAB,[250] none of the carbonyl compounds increased following MLF for the wines studied here. All three LAB strains showed an increase in diacetyl (**69**), with starter culture O producing the highest levels of this compound. Diacetyl is responsible for the typical buttery flavor associated with MLF, as reported by numerous authors.[249, 253] The other diketone, 2,3- pentanedione (**71**), decreased significantly in the MLF wines

produced by all three starter cultures. Furthermore, benzeneacetaldehyde (**88**), 2-butanone (**70**), hexanal (**85**), and 2-heptanone (**75**) were also found to decrease significantly following MLF. A decrease of acetaldehyde, 2-methyl-1-butanal, and 3-methyl-1-butanal has been reported in Chancellor wines following MLF.[263] A decrease of acetaldehyde was also reported by others.[261] On the other hand, the concentrations of 11 aldehydes in Syrah and Pinotage wines analyzed by Malherbe[288] using HS-SPME-GC-MS did not show any significant differences as a result of MLF. Starter culture V seemed to differ in its metabolic profile, because the concentrations of 3-penten-2-one (**72**) and isobutanal (**81**) decreased significantly compared to the control wines, as well as to those produced with starter cultures O and C. On the basis of the ability of dairy Leuconostoc species to reduce propanal to propanol, Liu[295] hypothesized that wine LAB are similarly able to reduce aldehydes to alcohols. The significant decrease of isobutanal (**81**) observed for wines fermented with starter culture V could indicate such ability for this culture. In addition, the corresponding alcohol isobutanol (**52**) increased significantly less in wines produced with starter culture V compared to cultures O and C. The remaining quantified carbonyl compounds showed no significant differences between the control and the MLF wines. Although diacetyl is one of the most studied compounds related to MLF, the change of other carbonyl compounds has not received much attention in

previous literature. Our findings could therefore contribute to the understanding of the impact of MLF on this potentially influential class of wine volatiles and aid in the interpretation of sensory data.

For the wines analyzed in this study no general conclusions could be drawn with regard to the changes of higher alcohols due to MLF. Three of the four alcohols that showed significant increase after MLF (1-butanol (**53**), 1-propanol (**51**), and isobutanol (**52**)) were also present at significantly lower levels in wines produced from starter culture V compared to the other MLF wines. This is once again indicative of metabolic differences between strain V and the other *O. oeni* strains used here.

Levels of four of the five quantified terpenoid compounds also significantly decreased for all three starter cultures following MLF. Decrease of this class of compounds due to MLF has been reported by other groups.[255, 256]

In the interpretation of the data reported here, it should be noted that the analyses in this study were performed 8 months after bottling due to practical constraints on instrumental availability, and therefore relative levels of volatile compounds were subjected to various reactions occurring naturally during wine aging. For instance, the levels of esters generally increase during wine aging, except for esters produced

by yeast during alcoholic fermentation in higher concentrations than those predicted by the law of mass action. Consequently, levels of those esters, for example, ethyl esters of fatty acids, decrease during aging.[296] This aspect hampers comparison of semi-quantitative data reported here with literature data for MLF wines. Nevertheless, this data set is consistent in the sense that all analyses were performed within 1 week, which allows accurate comparison between the wines produced with the *O. oeni* strains investigated here. The results therefore accurately reflect the effects of MLF on differences in volatile compounds in wines of the same age.

### 5.2.3 Multivariate data analysis

Principal component analysis (PCA) was used to identify the volatile components responsible for differentiation between control and MLF wines, as well as between MLF wines produced with different *O. oeni* starter cultures. For reasons of simplification only quantified compounds showing high correlation with the first two principal components (correlation coefficients > 0.8) were used for the presentation of the PCA model (Figure 5-3). The PCA biplot presented in Figure 5-3 provides an overview of the correlations of compounds with each of the MLF samples and the control wines. Excellent grouping of all biological repeats and duplicate injections was obtained for each MLF sample as well as for the control.

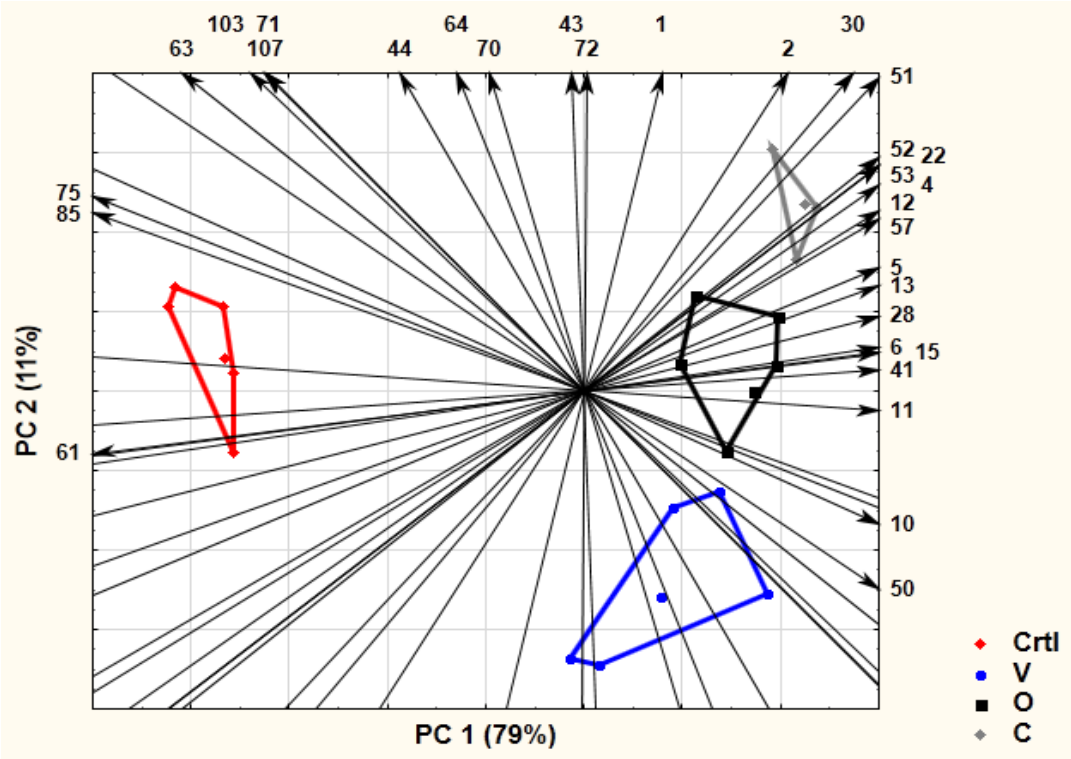


**Figure 5-3: PCA biplot of volatiles quantified with high regression coefficients ($R^2 > 0.8$) on the first two PCs. Samples for each treatment are presented in the same color; their grouping is demonstrated with colored convex hulls. Vectors indicate the different compounds, which are labeled corresponding to Table 5-1.**

Separation of all samples with different treatments was obtained by the first two PCs, which explained 90% of the variance in the sample set (PC1, 79%; PC2, 11%).

The control wines were separated from the MLF wines on PC1, whereas the variance between the different MLF wines was mainly explained by PC2. The control wines were positively correlated with 2-heptanone (**75**), hexanal (**85**), and 1-hexanol (**61**) and, to a lesser extent, with 1-heptanol (**63**), 2,3-pentanedione (**71**), limonene (**107**), 6-methyl-5 hepten-2-one (**103**), ethyl phenylacetate (**44**), 1-octanol-3-ol (**64**), and 2-butanone (**70**) (the MLF wines showed negative correlation with these compounds). These compounds were largely responsible for the differentiation between the MLF and the control wines. Interestingly, hexanal (**85**) and 1-hexanol (**61**) are both associated with green odor descriptors, [287, 288, 297] and a reduction in vegetative, green, grassy, herbaceous aromas following MLF has been reported previously.[252, 271, 287, 288]A decrease in concentrations of compounds with terpenoid character after MLF (such as 6-methyl- 5-hepten-2-one (**103**)) has been described previously.[255, 256] Boido[255] assumed that these aroma compounds are able to form stable linkages with bacterial polysaccharides, therefore explaining their lower levels in MLF wines. On the other hand, according to D'Incecco et al.,[275] partial metabolization of the liberated aglycon compounds by LAB may also be responsible

for the lower concentrations of these compounds in MLF wines. Increased levels of glycoside-related volatiles, such as linalool, farnesol, and β damascenone,[256] due to glycosidic activity during MLF, as reported by other groups,[256, 275, 276] could not be confirmed in this work because only a few of these compounds were quantified.

All MLF wines correlated positively with isobutanol (**52**), 1-butanol (**53**), 1-propanol (**51**), amyl alcohol (**57**), and most of the esters. Whereas the majority of wine esters originate from alcoholic fermentation by yeast, these results, in agreement with those of other researchers,[254, 262, 264, 294] show that LAB can influence the relative concentrations of esters in wine. It is assumed that this is a result of bacterial esterase activity. Although less is known about esterase activity of wine-associated LAB, the same conclusion was drawn regarding the esterase activity of dairy-associated lactic acid bacteria.[298] In fact, a variety of enzymatic activities have been related to wine LAB.[253, 298] Investigation of the esterase activity of commercial MLF starter cultures was previously carried out by Matthews et al.[299] Esterase from *O. oeni* was first characterized by Sumby et al.,[300] whereas the microbial modulation of esters in wine has recently been reviewed.[301]

The MLF wines produced with different LAB strains were primarily differentiated according to PC2. MLF wines from starter cultures C and O were distinguished from

those produced by starter culture V on the basis of the levels of esters and some alcohols. These two cultures therefore seem to be alike with regard to their metabolic activity in wine. Wines fermented with starter culture V differed in terms of negative correlation with the compounds 1-octen-3-ol (**64**), 2-butanone (**70**), methyl salicylate (**43**), 3-penten-2-one (**72**), and ethyl formate (**1**). The levels of these compounds, as well as diacetyl (**69**), isobutanal (**81**), isoamyl propanoate (**21**), methyl acetate (**2**), propyl acetate (**5**), butyl acetate (**12**), isobutanol (**52**), 1-propanol (**51**), and 1-butanol (**53**), were significantly lower compared to those in wines produced with the other MLF starter cultures, once again indicating possible metabolic differences between this culture and the other LAB strains.

Higher alcohols are primarily derived from amino acid metabolism of yeast.[302] Other groups, however, have also demonstrated that MLF, depending on the bacterial strain used, can have an impact on the concentration of higher alcohols.[261, 262, 264, 272] Ugliano et al.[254] reported only small increases for several alcohols in their experiments when they studied changes of yeast-derived volatile compounds in Aglinanico wines.

Sensory studies of the wines analyzed in this study were performed 5 months after bottling.[287] The incidence of the odor descriptor “buttery” was significantly lower for

starter culture V compared to starter cultures O and C and did not show any significant difference compared to the control. Although the chemical analyses for the current study were performed 3 months later, it is likely that lower levels of diacetyl in wines fermented with starter culture V were responsible for this difference.

## 5.3 Conclusions

In conclusion, in this study GC×GC has successfully been applied for the improved separation of volatile compounds in Pinotage wines subjected to MLF. This has allowed the detailed investigation of the impact of different MLF starter cultures on the volatile composition of Pinotage red wine. The improved separation offered by GC×GC coupled with the use of deconvoluted mass spectra obtained by TOFMS allowed the identification of a wide range of compounds in a single analysis and enhanced the integrity of quantitative results through the reduction of the risk of coelutions.

The accurate relative quantification of 60 compounds provided useful new information regarding the changes in levels of individual compounds following MLF. With few exceptions, our findings were in accordance with published results regarding MLF. Moreover, the inherent advantages of GC×GC-TOFMS in terms of

improved resolution and sensitivity, combined with careful quantification, allowed the identification of a number of compounds showing significant differences as a function of MLF for the first time. These include several minor esters (**1, 4, 5, 12, 13, 15, 18, 19, 21, 22, 34, 35, 39, 43, 48, 49**), 1-pentanol (**57**), the ketones 2-butanone (**70**), 3-penten-2- one (**72**), 2-heptanone (**75**) and 6-methyl-5-hepten-2-one (**103**), the aldehydes isobutanal (**81**), hexanal (**85**) and phenylacetaldehyde (**88**). Most of these compounds cannot be easily identified and/or quantified by 1D-GC, due either to their low levels in wine or to coelutions with other wine volatiles. The GC×GC-TOFMS method reported here overcomes some of these problems, and as a result has contributed significantly to knowledge on the effect of MLF on Pinotage volatiles in particular.

Whereas GC×GC is finding increasing application as a powerful screening tool for the identification of compounds in complex samples, the results presented here also indicate the utility of the technique for quantitative comparison of wine samples. However, when using GC×GC-TOFMS, the polar nature of many wine volatiles and the concomitant poor peak shapes in the second dimension necessitate extensive manual intervention to ensure reliable quantitative data.

PCA and results from ANOVA and LSD testing indicated not only significant differences in the volatile composition between the control and MLF wines, but also the effect of metabolic differences between the MLF starter cultures studied here. Especially starter culture V showed significant differences compared to starter cultures O and C, most markedly the lower amounts of diacetyl produced. Further investigation of the potential sensory contribution of the MLF-associated compounds reported here for the first time needs to be performed. More research on the biosynthesis pathways of LAB, wine aging following MLF, and the influence of grape cultivars on MLF, as well as the influence of winemaking practices on LAB, is also required to fully elucidate the impact of MLF on wine aroma.

# Chapter 6

# Characterization of the Flavor Profile of Blue Honeysuckle Berries

*Lonicera caerulea* L. (honeyberry, blue honeysuckle, edible honeysuckle, sweet berry honeysuckle; Caprifoliaceae) is a nutritionally valuable shrub native to cool temperate northern hemisphere, mostly in moderate climate regions.[303] Its berries are widely harvested in Russia, China and Japan, but are not well-known as edible berries in Europe and North America. Cultivation of these plants is easy, especially under Polish climatic and soil conditions. Fruit shapes are oval to long and dark navy blue to purple in color. Their flavor is similar to that of bilberries, black currants, and blueberries. They are characterized by extra-early ripening, high content of ascorbic acid and bioactive flavonoids.[304]

The health benefits of honeyberries, particularly decreasing the risk of cardiovascular diseases and various forms of cancer, are associated with their high antioxidant content.[305, 306] The major components of blue honeysuckles and their juice have been found to be ascorbic acid and polyphenols.[307] Previous studies have focused on the evaluation of phenolic compounds, saccharides, vitamins and amino acids present in L. *caerulea*.[303, 308] However, to the best of the author's knowledge, the

composition of the volatile fraction of blue honeysuckle berries has not been reported to date.

In the light of that, we were approached by our colleagues at Gdansk University of Technology in Poland in an international collaboration project to apply the powerful separation capabilities of GC×GC to investigate the volatile composition of honeyberries harvested at two plantations in northern Poland to obtain a qualitative characterization of the volatiles in these berries.

## 6.1 Experimental

### 6.1.1 Samples, chemicals and materials

Berries of 5 different blue honeysuckle cultivars: Wojtek (W), Zielona (Z), Brązowa (B), Mińsk (M) and type 44 (T) from two different plantations in northern Poland were harvested in May-June 2009-2010 and stored in a freezer prior to analysis. In addition, two different samples of honeysuckle berries juice (J) and jam (JM) were analyzed. NaCl (ACS grade) was obtained from EMD Chemicals (Gibbstown, NJ, USA), while $C_6$ to $C_{17}$ *n*-alkane (99%) used for linear retention index determination were from Sigma-Aldrich (St. Louis, MO, USA). A divinylbenzene / carboxen / polydimethylsiloxane (DVB/CAR/PDMS, 50/30 μm, 2 cm) SPME fiber (Supelco, Belletonte, PA, USA) was used.

### 6.1.2 Instrumentation

The same instrumentation and columns used in Chapter 4 were used in this study. The temperature program used was as follows: initial temperature 40 °C for 0.2 min, ramped at 4 °C/min to 200 °C, then ramped at 10 °C/min to 250 °C and held for 2 min. The injector was operated at 250 °C in the splitless mode, with splitless time of 2 min. Helium was used as the carrier gas at a constant flow of 1.8 ml/min. The transfer line was maintained at 250 °C. Ions in the mass range of 33 - 400 amu were acquired at a rate of 50 spectra/s. The ion source temperature was 225 °C and the detector voltage was set to -1800 V.

### 6.1.3 Sample preparation

For each cultivar, 50 g of frozen berries were thawed at refrigerator temperature (about 4°C). The fruits were blended for 1 min and 10 ml of berries' juice were transferred to a 40 ml vial. After 2 g of ACS grade NaCl (pre-heated to 250°C and cooled to room temperature) were added together with PTFE-coated stir bar, the vial was capped immediately with a PTFE-lined septum and an aluminum crimp-cap. The obtained solution was maintained at a temperature of 40 °C in a water bath before sampling for 60 min to promote the transfer of the compounds from the sample to the headspace. HS-SPME was performed for 60 min with stirring at 850

rpm, followed by desorption of the fiber in the GC split/splitless injector port at 250 °C for 2 min.

### 6.1.4 Data analysis

The obtained GC×GC total ion chromatograms (TIC) were processed using automated spectral deconvolution of ChromaTOF software (LECO Corp. version 4.41) at S/N threshold 100. Two commercial databases (NIST 05 and Wiley 275) were used. Mass spectral match factor, similarity > 750, was used to decide whether a peak was correctly identified or not. Tentative identification was verified by comparing the experimentally determined linear temperature-programmed retention indices (LTPRI) with literature values. Furthermore, some of the compounds were positively identified using authentic standards (when available). GC×GC analysis of $C_6$ to $C_{17}$ *n*-alkane series was performed for the calculation of LTPRI in the first dimension.

## 6.2 Results and discussion

Very few studies have been published to date on the analysis of blue honeysuckles[303, 307, 308]. These studies were mainly focused on the phenolic compounds present in that kind of berries.

A powerful separation method is required for separating complex matrices such as natural products (e.g. blue honeysuckles). Frequent coelutions are normally observed when any single stationary phase is used. The problem can be overcome using GC×GC as separation is based on two different separation mechanisms in this technique.

The use of HS-SPME combined with GC×GC-TOFMS allowed to fully characterize the composition of the volatile profile of blue honeysuckle fruits and selected products (juice and jam). In total, 152 compounds were tentatively assigned as honeysuckle aroma components after GC×GC–TOFMS analysis and LTPRI verification (Table 6-1 illustrates the aroma components found in blue honeysuckle fruits, juice and jam).

The sensitivity of SPME extraction technique depends greatly on the value of the distribution constant of analytes partitioned between the sample and fiber coating material.[309] The DVB/CAR/PDMS fiber used in this study proved to be the most universal assembly for sufficient isolation of analytes having wide range of physico-chemical properties.[208, 310, 311]

**Table 6-1: Volatile compounds identified in blue honeysuckle berries (fruits, juice and jam) using HS-SPME-GC×GC-TOFMS**

| No. | Compounds | LTPRI | | | | | | | | | |
|---|---|---|---|---|---|---|---|---|---|---|---|
| | | Calc.[a] | Lit.[b] | Stand[c] | W | T | Z | M | B | J | JM |
| **Terpenes** | | | | | | | | | | | |
| 1 | α-Pinene* | 940 | 949 | – | + | + | + | - | + | + | + |
| 2 | β-Thujene | 958 | 957 | – | + | + | - | + | + | - | - |
| 3 | β-Pinene | 982 | 981 | – | + | + | + | + | + | + | + |
| 4 | β-Myrcene | 988 | 988 | – | - | - | + | - | - | - | - |
| 5 | p-Cymene* | 1022 | 1022 | – | + | + | + | + | + | + | + |
| 6 | Eucalyptol* | 1034 | 1035 | 1035 | + | + | + | + | + | + | + |
| 7 | (Z)-ocimene* | 1043 | 1043 | – | + | + | + | + | + | - | - |
| 8 | β-Phellandrene | 1058 | 1056 | – | + | + | + | + | + | + | + |
| 9 | Linalool oxide | 1068 | 1068 | 1065 | + | + | + | + | + | + | + |
| 10 | (-)-Fenchone | 1083 | 1084 | 1083 | - | + | + | - | + | + | - |
| 11 | Linalool* | 1090 | 1089 | 1088 | + | + | + | - | + | - | - |
| 12 | Terpinolene* | 1092 | 1089 | – | + | + | + | + | + | + | + |
| 13 | Camphor | 1140 | 1139 | – | + | + | + | + | + | + | - |
| 14 | (-)-Menthol | 1173 | 1171 | 1170 | + | + | + | + | + | + | + |
| 15 | Terpinen-4-ol | 1178 | 1178 | – | + | + | + | + | + | + | + |
| 16 | α-Terpineol* | 1188 | 1184 | 1186 | + | + | + | + | + | + | + |
| 17 | β-Cyclocitral* | 1216 | 1202 | – | + | + | + | + | + | + | + |
| 18 | Geraniol* | 1245 | 1242 | 1242 | - | + | + | - | + | - | - |

| | | | | | | | | | | | |
|---|---|---|---|---|---|---|---|---|---|---|---|
| 19 | Geranial* | 1256 | 1256 | – | + | + | + | + | + | + | - |
| 20 | α-Ionone | 1427 | 1426 | 1423 | - | + | + | - | + | - | - |
| 21 | α-Ionone* | 1486 | 1484 | 1483 | + | + | + | + | + | - | + |
| 22 | α-Phellandrene | 1006 | 1009 | – | + | + | + | + | + | + | + |
| 23 | α-Terpinene* | 1008 | 1001 | – | + | + | - | + | - | - | - |
| **Aldehydes** | | | | | | | | | | | |
| 24 | Acetaldehyde | < 600[i] | 381 | – | + | + | + | + | + | + | + |
| 25 | 2-Propenal | < 600[i] | 469 | – | + | + | + | + | + | + | + |
| 26 | Propanal | < 600[i] | 472 | – | + | + | + | + | + | + | - |
| 27 | Butanal | < 600[i] | 587 | < 600[i] | + | + | + | + | + | + | + |
| 28 | 2-Butenal | 625 | 625 | – | + | + | + | + | + | + | + |
| 29 | Butanal, 3-methyl- | 630 | 627 | – | + | + | + | + | + | + | + |
| 30 | Butanal, 2-methyl- | 642 | 643 | – | + | + | + | + | + | + | + |
| 31 | Pentanal | 675 | 675 | – | + | + | + | + | + | + | + |
| 32 | 2-Pentenal, (E)- | 732 | 730 | – | + | + | + | + | + | + | + |
| 33 | (Z)-3-Hexenal | 777 | 778 | – | + | + | + | + | + | + | + |
| 34 | Hexanal | 780 | 780 | 779 | + | + | + | + | + | + | + |
| 35 | Furfural | 812 | 812 | 812 | + | + | + | + | + | + | + |
| 36 | (E)-2-Hexenal | 832 | 832 | – | + | + | + | + | + | + | + |
| 37 | Heptanal | 882 | 883 | – | + | + | + | + | + | + | + |
| 38 | 2,4-Hexadienal, (E,E)- | 889 | 883 | – | + | + | + | + | + | + | - |

| | | | | | | | | | | | |
|---|---|---|---|---|---|---|---|---|---|---|---|
| 39 | 2-Heptenal, (E)- | 928 | 927 | – | + | - | - | + | + | + | + |
| 40 | 2-Heptenal, (Z)- | 938 | 936 | – | + | + | + | + | + | + | + |
| 41 | Methylfurfural | 942 | 941 | 941 | - | + | - | - | - | + | + |
| 42 | Benzaldehyde | 945 | 944 | 943 | + | + | + | + | + | + | + |
| 43 | octanal | 987 | 987 | – | + | + | + | + | + | + | + |
| 44 | 2,4-Heptadienal, (E,E)- | 991 | 991 | – | + | + | + | + | + | + | + |
| 45 | 4-Ethyl-2-hexynal | 1018 | 958 | – | + | + | + | + | + | + | + |
| 46 | (E)-2-octenal | 1040 | 1039 | 1040 | + | + | + | + | + | + | + |
| 47 | Nonanal | 1089 | 1089 | 1088 | + | + | + | + | + | + | + |
| 48 | 2,4-octadienal, (E,E)- | 1092 | 1090 | – | + | + | + | + | + | - | + |
| 49 | 2,6-Nonadienal, (E,E)- i (E,Z)- | 1137 | 1131 | – | + | + | + | + | + | + | + |
| 50 | (E)-2-Nonenal | 1145 | 1142 | 1143 | + | + | + | + | + | + | + |
| 51 | Decanal | 1192 | 1191 | 1191 | + | + | + | + | + | + | + |
| 52 | 2,4-Nonadienal, (E,E)- | 1198 | 1187 | – | + | + | + | + | + | + | - |
| 53 | Undecanal | 1294 | 1294 | – | + | + | + | + | + | - | - |
| 54 | 2,4-Decadienal, (E,E)- | 1302 | 1293 | – | + | + | + | + | + | + | - |
| 55 | Dodecanal | 1398 | 1398 | – | + | + | + | + | + | + | - |
| **Ketones** | | | | | | | | | | | |
| 56 | Acetone | < 600[i] | 465 | – | + | + | + | + | + | + | + |
| 57 | 2-Butanone | < 600[i] | 567 | – | + | + | + | + | + | + | + |

| | | | | | | | | | | | |
|---|---|---|---|---|---|---|---|---|---|---|---|
| 58 | 2,3-Butanedione | < 600[i] | 586 | < 600[i] | + | + | + | + | + | + | + |
| 59 | 1-Penten-3-one | 663 | 662 | – | + | + | + | + | + | + | + |
| 60 | 2-Pentanone | 665 | 664 | 664 | + | + | + | + | + | + | + |
| 61 | 2,3-Pentanedione | 671 | 672 | 671 | + | + | + | + | + | - | + |
| 62 | 3-Penten-2-one, (E)- | 719 | 712 | – | + | + | + | + | + | + | + |
| 63 | 2-Hexanone | 769 | 770 | – | + | + | + | + | + | + | + |
| 64 | 2,3-octanedione | 965 | 967 | – | + | + | + | + | + | + | + |
| 65 | 6-methyl-5-hepten-2-one | 969 | 968 | – | + | + | + | + | + | + | + |
| 66 | 2-octanone | 974 | 975 | – | + | + | + | + | + | + | + |
| 67 | Benzeneacetaldehyde | 1024 | 1024 | – | + | + | + | + | + | + | + |
| 68 | Acetophenone | 1050 | 1048 | 1049 | + | + | + | + | + | + | + |
| 69 | 3,5-octadien-2-one, (E,E)- | 1063 | 1074 | – | + | + | + | + | + | - | - |
| 70 | (E)-Geranyl acetone | 1442 | 1434 | – | + | + | + | + | + | + | + |
| **Alcohols** | | | | | | | | | | | |
| 71 | 1-Propanol | <600[i] | 574 | < 600[i] | + | + | + | + | + | + | - |
| 72 | 2-Methyl-1-propanol | 613 | 612 | 613 | + | + | + | + | + | + | + |
| 73 | 1-Butanol | 647 | 647 | 647 | + | + | + | + | + | + | + |
| 74 | 3-Methylbutanol | 722 | 722 | 722 | + | + | + | + | + | + | + |
| 75 | 2-Methyl-1-butanol | 726 | 728 | 728 | + | + | + | + | + | + | + |
| 76 | 4-Methyl-2-pentanol | 746 | 744 | 746 | + | - | - | - | + | - | + |

| | | | | | | | | | | | |
|---|---|---|---|---|---|---|---|---|---|---|---|
| 77 | 2-Penten-1-ol, (E)- | 760 | 744 | – | + | + | + | + | + | - | - |
| 78 | 2-Penten-1-ol, (Z)- | 758 | 760 | – | + | + | + | + | + | - | + |
| 79 | (Z)-3-hexen-1-ol | 842 | 842 | 842 | + | + | + | + | + | + | + |
| 80 | (E)-2-hexen-1-ol | 854 | 853 | – | + | + | + | + | + | + | + |
| 81 | 1-Hexanol | 856 | 855 | 855 | + | + | + | + | + | + | + |
| 82 | 2-Heptanol | 889 | 887 | – | + | + | + | + | + | + | + |
| 83 | 1-octen-3-ol | 968 | 967 | 967 | + | + | + | + | + | + | + |
| 84 | 3-octanol | 985 | 985 | 985 | + | + | + | + | + | + | + |
| 85 | 2-octanol | 990 | 990 | 989 | + | + | + | + | + | + | + |
| 86 | 2-octen-1-ol, (E)- | 1058 | 1055 | – | + | + | + | + | + | + | + |
| 87 | octanol | 1061 | 1061 | – | + | + | + | + | + | + | + |
| 88 | Nonanol | 1165 | 1164 | – | + | + | + | + | + | + | + |
| 89 | 2-Butyl-1-octanol | 1312 | 1277 | – | - | + | - | + | + | + | - |
| 90 | Benzyl alcohol | 1024 | 1022 | 1023 | - | - | - | + | + | + | - |
| 91 | Phenylethyl alcohol | 1104 | 1102 | 1102 | - | - | - | - | + | + | - |
| 92 | p-Cymen-8-ol | 1177 | 1170 | – | + | + | + | + | + | + | + |
| **Esters** | | | | | | | | | | | |
| 93 | Methyl formate | < 600[i] | 407 | – | + | + | + | + | + | + | - |
| 94 | Ethyl formate | < 600[i] | 545 | < 600[i] | + | + | - | - | + | + | - |
| 95 | Ethyl acetate | 602 | 603 | 601 | + | + | + | + | + | + | + |
| 96 | n-Propyl acetate | 700 | 698 | – | + | + | + | + | + | - | + |

| | | | | | | | | | | | |
|---|---|---|---|---|---|---|---|---|---|---|---|
| 97 | Ethyl 2-methylpropanoate | 743 | 743 | 743 | + | + | + | + | + | + | - |
| 98 | Isobutyl acetate | 756 | 756 | 756 | + | + | - | + | + | + | + |
| 99 | Methyl 3-methylbutanoate | 760 | 758 | – | + | + | + | - | - | - | - |
| 100 | Ethyl butanoate | 784 | 783 | 783 | + | + | + | + | + | + | + |
| 101 | Acetic acid, butyl ester | 797 | 798 | – | + | + | + | + | + | + | + |
| 102 | Ethyl lactate | 800 | 799 | 798 | + | - | - | - | + | + | - |
| 103 | Methyl pentanoate | 809 | 810 | – | + | + | + | + | - | + | - |
| 104 | Ethyl-(2E)-2-butenoate | 825 | 823 | 823 | + | + | + | + | + | + | - |
| 105 | Ethyl 2-methylbutanoate | 836 | 835 | 835 | + | + | + | + | + | + | + |
| 106 | Ethyl 3-methylbutanoate | 838 | 840 | – | + | + | + | + | + | + | + |
| 107 | Isoamyl acetate | 861 | 860 | 860 | + | + | + | + | + | + | + |
| 108 | Butanoic acid, propyl ester | 882 | 881 | – | + | + | + | + | + | - | - |
| 109 | Ethyl pentanoate | 885 | 884 | 885 | - | + | - | + | + | + | - |
| 110 | Propanoic acid, butyl ester | 892 | 890 | – | + | + | + | + | + | - | - |
| 111 | Pentyl acetate | 897 | 897 | – | + | + | + | + | + | + | + |
| 112 | Methyl hexanoate | 909 | 908 | – | + | + | + | + | + | + | + |
| 113 | Methyl (Z)-3-hexenoate | 915 | 916 | – | + | + | + | + | + | - | - |

| | | | | | | | | | | | |
|---|---|---|---|---|---|---|---|---|---|---|---|
| 114 | Ethyl 3-hydroxybutanoate | 917 | 920 | – | + | - | + | + | - | - | - |
| 115 | Ethyl 2-hydroxy-3-methylbutanoate | 954 | 965 | – | + | + | + | + | + | - | - |
| 116 | Ethyl hexanoate | 984 | 985 | 985 | + | + | + | + | + | + | - |
| 117 | (Z)-3-Hexenyl acetate | 990 | 991 | – | + | + | + | + | + | + | + |
| 118 | (E)-2-Hexenyl acetate | 997 | 994 | – | + | + | + | + | + | + | + |
| 119 | Hexyl acetate | 997 | 997 | 996 | + | + | + | + | + | + | + |
| 120 | Butanoic acid, butyl ester | 980 | 982 | – | + | + | + | + | + | + | + |
| 121 | γ-Caprolactone | 1023 | 1023 | – | + | + | + | + | + | - | - |
| 122 | Methyl benzoate | 1082 | 1084 | 1086 | + | + | + | + | - | + | + |
| 123 | Hexyl propanoate | 1091 | 1091 | – | + | + | + | + | + | - | - |
| 124 | Ethyl 3-hydroxyhexanoate | 1111 | 1106 | 1109 | + | + | - | - | - | - | - |
| 125 | octanoic acid, methyl ester | 1111 | 1111 | – | + | + | + | + | + | + | + |
| 126 | Butanoic acid, 3-hexenyl ester, (E)- | 1130 | 1146 | – | + | + | + | + | + | + | + |
| 127 | Ethyl benzoate | 1159 | 1156 | – | + | + | + | + | + | + | - |
| 128 | Butanoic acid, 3-hexenyl ester, (Z)- | 1171 | 1170 | – | + | + | + | + | + | + | - |
| 129 | (E)-2-hexenyl butanoate | 1177 | 1191 | – | + | + | + | + | + | - | - |
| 130 | Ethyl octanoate | 1183 | 1182 | 1180 | + | + | + | + | + | + | - |

| | | | | | | | | | | | |
|---|---|---|---|---|---|---|---|---|---|---|---|
| 131 | Hexyl-2-methylbutanoate | 1225 | 1224 | – | + | + | + | + | + | + | + |
| 132 | Ethyl phenylacetate | 1226 | 1224 | 1226 | + | + | - | + | + | + | - |
| 133 | Hexyl-3-methylbutanoate | 1230 | 1220 | – | - | - | - | + | + | - | - |
| 134 | 2-Phenylethyl acetate | 1240 | 1244 | – | - | - | - | - | + | + | - |
| 135 | Hexyl hexanoate | 1375 | 1374 | – | + | + | + | + | + | - | + |
| 136 | Ethyl decanoate | 1384 | 1380 | 1380 | + | + | + | + | + | + | - |
| **Furans** | | | | | | | | | | | |
| 137 | 2,3-Dihydrofuran | < 600[i] | 571 | – | + | - | + | + | + | + | + |
| 138 | Furan, 2-methyl- | < 600[i] | 589 | – | + | + | + | + | + | + | + |
| 139 | Furan, 2-ethyl- | 693 | 692 | – | + | + | + | + | + | + | + |
| 140 | 2,2-Dimethyl-3(2H)-furanone | 817 | 877 | – | + | - | + | - | + | - | + |
| 141 | 2-n-Butyl furan | 884 | 887 | – | + | + | + | + | + | - | + |
| 142 | Furan, 2-pentyl- | 985 | 984 | – | + | + | + | + | + | + | + |
| 143 | 2,5-Furandione, 3,4-dimethyl- | 1002 | 996 | – | + | + | + | + | + | - | + |
| 144 | 5-Ethyl-2(5H)-furanone | 1003 | 984 | – | + | + | + | + | + | - | - |
| 145 | 3(2H)-Furanone, 4-methoxy-2,5-dimethyl- | 1039 | 1032 | – | + | + | + | + | + | + | + |
| **Volatile phenols** | | | | | | | | | | | |
| 146 | Phenol | 983 | 983 | – | + | + | + | - | - | - | - |

| | | | | | | | | | | | |
|---|---|---|---|---|---|---|---|---|---|---|---|
| 147 | p-sec-Butyl phenol | 1309 | 1314 | – | + | + | + | + | + | - | + |
| **Sulphur compunds** | | | | | | | | | | | |
| 148 | Methanethiol | < 600[i] | 464 | – | + | + | + | + | + | + | + |
| 149 | Dimethyl sulfide | < 600[i] | 506 | – | + | + | + | + | + | + | + |
| 150 | Dimethyl disulfide | 732 | 730 | 730 | + | + | + | + | + | + | + |
| 151 | Dimethyl trisulfide | 961 | 961 | – | + | + | + | + | + | - | + |
| **Acids** | | | | | | | | | | | |
| 152 | Hexanoic acid, 2-ethyl- | 1111 | 1116 | – | + | + | - | - | - | + | - |

[a]LTPRI experimentally determined, [b]LTPRI obtained from literature, [c]LTPRI experimentally determined for authentic standards, *compounds found in ordinary berry,[312] (+) compound was found, (-) compound was not found, [i] LTPRI < 600 estimated since $C_6$ was the lowest *n*-alkane analyzed.

Highlighted cells show potential markers that are unique to specific varieties of honeysuckle berries.

In the first step of data analysis, automated data processing was used to find all peaks in the GC×GC chromatograms with a signal-to-noise at a minimum of 100. After the peak detection, mathematical separation of spectra of co-eluted peaks was performed (peak deconvolution). In this work, the peak table generated automatically by ChromaTOF software has been further examined and the identification has been confirmed or changed based on the criteria described in Section 6.1.4. This resulted in several hundreds of peaks. Due to a lack of authentic standards for numerous compounds, they were tentatively identified by comparing the deconvoluted mass spectra with NIST 05 and Wiley 275 spectral libraries using ChromaTOF software and a match factor of 75% as a minimum requirement. In addition, linear temperature programmed retention indices (LTPRI) were experimentally determined [209] in the first dimension using a homologous series of *n*-alkanes and were compared to the literature values. The averaged $^{1}$D retention time for each analyte was used for the LTPRI calculation (Table 6-1). A maximum absolute retention index difference of 30 compared to literature values was used as the selection criterion in this work as before.

The compounds determined in honeysuckles are presented in Table 6-1. They were classified according to their chemical structure into esters (44), aldehydes (32), terpenes (23), alcohols (22), ketones (15), acids (1), volatile phenols (2), sulphur

compounds (4) and furans (9). 54 compounds were positively identified using authentic standards. It should be mentioned that many peaks detected with good spectral matches were excluded from the results presented here because there were no other means to confirm their identity.

As it is shown in Table 6-1, most of the low-boiling volatiles (e.g. propanal, propan-1-ol, methyl formate and acetate and propyl acetate) that were detected in honeysuckle fruits were not detected in samples of juice and jam. Overall, the jam sample was characterized by poorer profile of the volatile fraction. The reason for this may be the conditions of the manufacturing processes of juice or jam, and in particular the increased temperature during the cooking stage for the jam. Thus, compounds originally present in the fruit may undergo chemical change or uncontrolled release into the environment. For example, sulphur compounds (e.g. dimethylsulphide, which is mainly formed during the cooking process of the fruit) present in fruits in trace amounts, were among the major compounds of juice and jam samples.

Almost all of the aroma-impact compounds that were previously reported for European blueberries,[312] including aldehydes, terpenes, alcohols, ketones, acids, esters and "green leaf volatiles" (GLVs; $C_6$ aldehydes, alcohols and their esters),

were also found in this study (Table 6-1). GLVs (Figure 6-1) are named for the distinctive scent that is produced when leaves are crushed or otherwise injured.[313] They are typical aroma volatiles produced by plants as attractants to predatory insects or due to enzymatic reactions initiated by skin damage.

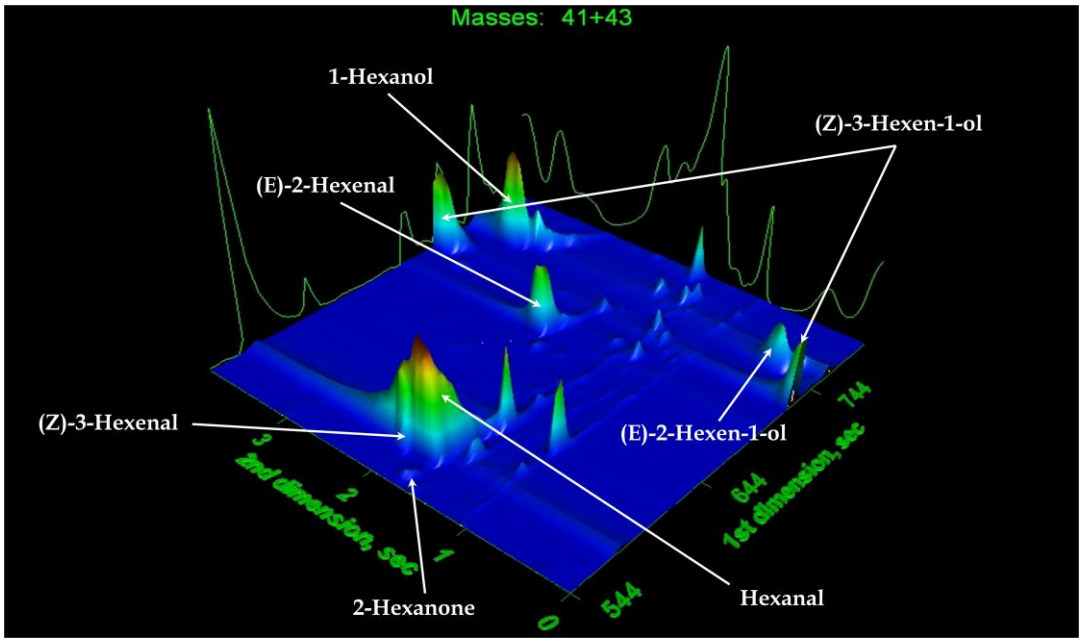


**Figure 6-1: Extracted ion surface plot chromatogram of green leaf volatiles found in blue honeysuckles.**

The most abundant volatiles determined in this study were esters (Table 6-1). Amongst the seven samples analyzed, 44 esters were detected. Of these, 17 were positively identified using authentic standards. Figure 6-2 shows some of the esters detected in honeysuckles. These esters contributed to the overall fruity flavor of honeysuckles.

Another major group that was found were aldehydes. Acetaldehyde was found

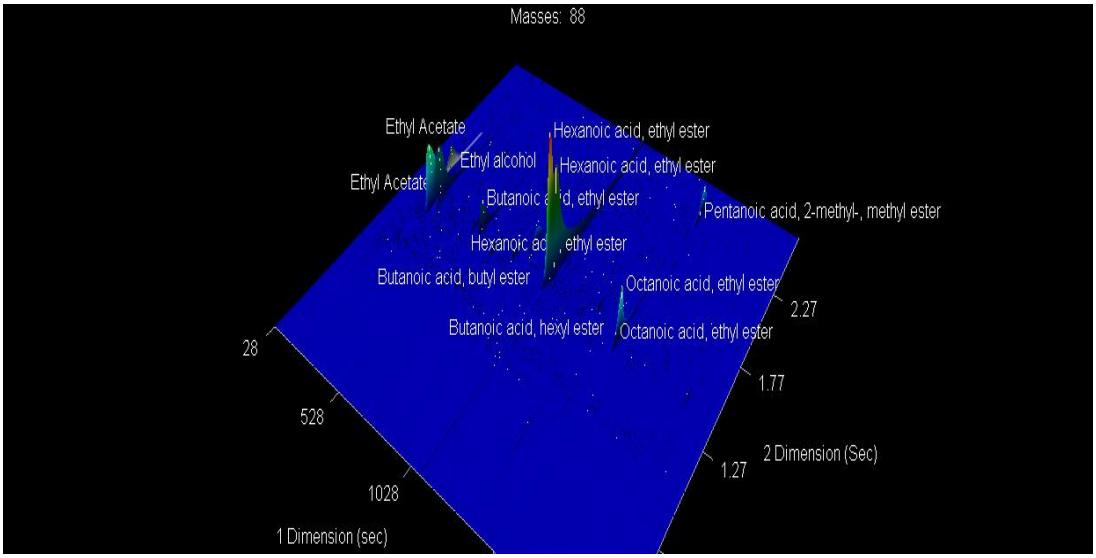


**Figure 6-2: Extracted ion surface plot chromatogram depicting selected esters in blue honeysuckle berries.**

in low concentration. This shows the capability of our GC×GC system to efficiently modulate even highly volatile analytes (acetaldehyde b.p. is 20.2 °C) (Figure 6-3). At low levels, acetaldehyde may be responsible for a pleasant fruity aroma, but at high concentrations it is characterized by a pungent, irritating odor.[314]

Terpenes (Figure 6-4) were also among the major groups that contributed to honeysuckle aroma. Terpene alcohols including linalool, $\alpha$-terpineol and geraniol impart the aroma of flower, rose and geranium. They have very low sensory thresholds and may contribute to aroma even when present in very low amounts

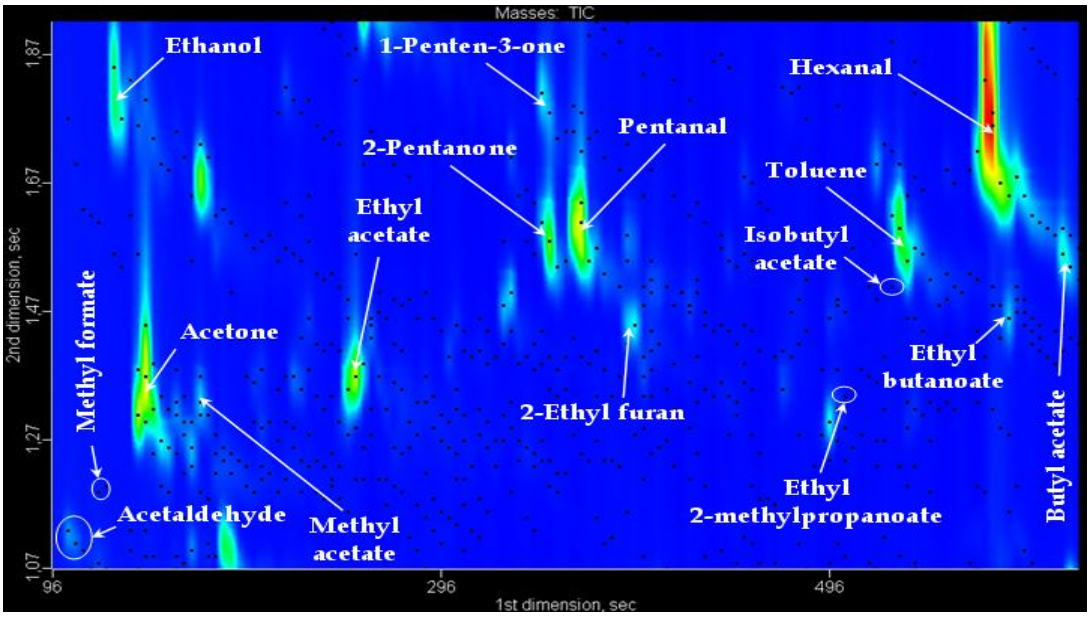


**Figure 6-3: GC×GC contour plot of the total ion chromatogram showing trapping of highly volatile components in honeysuckle berries.**

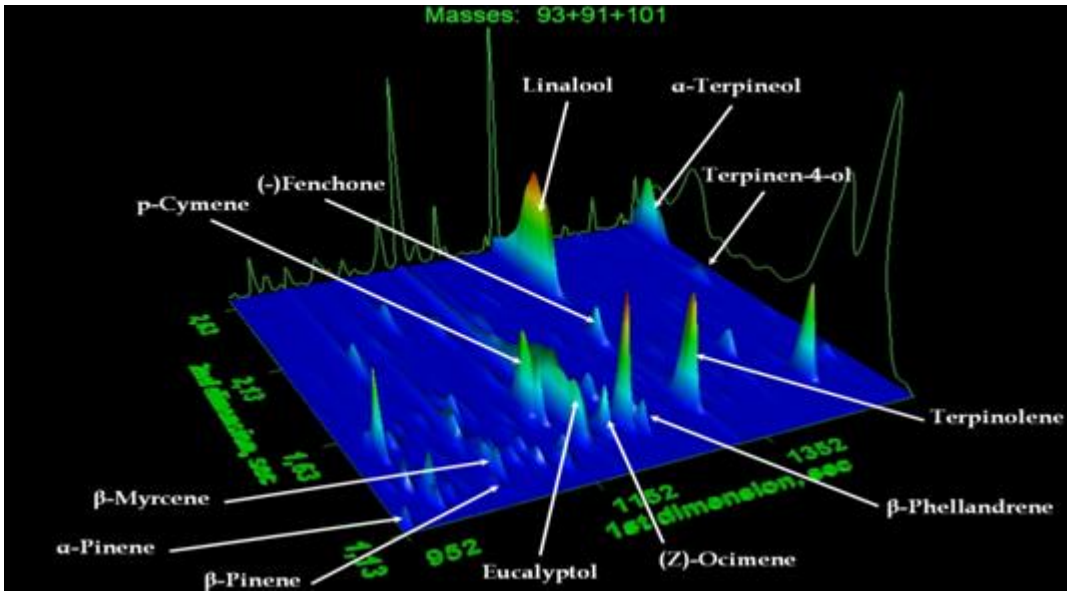


**Figure 6-4: Extracted ion chromatogram showing selected terpenes in blue honeysuckle berries.**

(linalool 100 μg/L, *α*-terpineol 400 μg/L;[315] and geraniol 18 μg/L [316]).

Besides strong aroma activity, some of the terpenes detected exhibit medicinal properties, acting e.g. as expectorants (eucalyptol, terpineol, menthol), analgesics (β-myrcene, (-)-menthol), antitumor (geraniol), as well as antivirus, antibacterial and antifungal agents (linalool, eucalyptol, α-terpineol, α-pinene, β-pinene). Moreover, terpinolene has been shown to effectively prevent low-density lipoprotein (LDL)-oxidation.[317]

An example of the separation power capabilities of GC×GC is shown in Figure 6-4 where linalool and terpinolene (woody aroma),[318] which are among the main

components of the volatile fraction of the fruit, had the same retention time in the $^{1}D$, but their separation was possible in the $^{2}D$ by using GC×GC.

Investigation of the results from this work has shown that many of the volatile compounds detected in samples of honeysuckles also occurs in more traditional blueberries. However, some volatiles were unique to honeysuckles, e.g. (-)-menthol (peppermint-spicy note) and (-)-fenchone (herb-woody note). In addition, studies also have shown that volatiles may be characteristic only for one or two varieties of the 5 studied varieties of honeysuckles. Some of the possible potential markers that are unique to specific varieties of honeysuckle berries are shown in the highlighted cells in Table 6-1. It should be pointed out that to decide that these are real markers, a large number of samples has to be analyzed.

## 6.3 Conclusions

GC×GC-TOFMS showed strong capabilities in the characterization of the complex aroma profile of blue honeysuckle berries. Esters, terpenes and aldehydes are the most abundant compounds influencing flavor profile of analyzed berry samples. 63 of the detected aroma compounds have also been reported for "common" blueberries. Some volatiles may be considered origin markers for a specific blue honeysuckle cultivar (e.g. phenylethyl alcohol for "Brązowa" berry). In order to

confirm that, a larger number of samples have to be analyzed. Some of the volatiles present in blue honeysuckles are distinctive for this type of berries. Quantitative analysis of the volatiles should lead to better characterization of blue honeysuckle berries for various purposes (e.g. determination of their quality, maturity and origin).

# Chapter 7

# Final Conclusions

The GC×GC research summarized in this thesis comprised of the recent advances in GC×GC fundamentals and instrumentation; and the development and application of GC×GC methods for the analysis of natural products.

The first study was the comparison of GC×GC sensitivity to that of 1D-GC using two different detectors; TOFMS, which is a selective detector, and FID, which is non-selective. The detector electronic noise was not the limiting factor for sensitivity. "Chemical or "chromatographic" noise was found to be the major contributing factor that affected sensitivity. Therefore, the ability of GC×GC to efficiently separate the anaytes of interest from any interfering components was of great importance and significantly enhanced sensitivity. At least an order of magnitude increase in sensitivity for *n*-alkanes was reported. The sensitivity gain decreased with the increase of modulation frequency.

HS-SPME-GC×GC (using dual-stage cryogenic loop modulator) in combination with TOFMS was applied for the analysis and characterization of natural products including South African Pinotage wines and Poland blue honeysuckle berries. In addition, the technique was applied for the interesting study of the effect of MLF on

Pinotage aroma during vinification. Chemometrics tools were used for multivariate data analysis to identify the volatile components responsible for aroma changes during MLF. These changes were not due to appearance or disappearance of volatile components; in contrast, they were mainly due to concentration changes of the volatiles already present.

GC×GC provided superior separation and sensitivity in the analysis of complex natural products samples. Use of 1D-GC in the analysis of these samples would have resulted in severe overlap and coelution of many components with matrix components. Therefore, GC×GC-MS provided more reliable identification than GC-MS owing to improved mass spectral quality. Analyte band focusing occurring in the cryogenic modulator increased peak intensities and enhanced the sensitivity, which allowed the detection of trace amounts of volatiles. On the other hand, the main disadvantage of GC×GC was the relatively tedious and time consuming data analysis. A further drawback was related to the dual-stage modulator including the high consumption of liquid $N_2$ and the challenging design of the modulator itself. A very careful adjustment of the carrier gas velocity and delay loop length whenever any of the chromatographic parameters was changed were required. Nevertheless, GC×GC advantages easily overweigh the disadvantages particularly in the analysis

of very complex matrices such as natural products. However, the development of cryogenic modulator free of the previously mentioned problems is needed.

Therefore, a new simple single-stage cryogenic modulator was developed during the course of this research. The revolutionary device developed rivals the performance of commercially available cryogenic modulators. It is able to modulate highly volatile compounds (~ $C_3$). Even solvent peaks such as $CS_2$ were efficiently trapped and modulated, which is impossible with any of the commercially available thermal modulators. Sample mixtures such as Grob mixture and Dimandja mixture were analyzed to test the modulator performance. In addition, selected real samples were analyzed including regular gasoline and diesel fuel samples. The new liquid $N_2$ delivery system developed reduced the consumption of liquid $N_2$ to ~30 L/day versus 50-100 L/day for commercially available cryogenic modulators.

In summary, the instrumentation and analytical methods of this study proved highly useful in the analysis of natural products samples and would be suitable for the analysis of different other types of complex samples. The newly developed modulator would be used for different applications in the analysis of several types of complex samples such as environmental, petrochemicals, etc. Meanwhile, the $LN_2$ delivery system can be further improved to reduce the $LN_2$ consumption. In

addition, different techniques would be applied for the direct heating of the modulator capillary for desorption instead of using compressed hot air, which would improve the modulator performance.

## 7.1 Author's Contribution to Research Presented in the Thesis

1. I was the lead author of the first part of the book chapter "History, evolution, and optimization aspects of comprehensive two-dimensional gas chromatography". My contribution in that chapter was devoted to the comprehensive review of GC×GC fundamentals, instrumentations, history and evolution till 2012 (Chapter 4, p.93-115). The second part of that chapter, "Optimization aspects", was written by Dr. P. Tranchida and Dr. L. Mondello, University of Messina, Italy. In addition, I also co-authored a review about history and evolution of the technique in Journal of Analytical and Bioanalytical Chemistry, which was mainly based on the book chapter mentioned above.

The first part of the thesis Introduction was based primarily on my section of the book chapter.

2. I was the lead author of a comprehensive review "Optimization aspects of comprehensive two-dimensional gas chromatography" in Journal of Chromatography A, which provided the reader with a comprehensive overview of

the optimization process in GC×GC separations. In this review, the second co-author participation was limited to the high resolution TOFMS section and the paragraph devoted to the modulation period optimization for valve-based modulators.

The second part of the thesis Introduction was mainly based on that review.

3. I was the lead author of the first experimental quantitative study to compare the sensitivity of GC×GC versus 1D-GC. I prepared the manuscript of the paper which is at the final stages of submission to Journal of Separation Science.

4. I developed the simple single-stage cryogenic modulator that performs better than most commercially-available cryogenic modulators. The paper describing the research is ready to be submitted to Analytical Chemistry. I presented this research at the 9th GC×GC symposium in Riva del Garda, Italy, May 27 to June 1, 2012 and won the "Best Innovative Poster Presentation" award.

5. I developed a new liquid nitrogen delivery system for the newly developed modulator. This delivery system reduced the liquid nitrogen consumption to ~30 L/day versus 50-100 L/day for commercially-available cryogenic modulators.

6. I participated in the first comprehensive study on the analysis and characterization of the volatile profile of South African Pinotage wines. This project was performed through international collaboration with the University of Stellenbosch, South Africa. The results of that project were published in Food

Chemistry. I did all the method development including standard analysis, retention index study and confirmation, and the positive identification of some of the volatiles. The aroma descriptors explanation and retention indices literature search and comparison were done by the co-authors. The data processing and analysis was initiated by the author and was completed at the University of Stellenbosch. However, I performed the data analysis independently and was able to confirm the results presented in the paper.

7. I spearheaded the analytical part for the GC×GC-based study of the effects of malolactic fermentation on Pinotage wine aroma during wine vinification. This project was also performed in collaboration with the University of Stellenbosch, South Africa. The results were published in Journal of Agricultural and Food Chemistry. In this project I developed the complete analytical methodology, from sample preparation through separation to method validation, performed all the sample preparation and all the chromatographic analyses (including standards analysis and confirmation, the retention index study and positive confirmation of the identity of some of the tentatively identified analytes). Data and chemometric analyses were done at the University of Stellenbosch, but I also performed data analysis independently.

8. I led the first comprehensive analysis and characterization study for the volatiles' profiles of Blue honeysuckle berries. The project was done through international collaboration with the Gdansk University of Technology, Poland. I was responsible for method development and validation, as well as sample preparation. I did the initial GC×GC analyses myself and supervised the rest of them. In addition, I did the analysis of all standards and performed the retention index study and confirmation. Data processing and analysis, as well as the tentative and positive identification of the compounds were done by me as well.

# References


1. Mostafa, A., Górecki, T., Tranchida, P. Q. and Mondello, L., in *in Comprehensive chromatography in combination with mass spectrometry,* ed. ed. L. Mondello, John Wiley & Sons, Inc., Hoboken, New Jersey, USA, 2011, pp.93.

2. Mostafa, A.; Edwards, M.; Górecki, T., J. Chromatogr. A In Press.

3. Giddings, J. C., Anal. Chem. 1967, 39: 1027-1028.

4. Bertsch, W., J. High Resolut. Chromatogr. 1999, 22: 647-665.

5. Giddings, J. C., J. Chromatogr. A 1995, 703: 3-15.

6. Simmons, M. C.; Snyder, L. R., Anal. Chem. 1958, 30: 32-35.

7. Giddings, J. C., Anal. Chem. 1984, 56: 1258A-1260A, 1262A, 1264A, 1266A, 1268A, 1270A.

8. Cortes, H. J., J. Chromatogr. 1992, 626: 3-23.

9. Liu, Z.; Phillips, J. B., J. Chromatogr. Sci. 1991, 29: 227-231.

10. Marriott, P.; Shellie, R., TrAC, Trends Anal. Chem. 2002, 21: 573-583.

11. Venkatramani, C. J.; Xu, J.; Phillips, J. B., Anal. Chem. 1996, 68: 1486-1492.

12. Gorecki, T.; Harynuk, J.; Panic, O., J. Sep. Sci. 2004, 27: 359-379.

13. Edwards, M.; Mostafa, A.; Gorecki, T., Analytical and Bioanalytical Chemistry 2011, 401: 2335-2349.

14. Murphy, R. E.; Schure, M. R.; Foley, J. P., Anal. Chem. 1998, 70: 1585-1594.

15. Blumberg, L. M., J. Chromatogr. A 2003, 985: 29-38.

16. Harynuk, J.; Gorecki, T.; Campbell, C., LCGC North Am. 2002, 20: 876, 878, 880-882, 884, 886-890, 892.

17. Bertsch, W., J. High Resolut. Chromatogr. 2000, 23: 167-181.

18. Dalluge, J.; Beens, J.; Brinkman, U. A. T., J. Chromatogr. A 2003, 1000: 69-108.

19. Gorecki, T.; Panic, O.; Oldridge, N., J. Liq. Chromatogr. Relat. Technol. 2006, 29: 1077-1104.

20. Adahchour, M.; Beens, J.; Vreuls, R. J. J.; Brinkman, U. A. T., TrAC, Trends Anal. Chem. 2006, 25: 540-553.

21. Amador-Munoz, O.; Marriott, P. J., J. Chromatogr. A 2008, 1184: 323-340.

22. Beens, J.; Boelens, H.; Tijssen, R.; Blomberg, J., J. High Resolut. Chromatogr. 1998, 21: 47-54.

23. Frysinger, G. S.; Gaines, R. B.; Ledford, E. B.,Jr, J. High Resolut. Chromatogr. 1999, 22: 195-200.

24. Penet, S.; Vendeuvre, C.; Bertoncini, F.; Marchal, R.; Monot, F., Biodegradation 2006, 17: 577-585.

25. Harynuk, J.; Gorecki, T., J. Chromatogr. A 2003, 1019: 53-63.

26. Reichenbach, S. E.; Ni, M.; Zhang, D.; Ledford, E. B., J. Chromatogr. A 2003, 985: 47-56.

27. Reichenbach, S. E.; Ni, M.; Kottapalli, V.; Visvanathan, A., Chemom. Intell. Lab. Syst. 2004, 71: 107-120.

28. Reichenbach, S. E.; Kottapalli, V.; Ni, M.; Visvanathan, A., J. Chromatogr. A 2005, 1071: 263-269.

29. Hollingsworth, B. V.; Reichenbach, S. E.; Tao, Q.; Visvanathan, A., J. Chromatogr. A 2006, 1105: 51-58.

30. Korytar, P.; Parera, J.; Leonards, P. E. G.; Santos, F. J.; de Boer, J.; Brinkman, U. A. T., J. Chromatogr. A 2005, 1086: 71-82.

31. Korytar, P.; Parera, J.; Leonards, P. E. G.; de Boer, J.; Brinkman, U. A. T., J. Chromatogr. A 2005, 1067: 255-264.

32. Beens, J.; Adahchour, M.; Vreuls, R. J. J.; van Altena, K.; Brinkman, U. A. T., J. Chromatogr. , A 2001, 919: 127-132.

33. Kinghorn, R. M.; Marriott, P. J., J. High Resolut. Chromatogr. 1999, 22: 235-238.

34. Oldridge, N.; Panic, O.; Gorecki, T., J. Sep. Sci. 2008, 31: 3375-3384.

35. Ong, R. C. Y.; Marriott, P. J., J. Chromatogr. Sci. 2002, 40: 276-291.

36. Bordajandi, L. R.; Ramos, L.; Gonzalez, M. J., J. Chromatogr. A 2005, 1078: 128-135.

37. Marriott, P. J.; Haglund, P.; Ong, R. C. Y., Clin. Chim. Acta 2003, 328: 1-19.

38. Van Stee, L. L. P.; Beens, J.; Vreuls, R. J. J.; Brinkman, U. A. T., J. Chromatogr. A 2003, 1019: 89-99.

39. Wang, F. C.; Robbins, W. K.; Greaney, M. A., J. Sep. Sci. 2004, 27: 468-472.

40. Winniford, B. L.; Sun, K.; Griffith, J. F.; Luong, J. C., J. Sep. Sci. 2006, 29: 2664-2670.

41. Hua, R.; Wang, J.; Kong, H.; Liu, J.; Lu, X.; Xu, G., J. Sep. Sci. 2004, 27: 691-698.

42. Phillips, J. B.; Luu, D.; Pawliszyn, J. B.; Carle, G. C., Anal. Chem. 1985, 57: 2779-2787.

43. Liu, Z.; Phillips, J. B., J. Microcolumn Sep. 1989, 1: 249-256.

44. Venkatramani, C. J.; Phillips, J. B., J. Microcolumn Sep. 1993, 5: 511-516.

45. Liu, Z.; Phillips, J. B., J. Microcolumn Sep. 1994, 6: 229-235.

46. Phillips, J. B.; Xu, J., J. Chromatogr. , A 1995, 703: 327-334.

47. Phillips, J. B.; Ledford, E. B., Field Anal. Chem. Technol. 1996, 1: 23-29.

48. Phillips, J. B.; Gaines, R. B.; Blomberg, J.; Van Der Wielen, F. W. M.; Dimandja, J.; Green, V.; Granger, J.; Patterson, D.; Racovalis, L.; De Geus, H.; De Boer, J.; Haglund, P.; Lipsky, J.; Sinha, V.; Ledford, E. B.,Jr, J. High Resolut. Chromatogr. 1999, 22: 3-10.

49. Beens, J.; Tijssen, R.; Blomberg, J., J. High Resolut. Chromatogr. 1998, 21: 63-64.

50. Frysinger, G. S.; Gaines, R. B., J. High Resolut. Chromatogr. 1999, 22: 251-255.

51. Harynuk, J.; Gorecki, T., J. Sep. Sci. 2002, 25: 304-310.

52. Burger, B. V.; Snyman, T.; Burger, W. J. G.; van Rooyen, W. F., J. Sep. Sci. 2003, 26: 123-128.

53. Goldstein, A. H.; Worton, D. R.; Williams, B. J.; Hering, S. V.; Kreisberg, N. M.; Panic, O.; Gorecki, T., J. Chromatogr. A 2008, 1186: 340-347.

54. Panic, O.; Gorecki, T.; McNeish, C.; Goldstein, A. H.; Williams, B. J.; Worton, D. R.; Hering, S. V.; Kreisberg, N. M., J. Chromatogr. A 2011, 1218: 3070-3079.

55. Worton, D. R.; Kreisberg, N. M.; Isaac, G.; Teng, A. P.; McNeish, C.; Górecki, T.; Hering, S. V.; Goldstein, A. H., Aerosol Sci. Technol. 2012, 46: 380-393.

56. Kinghorn, R. M.; Marriott, P. J., J. High Resolut. Chromatogr. 1998, 21: 620-622.

57. Marriott, P.; Kinghorn, R., J. High Resolut. Chromatogr. 1996, 19: 403-408.

58. Marriott, P. J.; Kinghorn, R. M., Anal. Chem. 1997, 69: 2582-2588.

59. Ledford, E. B., Presented at the 23rd Symposium on Capillary Gas Chromatography, Riva del Garda, Italy, June 2000.

60. Harynuk, J.; Górecki, T., Pittcon, New Orleans, LA, 2001.

61. Adahchour, M.; Beens, J.; Brinkman, U. A. T., Analyst (Cambridge, U. K. ) 2003, 128: 213-216.

62. Ledford, E. B.; Billesbach, C.; Termaat, J., Pittcon, New Orleans, LA, 2002.

63. Harynuk, J.; Gorecki, T., J. Sep. Sci. 2004, 27: 431-441.

64. Harynuk, J.; Gorecki, T., J. Chromatogr. A 2006, 1105: 159-167.

65. Libardoni, M.; Waite, J. H.; Sacks, R., Anal. Chem. 2005, 77: 2786-2794.

66. Libardoni, M.; Hasselbrink, E.; Waite, J. H.; Sacks, R., J. Sep. Sci. 2006, 29: 1001-1008.

67. Hyoetylaeinen, T.; Kallio, M.; Hartonen, K.; Jussila, M.; Palonen, S.; Riekkola, M., Anal. Chem. 2002, 74: 4441-4446.

68. Kallio, M.; Hyoetylaeinen, T.; Jussila, M.; Hartonen, K.; Palonen, S.; Shimmo, M.; Riekkola, M., Anal. Bioanal. Chem. 2003, 375: 725-731.

69. Kallio, M.; Jussila, M.; Raimi, P.; Hyoetylaeinen, T., Anal. Bioanal. Chem. 2008, 391: 2357-2363.

70. Bruckner, C. A.; Prazen, B. J.; Synovec, R. E., Anal. Chem. 1998, 70: 2796-2804.

71. Seeley, J. V.; Kramp, F.; Hicks, C. J., Anal. Chem. 2000, 72: 4346-4352.

72. Hamilton, J. F.; Lewis, A. C.; Bartle, K. D., J. Sep. Sci. 2003, 26: 578-584.

73. Mohler, R. E.; Prazen, B. J.; Synovec, R. E., Anal. Chim. Acta 2006, 555: 68-74.

74. Johnson, K. J.; Prazen, B. J.; Olund, R. K.; Synovec, R. E., J. Sep. Sci. 2002, 25: 297-303.

75. Bueno, P. A., Jr.; Seeley, J. V., J. Chromatogr. , A 2004, 1027: 3-10.

76. Sinha, A. E.; Prazen, B. J.; Fraga, C. G.; Synovec, R. E., J. Chromatogr. , A 2003, 1019: 79-87.

77. Sinha, A. E.; Johnson, K. J.; Prazen, B. J.; Lucas, S. V.; Fraga, C. G.; Synovec, R. E., J. Chromatogr. , A 2003, 983: 195-204.

78. Micyus, N. J.; McCurry, J. D.; Seeley, J. V., J. Chromatogr. , A 2005, 1086: 115-121.

79. Seeley, J. V.; Libby, E. M.; Seeley, S. K.; McCurry, J. D., J. Sep. Sci. 2008, 31: 3337-3346.

80. LaClair, R. W.; Bueno, P. A., Jr.; Seeley, J. V., J. Sep. Sci. 2004, 27: 389-396.

81. Seeley, J. V.; Micyus, N. J.; McCurry, J. D.; Seeley, S. K., Am. Lab. (Shelton, CT, U. S. ) 2006, 38: 24-26.

82. Poliak, M.; Fialkov, A. B.; Amirav, A., J. Chromatogr. , A 2008, 1210: 108-114.

83. Poliak, M.; Kochman, M.; Amirav, A., J. Chromatogr. , A 2008, 1186: 189-195.

84. Quimby, B.; McCurry, J.; Norman, W., LC. GC the Peak 2007, April (2007): 7-15.

85. Wang, F. C., J. Chromatogr. A 2008, 1188: 274-280.

86. Harynuk, J.; Gorecki, T., Am. Lab. (Shelton, CT, U. S. ) 2007, 39: 36-39.

87. Ramos, L. and Sanz, J., in *in Comprehensive Analytical Chemistry,* ed. ed. D. Barcelo, Elsevier, Amsterdam, Netherlands, 2009, pp.283-298.

88. Krupčík, J.; Májek, P.; Gorovenko, R.; Sandra, P.; Armstrong, D. W., J. Chromatogr. A 2011, 1218: 3186-3189.

89. Semard, G.; Gouin, C.; Bourdet, J.; Bord, N.; Livadaris, V., J. Chromatogr. A 2011, 1218: 3146-3152.

90. Libardoni, M.; Fix, C.; Waite, J. H.; Sacks, R., Anal. Methods 2010, 2: 936-943.

91. Haglund, P.; Harju, M.; Danielsson, C.; Marriott, P., J. Chromatogr. A 2002, 962: 127-134.

92. Ledford, E. B., Jr.; Billesbach, C., J. High Resolut. Chromatogr. 2000, 23: 202-204.

93. Mostafa, A., Gorecki, T., Pittcon, Atlanta, GA, USA 2011.

94. Gaines, R. B.; Frysinger, G. S., J. Sep. Sci. 2004, 27: 380-388.

95. LECO corporation, ; Training class lab manual of Pegasus 4D GCXGC Time of Flight Mass Spectrometer 2009, p. 270.

96. Harynuk, J.; Gorecki, T., J. Chromatogr. A 2005, 1086: 135-140.

97. Tranchida, P. Q.; Casilli, A.; Dugo, P.; Dugo, G.; Mondello, L., Anal. Chem. 2007, 79: 2266-2275.

98. Weldegergis, B. T.; de Villiers, A.; McNeish, C.; Seethapathy, S.; Mostafa, A.; Gorecki, T.; Crouch, A. M., Food Chem. 2011, 129: 188-199.

99. Adahchour, M.; Beens, J.; Vreuls, R. J. J.; Brinkman, U. A. T., TrAC, Trends Anal. Chem. 2006, 25: 438-454.

100. Dimandja, J. M. D.; Clouden, G. C.; Colon, I.; Focant, J.; Cabey, W. V.; Parry, R. C., J. Chromatogr. A 2003, 1019: 261-272.

101. Dimandja, J. D., Anal. Chem. 2004, 76: 167A-173A.

102. Cordero, C.; Rubiolo, P.; Sgorbini, B.; Galli, M.; Bicchi, C., J. Chromatogr. A 2006, 1132: 268-279.

103. Kohl, A.; Cochran, J.; Cropek, D. M., J. Chromatogr. A 2010, 1217: 550-557.

104. Ryan, D.; Morrison, P.; Marriott, P., J. Chromatogr. A 2005, 1071: 47-53.

105. Ryan, D.; Shellie, R.; Tranchida, P.; Casilli, A.; Mondello, L.; Marriott, P., J. Chromatogr. A 2004, 1054: 57-65.

106. Mondello, L.; Casilli, A.; Tranchida, P. Q.; Costa, R.; Chiofalo, B.; Dugo, P.; Dugo, G., J. Chromatogr. A 2004, 1035: 237-247.

107. Mondello, L.; Casilli, A.; Tranchida, P. Q.; Dugo, P.; Costa, R.; Festa, S.; Dugo, G., J. Sep. Sci. 2004, 27: 442-450.

108. Adahchour, M.; Beens, J.; Vreuls, R. J. J.; Batenburg, A. M.; Brinkman, U. A. T., J. Chromatogr. A 2004, 1054: 47-55.

109. Beens, J.; Boelens, H.; Tijssen, R.; Blomberg, J., J. High Resolut. Chromatogr. 1998, 21: 47-54.

110. Lewis, A.; Carslaw, N.; Marriott, P.; Kinghorn, R.; Morrison, P.; Lee, A.; Bartle, K.; Pilling, M., Nature 2000, 405: 778-781.

111. Harju, M.; Haglund, P., J. Microcolumn Sep. 2001, 13: 300-305.

112. Dimandja, J.; Stanfill, S.; Grainger, J.; Patterson, D., HRC-J. High Resolut. Chromatogr. 2000, 23: 208-214.

113. Ong, R.; Marriott, P.; Morrison, P.; Haglund, P., J. Chromatogr. A 2002, 962: 135-152.

114. Lu, X.; Cai, J.; Kong, H.; Wu, M.; Hua, R.; Zhao, M.; Liu, J.; Xu, G., Anal. Chem. 2003, 75: 4441-4451.

115. Zapadlo, M.; Krupcik, J.; Majek, P.; Armstrong, D. W.; Sandra, P., J. Chromatogr. A 2010, 1217: 5859-5867.

116. Seeley, J. V.; Bates, C. T.; McCurry, J. D.; Seeley, S. K., J. Chromatogr. A 2012, 1226: 103-109.

117. Anderson, J. L.; Ding, J.; Welton, T.; Armstrong, D. W., J. Am. Chem. Soc. 2002, 124: 14247-14254.

118. Anderson, J. L.; Armstrong, D. W., Anal. Chem. 2003, 75: 4851-4858.

119. Anderson, J. L.; Armstrong, D. W., Anal. Chem. 2005, 77: 6453-6462.

120. Seeley, J. V.; Seeley, S. K.; Libby, E. K.; Breitbach, Z. S.; Armstrong, D. W., Anal. Bioanal. Chem. 2008, 390: 323-332.

121. Reid, V. R.; Crank, J. A.; Armstrong, D. W.; Synovec, R. E., J. Sep. Sci. 2008, 31: 3429-3436.

122. Beens, J.; Tijssen, R.; Blomberg, J., J. Chromatogr. , A 1998, 822: 233-251.

123. Vendeuvre, C.; Bertoncini, F.; Thiebaut, D.; Martin, M.; Hennion, M., J. Sep. Sci. 2005, 28: 1129-1136.

124. Bieri, S.; Marriott, P. J., Anal. Chem. 2006, 78: 8089-8097.

125. Dorman, F. L.; Schettler, P. D.; Vogt, L. A.; Cochran, J. W., J. Chromatogr. A 2008, 1186: 196-201.

126. Karolat, B.; Harynuk, J., J. Chromatogr. A 2010, 1217: 4862-4867.

127. McGinitie, T. M.; Karolat, B. R.; Whale, C.; Harynuk, J. J., J. Chromatogr. A 2011, 1218: 3241-3246.

128. Seeley, J. V.; Libby, E. M.; Edwards, K. A. H.; Seeley, S. K., J. Chromatogr. A 2009, 1216: 1650-1657.

129. Adahchour, M.; Tasoez, A.; Beens, J.; Vreuls, R. J. J.; Batenburg, A. M.; Brinkman, U. A. T., J. Sep. Sci. 2003, 26: 753-760.

130. Ong, R.; Shellie, R.; Marriott, P., J. Sep. Sci. 2001, 24: 367-377.

131. Zhu, Z.; Harynuk, J.; Gorecki, T., J. Chromatogr. A 2006, 1105: 17-24.

132. Beens, J.; Janssen, H.; Adahchour, M.; Brinkman, U. A. T., J. Chromatogr. A 2005, 1086: 141-150.

133. Harynuk, J.; Gorecki, T.; de Zeeuw, J., J. Chromatogr. A 2005, 1071: 21-27.

134. Tranchida, P. Q.; Purcaro, G.; Conte, L.; Dugo, P.; Dugo, G.; Mondello, L., J. Chromatogr. A 2009, 1216: 7301-7306.

135. Tranchida, P. Q.; Purcaro, G.; Conte, L.; Dugo, P.; Dugo, G.; Mondello, L., Anal. Chem. (Washington, DC, U. S. ) 2009, 81: 8529-8537.

136. Junge, M.; Bieri, S.; Huegel, H.; Marriott, P. J., Anal. Chem. 2007, 79: 4448-4454.

137. von Muehlen, C.; Khummueng, W.; Zini, C. A.; Caramao, E. B.; Marriott, P. J., J. Sep. Sci. 2006, 29: 1909-1921.

138. Macedo da Silva, J.; Zini, C. A.; Caramao, E. B., Quim. Nova 2011, 34: 962-967.

139. Macedo da Silva, J.; Zini, C. A.; Caramao, E. B., J. Chromatogr. A 2011, 1218: 3166-3172.

140. Macedo da Silva, J.; Zini, C. A.; Caramao, E. B.; Canizares, E. M. P. N.; Leal, K. A., Quim. Nova 2010, 33: 591-597.

141. Muscalu, A. M.; Reiner, E. J.; Liss, S. N.; Chen, T., Int. J. Environ. Anal. Chem. 2010, 90: 1-13.

142. Muscalu, A. M.; Reiner, E. J.; Liss, S. N.; Chen, T.; Ladwig, G.; Morse, D., Anal. Bioanal. Chem. 2011, 401: 2403-2413.

143. Haglund, P.; Korytar, P.; Danielsson, C.; Diaz, J.; Wiberg, K.; Leonards, P.; Brinkman, U. A. T.; de Boer, J., Anal. Bioanal. Chem. 2008, 390: 1815-1827.

144. Bordajandi, L. R.; Ramos, L.; Gonzalez, M. J., J. Chromatogr. A 2006, 1125: 220-228.

145. Korytar, P.; Covaci, A.; Leonards, P. E. G.; de Boer, J.; Brinkman, U. A. T., J. Chromatogr. A 2005, 1100: 200-207.

146. Danielsson, C.; Wiberg, K.; Korytar, P.; Bergek, S.; Brinkman, U. A. T.; Haglund, P., J. Chromatogr. A 2005, 1086: 61-70.

147. Harju, M.; Bergman, A.; Olsson, M.; Roos, A.; Haglund, P., J. Chromatogr. A 2003, 1019: 127-142.

148. Korytar, P.; van Stee, L. L. P.; Leonards, P. E. G.; de Boer, J.; Brinkman, U. A. T., J. Chromatogr. A 2003, 994: 179-189.

149. Korytar, P.; Leonards, P. E. G.; de Boer, J.; Brinkman, U. A. T., J. Chromatogr. A 2002, 958: 203-218.

150. von Muhlen, C.; de Oliveira, E. C.; Morrison, P. D.; Zini, C. A.; Caramao, E. B.; Marriott, P. J., J. Sep. Sci. 2007, 30: 3223-3232.

151. Mateus, E. P.; Gomes da Silva, M. D. R.; Ribeiro, A. B.; Marriott, P. J., J. Chromatogr. A 2008, 1178: 215-222.

152. Ochiai, N.; Ieda, T.; Sasamoto, K.; Fushimi, A.; Hasegawa, S.; Tanabe, K.; Kobayashi, S., J. Chromatogr. A 2007, 1150: 13-20.

153. Ryan, D.; Marriott, P., J. Sep. Sci. 2006, 29: 2375-2382.

154. Khummueng, W.; Trenerry, C.; Rose, G.; Marriott, P. J., J. Chromatogr. A 2006, 1131: 203-214.

155. Ryan, D.; Watkins, P.; Smith, J.; Allen, M.; Marriott, P., J. Sep. Sci. 2005, 28: 1075-1082.

156. Yang, Y.; Wang, Z., Fenxi Huaxue 2010, 38: 1805-1808.

157. Mahe, L.; Dutriez, T.; Courtiade, M.; Thiebaut, D.; Dulot, H.; Bertoncini, F., J. Chromatogr. A 2011, 1218: 534-544.

158. Ruiz-Guerrero, R.; Vendeuvre, C.; Thiebaut, D.; Bertoncini, F.; Espinat, D., J. Chromatogr. Sci. 2006, 44: 566-573.

159. Hua, R.; Li, Y.; Liu, W.; Zheng, J.; Wei, H.; Wang, J.; Lu, X.; Kong, H.; Xu, G., J. Chromatogr. A 2003, 1019: 101-109.

160. Wang, F. C.; Robbins, W. K.; Di Sanzo, F. P.; McElroy, F. C., J. Chromatogr. Sci. 2003, 41: 519-523.

161. Marriott, P. J., in *in Comprehensive chromatography in combination with mass spectrometry,* ed. ed. L. Mondello, John Wiley & Sons, Inc, Hoboken, New Jersey, USA, 2011, pp.243.

162. Shellie, R. A.; Marriott, P. J.; Huie, C. W., J. Sep. Sci. 2003, 26: 1185-1192.

163. Purcaro, G.; Tranchida, P. Q.; Ragonese, C.; Conte, L.; Dugo, P.; Dugo, G.; Mondello, L., Anal. Chem. 2010, 82: 8583-8590.

164. Shellie, R.; Marriott, P. J., Anal. Chem. 2002, 74: 5426-5430.

165. Debonneville, C.; Chaintreau, A., J. Chromatogr. A 2004, 1027: 109-115.

166. Adahchour, M.; Brandt, M.; Baier, H. U.; Vreuls, R. J. J.; Batenburg, A. M.; Brinkman, U. A. T., J. Chromatogr. A 2005, 1067: 245-254.

167. Leclercq, P. A.; Cramers, C. A., Mass Spectrom. Rev. 1998, 17: 37-49.

168. van Deursen, M.; Beens, J.; Reijenga, J.; Lipman, P.; Cramers, C.; Blomberg, J., J. High Resolut. Chromatogr. 2000, 23: 507-510.

169. Dimandja, J. M. D., Am. Lab. 2003, 35: 42-53.

170. Tranchida, P., Mondello, L., Poynter, S. D. H. and Shellie, R., in *in Comprehensive chromatography in combination with mass spectrometry,* ed. ed. L. Mondello, John Wiley & Sons, Inc., 2011, pp.171.

171. Ieda, T.; Ochiai, N.; Miyawaki, T.; Ohura, T.; Horii, Y., J. Chromatogr. A 2011, 1218: 3224-3232.

172. Cao, G.; Shan, Q.; Li, X.; Cong, X.; Zhang, Y.; Cai, H.; Cai, B., Analyst (Cambridge, U. K. ) 2011, 136: 4653-4661.

173. Ochiai, N.; Ieda, T.; Sasamoto, K.; Takazawa, Y.; Hashimoto, S.; Fushimi, A.; Tanabe, K., J. Chromatogr. A 2011, 1218: 6851-6860.

174. Hashimoto, S.; Takazawa, Y.; Fushimi, A.; Tanabe, K.; Shibata, Y.; Ieda, T.; Ochiai, N.; Kanda, H.; Ohura, T.; Tao, Q.; Reichenbach, S. E., J. Chromatogr. A 2011, 1218: 3799-3810.

175. Reichenbach, S. E.; Tian, X.; Tao, Q.; Ledford, E. B., Jr.; Wu, Z.; Fiehn, O., Talanta 2011, 83: 1279-1288.

176. Takazawa, Y.; Hashimoto, S.; Ito, H.; Tanabe, K., Chromatography 2009, 30: 103-104.

177. Shunji, H.; Yoshikatsu, T.; Akihiro, F.; Hiroyasu, I.; Kiyoshi, T.; Yasuyuki, S.; Masa-aki, U.; Akihiko, K.; Kazuo, T.; Hideyuki, O.; Katsunori, A., J. Chromatogr. A 2008, 1178: 187-198.

178. Ochiai, N.; Ieda, T.; Sasamoto, K.; Fushimi, A.; Hasegawa, S.; Tanabe, K.; Kobayashi, S., Organohalogen Compd. 2007, 69: 414/1-414/4.

179. Taraszewski, W. J.; Haworth, D. T.; Pollard, B. D., Anal. Chim. Acta 1984, 157: 73-82.

180. Kinghorn, R. M.; Marriott, P. J., J. High Resolut. Chromatogr. 1998, 21: 32-38.

181. Marriott, P. J.; Kinghorn, R. M., J. Chromatogr. , A 2000, 866: 203-212.

182. De Geus, H.; De Boer, J.; Phillips, J. B.; Ledford, E. B., Jr.; Brinkman, U. A. T., J. High Resolut. Chromatogr. 1998, 21: 411-413.

183. Habram, M.; Welsch, T., J. High Resolut. Chromatogr. 1999, 22: 335-338.

184. Lee, A. L.; Bartle, K. D.; Lewis, A. C., Anal. Chem. 2001, 73: 1330-1335.

185. U.S. Environmental Protection Agency, Part 136, Appendix B, Revision 1.11, 40 CFR.; Ch 1, 1986, p. 537-539, at URL http://ecfr.gpoaccess.gov/cgi/t/text/text-

idx?c=ecfr&sid=44c46aef5b71fe4102de80b1b36cad17&rgn=div5&view=text&node=40:22.0.1.1.1&idno=40#40:22.0.1.1.1.0.1.7.2, accessed on October 27, 2010.

186. Papoulis, A., *Probability, Random Variables, and Stochastic Processes*, McGraw-Hill, New York, 1965.

187. Frysinger, G. S.; Gaines, R. B., J. High Resolut. Chromatogr. 2000, 23: 197-201.

188. Frysinger, G. S.; Gaines, R. B., J. Sep. Sci. 2001, 24: 87-96.

189. Alves, R. F.; Nascimento, A. M. D.; Nogueira, J. M. F., Anal. Chim. Acta 2005, 546: 11-21.

190. Webster, D. R.; Edwards, C. G.; Spayd, S. E.; Peterson, J. C.; Seymour, B. J., Am. J. Enol. Vitic. 1993, 44: 275-284.

191. Marais, J., S. Afr. J. Enol. Vitic. 2003, 24: 70-75.

192. Van Wyk, C. J.; Augustyn, O. P. H.; De Wet, P.; Joubert, W. A., Am. J. Enol. Vitic. 1979, 30: 167-173.

193. Castro, R.; Natera, R.; Benitez, P.; Barroso, C. G., Anal. Chim. Acta 2004, 513: 141-150.

194. del Alamo Sanza, M.; Nevares Dominguez, I.; Carcel Carcel, L. M.; Navas Gracia, L., Anal. Chim. Acta 2004, 513: 229-237.

195. Tredoux, A.; de Villiers, A.; Majek, P.; Lynen, F.; Crouch, A.; Sandra, P., J. Agric. Food Chem. 2008, 56: 4286-4296.

196. Weldegergis, B. T.; Tredoux, A. G. J.; Crouch, A. M., J. Agric. Food Chem. 2007, 55: 8696-8702.

197. Gogus, F.; Ozel, M. Z.; Lewis, A. C., J. Sep. Sci. 2006, 29: 1217-1222.

198. Cardeal, Z. L.; Gomes da Silva, M. D. R.; Marriott, P. J., Rapid Commun. Mass Spectrom. 2006, 20: 2823-2836.

199. Mondello, L.; Casilli, A.; Tranchida, P. Q.; Dugo, P.; Dugo, G., J. Chromatogr. A 2003, 1019: 187-196.

200. Adahchour, M.; Van Stee, L. L. P.; Beens, J.; Vreuls, R. J. J.; Batenburg, M. A.; Brinkman, U. A. T., J. Chromatogr. A 2003, 1019: 157-172.

201. Ryan, D.; Shellie, R.; Tranchida, P.; Casilli, A.; Mondello, L.; Marriott, P., J. Chromatogr. A 2004, 1054: 57-65.

202. Hajslova, J.; Pulkrabova, J.; Poustka, J.; Cajka, T.; Randak, T., Chemosphere 2007, 69: 1195-1203.

203. LECO, 2008, Review number 1. <http://leco.com/ resources/application_note_subs/pdf/ separation_science/-270.pdf>.

204. Rocha, S. M.; Coelho, E.; Zrostlikova, J.; Delgadillo, I.; Coimbra, M. A., J. Chromatogr. A 2007, 1161: 292-299.

205. Banerjee, K.; Patil, S. H.; Dasgupta, S.; Oulkar, D. P.; Patil, S. B.; Savant, R.; Adsule, P. G., J. Chromatogr. A 2008, 1190: 350-357.

206. Marais, J.; Van Rooyen, P. C.; Du Plessis, C. S., S. Afr. J. Enol. Vitic. 1981, 2: 19-23.

207. Van Rooyen, P. C.; Ellis, L. P.; Du Plessis, C. S., S. Afr. J. Enol. Vitic. 1984, 5: 29-34.

208. Setkova, L.; Risticevic, S.; Pawliszyn, J., J. Chromatogr. A 2007, 1147: 213-223.

209. Marques, F. D. A.; McElfresh, J. S.; Millar, J. G., J. Braz. Chem. Soc. 2000, 11: 592-599.

210. Rodrigues, F.; Caldeira, M.; Camara, J. S., Anal. Chim. Acta 2008, 609: 82-104.

211. Bosch-Fuste, J.; Riu-Aumatell, M.; Guadayol, J. M.; Caixach, J.; Lopez-Tamames, E.; Buxaderas, S., Food Chem. 2007, 105: 428-435.

212. Campo, E.; Cacho, J.; Ferreira, V., J. Chromatogr. A 2006, 1137: 223-230.

213. Cardeal, Z. L.; de Souza, P. P.; Gomes da Silva, M. D. R.; Marriott, P. J., Talanta 2008, 74: 793-799.

214. Quijano, C. E.; Pino, J. A., J. Essent. Oil Res. 2007, 19: 527-533.

215. Ferreira, V.; Lopez, R.; Cacho, J. F., J. Sci. Food Agric. 2000, 80: 1659-1667.

216. Campo, E.; Ferreira, V.; Escudero, A.; Cacho, J., J. Agric. Food Chem. 2005, 53: 5682-5690.

217. Campo, E.; Cacho, J.; Ferreira, V., J. Chromatogr. A 2007, 1140: 180-188.

218. Zhu, S.; Lu, X.; Ji, K.; Guo, K.; Li, Y.; Wu, C.; Xu, G., Anal. Chim. Acta 2007, 597: 340-348.

219. VCF (2000). Database of volatile compounds in food. Boelens Aroma Chemical Information Service (BACIS).

220. Ortega-Heras, M.; Gonzalez-Huerta, C.; Herrera, P.; Gonzalez-Sanjose, M. L., Anal. Chim. Acta 2004, 513: 341-350.

221. Romano, P.; Granchi, L.; Caruso, M.; Borra, G.; Palla, G.; Fiore, C.; Ganucci, D.; Caligiani, A.; Brandolini, V., Int. J. Food Microbiol. 2003, 86: 163-168.

222. Campo, E.; Ferreira, V.; Escudero, A.; Marques, J. C.; Cacho, J., Anal. Chim. Acta 2006, 563: 180-187.

223. Camara, J. S.; Marques, J. C.; Alves, M. A.; Ferreira, A. C. S., J. Agric. Food Chem. 2004, 52: 6765-6769.

224. Guth, H., J. Agric. Food Chem. 1997, 45: 3027-3032.

225. Nykanen, L., Am. J. Enol. Vitic. 1986, 37: 84-96.

226. Caven-Quantrill, D. J.; Buglass, A. J., J. Chromatogr. A 2006, 1117: 121-131.

227. Fang, Y.; Qian, M., Flavour Fragrance J. 2005, 20: 22-29.

228. Camara, J. S.; Marques, J. C.; Alves, A.; Silva Ferreira, A. C., Anal. Bioanal. Chem. 2003, 375: 1221-1224.

229. Morales, M. L.; Benitez, B.; Troncoso, A. M., Food Chem. 2004, 88: 305-315.

230. Masson, E.; Baumes, R.; Moutounet, M.; Puech, J., Am. J. Enol. Vitic. 2000, 51: 201-214.

231. Chatonnet, P., Am. J. Enol. Vitic. 1999, 50: 479-494.

232. Spillman, P. J.; Pollnitz, A. P.; Liacopoulos, D.; Pardon, K. H.; Sefton, M. A., J. Agric. Food Chem. 1998, 46: 657-663.

233. Fedrizzi, B.; Magno, F.; Badocco, D.; Nicolini, G.; Versini, G., J. Agric. Food Chem. 2007, 55: 10880-10887.

234. Mataix, E.; Luque de Castro, M. D., Analyst (Cambridge, U. K. ) 1998, 123: 1547-1549.

235. Marais, J., Vitis 1979, 18: 254-260.

236. Mauricio, J. C.; Ortega, J. M., Biotechnol. Bioeng. 1997, 53: 159-167.

237. Ribereau-Gayon, P., Glories, Y., Maujean, A. and Dubourdieu, D., *Handbook of enology and viticulture*, John Wiley and Sons Ltd., UK, 2000.

238. Alberts, P.; Stander, M. A.; Paul, S. O.; de Villiers, A., J. Agric. Food Chem. 2009, 57: 9347-9355.

239. Mateo, J. J.; Jimenez, M., J. Chromatogr. A 2000, 881: 557-567.

240. Ebeler, S. E., Food Rev. Int. 2001, 17: 45-64.

241. Williams, P. J.; Strauss, C. R.; Wilson, B., J. Agric. Food Chem. 1980, 28: 766-771.

242. Rapp, A., Nahrung 1998, 42: 351-363.

243. Simpson, R. F., Vitis 1978, 17: 274-287.

244. Mazzoleni, V.; Caldentey, P.; Careri, M.; Mangia, A.; Colagrande, O., Am. J. Enol. Vitic. 1994, 45: 401-406.

245. Baldock, G. A.; Hayasaka, Y., Aust. J. Grape Wine Res. 2004, 10: 17-25.

246. Jordao, A. M.; Ricardo-da-Silva, J. M.; Laureano, O.; Adams, A.; Demyttenaere, J.; Verhe, R.; De Kimpe, N., J. Wood Sci. 2006, 52: 514-521.

247. Demyttenaere Jan, C. R.; Dagher, C.; Sandra, P.; Kallithraka, S.; Verhe, R.; De, K. N., J. Chromatogr. A 2003, 985: 233-246.

248. Vestner, J.; Malherbe, S.; Du Toit, M.; Nieuwoudt, H. H.; Mostafa, A.; Gorecki, T.; Tredoux, A. G. J.; de Villiers, A., J. Agric. Food Chem. 2011, 59: 12732-12744.

249. Bartowsky, E.; Henschke, P.; Hoj, P.; Pretorious, I., Wine Industry Journal 2004, 19: 24.

250. Ribereau-Gayon, P., Glories, Y., Maujean, A. and Dubourdieu, D., *Handbook of Enology Vol. 1: The Microbiology of Wine and Vinifications, 2nd ed.*, Wiley, Chichester, U.K., 2006.

251. Lerm, E.; Engelbrecht, L.; du Toit, M., S. Afr. J. Enol. Vitic. 2010, 31: 186-212.

252. Bartowsky, E.; Henschke, P., Aust. Grapegrower Winemaker 1995, 379a: 83-94.

253. Davis, C. R.; Wibowo, D.; Eschenbruch, R.; Lee, T. H.; Fleet, G. H., Am. J. Enol. Vitic. 1985, 36: 290-301.

254. Ugliano, M.; Moio, L., J. Agric. Food Chem. 2005, 53: 10134-10139.

255. Boido, E.; Lloret, A.; Medina, K.; Carrau, F.; Dellacassa, E., J. Agric. Food Chem. 2002, 50: 2344-2349.

256. Ugliano, M.; Moio, L., J. Sci. Food Agric. 2006, 86: 2468-2476.

257. Pripis-Nicolau, L.; De Revel, G.; Bertrand, A.; Lonvaud-Funel, A., J. Appl. Microbiol. 2004, 96: 1176-1184.

258. Bartowsky, E.; Costello, P.Henschke, P., ; 11th Australian Wine Industry Technical Conference 2002.

259. Sauvageot, F.; Vivier, P., Am. J. Enol. Vitic. 1997, 48: 187-192.

260. Gambaro, A.; Boido, E.; Zlotejablko, A.; Medina, K.; Lloret, A.; Dellacassa, E.; Carrau, F., Aust. J. Grape Wine Res. 2001, 7: 27-32.

261. Pozo-Bayon, M. A.; G.-Alegria, E.; Polo, M. C.; Tenorio, C.; Martin-Alvarez, P. J.; Calvo de la Banda, M. T.; Ruiz-Larrea, F.; Moreno-Arribas, M. V., J. Agric. Food Chem. 2005, 53: 8729-8735.

262. Boido, E.; Medina, K.; Farina, L.; Carrau, F.; Versini, G.; Dellacassa, E., J. Agric. Food Chem. 2009, 57: 6271-6278.

263. Delaquis, P.; Cliff, M.; King, M.; Girard, B.; Hall, J.; Reynolds, A., Am. J. Enol. Vitic. 2000, 51: 42-48.

264. Fernandes, L.; Relva, A. M.; Gomes da Silva, M. D. R.; Costa Freitas, A. M., J. Chromatogr. , A 2003, 995: 161-169.

265. Swiegers, J. H.; Bartowsky, E. J.; Henschke, P. A.; Pretorius, I. S., Aust. J. Grape Wine Res. 2005, 11: 139-173.

266. Lonvaud-Funel, A., Antonie Van Leeuwenhoek 1999, 76: 317-331.

267. Martineau, B.; Henick-Kling, T.; Acree, T., Am. J. Enol. Vitic. 1995, 46: 385-388.

268. de Revel, G.; Bloem, A.; Augustin, M.; Lonvaud-Funel, A.; Bertrand, A., Food Microbiol. 2005, 22: 569-575.

269. Bauer, R.; Dicks, L. M. T., S. Afr. J. Enol. Vitic. 2004, 25: 74-88.

270. Versari, A.; Parpinello, G. P.; Cattaneo, M., J. Ind. Microbiol. Biotechnol. 1999, 23: 447-455.

271. Henick-Kling, T., Soc. Appl. Bacteriol. Symp. Ser. 1995, 24: 29S-37S.

272. Maicas, S.; Gil, J.; Pardo, I.; Ferrer, S., Food Res. Int. 1999, 32: 491-496.

273. Osborne, J. P.; Mira de Orduna, R.; Pilone, G. J.; Liu, S. -., FEMS Microbiol. Lett. 2000, 191: 51-55.

274. Sefton, M. A.; Francis, I. L.; Williams, P. J., Am. J. Enol. Vitic. 1993, 44: 359-370.

275. D'Incecco, N.; Bartowsky, E.; Kassara, S.; Lante, A.; Spettoli, P.; Henschke, P., Food Microbiol. 2004, 21: 257-265.

276. Hernandez-Orte, P.; Cersosimo, M.; Loscos, N.; Cacho, J.; Garcia-Moruno, E.; Ferreira, V., Food Res. Int. 2009, 42: 773-781.

277. Lloret, A.; Boido, E.; Lorenzo, D.; Medina, K.; Carrau, F.; Dellacassa, E.; Versini, G., Ital. J. Food Sci. 2002, 14: 175-180.

278. Cortes, H., *Multidimensional Chromatography: Techniques and Applications*; Dekker: New York, 1990; Vol. 50.

279. Cordero, C.; Liberto, E.; Bicchi, C.; Rubiolo, P.; Schieberle, P.; Reichenbach, S. E.; Tao, Q., J. Chromatogr. A 2010, 1217: 5848-5858.

280. Cordero, C.; Bicchi, C.; Rubiolo, P., J. Agric. Food Chem. 2008, 56: 7655-7666.

281. Schmarr, H.; Bernhardt, J., J. Chromatogr. A 2010, 1217: 565-574.

282. Vaz-Freire, L. T.; Gomes da Silva, M. D. R.; Freitas, A. M. C., Anal. Chim. Acta 2009, 633: 263-270.

283. Weldegergis, B. T.; Crouch, A. M.; Gorecki, T.; de Villiers, A., Anal. Chim. Acta 2011, 701: 98-111.

284. Schmarr, H.; Bernhardt, J.; Fischer, U.; Stephan, A.; Mueller, P.; Durner, D., Anal. Chim. Acta 2010, 672: 114-123.

285. Robinson, A. L.; Boss, P. K.; Heymann, H.; Solomon, P. S.; Trengove, R. D., J. Chromatogr. A 2011, 1218: 504-517.

286. Robinson, A. L.; Boss, P. K.; Heymann, H.; Solomon, P. S.; Trengove, R. D., J. Agric. Food Chem. 2011, 59: 3273-3284.

287. Malherbe, S.; Tredoux, A.; Nieuwoudt, H. H.; du Toit, M., J. Ind. Microbiol. Biotechnol. 2011, 1050-1054.

288. Malherbe, S. *Investigation of the impact of commercial malolactic fermentation starter cultures on red wine aroma compounds, sensory properties and consumer preference*, Ph.D., Stellenbosch University, 2011; http://scholar.sun.ac.za/bitstream/handle/10019.1/6587/malherbe_investigation 2011.pdf?sequence=1.

289. Gower, J.; Hand, D. Biplots. *Mg Stat Pro*; Chapman & Hall: London, U.K., 1996.

290. R Development Core Team, ; 2010, Vienna, Austria, 2010; http://www.R-project.org.

291. Stein, S.; Mirokhin, Y.; Tchekhovskoi, D.; Mallard, G. The NIST Mass Spectral Search Program, National Institute of Standards and Technology, Gaithersburg, MD, 2008.

292. Linstrom, P. J.; Mallard, W. G. *NIST Chemistry WebBook*; NIST Standard References Database 69; National Institute of Standards and Technology: Gaithersburg, MD, 2011.

293. Siebert, T. E.; Smyth, H. E.; Capone, D. L.; Neuwoehner, C.; Pardon, K. H.; Skouroumounis, G. K.; Herderich, M. J.; Sefton, M. A.; Pollnitz, A. P., Anal. Bioanal. Chem. 2005, 381: 937-947.

294. Bartowsky, E.; Costello, P.; Krieger-Weber, S.; Markides, A.; Francis, L.; Travis, B. Influence of malolactic fermentation on the fruity characters of red wine _ bringing wine chemistry and sensory together. *Internationaler IVIF-Kongress* 2010, Stuttgart, Germany; Deutscher Weinbauverband e.V.: Bonn, Germany, 2010.

295. Liu, S., J. Appl. Microbiol. 2002, 92: 589-601.

296. Ribereau-Gayon, P., Glories, Y., Maujean, A. and Dubourdieu, D., *Handbook of Enology Vol. 2: The Chemistry of Wine and Stabilization and Treatments, 2nd ed.*, Wiley, Chichester, U.K., 2006.

297. Escudero, A.; Campo, E.; Farina, L.; Cacho, J.; Ferreira, V., J. Agric. Food Chem. 2007, 55: 4501-4510.

298. Matthews, A.; Grimaldi, A.; Walker, M.; Bartowsky, E.; Grbin, P.; Jiranek, V., Appl. Environ. Microbiol. 2004, 70: 5715-5731.

299. Matthews, A.; Grbin, P. R.; Jiranek, V., Appl. Microbiol. Biotechnol. 2007, 77: 329-337.

300. Sumby, K. M.; Matthews, A. H.; Grbin, P. R.; Jiranek, V., Appl. Environ. Microbiol. 2009, 75: 6729-6735.

301. Sumby, K. M.; Grbin, P. R.; Jiranek, V., Food Chem. 2010, 121: 1-16.

302. Howell, K. S.; Klein, M.; Swiegers, J. H.; Hayasaka, Y.; Elsey, G. M.; Fleet, G. H.; Hoj, P. B.; Pretorius, I. S.; de Barros Lopes, M. A., Appl. Environ. Microbiol. 2005, 71: 5420-5426.

303. Palikova, I.; Heinrich, J.; Bednar, P.; Marhol, P.; Kren, V.; Cvak, L.; Valentova, K.; Ruzicka, F.; Hola, V.; Kolar, M.; Simanek, V.; Ulrichova, J., J. Agric. Food Chem. 2008, 56: 11883-11889.

304. Plekhanova, M. N., Acta Hort. 2000, 538: 159-164.

305. Wang, S. Y.; Lin, H., J. Agric. Food Chem. 2000, 48: 140-146.

306. Kaehkoenen, M. P.; Hopia, A. I.; Heinonen, M., J. Agric. Food Chem. 2001, 49: 4076-4082.

307. Svarcova, I.; Heinrich, J.; Valentova, K., Biomed Pap Med Fac Univ Palacky Olomouc Czech Repub 2007, 151: 163-174.

308. Skupien, K.; Ochmian, I.; Grajkowski, J., J. Fruit Ornam. Plant Res. 2009, 17/(1): 101-111.

309. Wardencki, W.; Michulec, M.; Curylo, J., Int. J. Food Sci. Technol. 2004, 39: 703-717.

310. Diaz, P.; Ibanez, E.; Senorans, F. J.; Reglero, G., J. Chromatogr. A 2003, 1017: 207-214.

311. Sanchez-Palomo, E.; Diaz-Maroto, M. C.; Perez-Coello, M. S., Talanta 2005, 66: 1152-1157.

312. Rohloff, J.; Nestby, R.; Nes, A.; Martinussen, I., Latvian Journal of Agronomy 2009, 12: 98-103.

313. Hatanaka, A., Phytochemistry 1993, 34: 1201-1218.

314. Keinanen, M., J. Agric. Food Chem. 1993, 41: 1986-1990.

315. Etievant, P. X. E., in *in Wine,* ed. ed. H. Maarse, 1991, pp.483-546.

316. Meilgaard, M., Food Quality Preference 1993, 4: 153-167.

317. Grassmann, J.; Hippeli, S.; Spitzenberger, R.; Elstner, E. F., Phytomedicine 2005, 12: 416-423.

318. Lukic, I.; Milicevic, B.; Banovic, M.; Tomas, S.; Radeka, S.; Persuric, D., J. Agric. Food Chem. 2010, 58: 7351-7360.